Tesis doctoral

BIOGEOGRAFÍA APLICADA DE LOS PRIMATES: DESDE EL PAPEL DE LAS BARRERAS GEOGRÁFICAS HASTA LA SALUD HUMANA

ALISA G. ALIAGA SAMANEZ
Dirigida por: Jesús Olivero Anarte y
Raimundo Real Giménez

2023

Universidad de Málaga
Facultad de Ciencias
Departamento de Biología Animal
Programa de Doctorado en Diversidad Biológica y Medio Ambiente

TESIS DOCTORAL

Biogeografía aplicada de los primates: desde el papel de las barreras geográficas hasta la salud humana

PhD Thesis

Applied primate biogeography: from the role of geographic barriers to implications for the human health

2023

por/by Alisa G. Aliaga Samanez

dirigida por/supervised by Prof. Dr. Jesús Olivero Anarte

& Dr. Raimundo Real Giménez

Programa de Doctorado en Diversidad Biológica y Medio Ambiente

DEPARTAMENTO DE BIOLOGÍA ANIMAL

FACULTAD DE CIENCIAS

UNIVERSIDAD DE MÁLAGA

AUTORA: Alisa Guadalupe Aliaga Samanez
https://orcid.org/0000-0002-8721-6896

EDITA: Publicaciones y Divulgación Científica. Universidad de Málaga

DECLARACIÓN DE AUTORÍA Y ORIGINALIDAD DE LA TESIS PRESENTADA PARA OBTENER EL TÍTULO DE DOCTOR

D./Dña ALISA G. ALIAGA SAMANEZ
Estudiante del programa de doctorado DIVERSIDAD BIOLOGICA Y MEDIO AMBIENTE de la Universidad de Málaga, autor/a de la tesis, presentada para la obtención del título de doctor por la Universidad de Málaga, titulada: BIOGEOGRAFÍA APLICADA DE LOS PRIMATES: DESDE EL PAPEL DE LAS BARRERAS GEOGRÁFICAS HASTA LA SALUD HUMANA

Realizada bajo la tutorización de DR. JESÚS OLIVERO ANARTE y dirección de DR. JESÚS OLIVERO ANARTE Y DR. RAIMUNDO REAL GIMÉNEZ (si tuviera varios directores deberá hacer constar el nombre de todos)

DECLARO QUE:

La tesis presentada es una obra original que no infringe los derechos de propiedad intelectual ni los derechos de propiedad industrial u otros, conforme al ordenamiento jurídico vigente (Real Decreto Legislativo 1/1996, de 12 de abril, por el que se aprueba el texto refundido de la Ley de Propiedad Intelectual, regularizando, aclarando y armonizando las disposiciones legales vigentes sobre la materia), modificado por la Ley 2/2019, de 1 de marzo.

Igualmente asumo, ante a la Universidad de Málaga y ante cualquier otra instancia, la responsabilidad que pudiera derivarse en caso de plagio de contenidos en la tesis presentada, conforme al ordenamiento jurídico vigente.

En Málaga, a 20 de MARZO de 2023

Fdo.: ALISA G. ALIAGA SAMANEZ Doctorando/a	Fdo.: JESÚS OLIVERO ANARTE Tutor/a
Fdo.: JESÚS OLIVERO ANARTE Y RAIMUNDO REAL GIMÉNEZ Director/es de tesis	

Raimundo Real Giménez, Catedrático de Universidad, y **Jesús Olivero Anarte**, Profesor Titular de Universidad, ambos del Departamento de Biología Animal de la Universidad de Málaga,

ACREDITAN QUE:

Dª Alisa G. Aliaga Samanez, doctoranda del Programa de Doctorado en Diversidad Biológica y Medio Ambiente, ha realizado, en el Departamento de Biología Animal de la Universidad de Málaga, las investigaciones que han conducido a la redacción de la presente Memoria de Tesis Doctoral, titulada "**Biogeografía aplicada de los primates: desde el papel de las barreras geográficas hasta la salud humana**".

La presente memoria, que recoge los resultados obtenidos y su interpretación, reúne los requisitos necesarios para ser sometida al juicio de la Comisión correspondiente. Por tanto, como directores y tutor de la tesis, autorizamos su exposición y defensa para optar al Grado de Doctor por la Universidad de Málaga.

Y para que así conste, en cumplimiento de las disposiciones vigentes, firmamos la presente acreditación en Málaga, a 20 de marzo de 2023.

Fdo.: Raimundo Real Giménez, director
Dpto. Biología Animal, Univ. de Málaga

Fdo.: Jesús Olivero Anarte, director y tutor
Dpto. Biología Animal, Univ. de Málaga

INFORME DE AVAL DE LAS PUBLICACIONES EN COAUTORÍA

Los directores de la tesis titulada "**Biogeografía aplicada de los primates: desde el papel de las barreras geográficas hasta la salud humana**" y presentada por la doctoranda **Alisa G. Aliaga Samanez**, del Programa de Doctorado en Diversidad Biológica y Medio Ambiente de la Universidad de Málaga, hacen constar que la tesis cumple con los requisitos de calidad del programa de doctorado. Además, los artículos publicados durante la tesis en revistas indexadas cumplen los criterios especificados por la ANECA, y **no han sido utilizados en tesis anteriores**.

A continuación, se indican los artículos publicados:

- Aliaga-Samanez, A., Real, R., Vermeer, J., Olivero, J. (2020). Modelling species distributions limited by geographical barriers: A case study with African and American primates. *Global Ecology and Biogeography*, 29(3), 444-453.
- Farfán, M., Aliaga-Samanez, A., Olivero, J., Williams, D., Dupain, J., Guian, Z., Fa, J.E. (2019). Spatial modelling for predicting potential wildlife distributions and human impacts in the Dja Forest Reserve, Cameroon. *Biological Conservation*, 230, 104-112.
- Aliaga-Samanez, A., Cobos-Mayo, M., Real, R., Segura, M., Romero, D., Fa, J.E., Olivero, J. (2021) Worldwide dynamic biogeography of zoonotic and anthroponotic dengue. *PloS Neglected Tropical Diseases*, 15(6), e0009496.
- Aliaga-Samanez, A., Real, R., Segura, M., Marfil-Daza, C., Olivero, J. (2022) Yellow fever surveillance suggests zoonotic and anthroponotic emergent potential. *Communications Biology*, 5(1), 1-12.

En Málaga, a 20 de marzo de 2023

Fdo.: Jesús Olivero Anarte, director
Dpto. Biología Animal, Univ. de Málaga

Fdo.: Raimundo Real Giménez, director
Dpto. Biología Animal, Univ. de Málaga

Cita recomendada para esta tesis doctoral:

Aliaga-Samanez, A. 2023. Biogeografía aplicada de los primates: desde el papel de las barreras geográficas hasta la salud humana. Tesis doctoral. Universidad de Málaga, Málaga, España.

This thesis should be cited as:

Aliaga-Samanez, A. 2023. Applied primate biogeography: from the role of geographic barriers to implications for the human health. PhD thesis. University of Malaga, Spain.

Dibujos de primates en la tesis / Drawing of primates in the thesis:	Artista de la Naturaleza
Dibujos de mosquitos en la tesis / Drawing of mosquitoes in the thesis:	Mathieu Contreras
Diseño de portada y contraportada / Covers design:	Alisa G. Aliaga Samanez

Esta es la tesis doctoral nº 23 que produce el Grupo de Investigación "Biogeografía, Diversidad y Conservación" (Código RNM-262), del Departamento de Biología Animal de la Universidad de Málaga, dirigido por el Catedrático Raimundo Real Giménez.

This is the thesis number 23 produced by the Research Group "Biogeography, Diversity and Conservation" (Code RNM-262), Department of Animal Biology, University of Málaga, headed by Professor Raimundo Real Giménez.

A mi familia y amigos

INDICE GENERAL / TABLE OF CONTENTS

0. Organización de la tesis 19

0. Outline of the Thesis 30

1. Introducción 41

1.1. Biogeografía de los primates 41

1.1.1. Clasificación taxonómica de los primates 41

1.1.2. Distribución global de los primates 42

1.1.3. Factores que afectan la distribución de los primates 43

1.1.4. Factores antrópicos 44

1.2. Conservación de los primates 45

1.3. Zoonosis en primates 47

1.3.1. ¿Qué es "zoonosis"? 47

1.3.2. Implicación de primates y mosquitos en las zoonosis 48

1.3.3. Efecto del cambio climático en la salud humana 51

1.3.4. Aplicación de herramientas biogeográficas 52

2. Objetivos de la Tesis Doctoral 55

2. Aims of the Doctoral Thesis 57

3. Material y métodos generales 59

3.1. Controles previos 60

3.2. Función de Favorabilidad y lógica difusa 61

3.3. Evaluación, comparación y validación de modelos 64

4. Modelling species distributions limited by geographic barriers: a case study with African and American primates 68

4.1. Abstract 68

4.2. Introduction 70

4.3. Material and Methods 72

4.3.1. Study area and distribution data 72

4.3.2. Predictor variables used for distribution modelling 74

4.3.3. Favourability models 75

4.3.4. Model assessment and comparison 76

4.3.5. Variation partitioning analysis 76
4.4. Results 77
4.5. Discussion 80
5. Spatial modelling for predicting potential wildlife distributions and human impacts in the Dja Forest Reserve, Cameroon 88
5.1. Abstract 88
5.2. Introduction 89
5.3. Material and methods 91
5.3.1. Study area 91
5.3.2. Patrol data 92
5.3.3. Modelling variables 94
5.3.3.1. Dependent variables 94
5.3.3.2. Independent variables 96
5.3.4. Predictive models 96
5.3.4.1. Model fitting and evaluation 96
5.3.4.2. Model extrapolation 98
5.3.5. Wildlife and risk maps 98
5.4. Results 99
5.4.1. Wildlife models 99
5.4.2. Threat models 102
5.4.3. Combining wildlife and threat models 104
5.5. Discussion 105
6. Worldwide dynamic biogeography of zoonotic and anthroponotic dengue 112
6.1. Abstract 112
6.2. Introduction 113
6.3. Material and methods 116
6.3.1. Study area and time period 116
6.3.2. Methodological framework 117
6.3.3. Vector models 120
6.3.4. Disease model 122
6.3.5. Dengue transmission-risk model 125
6.3.6. Transmission-model refinement 125
6.3.7. Model assessment and validation 126

6.3.8. Contribution of the zoonotic factor 127
6.4. Results 128
6.4.1. Vector models 128
6.4.1.1. Urban mosquitoes 128
6.4.1.2. Sylvatic mosquitoes 129
6.4.1.3. Integrated vector models 129
6.4.2. Disease models 130
6.4.3. Dengue transmission-risk models 132
6.4.4. Model assessment 133
6.4.4.1. Model evaluation 133
6.4.4.2. Predictive capacity 134
6.4.5. Contribution of the sylvatic cycle 137
6.5. Discussion 139
7. Yellow fever surveillance suggests zoonotic and anthroponotic emergent potential 153
7.1. Abstract 153
7.2. Introduction 154
7.3. Material and Methods 157
7.3.1. Lattice data geoprocessing and temporal extent 157
7.3.2. Yellow fever datasets 158
7.3.3. Vector dataset 159
7.3.4. Zoogeographic, spatial and environmental variables 160
7.3.5. Pathogeographical approach to transmission risk modelling 161
7.3.6. Baseline disease models 162
7.3.7. Vector models 163
7.3.8. Model fit assessment and validation of its predictive capacity 164
7.3.9. Relative importance of the zoogeographical factor 165
7.4. Results 165
7.4.1. Zoogeographic Factor 165
7.4.2. Baseline disease models 166
7.4.3. Relative importance of the zoogeographical factor 169
7.4.4. Vector models 169
7.4.5. Yellow fever transmission-risk model 170

7.4.6. Model fit assessment 171
7.4.7. Validation of model predictive capacity 173
7.5. Discussion 174
8. Climate change might be aggravating dengue and yellow fever vectors spread 184
8.1. Abstract 184
8.2. Introduction 185
8.3. Material and Methods 186
8.3.1. Methodological framework and temporal context 186
8.3.2. Forecasting the future distribution of vectors 187
8.3.3. Expected rates of change in favourability 188
8.3.4. Uncertainty in the forecasts 188
8.4. Results 189
8.4.1. *Ae. aegypti* and *Ae. albopictus* models projected into the future 189
8.4.2. Sylvatic vector models projected into the future 189
8.4.3. Combined (urban and sylvatic) vector models projected into the future 192
8.5. Discussion 195
9. Discusión general 200
10. Conclusiones 206
10. Conclussions 210
11. Referencias bibliográficas 214
12. Apéndices 262
13. Producción científica asociada a esta tesis doctoral / Scientific outputs of this PhD thesis 312
14. Breve *curriculum vitae* / Brief cv 318

Agradecimientos

Estoy muy agradecida con todas las personas que se han ido cruzando en mi camino durante toda mi etapa predoctoral, agradecida por lograr que sintiera un ambiente tan agradable y alegre, un hogar. Ha sido difícil estar tanto tiempo lejos de mi familia, pero siempre me ha reconfortado el haber tenido su amor, confianza y ánimo a pesar de la distancia.

Esta tesis doctoral ha sido financiada por el contrato FPU16/06710 del Ministerio de Universidades. Durante su desarrollo, he estudiado y analizado la biogeografía aplicada a los primates, desde el papel de las barreras geográficas hasta la salud humana. De alguna forma, mi inquietud por el estudio de los primates ha ido guiando mi camino, probablemente Jesús, mi director de tesis doctoral, así lo afirme. Antes de llegar a España, durante y al finalizar la carrera de biología, pude colaborar como voluntaria y luego como asistente de campo en diferentes proyectos de investigación enfocados en la conservación de primates en Perú y en Venezuela. En un primer momento, al llegar a España para realizar el máster, pensé que no podría seguir estudiando los primates desde aquí, sin embargo, Raimundo y Jesús me propusieron un trabajo fin de máster con primates como grupo de estudio, y no lo podía creer, estaba tan feliz. Más tarde, al continuar con el doctorado, de nuevo surgió la oportunidad de incluir a los primates como hilo conductor.

Deseo expresar mi más sincero agradecimiento:

A mi familia, a mi padre Helmo, a mi madre Guadalupe, a mis hermanas Cynthia y Gabriela, y a mi sobrina Sofía, a pesar de estar lejos todos estos años, siempre me han hecho sentir su amor, su confianza y su inmenso apoyo, sin todo esto tan cerca aún en la distancia, siento que no habría sido posible recorrer este camino.

No hay palabras para agradecer a Jesús, tutor, director, amigo y familia, en estos siete años que llevo en España, brindándome parte de su tiempo con mucha dedicación para guiarme y acompañarme, empezando por el trabajo fin de máster y ahora con esta tesis doctoral, agradezco haber sido tutorizada por alguien con una calidad científica tan alta pero sobre todo agradezco su calidad humana, sin su apoyo y consejos, no hubiese sido posible realizar esta tesis doctoral. Agradezco a Raimundo Real, por haberme abierto la puerta a esta gran familia, ofreciéndome la oportunidad de realizar mi trabajo fin de máster en el equipo, y aprender una forma de trabajar, y un compañerismo, que me conquistaron, e hizo que quisiera continuar investigando. Le doy las gracias por todas las charlas, que sin esperarlo surgían en el Alcornocal, por sus ganas y forma de explicarlo todo de la manera más simple. Agradezco el enorme apoyo brindado en el desarrollo de esta tesis.

A los miembros del Grupo de Biogeografía, Diversidad y Conservación, que han sido mi familia aquí en España, un grupo donde prima la cooperación, la generosidad y la calidad científica. A mis compañeros y amigos del Alcornocal, quiero agradecer a Marina, por su constante apoyo incondicional, por sus buenos consejos, por siempre animarme, por esas charlas en Casa Lola y por haber sido una elemento clave para uno de los capítulos de esta tesis; a Darío, por ser buen consejero y un apoyo durante el desarrollo de esta tesis; a José Antonio, por siempre animarme y, sobre todo, por esas lindas charlas; a Chema, por su humor pícaro y sus buenos consejos; a Sandro, por siempre ayudarme con una sonrisa y alentarme; a Juan Diego, por alegrarnos siempre con sus ocurrencias y sus locos, y siempre, acertados consejos; a Olga, por transmitir siempre alegría y a través de su contagio alentarme. A Inma, por preocuparse siempre y por esas risas; a Víctor, por esas salidas de campo tan alegres; a Ernesto, por sus preguntas constantes y por sus bromas tan únicas; a Adrián, por siempre ofrecer su ayuda y apoyo; a Baro, por ser tan alegre y por haberme ayudado con la recopilación de

información para uno de los capítulos de esta tesis; a Clara, por ayudarme a obtener algunas variables para esta tesis, por siempre querer juntarnos todos y hacerlo a través de su alegría constante; a Germán, por sus bromas y su apoyo en una idea que tuve "Naturmunayki"; A Estefanía Torreblanca, por esas charlas y salidas en bicicleta. A todas las personas que han ido pasando por el Alcornocal a Sara, Isabel, Ibeti, Ceci, Manu, Cecilia....

A los profesores del grupo, a David, por ser un buen amigo, por siempre preocuparse y animarme a que todo va a salir bien, por ser un buen consejero, por su apoyo incondicional, acompañado de charlas también sobre la vida; a Ana Luz, por siempre estar allí para ayudarme y por sus ajíes; a Lucrecia, por ayudarme durante el proceso de entrega de la tesis; a Farfán, por brindarme siempre su apoyo con una sonrisa; a Paco, por siempre estar allí para motivarme; a Serge, sin él nada de esto hubiese empezado, gracias a él pude hacer el máster; a Carmen Salas, por siempre preocuparse por todos nosotros; a Javivi, por su gran cariño, a Mamen, por ser siempre muy positiva; a Mara, por sus consejos y por haberme ofrecido la oportunidad de escribir parte de mi tesis en su linda casa, a Antonio Román, por todo su apoyo; a Ana Carmen, por siempre ayudarnos con todas las gestiones del Programa de Doctorado; a Estefanía Santos, por su alegría y sus dulces y a Oscar por siempre enseñarte cosas nuevas y por sus helechos.

A Marina Segura por todo su apoyo y consejos para la realización de tres capítulos de esta tesis. A Antonio Picornel y a Unzu, por sus consejos y siempre alentarme.

A Kris Murray, por su buena disposición durante mi estancia en el MRC Unit The Gambia, y por haberme supervisado la estancia, gracias a todo su equipo, a Ana, a Sariba y a Franca. A todas las personas de la Estación de Entomología en Walikunda, a Amadou por siempre querer ayudarme en todo.

A Miguel, por su gran cariño, por su espíritu aventurero y por esas risas sobre los impuestos; a Ángel, por siempre haber sido crítico y por esas risas y a Mamen Merino por esas charlas comiendo siempre dulces.

A mis amigos en Perú y en otras partes del mundo, que, aunque estén lejos siempre me han hecho sentir su apoyo, a Paola, Kattya, Angelito, Alexis, Helen, Fiorella, Pierina, Oscar Vilca, Antonio Bóveda…

Finalmente, a Carlos Marfil, por su amor, por siempre haber estado allí para apoyarme y por haberme alentado en los momentos difíciles durante esta tesis doctoral. A Paco Marfil y a María del Mar Daza, por haberme hecho sentir como parte de su familia y por siempre haber sido un gran apoyo.

Primatus sum, nihil primatum mihi alienum puto

Yo soy un primate; nada acerca de los primates me es extraño

[Hooton, 1955]

Capítulo 0

Organización de la Tesis

Outline of the Thesis

0. Organización de la tesis

La biodiversidad desempeña un papel fundamental en el funcionamiento de los ecosistemas y en la salud humana. La conservación y el uso sostenible de la biodiversidad podría beneficiar a la salud humana manteniendo los servicios de los ecosistemas y reduciendo el riesgo de enfermedades zoonóticas (Keesing *et al.*, 2010; WHO, 2015a). Sin embargo, los recursos biológicos de nuestro planeta no sólo están formados por procesos evolutivos naturales, sino que también se transforman cada vez más por la actividad antropogénica, las presiones demográficas, por la globalización y por el cambio climático (McMichael, 2013). Por lo tanto, desafíos sanitarios mundiales como la lucha contra las enfermedades infecciosas están ligados a las complejas interacciones entre los ecosistemas, las personas y los procesos socioeconómicos.

Considerando la estrecha relación entre la conservación y la salud humana, y con el objetivo de tener una perspectiva unificadora, con esta tesis se pretende estudiar y analizar algunos de los factores que conforman esta relación. Para ello, se ha considerado la biogeografía de los primates como hilo conductor. Los primates no humanos, nuestros parientes biológicos vivos más cercanos, son resultado de la tercera radiación de mamíferos con mayor número de especies: los primates incluyen 517 especies existentes, y solo Rodentia y Chiroptera tienen más especies (IUCN, 2022). Son un componente esencial de la biodiversidad y juegan un papel importante en la regeneración de los bosques (Estrada *et al.*, 2022). Enfocar los análisis de la presente tesis en un único taxón ha permitido profundizar en diversos análisis biogeográficos que convergen en la conservación de la biodiversidad y la preservación de la salud humana. Para ello, es necesario tener en cuenta la historia biogeográfica que puede afectar y condicionar las áreas de presencia de las especies, ya que de esta manera se mejora el rendimiento de los modelos utilizados para analizar su distribución.

La organización general de la tesis se explica a continuación:

En el **capítulo 1** de la presente tesis doctoral se introducen las primeras ideas sobre la biogeografía de los primates, dando a conocer su clasificación taxonómica actual y un pequeño recorrido histórico sobre la evolución de su distribución. También se introduce cómo los factores físicos y antrópicos pueden afectar a estas especies, por ejemplo, limitando sus distribuciones, alterando sus dinámicas poblacionales, disminuyendo sus poblaciones y alterando sus funciones en los ecosistemas a los que pertenecen. En dicho contexto, se introduce la importancia de los primates para que sean especies de interés en los planes de manejo de la conservación, y también se hace referencia a medidas de conservación implementadas a nivel global. Finalmente, se introduce la participación de los primates en las enfermedades zoonóticas, profundizando en la vinculación de la actividad humana en la emergencia de enfermedades zoonóticas; así como el posible efecto del cambio climático en el riesgo de propagación de estas enfermedades. Además, se hace mención del papel de la biogeografía como aproximación metodológica y conceptual para entender y analizar las enfermedades zoonóticas. La presente tesis doctoral utiliza los modelos de distribución como herramienta para analizar la historia, la conservación y la salud humana, teniendo como hilo conductor la biogeografía de los primates con la finalidad de aportar información e identificar áreas que deben ser priorizadas para implementar estrategias de conservación y tomar medidas de vigilancia sanitaria.

En el **capítulo 2** se mencionan los objetivos generales de la presente tesis.

En el **capítulo 3** se profundiza en las aproximaciones metodológicas que son comunes a los distintos capítulos de esta tesis doctoral. Se detalla el uso de la Función de Favorabilidad como herramienta metodológica de modelación aplicada, el procedimiento de control y selección de variables que resultarán

significativas en los modelos, así como los índices de evaluación utilizados para valorar la capacidad descriptiva y predictiva de los modelos resultantes. Los enfoques metodológicos están descritos con mayor detalle en sus respectivos capítulos.

En el **capítulo 4** se desarrolla un enfoque metodológico basado en la Función de Favorabilidad, para evaluar si es posible integrar en los modelos de distribución de especies el papel de las barreras geográficas como elementos que se interponen en el proceso de dispersión. Los límites de las distribuciones de especies a menudo están formados por barreras naturales, como montañas y ríos, pero los modelos de distribución de especies generalmente no incluyen estas restricciones. Se prueban varios enfoques metodológicos que incluyen el análisis de la estructura puramente espacial de la distribución de las especies, y también las barreras geográficas como variables explicativas en los modelos de distribución. Se consideran, como casos de estudio, los primates en la Cuenca del Congo (África central) y en la Región San Martín (Perú). En África Central, el río Congo pone límite a algunas especies de primates, como el chimpancé (*Pan troglodytes*) y el bonobo (*Pan paniscus*); y en Perú, el río Huallaga parece representar también una barrera geográfica para la distribución de algunas especies de mono tocón (*Plecturocebus oenanthe* y *Plecturocebus discolor*). Los resultados permiten afirmar que la Función de Favorabilidad es útil como herramienta para describir barreras geográficas con el fin de mejorar el rendimiento de los modelos de distribución cuando las especies están condicionadas biogeográficamente por barreras. Además, se concluye que el análisis de la estructura espacial de una distribución permite reflejar en los mapas resultantes la forma de distribuciones de especies parcialmente condicionadas por la presencia de una barrera geográfica. Los modelos a los que se permite mayor flexibilidad en el análisis de la estructura espacial describen mejor la forma de la distribución; en cambio, una estructura espacial menos flexible permite que

las variables ambientales capaces de explicar la distribución de las especies estén mejor representadas en la fórmula matemática del modelo. Se ha podido caracterizar la naturaleza de una barrera geográfica a través de variables diseñadas para representar dicha barrera como física o ecológica. Entre estas dos posibilidades, el modelo que describe la barrera como física ha sido el mejor valorado. El enfoque metodológico podría aplicarse a otras especies que estén limitadas por barreras geográficas, debido a que, en este capítulo, se ha considerado diferentes especies en diferentes contextos geográficos.

En el **capítulo 5** se plantea comprender el modo en que influyen sobre la distribución de varias especies, en un área protegida, de diferentes amenazas de origen humano como la caza furtiva, la deforestación y los incendios forestales. El estudio se centra en el chimpancé (*Pan troglodytes*), el gorila de las tierras bajas occidentales (*Gorilla gorilla gorilla*) y el elefante africano del bosque (*Loxodonta cyclotis*), dentro y en el entorno de la Reserva Forestal de Dja, en el sur de Camerún. Esta reserva es una de las selvas tropicales con mayor biodiversidad de África. Sin embargo, el éxito de su conservación es bajo debido al impacto de actividades ilegales, como la caza furtiva. Por lo tanto, se necesitan herramientas que permitan la gestión y conservación de vida silvestre dentro de las áreas protegidas. El software SMART (Spatial Monitoring And Reporting Tool) permite, al personal de vigilancia de fauna en la reserva, recopilar información directamente en el campo sobre la presencia de fauna y sobre la observación de amenazas. El objetivo del estudio ha sido dar uso a esta información sobre la distribución de las especies objetivo y las presiones sobre estas, para generar mapas de áreas de riesgo para la fauna utilizando la modelación espacial mediante el uso de la Función de Favorabilidad. Los modelos de riesgo constituyen una herramienta de evaluación rápida para ser utilizada en el manejo y conservación de la fauna de interés en la Reserva Forestal de Dja. Los modelos realizados sugieren que las áreas más favorables para el chimpancé, el gorila y el

elefante se encuentran dentro del núcleo del área protegida estudiada. Las mayores distancias a la carretera se asociaron a una mayor favorabilidad para la presencia de las tres especies. Las áreas más favorables para la superposición espacial de amenazas se encuentran a lo largo del límite occidental. Los mapas de riesgo, por tanto, muestran que la fauna mejor protegida se concentra en el núcleo de la reserva, lo que coincide con actividades de caza furtiva, en contraste con el mayor riesgo de pérdida de bosque e incendios, que se concentra fuera de los límites de la reserva. Los modelos resultantes proporcionan información valiosa a los administradores de áreas protegidas al resaltar las áreas vulnerables y guiar las acciones de gestión sobre el terreno.

En el **capítulo 6** se investigan los cambios geográficos en el riesgo de transmisión de dengue desde finales del siglo XX, utilizando como base el conjunto de datos global de casos registrados más completo hasta la fecha. Se ha tenido en cuenta, por primera vez, el papel potencial que juegan la biogeografía de los primates y los vectores selváticos en el aumento del riesgo de transmisión de enfermedades arbovirales. El ciclo de transmisión del dengue es complejo. Los seres humanos son los principales huéspedes, y los mosquitos del género *Aedes* son los principales vectores. Sin embargo, existen ciclos selváticos en África y Asia en los que los primates no humanos se infectan de manera asintomática con el virus del dengue a través de diversas especies de mosquitos. Aunque no hay aún constancia demostrada de la presencia de dengue zoonótico en América, los ciclos enzoóticos (basados en primates no humanos) en el neotrópico sí están involucrados en la diversificación y transmisión a humanos del virus de la fiebre amarilla. Este virus comparte vectores con el virus de la fiebre amarilla, por lo que es probable que también ocurra un ciclo selvático en el caso del dengue. A través de la Función de Favorabilidad, se han combinado diferentes modelos de distribución. Por un lado, se ha realizado un modelo de vector a través de la unión difusa de modelos realizados para cada especie de mosquito capaz de transmitir

el virus (es decir, se ha asumido que la transmisión requiere la presencia de, al menos, una especie de vector). Por otro lado, se ha realizado un modelo de enfermedad que describe las zonas favorables para la aparición de infecciones humanas mediante la combinación de predictores ambientales, espaciales, socioeconómicos y de variables zoogeográficas (corotipos de primates). Finalmente, se ha obtenido un modelo de riesgo de transmisión a través de la intersección difusa entre el modelo de vector y el modelo de enfermedad. La evaluación de estos modelos muestra una gran capacidad predictiva, que incluso supera su capacidad descriptiva. Es decir: los modelos obtenidos anticipan tendencias de cambio espacial en el riesgo que ya se están observando. Los modelos sugieren que la propagación de la enfermedad es probable en áreas que, en la actualidad, apenas están afectadas por el dengue (por ejemplo, el sureste de China, Papúa Nueva Guinea, el norte de Australia, el sur de los Estados Unidos, las regiones interiores de Colombia y Venezuela, Madagascar, y el sur de Europa y de Japón). Además, según los análisis, la contribución del ciclo selvático a la transmisión representa un pequeño porcentaje, lo que podría ser una subestimación debido a que solo se han mapeado áreas donde la contribución de los primates no se correlaciona con factores ambientales. Las áreas de influencia potencial de los ciclos selváticos en la presencia de dengue en humanos en el neotrópico son la cuenca del Amazonas y los bosques atlánticos del sur de Brasil. El enfoque metodológico utilizado ha permitido que se puedan proporcionar distintos escenarios geográficos con el fin de que las autoridades sanitarias puedan focalizar las estrategias de vigilancia: (1) Zonas con condiciones favorables tanto para los casos de dengue como para los vectores, siendo alto el riesgo de transmisión. Esto es evidente al sur de Asia. Así, zonas que estaban libres de dengue hace dos décadas, como Pakistán, se han visto favorecidas ambientalmente para la presencia de dengue y de sus vectores. Los modelos han predicho el riesgo de transmisión en esta zona a finales del siglo XX, y los nuevos casos reportados en los informes epidemiológicos a inicios del siglo XXI han

validado esta predicción. En este caso, las entidades sanitarias deben asegurar una estrecha vigilancia microbiológica e epidemiológica. (2) Zonas ambientalmente favorables para la presencia de vectores, pero no para el virus. Este caso sucede, por ejemplo, en el sur de Europa. En España, el mosquito tigre (*Aedes albopictus*) comenzó a establecerse con éxito en los primeros años del presente siglo. Si bien la región se encuentra lejos de las áreas endémicas de dengue, continuamente llegan viajeros que padecen la enfermedad. En 2018 se notificaron por primera vez algunos casos autóctonos en Andalucía, Murcia y Cataluña. En escenarios como este, las entidades sanitarias deben considerar la aplicación de medidas de concienciación orientada a la población local y, en especial, a los viajeros con destino a zonas endémicas de dengue. (3) Zonas con condiciones ambientalmente favorables para los casos de dengue, pero no para los vectores. Este caso se evidenció en Sudamérica, donde los modelos realizados con datos de finales del siglo XX han descrito zonas favorables para los casos de dengue, pero no para los vectores. En la actualidad, la región muestra un panorama diferente, en el que los vectores encuentran ya condiciones ambientalmente favorables, y como consecuencia se asientan exitosamente, aumentando el riesgo de transmisión entre seres humanos. La rápida dispersión de *Aedes*, influida por los seres humanos y por su propio potencial adaptativo, hacen que el ambiente donde actualmente habita pueda no representar el rango de condiciones idóneas que podrían permitirles establecer nuevas poblaciones. Por ello, se considera que las zonas favorables para los vectores, según predicen los modelos obtenidos, deberían tomarse en serio con la finalidad de prevenir la llegada de mosquitos invasores.

En el **capítulo 7** se sigue el mismo enfoque metodológico mencionado en el capítulo 6. Así, se ha construido un modelo que describe las condiciones favorables para la presencia de vectores; otro sobre la favorabilidad ambiental y zoogeográfica para la presencia de casos de fiebre amarilla en los seres humanos;

y, por último, mediante la combinación de los dos anteriores, un modelo que describe las zonas de riesgo de transmisión de la enfermedad. Se ha realizado un análisis patogeográfico para evaluar si los ciclos enzoóticos, basados en corotipos de primates, podrían estar amplificando el riesgo de infecciones por fiebre amarilla en humanos, en un contexto de cambios espaciales mostrados por la enfermedad desde finales del siglo XX. En las últimas décadas se están detectando casos de fiebre amarilla en áreas que habían estado libres de esta durante décadas, probablemente como consecuencia de la rápida propagación de los mosquitos vectores y de la dinámica evolutiva del virus, en la que están involucrados los primates no humanos. En Sudamérica, el potencial de transmisión zoonótica de la fiebre amarilla afecta a regiones dentro de la cuenca occidental, oriental y central del Amazonas, y también en gran parte los bosques atlánticos de Brasil (Mata Atlántica). En África, este potencial podría afectar a algunas sabanas abiertas y boscosas al norte y al sur de las selvas tropicales centroafricanas. Sin embargo, la estimación realizada de la relevancia geográfica del ciclo zoonótico de la fiebre amarilla podría ser conservadora, ya que se hizo sobre la base del efecto puro de las distribuciones de primates no humanos, excluyendo áreas en las que su contribución podría correlacionarse con la de otros factores ambientales. La participación de los primates en la transmisión del virus a humanos, por ejemplo, en la Mata Atlántica, y la alta tasa de evolución mostrada recientemente por este patógeno, podrían llevar a que nuevas variantes alcancen finalmente las poblaciones humanas, considerando que los ciclos zoonóticos en el sudeste de Brasil están estrechamente relacionados con las áreas urbanas. La fragmentación forestal también podría amplificar el riesgo de transmisión de la enfermedad, al aumentar la proximidad de las poblaciones humanas a la fauna silvestre. Se ha realizado una lista de especies pertenecientes a corotipos significativamente relacionados con la distribución de los casos de la enfermedad, útil para considerarla en medidas la vigilancia activa de la fiebre amarilla en primates no humanos. Estos corotipos representan la distribución de

la diversidad de primates no humanos con potencial biogeográfico de ser infectados por el virus de la fiebre amarilla, y geográficamente relacionados con la distribución de casos en humanos. Al igual que en el capítulo 6, los análisis han identificado nuevas áreas que podrían ser prioritarias para vigilancia y vacunación, para lo cual se ha considerado tres escenarios geográficos de transmisión de la fiebre amarilla. El primer escenario implica zonas con condiciones muy favorables, tanto para la presencia del virus, como para la de mosquitos vectores. Este es el caso de algunas zonas de África Occidental y Central y del sur de Brasil. Los modelos apoyan el programa de vacunación previsto por el Ministerio de Salud brasileño en 2019 en muchos estados del este de Brasil, aunque esta zona aún no está considerada por la OMS y la CDC como prioritaria para la vacunación. El segundo escenario describe zonas con un riesgo bajo, pero no despreciable de transmisión de la fiebre amarilla, como es el caso del norte de Namibia, el oeste de Zambia, el este de Etiopía y algunas regiones de Somalia. La OMS y la CDC tampoco consideran estas zonas como prioritarias para la vacunación. Por último, el tercer escenario implica zonas ambientalmente favorables para la presencia de mosquitos vectores, pero no tanto para la aparición del virus. Esta situación se da, por ejemplo, en Norteamérica, el sur de Europa, Asia y Oceanía, que están fuera de la zona endémica de fiebre amarilla. En esta situación, la política más adecuada es la prevención de la introducción del virus a través de los viajes internacionales. Los resultados obtenidos son útiles, por tanto, para identificar nuevas áreas que deben priorizarse para la vacunación, y sugieren la necesidad de vigilancia profunda de la fiebre amarilla en primates de América del Sur y África.

En el **capítulo 8** se evalua el efecto del cambio climático en la distribución de los mosquitos vectores urbanos y selváticos, a partir de los modelos de vector obtenidos en los capítulos 6 y 7. El aumento de las temperaturas provoca la propagación de huéspedes y vectores de enfermedades, lo que aumenta la

población humana expuesta a enfermedades, como el dengue y la fiebre amarilla. El aumento de la favorabilidad para la presencia de mosquitos urbanos y selváticos en los trópicos podría contribuir a aumentar la extensión de las zonas de riesgo de transmisión del dengue y la fiebre amarilla. En Europa, algunas zonas costeras son, y seguirán siendo favorables a la introducción y el posible establecimiento de *Ae. aegypti*. El riesgo podría concentrarse en ciudades con grandes puertos y/o aeropuertos, aunque muy probablemente favorecido por la posibilidad de llegada de individuos más que por el cambio climático. Los modelos sugieren que, actualmente, *Ae. albopictus* tiene condiciones favorables para aparecer en los 7 países europeos en los que aún no está establecido, y que seguirá teniéndolas en 2080. Considerando la respuesta de los mosquitos selváticos al cambio climático, los resultados sugieren que las zonas favorables para la presencia de *Ae. niveus* y *Ae. vittatus* podrían extenderse en el interior de la India, en el sureste de China y en los países del sur de Asia, especialmente en Borneo. En África subsahariana occidental y central, habría que prestar atención a *Ae. vittatus*, *Ae. luteocephalus* y *Ae. africanus*, especialmente en Camerún, la República Centroafricana y el norte de la República Democrática del Congo. Dado que los brotes de arbovirus transmitidos por *Aedes* siguen aumentando en África, sería fundamental establecer una sólida infraestructura entomológica de salud pública para los mosquitos *Aedes* con el fin de contener y prevenir nuevos brotes. Detectar qué especies de mosquitos podrían encontrar nuevas zonas favorables, y dónde, es un paso importante para establecer un protocolo de vigilancia que permita prevenir nuevos casos de dengue y fiebre amarilla. Se propone, como siguiente paso, evaluar el efecto del cambio climático en el riesgo de transmisión de estas enfermedades en el futuro teniendo en cuenta el efecto del cambio climático en la distribución de los primates.

En el **capítulo 9** se discute de forma general los objetivos y conclusiones abordados en la tesis doctoral, integrando el sentido de su estructura y resaltando

los principales logros, además de sugerir algunas estrategias de actuación frente a las distintas cuestiones metodológicas evaluadas.

En el **capítulo 10** se recogen las conclusiones generales más significativas obtenidas en esta tesis doctoral.

En el **capítulo 11** se recogen, por orden alfabético, las referencias bibliográficas utilizadas para redactar la presente tesis doctoral.

Finalmente, en el **capítulo 12** se agrupan los apéndices que pertenecen a los capítulos 4, 5, 6, 7 y 8. Al final de este capítulo se detallan las contribuciones científicas que avalan la presente tesis doctoral, así como otras contribuciones obtenidas, las noticias en canales, periódicos y blogs científicos que se desarrollaron durante realización de la tesis, y un breve *curriculum vitae* de la doctoranda.

0. Outline of the Thesis

Biodiversity plays a key role in ecosystem functioning and human health. The conservation and sustainable use of biodiversity could benefit human health by maintaining ecosystem services and by reducing the risk of zoonotic diseases (Keesing *et al.*, 2010; WHO, 2015a). However, the biological resources of our planet are not only shaped by natural evolutionary processes, but are also increasingly transformed by anthropogenic activity, population pressures, globalisation and climate change (McMichael, 2013). Therefore, global health challenges such as the fight against infectious diseases are linked to the complex interactions between ecosystems, people and socio-economic processes.

Considering the close relationship between conservation and human health, and with the aim of having a unifying perspective, this thesis aims to study and analyse some of the factors that shape this relationship. To this end, primate biogeography has been considered as a guiding thread. Non-human primates, our closest living biological relatives, are the third largest mammalian radiation with the highest number of species: Primates include 517 extant species, and only Rodentia and Chiroptera have more species than it (IUCN, 2022). They are an essential component of biodiversity and play an important role in forest regeneration (Estrada *et al.*, 2022). Focusing the analyses in this thesis on a single taxon has allowed us to delve into various biogeographical analyses that converge in the conservation of biodiversity and the preservation of human health. To this end, it is necessary to take into account the biogeographical history that can affect and condition where species occur, as this improves the performance of the models used to analyse their distribution.

The general organisation of the thesis is explained below:

Chapter 1 introduces the first ideas on primate biogeography, presenting the current taxonomic classification and a brief historical overview of the evolution of their distribution. It also introduces how physical and anthropogenic factors can affect these species, for example, by limiting their distributions, altering their population dynamics, reducing their populations and altering their functions in the ecosystems to which they belong. In this context, the importance of primates as species of concern in conservation management plans is introduced. Reference is also made to conservation measures implemented at the global level. Finally, the involvement of primates in zoonotic diseases is introduced, with the link between human activity and the emergence of zoonotic diseases, as well as the possible effect of climate change on the risk of the spread of these diseases. In addition, mention is made of the role of biogeography as a methodological and conceptual approach to understanding and analysing zoonotic diseases. This PhD thesis uses distribution modelling as a tool to analyse history, conservation and human health, using primate biogeography as a common thread to provide information and identify areas that should be prioritised in order to implement conservation strategies and health surveillance measures.

Chapter 2 outlines the general objectives of this thesis.

Chapter 3 deepens the methodological approaches common to the different chapters of this doctoral thesis. Details of the use of the Favourability Function, as a methodological tool for applied modelling, are given, together with the procedures for control and selection of variables that will be significant in the models. Finally, this chapter describes the indices used to assess the descriptive and predictive capacities of the resulting models. Methodological approaches are described in more detail in their respective chapters.

In **chapter 4**, a methodological approach based on the Favourability Function has been developed to assess whether it is possible to integrate the role of

geographic barriers as intervening elements in the dispersal process into species distribution models. Boundaries of species distributions are often formed by natural barriers, such as mountains and rivers, but species distribution models generally do not include these constraints. Several methodological approaches are tested that include the analysis of the purely spatial structure of species distributions. Also, geographical barriers are used as explanatory variables. Primates in the Congo Basin (Central Africa) and in the San Martin Region (Peru) are considered as case studies. In Central Africa, the Congo River limits de distribution of some primate species, such as chimpanzee (*Pan troglodytes*) and bonobo (*Pan paniscus*). In Peru, the Huallaga River also seems to represent a geographical barrier for the distribution of some species of titi monkey (*Plecturocebus oenanthe* and *Plecturocebus discolor*). The results of this research allow us to affirm that the Favourability Function is useful as a tool to describe geographical barriers in order to improve the performance of distribution models when species are biogeographically conditioned by them. Furthermore, the analysis of the spatial structure of a distribution allows resulting maps to reflect the shape of species distributions partially conditioned by the presence of a geographical barrier. Allowing greater flexibility in the analysis of the spatial structure enhances descriptions of the shape of the distribution, whereas a less flexible spatial structure allows entry, in the mathematical formula of the model, to environmental variables that can explain the species distribution. The nature of a geographical barrier has been also characterized using variables designed to represent such a barrier as physical or ecological. Between these two possibilities, the model describing the barrier as physical got the best evaluation. The methodological approach used in this chapter could be applied to other species that are limited by geographical barriers, as different species in different geographical contexts have been used in this case study.

Chapter 5 aims to understand how the distribution of several species in an African protected area is influenced by human-induced threats such as poaching,

deforestation and forest fires. The study focuses on chimpanzee (*Pan troglodytes*), western lowland gorilla *(Gorilla gorilla gorilla*) and African forest elephant (*Loxodonta cyclotis*), in and around the Dja Forest Reserve, in southern Cameroon. This reserve is one of the most biodiverse rainforests in Africa. However, its conservation success is low due to the impact of illegal activities such as poaching. Therefore, tools are needed to enable the management and conservation of wildlife within protected areas. The SMART (Spatial Monitoring And Reporting Tool) software allows wildlife rangers in the reserve to collect information, directly in the field, on the presence of wildlife and on the observation of threats. The aim of the study was to use this information on the distribution of target species and of pressures on them, in order to generate maps of areas at risk of human impact on the target mammals, using spatial modelling with the Favourability Function. Risk models provide a rapid assessment tool for the management and conservation of wildlife in the Dja Forest Reserve. The models suggest that the most favourable areas for chimpanzee, gorilla and elephant are within the core of the protected area. Greater distances from roads were associated to greater favourability for the presence of the three species. The most favourable areas for spatial overlap of threats are located along the western boundary of the reserve. Risk maps, therefore, show that the best protected fauna is concentrated in the core of the reserve, which coincides with poaching activities, in contrast to the highest risk of forest loss and fire, which is concentrated outside the reserve boundaries. The resulting models provide valuable information to the managers of protected areas, by highlighting vulnerable areas and guiding management actions on the ground.

Chapter 6 investigates geographical changes in the risk of dengue transmission since the late 20th century, using as a basis the most complete global dataset of reported cases to date. The potential role of primate biogeography and sylvatic vectors in increasing the risk of arboviral disease transmission has been

considered for the first time. The transmission cycle of dengue is complex. Humans are the main hosts, and *Aedes* mosquitoes are the main vectors. However, there are sylvatic cycles in Africa and Asia in which non-human primates are asymptomatically infected with dengue virus by several mosquito species. Although there is as yet no proven evidence of zoonotic dengue in the Americas, enzootic (i.e., non-human primate based) cycles in the neotropics are involved in the diversification and transmission of yellow fever virus to humans. This virus shares vectors with the yellow fever virus, so it is likely that a sylvatic cycle also occurs in the case of dengue. By means of the Favourability Function, different distribution models have been combined. On the one hand, a vector model has been made through the fuzzy union of models based on each mosquito species capable of transmitting the virus (i.e., it has been assumed that transmission requires the presence of at least one vector species). On the other hand, a disease model describing favourable areas for the occurrence of human infections has been developed by combining environmental, spatial, socio-economic and zoogeographical predictors (i.e., primate chorotypes). Finally, a transmission risk model has been obtained through the fuzzy intersection between the vector model and the disease model. The evaluation of these models shows a high predictive capacity, which even exceeds their descriptive capacity. That is, the models obtained anticipate trends of spatial change in risk that are already being observed. The models suggest that the spread of the disease is likely in areas that are currently hardly affected by dengue (e.g., southeast China, Papua New Guinea, northern Australia, southern United States, inland regions of Colombia and Venezuela, Madagascar, southern Europe, and Japan). Furthermore, analyses suggest that the contribution of the sylvatic cycle to transmission represents a small percentage, which may be an underestimation because only areas where the contribution of primates does not correlate with environmental factors have been mapped. The areas of potential influence of forest cycles on the occurrence of dengue in humans in the neotropics are the Amazon basin and the Atlantic

forests of southern Brazil. The methodological approach used has allowed different geographical scenarios to be provided so that health authorities can focus surveillance strategies: (1) Areas with favourable conditions for both dengue cases and vectors, with a high risk of transmission. This is evident in South Asia. Thus, areas that were dengue-free two decades ago, such as Pakistan, have become environmentally favourable for the presence of dengue and its vectors. The models have predicted the risk of transmission in this area in the late 20th century, and new cases reported in epidemiological reports in the early 21st century have validated this prediction. In this case, health entities should ensure close microbiological and epidemiological surveillance. (2) Areas environmentally favourable for the presence of vectors, but not for the virus. This is the case, for example, in southern Europe. In Spain, the tiger mosquito (*Aedes albopictus*) began to establish itself successfully in the early years of the current century. Although the region is far from dengue endemic areas, travellers suffering from the disease are continuously arriving. In 2018, some autochthonous cases were reported for the first time in Andalusia, Murcia and Catalonia. In scenarios such as this, health entities should consider the implementation of awareness-raising measures aimed at the local population and, in particular, at travellers to dengue-endemic areas. (3) Areas with environmentally favourable conditions for dengue cases, but not for vectors. This was the case in South America, where modelling using data from the late 20th century has described areas favourable for dengue cases but not for vectors. Today, the region shows a different scenario, where vectors already find environmentally favourable conditions and, as a consequence, they establish successfully themselves, increasing the risk of human-to-human transmission. The rapid dispersal of *Aedes* influenced by humans, and their own adaptive potential, means that the environments where they currently inhabit may not represent the range of ideal conditions that would allow them to establish new populations. Therefore, it is considered that vector

favourable areas, as predicted by the models obtained, should be taken seriously in order to prevent the arrival of invasive mosquitoes.

In **chapter 7**, the same methodological approach mentioned in Chapter 6 has been followed. Thus, a model has been constructed describing the favourable conditions for the presence of vectors; another on the environmental and zoogeographical favourability for the presence of yellow fever cases in humans; and finally, by combining the two previous ones, a model describing the areas at risk of disease transmission. A pathogeographic analysis has been carried out to assess whether enzootic cycles, based on primate chorotypes, could be amplifying the risk of yellow fever infections in humans, in a context of spatial changes shown by the disease since the end of the 20th century. In recent decades, yellow fever cases are being detected in areas that had been free of yellow fever for decades, probably as a consequence of the rapid spread of mosquito vectors and the evolutionary dynamics of the virus, in which non-human primates are involved. In South America, the potential for zoonotic transmission of yellow fever affects regions within the western, eastern and central Amazon basin, and also to a large extent the Atlantic forests of Brazil (Mata Atlantica). In Africa, this potential could affect some open and wooded savannahs north and south of the Central African rainforests. However, the estimate made of the geographical relevance of the yellow fever zoonotic cycle may be conservative, as it was made on the basis of the pure effect of non-human primate distributions, excluding areas where their contribution could be correlated with that of other environmental factors. The involvement of primates in the transmission of the virus to humans, for example in the Atlantic Forest, and the high rate of evolution recently shown by this pathogen, could lead to new variants eventually reaching human populations, considering that zoonotic cycles in southeastern Brazil are closely related to urban areas. Forest fragmentation could also amplify the risk of disease transmission by increasing the proximity of human populations to wildlife. A list of species

belonging to chorotypes significantly related to the distribution of disease cases has been compiled, useful for consideration in active surveillance measures for yellow fever in non-human primates. These chorotypes represent the distribution of the diversity of non-human primates with biogeographical potential to be infected by yellow fever virus, and geographically related to the distribution of human cases. As in chapter 6, the analyses have identified new areas that could be prioritised for surveillance and vaccination, for which three geographical scenarios of yellow fever transmission have been considered. The first scenario involves areas with very favourable conditions for both the presence of the virus and mosquito vectors. This is the case in parts of West and Central Africa and southern Brazil. The models support the vaccination programme planned by the Brazilian Ministry of Health in 2019 in many eastern Brazilian states, although this area is not yet considered by the WHO and the CDC as a priority for vaccination. The second scenario describes areas with a low but not negligible risk of yellow fever transmission, such as northern Namibia, western Zambia, eastern Ethiopia and some regions of Somalia. These areas are also not considered by the WHO and the CDC as priority areas for vaccination. Finally, the third scenario involves areas that are environmentally favourable for the presence of mosquito vectors, but not so favourable for virus emergence. This situation occurs, for example, in North America, southern Europe, Asia and Oceania, which are outside the yellow fever endemic zone. In this situation, the most appropriate policy is to prevent the introduction of the virus through international travelling. The results obtained are, therefore, useful for identifying new areas to be prioritised for vaccination, and suggest the need for in-depth surveillance of yellow fever in primates in South America and Africa.

In **chapter 8,** the effect of climate change on the distribution of urban and sylvatic mosquito vectors has been assessed, based on the vector models obtained in Chapters 6 and 7. Rising temperatures cause the spread of disease hosts and

vectors, increasing the human population exposed to diseases such as dengue and yellow fever. Increased favourability for urban and sylvatic mosquitoes in the tropics could contribute to the spread of areas at risk of dengue and yellow fever transmission. In Europe, some coastal areas are, and will remain, favourable for the introduction and possible establishment of *Ae. aegypti*. The risk could be concentrated in cities with large ports and/or airports, although it is most likely favoured by the possibility of arrival of individuals rather than climate change. Modelling suggests that *Ae. albopictus* currently has favourable conditions for occurrence in the 7 European countries where it is not yet established, and will continue to do so in 2080. Considering the response of sylvatic mosquitoes to climate change, the results suggest that favourable areas for *Ae. niveus* and *Ae. vittatus* could extend into inland India, southeast China and South Asian countries, especially Borneo. In western and central Sub-Saharan Africa, attention should be focused on *Ae. vittatus*, *Ae. luteocephalus* and *Ae. africanus*, especially in Cameroon, Central African Republic and northern Democratic Republic of Congo. As outbreaks of *Aedes*-borne arboviruses continue to increase in Africa, it would be critical to establish a robust public health entomological infrastructure for *Aedes* mosquitoes to contain and prevent further outbreaks. Detecting which mosquito species might find new favourable areas, and where, is an important step in establishing a surveillance protocol to prevent new cases of dengue and yellow fever. As a next step, assessessments of the effect of climate change on the future risk of transmission of these diseases are proposed, taking into account the effect of climate change on the distribution of primates.

Chapter 9 discusses, in general terms, the objectives and conclusions addressed in this PhD thesis, integrating the sense of its structure and highlighting the main achievements, as well as suggesting some strategies for action against the different methodological issues evaluated.

Chapter 10 contains the most significant general conclusions obtained in this doctoral thesis.

Chapter 11 lists, in alphabetical order, the bibliographical references used to write this doctoral thesis.

Finally, in **chapter 12**, the appendices belonging to chapters 4, 5, 6, 7 and 8 have been grouped together. At the end of this chapter, the scientific contributions that support this doctoral thesis are detailed, as well as other contributions: news on scientific channels, newspapers and blogs that were developed during the thesis, and a brief *curriculum vitae* of the doctoral student.

CAPÍTULO 1

Introducción General

1. Introducción

1.1. Biogeografía de los primates

1.1.1. Clasificación taxonómica de los primates

El Orden Primates está conformado por 16 familias (Burgin *et al.*, 2020). Éstas contienen un total de 517 especies, según el libro *Illustrated checklist of the mammals of the world* (Burgin *et al.*, 2020), y 521 especies según la IUCN Red List (IUCN, 2022). La clasificación de los Primates divide este orden en dos subórdenes: Strepsirrhini y Haplorhini. Los Strepsirrhini incluyen a los lémures, lorises, y gálagos, que habitan en África y Asia; mientras los Haplorrinos incluyen al infraorden Tarsiformes (tarseros), que habitan en el continente asiático, y al infraorden Simiiformes. Este último incluye a los parvórdenes Catarrhini y Platyrrhini, conocidos respectivamente como primates del Viejo Mundo y del Nuevo Mundo (Mittermeier *et al.*, 2013). Los catarrinos se distribuyen por los continentes africano y asiático, con la excepción de una sola especie del género *Macaca* que fue introducida en el Peñón de Gibraltar (Ballesta, 2017). Dos superfamilias forman parte de los catarrinos: los cercopithecidos y los hominoideos. Los primeros incluyen a los macacos, los mangabeys, los mandriles, los papiones, los géladas, los colobos, los langures, los rinopitecos y los monos patas, entre otros. La superfamilia Hominoidea está conformada por las familias Hylobatidae (gibones y siamangs) y Hominidae (oranguntanes, gorilas, chimpancés, bonobos y humanos) (Burgin *et al.*, 2020). Por último, los plathyrrhinos se distribuyen por la región neotropical, que abarca Centro y Sudamérica, y se interna levemente en Norteamérica. Está conformado por 5 familias: Callitrichidae (titis y tamarinos), Aotidae (monos nocturnos), Cebidae (monos ardillas y monos capuchinos), Pitheciidae (titis, sakis y uacaris) y Atelidae (monos aulladores, monos araña, monos choro y muriquis) (Burgin *et al.*, 2020).

1.1.2. Distribución global de los primates

La biogeografía es el estudio de cómo se distribuye la biodiversidad en el tiempo y el espacio (Lomolino *et al.*, 2006). El orden de los primates evolucionó en el período Cretácico hace alrededor de 81,5 millones de años a partir de un grupo ancestral de mamíferos (Tavaré *et al.*, 2002). La evidencia fósil de los primeros primates conocidos comienza hace unos 55 a 60 millones de años (Paleoceno tardío/Eoceno temprano) (Smith & Burrows, 2004). La distribución y evolución de los primates durante los últimos millones de años ha tenido lugar en el contexto de una Tierra dinámica, en la que han ocurrido cambios en la geografía y el clima, en la posición y la composición de los continentes y, especialmente, en sus interconexiones, que han cambiado considerablemente (Fleagle & Gilbert, 2006).

Al inicio del Cenozoico, su rango latitudinal era mucho más amplio que el actual. Durante el calentamiento climático del Eoceno, hace entre 56 y 34 millones de años, abundaban en las latitudes altas, hasta unos 50° Norte, tanto en América del Norte como en Europa (alcanzando lo que hoy es Reino Unido, Francia y Alemania) (Fleagle & Gilbert, 2006). Durante el Oligoceno, debido al enfriamiento global, América del Norte quedó desprovista de primates, con la excepción del omomíido *Ekgmowechashala*. Se conocen fósiles del Mioceno temprano en Dakota del Sur (Harrison, 2016). En Eurasia, sobrevivieron primates en Indo-Pakistán, el sur de China y Tailandia (Harrison, 2016). Durante el Mioceno temprano, la colisión de la placa afroárabe con Eurasia permitió la afluencia de mamíferos a este continente desde África (Andrews *et al.*, 1996). Durante el pico de calentamiento del Mioceno temprano-medio, los primates vivían en latitudes altas en los extremos más meridionales de Sudamérica, así como en el norte de Europa y Asia (Fleagle & Gilbert, 2006).

Actualmente, los primates no humanos están asociados a climas tropicales o subtropicales, y la mayoría de los taxones se encuentran entre las latitudes de 30°

Norte y 30° Sur. No obstante, hay excepciones notables, como los macacos japoneses que habitan una latitud de más de 40°. No hay primates no humanos en América del Norte al norte de México Central, y ninguno en Europa salvo los macacos de Berbería en Gibraltar (Fleagle & Gilbert, 2006). En el hemisferio sur, algunas especies se extienden más allá del paralelo 30° hasta el extremo de África y los bosques templados de Argentina (Fleagle & Gilbert, 2006). Los primates tienen una tolerancia relativamente menor a los climas más fríos que otros órdenes de mamíferos como los Carnivora, que se extienden desde el Ártico a la Tierra de Fuego, o los murciélagos y los roedores, que tienen bastante éxito en climas templados. En resumen, los primates actuales se distribuyen en las regiones biogeográficas Neotropical, Afrotropical (África continental y Madagascar) e Indomalaya (Estrada *et al.*, 2022).

1.1.3. Factores que afectan la distribución de los primates

Existen factores que pueden afectar las áreas de distribución de los primates, determinando su posición geográfica, su forma, y su configuración. Entre estos factores se encuentran las barreras a la dispersión (Rapoport, 1975). En biogeografía se entiende como barrera a cualquier factor que se opone a la difusión (en inglés, *dispersion*) y a la dispersión (en inglés, *dispersal*) de una especie, grupo taxonómico o asociación biótica (Lomolino *et al.*, 2006). Barreras físicas importantes pueden ser la existencia de condiciones climáticas desfavorables y los accidentes geográficos y topográficos; y barreras biológicas pueden ser la competencia interespecífica y los cambios en la vegetación (Rapoport, 1975). Las influencias combinadas de los factores abióticos, las respuestas individuales y de la población a la calidad y disponibilidad del hábitat, y las interacciones ecológicas suelen controlar la dispersión más allá de los márgenes de distribución observados (Mott, 2010).

A su vez, a lo largo del tiempo, se han ido alterando los equilibrios de los ecosistemas debido a factores antrópicos que han modificado la configuración

biogeográfica de los primates (véase el apartado 1.1.4). Por consiguiente, la razón por la que las especies habitan áreas particulares y, por lo general, no se dispersan más allá de los límites de su área de distribución, es que ésta resulta de la relación entre la historia evolutiva (dónde y por qué se originó la especie, qué barreras se interpusieron en su dispersión), las características ambientales, y un impacto creciente de las actividades del ser humano (transformación de hábitats, sobreexplotación, contaminación) (Kamilar, 2017).

1.1.4. Factores antrópicos

Los primates son parte importante de la biodiversidad tropical, y contribuyen al mantenimiento de ecosistemas saludables (Estrada *et al.*, 2022). Algunas actividades humanas explican que algunas especies de primates estén en peligro de extinción (Estrada *et al.*, 2017). La IUCN considera que las principales amenazas son la pérdida de hábitat causada por la agricultura (76%), la tala y extracción de madera (60%) y la ganadería (31%), así como la pérdida directa por caza y captura (60%) (Estrada *et al.*, 2017). La pérdida y fragmentación de hábitats es la amenaza más grave porque reduce la cantidad total de superficie disponible para una especie (Wich & Marshall, 2016).

Una de sus principales causas es la conversión en tierras agrícolas (Gibbs *et al.*, 2010). Durante las décadas de 1980 y 1990, más del 55% de nuevas tierras agrícolas provinieron de bosques intactos en los trópicos (Gibbs *et al.*, 2010). La mayoría de las especies de primates disminuyen el tamaño de su población o desaparecen una vez que se deforesta su hábitat. Así ocurrió en Costa de Marfil, donde el aumento en más del 50% de la población humana pudo ser la causa de una disminución alarmante de la población de chimpancés, presumiblemente a través del aumento del furtivismo y de la tasa de deforestación (Campbell *et al.*, 2008).

A su vez, la caza comercial de carne de animales silvestres ha aumentado en relación con la caza de subsistencia en muchas partes del mundo, debido al crecimiento de la población humana y al aumento de su poder adquisitivo (Estrada *et al.*, 2017). Ésta se ha convertido en una de las principales fuerzas impulsoras de la disminución de la población de primates, especialmente en África y el sudeste asiático (Meijaard *et al.*, 2011). La caza se produce tanto dentro de los bosques, cuando las personas cazan primates para su propio consumo o para el comercio, como en el límite entre los bosques y las tierras agrícolas, cuando los primates buscan alimentos en los cultivos (Fa & Brown, 2009; Meijaard *et al.*, 2011). También se captura a los primates a menudo para el comercio de animales de compañía, lo cual conlleva la frecuente matanza de las madres (Nijman *et al.*, 2011). Otras causas de la pérdida, fragmentación y degradación de los hábitats de estas y otras especies son la extracción de madera, el desarrollo de infraestructuras y los incendios (Silveira *et al.*, 2016; Geist & Lambin, 2022).

Aunque los efectos de la pérdida, fragmentación y degradación del hábitat sobre los primates están mediados por variaciones en los rasgos específicos de la especie (rareza, niveles tróficos, modo de dispersión, biología reproductiva, historia de vida, dieta y comportamiento de distribución), la respuesta común entre los taxones es la disminución de la población (Estrada *et al.*, 2017). Teniendo en cuenta todas las amenazas que afectan a los ecosistemas donde habitan los primates, es necesario aumentar los esfuerzos para su conservación.

1.2. Conservación de los primates

Más allá del derecho intrínseco a existir de las especies, es posible encontrar razones "utilitarias" para esforzarse en la conservación de los primates, pues desempeñan funciones fundamentales como proveedores de servicios ecosistémicos. Proporcionan servicios de polinización en algunos ecosistemas (Marshall & Wich, 2016), son ampliamente reconocidos como dispersores de semillas, influyen en la estructura de la comunidad en múltiples niveles tróficos, y

pueden desempeñar un papel de amortiguación de los efectos perjudiciales del cambio climático global. Como dispersores de semillas, se reconoce su importancia para las especies de plantas con semillas de gran tamaño (Howe, 1986). Precisamente, las especies de árboles con semillas grandes suelen tener una mayor densidad de carbono que los árboles con semillas pequeñas (Queenborough *et al.*, 2009), de ahí que la presencia de primates promueva el secuestro de carbono adicional en los bosques tropicales, sirviendo como amortiguadores clave contra el cambio climático global (van der Werf *et al.*, 2009). De hecho, la evolución de los primates está estrechamente ligada al uso de los bosques tropicales.

Sin embargo, el 60% de las especies de primates está amenazado de extinción, es decir, clasificado como "En Peligro Crítico", "En Peligro" o "Vulnerable" por la Lista Roja IUCN, y esto afecta a las 16 familias existentes. Por esta razón, es urgente desarrollar conocimiento científico que permita aplicar medidas que garanticen la conservación de los primates a largo plazo y de sus hábitats (Cowlishaw & Dunbar, 2000).

La conservación de los primates requiere hacer un mayor esfuerzo en la creación de nuevas áreas protegidas, y en mejorar el cumplimiento de las medidas de protección que rigen las áreas protegidas actuales para salvaguardar los hábitats preferidos, reducir la fragmentación del hábitat y prevenir la caza y recolección ilegal de primates. Existe evidencia de que garantizar la aplicación de medidas de conservación en las áreas protegidas es más efectivo que la mayoría de las otras iniciativas (Junker *et al.*, 2020). Sin embargo, es necesario reconocer que muchas áreas protegidas son esencialmente "parques de papel", sin una aplicación efectiva de la normativa, y además muchas poblaciones de primates se encuentran fuera de las áreas protegidas (Murai *et al.*, 2013; Hoskins *et al.*, 2020). Es importante resaltar también un factor sustancial y que no se suele tener en cuenta para la conservación de la biodiversidad, que es respetar a los pueblos indígenas por su conocimiento del medio y considerarlos como poseedores de

información esencial para salvarguardar la biodiversidad. El conocimiento ecológico indígena (TEK, del inglés *Traditional Ecological Knowledge*) puede contribuir a conservar los ecosistemas locales, regionales y globales, ofreciendo una gran oportunidad para prevenir la extinción de primates (Berkes *et al.*, 2000; Omotayo & Musa, 2008; Olivero *et al.*, 2016a; Estrada *et al.*, 2022).

Existen herramientas para monitorear los hábitats de los primates, el estado de la población y las amenazas antropogénicas. Éstas involucran los sistemas de telecomunicaciones globales e Internet inalámbrico, softwares, imágenes satelitales y aéreas, tecnología de drones, dispositivos portátiles cada vez más potentes y cámaras trampa (Estrada *et al.*, 2017). En combinación con los sistemas de información geográfica y los estudios sobre el terreno, parte de esta tecnología ha sido utilizada con el fin de realizar una planificación espacial sostenible del uso de la tierra y de los conflictos entre humanos y primates (Estrada *et al.*, 2017).

1.3. Zoonosis en primates

1.3.1. ¿Qué es "zoonosis"?

El término "zoonosis" deriva de dos vocablos griegos: *zoon*, o "animal", y *nosos*, o "enfermedad". Fue acuñado a finales del siglo XIX por Rudolph Virchow (Virchow, 1855). Desde entonces, la literatura científica ha propuesto términos como "antropozoonosis" para definir a las enfermedades transmitidas de animales a humanos, y "zooantroponosis" para definir a las enfermedades transmitidas de los seres humanos a otros animales (Chomel, 2009). Desafortunadamente, muchos científicos han utilizado estos términos en sentido inverso o indiscriminadamente, lo que condujo a que un comité de expertos conformado por la Organización Mundial de la Salud (OMS) y la Organización de las Naciones Unidas para la Alimentación y la Agricultura (FAO) recomendase, a mediados del s. XX, evitar confusiones evitando el uso de estos dos términos (WHO & FAO, 1959). En cambio, se recomendó definir "zoonosis" como "enfermedades e

infecciones que se transmiten, en forma natural, entre animales vertebrados y el ser humano". Sin embargo, el término "zoonosis" generalmente se refiere a una enfermedad que se transmite de animales a humanos (antropozoonosis).

En *The Tripartite Zoonoses Guide*, la FAO, la OMSA (Organización Mundial de Sanidad animal) y la OMS definen como zoonosis a las enfermedades que pueden ser propagadas entre animales y humanos a través de los alimentos, el agua, especies que actúan como vectores, y materias inertes que también contribuyen a la transmisión (denominadas "fómites"). En esta tesis se ha considerado el término *zoonosis* teniendo en cuenta esta última definición. Además, se han considerado también los términos "antroponótico", cuando la fuente es un ser humano infeccioso y la transmisión interhumana es típica, y "zoonótico" cuando la fuente es un animal infeccioso y la transferencia interhumana es poco común (Hubálek, 2003).

1.3.2. Implicación de primates y mosquitos en las zoonosis

De las enfermedades infecciosas, un 61% son enfermedades zoonóticas, transmitidos directa o indirectamente a partir de animales (Taylor *et al.*, 2001). Debido a la estrecha relación genética que existe entre los primates no humanos y los humanos, los organismos que causan enfermedades se intercambian fácilmente entre ellos. Los primates no humanos ocupan un lugar importante en los ciclos de estas enfermedades, pudiendo participar como reservorios o amplificadores de agentes de enfermedad, o "patógenos". Estos últimos pueden ser virus, bacterias, hongos y protozoos (Nunn & Altizer, 2006). Los patógenos se pueden transmitir a través de vectores (frecuentemente artrópodos), rasguños, mordeduras, ingestión, etc. (Virginia Department of Health, 2011).

En las últimas décadas se ha demostrado una relación significativa entre la aparición de enfermedades zoonóticas emergentes y la ocupación de los bosques tropicales por parte del ser humano (Wolfe *et al.*, 2005; Wallace *et al.*, 2014; Castro

et al., 2019). Los seres humanos pueden exponerse a la infección mediante la invasión de los bosques a través de la caza, o bien de la deforestación con fines agrícolas o de urbanización (Olivero *et al.*, 2017a). Este aumento de contacto entre los seres humanos y la fauna silvestre se puede ver intensificado debido a la alta densidad de los bordes de los bosques fragmentados (Bloomfield *et al.*, 2020; Olivero, 2021). Además, la pérdida de bosques interrumpe los movimientos de los animales y las densidades locales y, por lo tanto, influye en sus interacciones y en el potencial de que un patógeno se transmita entre individuos y entre especies (Olivero *et al.*, 2017b). Como sucedió en EE.UU., como consecuencia de la destrucción y fragmentación de bosques se redujo la diversidad de especies de mamíferos y se elevó la densidad de población de ratones de patas blancas (*Peromyscus leucopus*), siendo éste el principal reservorio natural de la bacteria que transmite la enfermedad de Lyme, *Borrelia burgdorferi*. Se incrementó de esta forma la probabilidad de que las garrapatas, vectores de esta enfermedad, que se alimentan de estos ratones, se infectasen con la bacteria. Cuanto más pequeños eran los parches de bosques, aumentaba dramáticamente la densidad de ninfas infectadas y, por lo tanto, el riesgo de transmisión de la enfermedad de Lyme. Por lo tanto, la fragmentación del hábitat puede influir en la composición de la comunidad de huéspedes vertebrados de vectores portadores de enfermedades y en la salud humana (Allan *et al.*, 2003).

Los primates ocupan un lugar importante en los "derrames zoonóticos" (*zoonotic spillovers*) (Vasilakis *et al.*, 2011; Narat *et al.*, 2018), es decir, el ciclo de transmisión selvática se ha "derramado" en un ciclo de transmisión urbano, en ocasiones a través de mosquitos vectores. Una vez en los entornos urbanos, las infecciones contraídas en el bosque se pueden propagar rápidamente a través de vectores propios de este medio (Valentine *et al.*, 2019). Esto sucede en el caso del virus de la fiebre amarilla, cuyas infecciones en primates preceden y conducen a brotes en las personas. Algunos arbovirus (es decir, virus transmitidos por mosquitos), como

el dengue, el chikungunya y el zika, se han adaptado completa o parcialmente a los ciclos humanos. Sin embargo, los ciclos selváticos podrían seguir estando implicados en las infecciones en los humanos (Valentine *et al.*, 2019), como ocurre con el dengue en África y en Asia. En este caso, los primates actuarían como reservorios animales, pues suelen cursar la infección de forma asintomática (Holmes & Twiddy, 2003). Además, los ciclos selváticos favorecen la dinámica evolutiva de los virus como por ejemplo, ocurrió en Sudamérica donde un linaje moderno causó brotes de fiebre amarilla en regiones no endémicas (Mir *et al.*, 2017). El papel de los vectores es fundamental en estos derrames zoonóticos, ya que sin la presencia de ellos no sería posible la transmisión de estas enfermedades.

Según la OMS, las enfermedades que son transmitidas por vectores son de importancia para la salud pública a nivel global pues representan una alta carga de morbilidad y mortalidad para los seres humanos, así como altos costes y sobrecargas de los sistemas de salud (PAHO, 2022). La morbilidad y mortalidad que infligen es más alta en las áreas tropicales y subtropicales (Chala & Hamde, 2021). En América, una de cada dos personas está en riesgo a causa de enfermedades transmitidas por vectores, por ejemplo el dengue, la malaria, la fiebre amarilla, el chikungunya y la enfermedad de changas (PAHO, 2014). A escala mundial, se ha señalado que las enfermedades infecciosas transmitidas por vectores representan el 17% de todas las enfermedades infecciosas y que causan más de 700.000 muertes al año (WHO, 2020b). Sus distribuciones son dinámicas y su propagación aumenta a lo largo del tiempo debido a diversos factores, por ejemplo: (1) la globalización, que a través de viajeros han transportado el virus con facilidad y a la rápida expansión de vectores; y (2) el cambio climático, que posiblemente afectará a largo plazo la geografía de la salud humana (véase el apartado 1.3.3).

La globalización ha permitido que especies como *Aedes albopictus* se hayan extendido por todo el mundo en los últimos 50 años (Ebi & Nealon, 2016). Su expansión mundial, junto con la de *Ae. aegypti*, ha hecho que la población susceptible a infección de muchas enfermedades haya aumentado considerablemente. Esto ha hecho posible que los patógenos asociados a los mosquitos del género *Aedes*, como el virus de la fiebre amarilla, el virus del dengue, el virus del zika y el virus de la chikunyunga, que tienen orígenes selváticos, se hayan expandido al viejo mundo y a otros continentes (Gould *et al.*, 2017). Aunque el transporte internacional ha jugado un papel muy importante en la dispersón de *Ae. aegypti* y sus arbovirus asociados, un factor más, muy relevante para la emergencia global de estos patógenos, es la adaptación del vector a ambientes urbanos. Esta especie, en concreto, ha adoptado preferencia por alimentarse de sangre humana (Gould *et al.*, 2017).

1.3.3. Efecto del cambio climático en la salud humana

El cambio climático es un "multiplicador de amenazas" para el medioambiente, una amenaza para la salud humana y un factor de deterioro de la biodiversidad (WHO Regional Office for Europe, 2022). Las actividades humanas están impulsando la tendencia al calentamiento global desde mediados del siglo XX (IPCC, 2014). El cambio climático y el aumento de las temperaturas provocan la propagación de huéspedes y vectores, lo que aumenta la población humana expuesta a enfermedades transmitidas por vectores como el dengue, la fiebre amarilla, el chikungunya, el zika y la encefalitis japonesa (WHO, 2022). El aumento de las temperaturas estimula aún más la tasa de reproducción tanto de los patógenos como de los vectores (WHO, 2022). Como sucedió en las tierras altas de África, entre 1950 y 2002, el aumento de las temperaturas coincidió con el aumento de la incidencia de la malaria, probablemente debido al aumento de las poblaciones de mosquitos (WHO Regional Office for Europe, 2022). Los periodos de incubación de los patógenos disminuyen y sus tasas de replicación aumentan

con las temperaturas elevadas, ampliando la carga de patógenos en los vectores. Por ejemplo, en un experimento en laboratorio, la tasa de replicación del virus del dengue en los mosquitos *Aedes aegypti* aumentó directamente con la temperatura (Mills *et al.*, 2010).

El aumento de las temperaturas impulsa la expansión del área de distribución de los vectores de enfermedades (como pulgas, garrapatas, pulgones y mosquitos) y de los huéspedes zoonóticos al facilitar la supervivencia en latitudes y altitudes más altas (como en el caso del mosquito *Ae. albopictus*) (Patz & Hahn, 2012). Varias enfermedades tropicales desatendidas, es decir, enfermedades infecciosas que afectan principalmente a las poblaciones más pobres y con un limitado acceso a los servicios de salud (PAHO, 2011), como por ejemplo, el dengue y la chikungunya, se encuentran ahora en latitudes más altas (WHO, 2021a).

El cambio climático también aumenta la tasa de fenómenos meteorológicos extremos y de catástrofes meteorológicas, como las inundaciones y los incendios. Estas catástrofes meteorológicas destruyen los hábitats naturales creando una amenaza para la biodiversidad, que es importante para el control de las zoonosis (WHO Regional Office for Europe, 2022). Las temperaturas extremas y la sequía provocan estrés en la fauna y flora silvestres y deterioran la respuesta inmunitaria, lo que aumenta la diseminación de patógenos zoonóticos (Acevedo-Whitehouse & Duffus, 2009). Por lo tanto, el cambio climático podría afectar negativamente a los seres humanos, si bien ya las oscilaciones meteorológicas a corto plazo influyen en el riesgo de enfermedades, el cambio climático a largo plazo, seguramente tendrá graves efectos en la salud humana (Olivero, 2021).

1.3.4. Aplicación de herramientas biogeográficas

La mayoría de los patógenos se transmiten interaccionando con vectores, reservorios y hospedadores. Esto hace que los enfoques biogeográficos para analizar los ciclos de transmisión de estos patógenos sean complejos (Olivero,

2021). Muchos estudios han destacado la necesidad de mejorar los métodos y los enfoques conceptuales para la cartografía de las enfermedades (Kraemer *et al.*, 2016). La iniciativa internacional "One Health" (Gibbs, 2004) fomenta el estudio de las enfermedades zoonóticas a través del análisis de las interconexiones entre animales, ecosistemas y salud humana. Por ello, los estudios biogeográficos sobre patógenos deben ser multidisciplinares, que requieren métodos y conceptos de diversos campos del conocimiento (Ramette & Tiedje, 2007).

El incremento en el interés de las enfermedades infecciosas (Peterson, 2008; Stephens *et al.*, 2016; Murray *et al.*, 2018) ha definido la especialización de una rama biogeográfica denominada patogeografía (Murray *et al.*, 2018). La patogeografía permite que los modelos de distribución puedan captar la complejidad de la transmisión de enfermedades considerando los procesos detrás de los patrones correlacionales (Peterson, 2015). Los modelos han descuidado a menudo la contribución potencial de las distribuciones animales como predictores explícitos del riesgo de enfermedad, asumiendo que está representada por correlaciones con el clima y otras variables (Olivero, 2021). Sin embargo, los biogeógrafos que estudian la cartografía de enfermedades han empezado a incluir reservorios y/o vectores como factores de predicción en los modelos de distribución (por ejemplo, Messina *et al.*, 2014a; Pigott *et al.*, 2014; Olivero *et al.*, 2017a; Aliaga-Samanez *et al.*, 2021, 2022).

CAPÍTULO 2

Objetivos de la Tesis Doctoral

Aims of the Doctoral Thesis

2. Objetivos de la Tesis Doctoral

El objetivo general de esta tesis doctoral es desarrollar aspectos aplicados de la dinámica biogeográfica de los primates.

Los objetivos específicos son los siguientes:

- Comparar diversas técnicas para la integración de barreras geográficas en los modelos de distribución para diferentes especies de primates y diferentes contextos geográficos.

- Generar mapas de riesgo, en el contexto de un área protegida en África Central en la que los vigilantes colaboran en la recopilación de información, con el fin de mostrar dónde es más probable que la fauna se vea afectada por amenazas antropogénicas.

- Generar mapas de riesgo de transmisión del dengue y de la fiebre amarilla a nivel global.

- Analizar dónde podría amplificarse el riesgo de infecciones de dengue y de fiebre amarilla en humanos por la contribución de los ciclos enzoóticos basados en ensamblajes de primates y de mosquitos vectores selváticos.

- Contribuir al sistema de salud internacional con pronósticos confiables sobre áreas donde la transmisión del dengue y fiebre amarilla entre humanos podría aumentar en un futuro cercano, aportando diferentes escenarios geográficos para que focalizar las estrategias de vigilancia.

- Analizar cómo el cambio en las condiciones climáticas podría alterar la distribución de las áreas favorables para las especies de vectores urbanas y selváticas.

- Analizar la incertidumbre en las proyecciones de futuro para detectar las zonas con predicciones más fiables.

2. Aims of the Doctoral Thesis

The general objective of this doctoral thesis is to develop applied aspects of primate biogeographic dynamics.

The specific objectives are as follows:

- To compare several techniques for integrating geographical barriers into distribution models for different primate species and different geographical contexts.

- To generate risk maps, in the context of a protected area in Central Africa where rangers collaborate in the collection of information, in order to show where wildlife is most likely to be affected by anthropogenic threats.

- To generate global dengue and yellow fever transmission risk maps.

- To analyse where the risk of dengue and yellow fever infections in humans could be amplified by the contribution of enzootic cycles based on primate assemblages and sylvatic mosquito vectors.

- To contribute to the international health system with reliable forecasts of areas where transmission between humans of dengue and yellow fever may increase in the near future, providing different geographical scenarios to focus surveillance strategies.

- To analyse how changing climatic conditions could alter the distribution of favourable areas for urban and sylvatic vector species.

- To analyse uncertainty in future projections to detect areas with more reliable predictions.

CAPÍTULO 3

Material y métodos generales

3. Material y métodos generales

En biogeografía, la modelación de la distribución de especies es una herramienta que facilita la comprensión de las relaciones entre las especies y su entorno. La Función de la Favorabilidad ha sido empleada para comprender en profundidad varios aspectos relacionados con la biogeografía de los primates. En el **capítulo 4** se ha utilizado para analizar el papel de las barreras geográficas (por tanto, de factores biogeográficos históricos), representadas por ríos, sobre la distribución de cuatro especies de primates en Suramérica y en África; en el **capítulo 5**, para generar mapas de riesgo con el fin de resaltar las áreas más vulnerables para especies de interés, como el chimpancé, el gorila y el elefante, dentro y en el entorno de la Reserva de Dja, en Camerún.

En los capítulos posteriores se ha utilizado modelación para analizar el riesgo global de transmisión del virus causante del dengue y de la fiebre amarilla, que tienen ciclos de transmisión complejos donde participan agentes como los mosquitos urbanos y selváticos, actuando como vectores; y los primates, como hospedadores y posibles reservorios de estos virus en los bosques tropicales. En concreto, en el **capítulo 6**, se ha analizado mediante modelación los cambios geográficos experimentados en el riesgo de transmisión del dengue desde finales del siglo XX y también se ha mapeado las áreas donde los ciclos zoonóticos (que involucran a primates y mosquitos selváticos) podrían estar favoreciendo la transmisión a humanos. En el **capítulo 7** se ha abordado el mismo objetivo que en el capítulo 6, si bien orientado al riesgo de transmisión de la fiebre amarilla. En estos dos últimos capítulos se ha incluido información zoogeográfica en el conjunto de variables predictoras sobre las que se construyen los modelos. Esta información ha sido definida por los tipos de distribución (es decir, los corotipos) que presentan los primates no humanos. Finalmente, en el **capítulo 8**, se han proyectado los modelos sobre mosquitos realizados en los capítulos 6 y 7 para

evaluar el efecto del cambio climático en la distribución de estas especies, que son transmisoras de dengue y de fiebre amarilla.

En el presente capítulo metodológico se detallan las herramientas metodológicas que tienen todos los capítulos en común. Concretamente, se describe la Función de Favorabilidad, en la que se basa el método de modelación utilizado; los controles previos sobre los datos que se han realizado antes de la modelación; así como los índices con los que se ha evaluado la capacidad descriptiva y la capacidad predictiva de los modelos de distribución.

3.1. Controles previos

Se ha controlado la multicolinearidad en los modelos, calculando una matriz de coeficientes de correlación de Spearman entre las variables predictoras o independientes propuestas para formar parte del modelo. El objetivo ha sido evitar la posible entrada de variables redundantes en un modelo, por estar altamente correlacionadas entre sí ($R > 0,8$). Cuando la correlación entre dos variables ha sido mayor que 0,95, se ha eliminado del análisis la variable menos significativa, de acuerdo con el estadístico de puntuación de Rao (Radhakrishna Rao, 1948). Si la correlación entre dos variables se encuentra entre 0,8 y 0,95, sólo se ha eliminado una de ellas cuando ambas han sido seleccionadas por el modelo. Las variables ingresan a la ecuación por selección por pasos, de manera que la primera variable que entra es la que explica la mayor proporción de la variación observada en la variable dependiente, la segunda variable explica la mayor proporción de la variación residual (es decir, la variación no explicada por la primera variable), y así sucesivamente. Además, el método hacia adelante y hacia atrás utilizado permite que variables ya incorporadas al modelo salgan de éste si su correlación con una nueva es excesiva (se dan detalles de este procedimiento más adelante). Por ello, incluso si no se llevase a cabo un control previo de

multicolinearidad, el modelo final suele evitar la entrada de variables muy correlacionadas.

El error de tipo I, potencialmente derivado del uso de un gran número de variables predictoras (Muñoz & Real, 2013), se ha controlado utilizando la tasa de falso descubrimiento (FDR) de Benjamini & Hochber (1995). Cometer error de tipo I significa admitir una hipótesis como verdadera siendo falsa; y en este caso concreto, es aceptar que una variable tiene poder explicativo sobre la distribución de la especie cuando su relación espacial con ella podría ser fruto del azar. Para utilizar la FDR, se ha obtenido el grado de significación entre la presencia de la especie y cada una de las variables predictoras de acuerdo con el estadístico de puntuación de Rao con el software IBM SPSS Statistics 25. Las variables se han ordenado en forma creciente de acuerdo con su grado de significación. Con la aplicación de la FDR, sólo se aceptan las variables en las que $p < i \times q/V$ (Benjamini & Hochberg, 1995), donde p es el grado de significación de la prueba de puntuación, i es la posición de la variable en el orden indicado, q la significación umbral de la FDR (se ha tomado $q = 0{,}05$), y V el número total de variables consideradas. El resto de las variables han sido excluidas antes de construir el modelo de distribución.

3.2. Función de Favorabilidad y lógica difusa

La definición de los modelos de distribución se ha realizado utilizando la Función de Favorabilidad (F) (Real *et al.*, 2006; Acevedo & Real, 2012):

$$F = \frac{\frac{P}{1-P}}{\frac{n_1}{n_0} + \frac{P}{1-P}}$$

donde P es la probabilidad de que la especie analizada esté presente, y n_1 y n_0 son el número de presencias observadas y el número de ausencias, respectivamente. Los valores de P se calcularon a través de una regresión logística

por pasos hacia adelante y hacia atrás (utilizando IBM SPSS Statistics 23), en la que las variables predictoras se seleccionaron, en pasos sucesivos, de acuerdo con las pruebas de puntuación de Rao (Radhakrishna Rao, 1948); mientras que las variables que ya están en el modelo pueden salir de éste de acuerdo con la significación de su coeficiente a través de la prueba de Wald. En la regression logística, *P* se formula según la siguiente ecuación:

$$P = \frac{e^y}{1 + e^y}$$

donde *e* es la base de los logaritmos neperianos, e *y* es la "ecuación *logit*", es decir, una combinación lineal de las variables predictoras seleccionadas. La favorabilidad *(F*, cuyos valores se mueven en el rango entre 0 y 1) también puede expresarse mediante esta otra ecuación:

$$F = \frac{e^y}{\left(\frac{n_1}{n_0}\right) + e^y}$$

Esta formulación es la que se ha utilizado para proyectar los modelos, procedimiento que se ha realizado para trasladar los valores de favorabilidad a una red de unidades geográficas con resolución mayor a la utilizada para realizar el modelo (es decir, un "downscaling"); y también para estimar los valores de favorabilidad en escenarios futuros de cambio climático. Para ello, se ha aplicado la fórmula sustituyendo en la ecuación logit (*y*) los valores de las variables predictoras por otros correspondiente a la nueva situación.

Los resultados de los modelos, por tanto, se han expresado como valores de favorabilidad. Estos valores representan el grado en que las condiciones ambientales, en una unidad espacial determinada, favorecen la ocurrencia de un evento dado. Así, los valores de favorabilidad pueden describirse como el grado de pertenencia de diferentes localidades al conjunto difuso de lugares con condiciones favorables para la especie (Real *et al.*, 2006). Por esta razón, los

modelos basados en la favorabilidad pueden compararse y combinarse mediante la aplicación de herramientas de la teoría de conjuntos difusos (Zadeh, 1965; Barbosa & Real, 2012). La condición necesaria para que esto sea posible es que el resultado de los modelos esté expresado en unidades conmensurables, es decir, que un mismo valor tenga el mismo significado en los diferentes modelos que se pretende comparar o combinar. La favorabilidad cumple con esta condición pues, a diferencia de la probabilidad, es independiente de la prevalencia. Es decir, en un modelo de probabilidad como el que resultaría de la aplicación de una regresión logística, el valor de *P* depende, por una parte, de las condiciones ambientales definidas por las variables incluidas en el modelo; y, por otra parte, de la proporción de unidades geográficas ocupadas por las presencias (es decir, de la prevalencia). Por esta razón, los valores de probabilidad basados en distribuciones con distintas prevalencias no son conmensurables entre sí. En cambio, la favorabilidad anula el efecto de la prevalencia, dependiendo sólo del grado en que las condiciones ambientales de un lugar son favorables a la presencia de la especie analizada (Acevedo & Real, 2012). Otros métodos de calidad reconocida y ampliamente utilizados, como el modelado de máxima entropía (MaxEnt, Phillips *et al.*, 2006), ofrecen como resultado de sus análisis valores de idoneidad o, en inglés, *suitability*. No hay, sin embargo, demostración de que los valores de idoneidad obtenidos en diferentes modelos sean conmensurables (Acevedo & Real, 2012).

La necesidad de utilizar la Función de Favorabilidad en esta tesis, en todos los capítulos, se justifica porque en ellos se combinan modelos a través de operaciones de lógica difusa. Por una parte, la intersección difusa, que consiste en seleccionar, para cada unidad espacial, el valor más bajo de favorabilidad de entre los modelos que se combinan; por otra, la unión difusa, que consiste en seleccionar, para cada unidad geográfica, el valor más alto de favorabilidad (Zadeh, 1965; Kosko, 1986). Por ello, un valor alto de favorabilidad en la

intersección difusa entre dos modelos requiere que ambos modelos señalen una favorabilidad alta; mientras que un valor alto derivado de la unión difusa se obtiene con que al menos uno de ellos apunte en ese sentido. En los capítulos siguientes se justifica el uso de estas operaciones, atendiendo a la finalidad con la que se apliquen.

3.3. Evaluación, comparación y validación de modelos

Se han utilizado seis índices para evaluar la capacidad de clasificación de los modelos (Fielding & Bell, 1997; Barbosa *et al.*, 2013): (1) sensibilidad (es decir, proporción de presencias clasificadas en unidades geográficas favorables), (2) especificidad (es decir, proporción de ausencias clasificadas en unidades desfavorables), (3) tasa de clasificación correcta (TCC, en ingles *CCR* de *Correct Classification Rate*, que cuantifica la proporción del total de unidades en la que las presencias y ausencias han sido clasificadas en unidades favorables y desfavorables, respectivamente), (4) estadística de habilidad verdadera (en inglés *TSS* de *True Skill Statistic*, que se obtiene de la sensibilidad + especificidad - 1), (5) Kappa de Cohen (que computa entre -1 y +1 la capacidad de clasificación compensada por la probabilidad de clasificaciones aleatorias correctas), (6) tasa de infrapredicción (es decir, proporción de áreas desfavorables que registran presencia) y (7) tasa de sobrepredicción (es decir, proporción de zonas favorables que no registran presencia).

La capacidad de discriminación se ha evaluado mediante el área bajo la curva (AUC, del inglés *Area Under the Curve*), haciendo referencia a la curva denominada "característica operativa del receptor" (ROC, del inglés *Receiver Operative Caracteristic*) (Lobo *et al.*, 2008). Además, se ha utilizado el criterio de información Akaike (índice de AIC, Akaike *et al.*, 1973) para comparar los modelos según el criterio de parsimonia en el capítulo 4.

Cuando la evaluación se ha referido a los datos presencia y ausencia de la especie utilizados para construir el modelo, el objeto de la misma ha sido la capacidad de descripción del modelo. En cambio, se ha evaluado la capacidad predictiva de un modelo utilizando información de presencia y ausencia no empleada para su definición. Esto

último se ha aplicado en los capítulos 6 y 7, de forma que las presencias y ausencias consideradas han correspondido a periodos temporales diferentes del contexto temporal del modelo (específicamente, periodos inmediatamente posteriores). Se dan detalles al respecto en los respectivos capítulos.

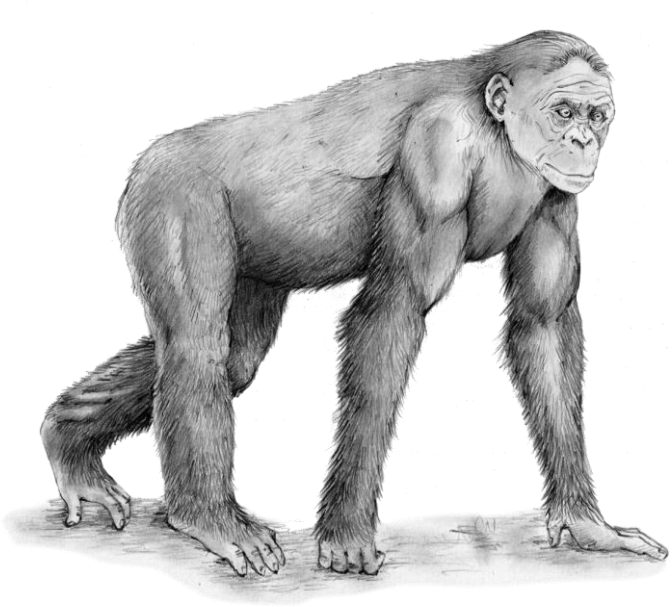

CAPÍTULO 4

Modelling species distributions limited by geographic barriers:

a case study with African and American primates

Modelación de la distribución de las especies limitadas por barreras geográficas:

un caso de estudio con primates africanos y americanos

Este capítulo se basa en/ This chapter is based on:

Aliaga-Samanez, A., Real, R., Vermeer, J., & Olivero, J. (2020). Modelling species distributions limited by geographical barriers: A case study with African and American primates. Global ecology and biogeography, 29(3), 444-453. https://doi.org/10.1111/geb.13041 **(Q1)**.

4 Modelling species distributions limited by geographic barriers: a case study with African and American primates

4.1. Abstract

The boundaries of species distributions are often shaped by natural barriers, such as mountains and rivers, but species distribution models usually fail to include these constraints. We tested several approaches that include barriers as explanatory variables in species distribution models. We modelled the ranges of pairs of primate species separated by a river in Africa and South America taking into account three explanatory components: the environment (ecosystems, topo-hydrography, climate, human pressure), the spatial structure shaped by history and population dynamics (using a trend-surface approach), and rivers as naturals barriers to dispersal (using a binary *cis-trans* variable that describes both sides of the river). To assess how the addition of a spatial structure and the barrier could improve distribution models, we used a nested approach by comparing models based on: a) the environment; b) the environment and the spatial structure; and c) the environment, the spatial structure and the river. These models were constructed using the favourability functions. There was a decreased occurrence of high-favourability values in the opposite side of the rivers in models that included the spatial structure of distributions, compared to models based on environment alone. This decrease was more marked when the description of the spatial structure was made more flexible. However, model performance was significantly improved by the inclusion of *cis-trans* variables that identified areas on the opposite side as totally unfavourable. The performance of distribution models can improve by the use of approaches that describe barriers. Although adding the location of geographic units in relation to a river appears to be the most accurate way to define the presence of a barrier, defining this variable may

be challenging. A suitable alternative is to analyse the spatial structure of distributions using a flexible approach.

4.2. Introduction

The spatial distribution of species can be influenced by multiple factors, such as environmental conditions, which may favour or hinder the presence of a species (Lomolino *et al.*, 2006). Other factors, which are typically difficult to quantify, can maintain the spatial structure of a distribution. Rapoport (1975) suggested that in the absence of anisotropic factors species tend to take the simplest form of maximum entropy possible, which would correspond to a circle. Nevertheless, the spatial structure of a distribution is also due to the effect of species' biogeographic history (e.g., continental drifts, past glaciations, evolutionary history), the spatial pattern of the habitat, and the species population dynamics (Legendre & Legendre, 1998). In turn, these factors may be affected by natural barriers to dispersal. Barriers are physical and biological factors that hinder species dispersal and specifically affect population dynamics (Cozzi *et al.*, 2013). Relevant physical barriers may include geographical and topographical accidents, and biological barriers may include interspecific competition and changes in both vegetation and trophic habitat (Rapoport, 1975). In most cases, geographic barriers isolate entire areas along with all the species that inhabit them, thereby facilitating vicariance events that, in turn, involve speciation (Peterson & Cohoon, 1999; Whitaker *et al.*, 2003). In other cases, barriers can be partially permeable (Cozzi *et al.*, 2013).

In modern biogeography, distribution modelling is a relevant tool that brings us closer to understanding the origins of species ranges and the factors that contribute to their current shapes (Braby *et al.*, 2014). Models have also been used to assess biogeographic relationships between taxa (e.g., Márquez *et al.*, 2004; Real *et al.*, 2009; Acevedo *et al.*, 2010; Acevedo & Real, 2012; Mpakairi *et al.*, 2017; Wilkinson *et al.*, 2018; Tobler *et al.*, 2019), to assess risk (e.g., Olivero *et al.*, 2017b; Farfán *et al.*, 2019), and to assist conservation efforts (e.g., Estrada *et al.*, 2008a; Fa *et al.*, 2014). It has been shown that the spatial factor must be warranted in species distribution models when ecological or evolutionary processes prevent

taxa from shifting their distributions (Record *et al.*, 2013). Thus, both environmental and purely spatial factors must be taken into account when a model is used to represent the factors influencing species distribution. These factors can be readily measured using predictor variables (Legendre, 1993; Márquez *et al.*, 2011; Romero *et al.*, 2016). Nevertheless, the issue of how to include natural barriers in distribution modelling remains to be addressed.

Alfred Russel Wallace was the first person to hypothesize that rivers are effective barriers to the distribution of primates (Wallace, 1852). This hypothesis has been confirmed in specific cases in South America (Ayres & Clutton-Brock, 1992) and in Africa (Harcourt & Wood, 2012).

In the present study, we analysed several approaches to the integration of barriers as explanatory variables in distribution models. We used two case studies, one conducted in Central Africa and the other in Peru. Both case studies addressed pairs of parapatric and congeneric primate species separated by a river. In Africa, the common chimpanzee (*Pan troglodytes* Blumenbach, 1775) and the bonobo (*Pan paniscus* Schwarz, 1929) are separated by the Congo River (Takemoto *et al.*, 2015). In Peru, the San Martin titi monkey (*Plecturocebus oenanthe* Thomas, 1924) and the red-crowned titi monkey (*Plecturocebus discolor* I. Geoffroy Saint-Hilaire & Deville, 1848) are partly separated by the Huallaga river. These rivers do not involve any relevant changes in environmental factors, but they can be efficient barriers to dispersal.

The specific objectives of this study were to address the following questions.

1) Can a model of the spatial structure of a distribution alone reflect the biogeographic effect of a barrier?

2) Can variables specifically designed to describe barriers significantly contribute to improving model performance?

4.3. Material and Methods

4.3.1. Study area and distribution data

The African study area comprised a rectangle with limits 9.3ºN, 13.5ºS, 2.7ºW, 34.1ºE (Fig. 4.1). This area includes the Congo basin, the ranges of the Common Chimpanzee subspecies inhabiting this basin (i.e. *P. t. troglodytes*, *P. t. ellioti* and *P. t. schweinfurthii*), and the Bonobo's distribution range. The Congo Basin is one of the largest inland sedimentary basins in the world, covering 1.2 million km^2. The Congo River is the southern boundary of a large part of the Common Chimpanzee's distribution in Central Africa. It also limits the Bonobo's distribution to the north, east, and west (Pilbrow & Groves, 2013). For modelling purposes, we divided the African study area into 10 × 10-km UTM squares (n= 55,454). Data on the Common Chimpanzee's and Bonobo's presence/absence in these units were extracted by overlapping them with the IUCN Red List maps (IUCN, 2017). Hurlbert & Jetz (2007) recommended not to analyze polygon data using grids lower than 1° × 1°, at least in the case of lowly known species such as amphibians and insects. Here, we have addressed the analyses at both 1° × 1° and 10 x 10-km resolutions, then we have downscaled the 1° × 1° outputs to a 10 x 10-km resolutions, and have analyzed the correlation (Pearson's R) between the 10 x 10-km models obtained through both methodological pathways. The model initially trained with a 10 x 10-km resolution was selected if R was higher than 0.80 and statistically significant.

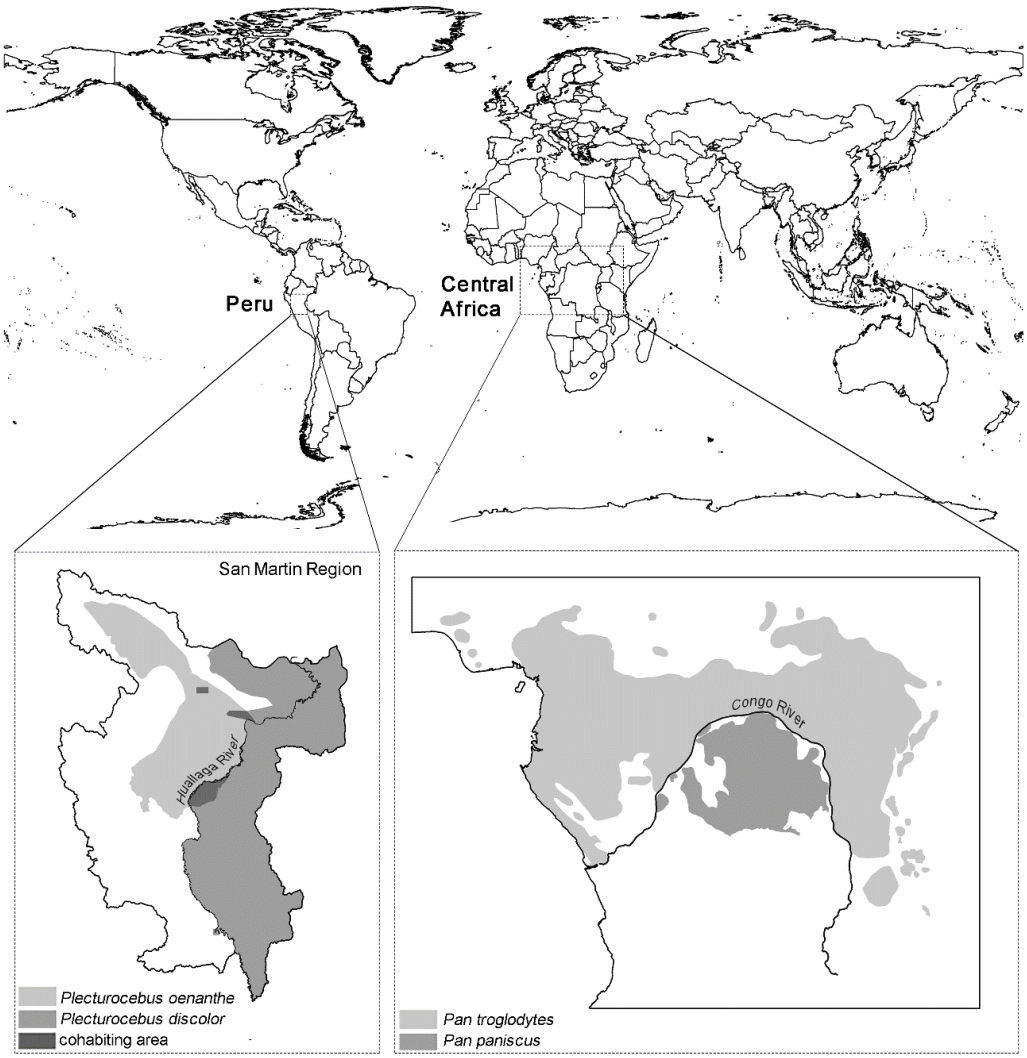

Fig. 4.1. Study area and species distributions: *Plecturocebus oenanthe* and *P. discolor* in Peru; *Pan paniscus* and *P. troglodytes* in Central Africa

The Peruvian study area comprised the San Martin region, which is located in the northern and central sector of the country on the eastern flank of the Andean range (Fig. 4.1). This region includes the San Martin Titi Monkey's entire distribution and the southern part of the Red-Crowned Titi Monkey's range. In this area, the Huallaga River delimits the distributions of both species which, unlike the African case, cohabit in small populations on the right bank of the river (Bóveda-Penalba *et al.*, 2009). This study area was divided into 5 × 5-km squares (n= 2,280). Data on the Titi Monkeys presence/absence in these units were obtained by overlapping them with presence points (see Vermeer *et al.*, 2011),

which were modified according to data provided by Proyecto Mono Tocón (http://www.monotocon.org/ and Primate of Peru, Pocket Identification Guide by Conservation International). In this case study, the distribution data are based on the most accurate information available, provided by the experts on this species. The data that support the findings of this study are openly available in Dryad Digital Repository at https://doi.org/10.5061/dryad.8pk0p2nj0.

4.3.2. Predictor variables used for distribution modelling

An environmental model (E-Model) was constructed for every species according to a set of variables that account for environmental conditions that potentially favour or limit the species' occurrence. These variables represent climate, ecosystem types, topography, hydrography, and human pressure (see variable descriptions and sources in Appendix 1). We also constructed a model in which environmental descriptors were complemented by a variable depicting the basic spatial structure of the distribution. We called this model the 0-Model (from "null model") due to its lack of specific measures for barrier identification in the description of the spatial variable. This spatial variable was constructed according to a 3rd-degree trend-surface approach as suggested by Legendre and Legendre (1998). In the present study, the spatial descriptor was calculated by performing a backward-stepwise logistic regression of the species presence/absence on a set of variables defined by combinations of longitude (X) and latitude (Y) in monomials up to the 3rd degree: X, Y, XY, X^2, Y^2, X^2Y, XY^2, X^3, and Y^3. The logit function resulting from the logistic regression (i.e. a linear combination of these variables) was taken as descriptor variable of the species' spatial structure, which we called $Spay^3$.

Two additional models were constructed for each species to test whether taking the presence of a barrier into account could improve model performance. These models were the *F-Model* (from "flexible model") and the *R-Model* (from "river model"). In the *F-model*, the $Spay^3$ spatial variable was replaced by a more flexible

trend-surface, by using monomials up to the 4th degree (*Spay*^{4}): X, Y, X^2, Y^2, X^3, Y^3, X^4, Y^4, XY, X^2Y, XY^2, X^3Y, XY^3 and X^2Y^2. Thus, the limits of favourable areas for species presence were expected to better fit the curves defined by river meanders. In the *R-model*, the variables included in the *0-Model* were complemented by a new binary *cis-trans* variable (*Briv*) that took value 0 for squares located on the same side of the river where the species occurs, and value 1 on the opposite side of the river.

The aim was to test whether the occurrence of a potentially competing species on the opposite side of the river would be a more explanatory factor than the barrier effect in our case studies. Thus, we constructed a competition model (*C-Model*) for each species, by complementing the variable set employed to run the *0-Model* using a new predictor defined as the presence/absence of the potential competitor (i.e. the corresponding parapatric species). We then compared the performance of the *C-Model* with that of the *F-* and *R-Models*.

4.3.3. Favourability models

Distribution models were performed according to the Favourability Function (Real *et al.*, 2006; Acevedo & Real, 2012), using the following equation:

$$F = \frac{\frac{P}{1-P}}{\frac{n_1}{n_0} + \frac{P}{1-P}}$$

where n_1 and n_0 are the numbers of species presences and absences, respectively, within the study area, and *P* is the probability of presence. *P* was calculated through logistic regression using the IBM-SPSS Statistics 23 software package. Favourability values are independent of the presence prevalence in the study area (Acevedo & Real, 2012). In this way, models of different species with different prevalences can be compared and combined (Real *et al.*, 2009), as in the present case.

Benjamini and Hochberg's (1995) False Discovery Rate (FDR) was used to control for Type I errors, which may result from the increase in the number of variables considered (Muñoz & Real, 2013). Only variables that were significant under a FDR of $q < 0.05$ were considered for model parameterization. We used a forward-backward stepwise procedure to avoid the inclusion of redundant variables in the models, according to the significance of Rao's score test and the Akaike information criterion (AIC; Akaike, 1973). To avoid high multicollinearity, variables with Spearman correlation coefficients >0.8 were not allowed in the same model; in this case, the least significant variable was deleted and the model was trained again. Model parameterization was performed using iterative log-likelihood maximization, goodness of fit was assessed using χ^2 tests, and the contribution of variables in the model was assessed using Wald tests.

4.3.4. Model assessment and comparison

Favourability models were assessed and compared according to their classification and discrimination capacity. Four classification assessment indices were used (Fielding & Bell, 1997): sensitivity (i.e. the proportion of correctly classified presences), specificity (i.e. the proportion of correctly classified absences), correct classification rate (CCR) (i.e. the proportion of correctly classified presences and absences), and Cohen's kappa. The latter index ranges from -1 to +1 and takes the probability of random correct classifications into account. Classification was based on the 0.5 favourability value, which is the threshold at which local probability is equivalent to overall prevalence (Acevedo & Real, 2012). Discrimination capacity was assessed using the area under the ROC curve (AUC) (Lobo *et al.*, 2008). In addition, the AIC was used to compare the models according to the parsimony criterion.

4.3.5. Variation partitioning analysis

We used variation partitioning analysis (Borcard *et al.*, 1992), according to the approach proposed by Muñoz *et al.* (2005), to assess the percentage of relative

contribution in the models of the factors defining spatial and environmental influences on a species range. The spatial factor was represented by the variable *Spay*^{3} in the *0-Model*; by the variable *Spay*^{4} in the *F-Model*; and by variables *Spay*^{3} and *Briv* in the *R-Model*, where the partial contribution of both *Spay*^{3} and *Briv* were analyzed separately. This analysis provided pure and shared effects of each factor. A pure effect is the contribution of a factor to explaining favourability for the presence of a species that is not influenced by the covariation of the other factors. A shared effect is the contribution of a factor that cannot be distinguished from the contribution of another factor.

4.4. Results

In the African case study, the correlation of favourability values trained on 10 x10-km squares with those of a downscaled model initially trained at a 1° x 1° resolution was highly significant for both *P. troglodytes* (R = 0.84; N = 55,454; P < 0.00001) and *P. paniscus* (R = 0.90; N = 55,454; P < 0.00001). Correlation even increased to R = 0.87 and R = 0.92, respectively, when only the area located in the "suitable side" of the barrier was considered. For this reason, only results regarding the 10 x 10-km model are shown.

All the models included variables representing a variety of explanatory factors. The spatial structure, represented by variables *Spay*^{3} and *Spay*^{4}, reached significance in all cases when used for model training. This was also the case for the variable “being on the other side of the River” (*Briv*) in *R-Models*. The Wald-parameter values of the spatial variables were always higher than those of the other variables in the model. The only exception was in the *R-Models*, where they were outperformed by *Briv*, which was always negatively associated with the species presence (see Appendix 2). All the models showed a high capacity for classification (sensitivity, specificity, and CCR >0.80; Kappa >0.53 or >0.65 if the spatial variable was included) and discrimination (AUC >0.88).

Without exception, the inclusion of the spatial factor (i.e. *0-Models*, *F-Models*, and *R-Models*) improved model performance compared to the use of environmental descriptors alone (i.e. *E-Models*) (see Table 4.1). In addition, the models that used specifically designed variables to represent the presence of a barrier (i.e. *F-Models* and *R-Models*) generally outperformed their corresponding *0-Models*. This improvement in performance was achieved by all *R-Models* and also by the *F-Models* of *P. troglodytes* and *P. oenanthe*. The *F-Model* of *P. paniscus* had slightly lower kappa than that of the *0-Models*, and the *F-Model* of *P. discolor* had slightly lower sensitivity (Table 4.1). *R-Models* outperformed *F-Models* for all species except for *P. oenanthe*.

Table 4.1 Model assessment based on classification capacity, discrimination capacity, and parsimony. For better model performance, Cohen's kappa, sensitivity, specificity, correct classification rate (CCR), and area under the ROC curve (AUC) values should be higher, and the Akaike information criterion (AIC) should be lower.

Species	Favourability models	kappa	Sensitivity	Specificity	CCR	AUC	AIC
Plecturocebus oenanthe	*E-Model*	0.773	0.936	0.910	0.915	0.980	709.55707
	0-Model	0.817	0.942	0.931	0.933	0.988	562.940693
	F-Model	0.907	0.984	0.962	0.967	0.997	288.885214
	R-Model	0.846	0.958	0.941	0.944	0.992	464.269053
	C-Model	0.830	0.954	0.934	0.938	0.990	518.893068
Plecturocebus discolor	*E-Model*	0.914	0.966	0.954	0.959	0.993	504.30203
	0-Model	0.939	0.979	0.965	0.971	0.997	357.518115
	F-Model	0.940	0.978	0.966	0.971	0.997	352.454852
	R-Model	0.984	0.990	0.993	0.992	0.999	163.201726
	C-Model	0.939	0.979	0.965	0.971	0.997	357.518115
Pan troglodytes	*E-Model*	0.569	0.811	0.807	0.809	0.883	42379.690
	0-Model	0.655	0.880	0.833	0.846	0.941	30814.283
	F-Model	0.759	0.920	0.885	0.895	0.965	24226.711
	R-Model	0.799	0.908	0.918	0.915	0.975	19981.955
	C-Model	0.750	0.897	0.891	0.893	0.963	24526.859
Pan paniscus	*E-Model*	0.531	0.959	0.903	0.906	0.980	9535.879
	0-Model	0.794	0.990	0.968	0.969	0.997	4055.177
	F-Model	0.792	0.991	0.968	0.969	0.997	3956.427
	R-Model	0.834	0.995	0.975	0.976	0.997	3798.397

	C-Model	0.831	0.994	0.975	0.976	0.997	3824.892

Variation partitioning analyses revealed that the pure effect of the flexible trend surface variable ($Spay^4$) in the *F-Models* was always higher than the pure effect of the trend surface variable ($Spay^3$) in the *0-Models* (Fig. 4.2). The higher pure effect of $Spay^4$ was at the expenses of a lower contribution of the environmental factor to the models. In contrast, the pure effect of $Spay^3$ in the *R-Models* was lower than the pure effect of $Spay^3$ in the *0-Models,* except in the *P. paniscus* case. This was paired with the higher contribution of either the environmental factor or the *Briv* variable pointing to the presence of a barrier.

In all *C-Models*, except in that one for *P. discolor*, the variable representing the presence/absence of the parapatric species was significantly and negatively associated with the modelled species (Table 4.1). *C-Models* either outperformed or equalled *0-Models*, but none of the *R-Models* were outperformed by *C-Models*. Classification values were sometimes higher in *C-Models* than in *F-Models*.

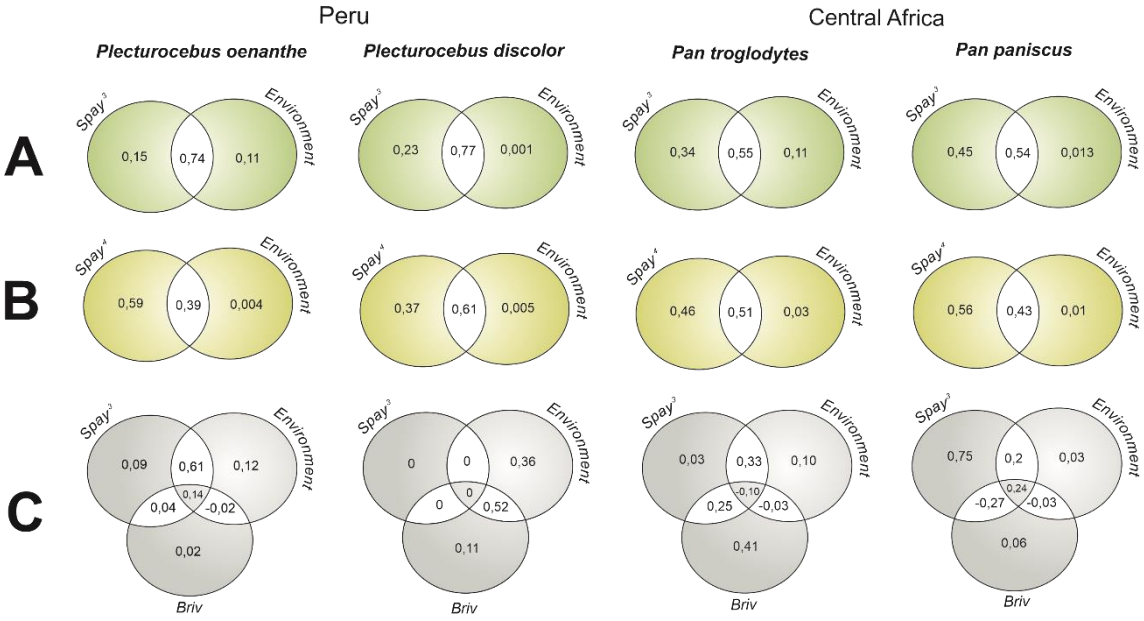

Fig. 4.2 Variation partitioning analysis. Venn diagrams displaying the results of variation partitioning analyses of models combining two factors: space (trend surface, binary *cis-trans* variable respect to the river) and environment (types of ecosystems, topography, hydrography,

climate, human concentration, infrastructures). A. *O-Model,* where the spatial factor is represented by $Spay^3$. B. *F-Model*, where the spatial factor is represented by $Spay^4$. C. *R-Model*, where the spatial factor is represented by the binary *cis-trans* variable (*Briv*) and also by $Spay^3$.

4.5. Discussion

The results show that the use of specific tools to describe barriers can improve the performance of distribution models when species are biogeographically conditioned by geographic barriers. This happened beyond the fact that polygon data defining interpolated presence points are, by definition, representing a certain spatial pattern. This finding applies to permeable and impermeable barriers. It has been suggested that a trend-surface approach is an effective way to integrate barriers in a model (Legendre & Legendre, 1998) in order to take the spatial structure of species distributions into account. Our results showed that, compared to purely environmental models, this technique decreased the occurrence of high-favourability values for species presence in the areas located on the opposite side of the river (e.g., different models for the same species can be compared in Fig. 4.3). This decrease was more marked when the description of the spatial structure was made more flexible. This was achieved by increasing the order of the polynomial representing species' trend surfaces in order to model structures of increasing complexity and refinement, as recommended by Legendre & Legendre (1998). This approach provided the model with sufficient flexibility to adapt to river meanders.

However, trend-surface approaches did not prevent the model from predicting the occurrence of areas on the other side of the river with intermediate favourability values (0.2 – 0.8). In most cases, this objective was achieved by including in the models a predictor binary *cis-trans* variable (*Briv*) that described the location of each geographic unit in relation to the barrier. The only exception was in the case of *P. oenanthe* case, for which the best fit was obtained using a model based on a flexible trend–surface. However, this result could have been a

consequence of the small overlap between the distribution limits of this species and the river.

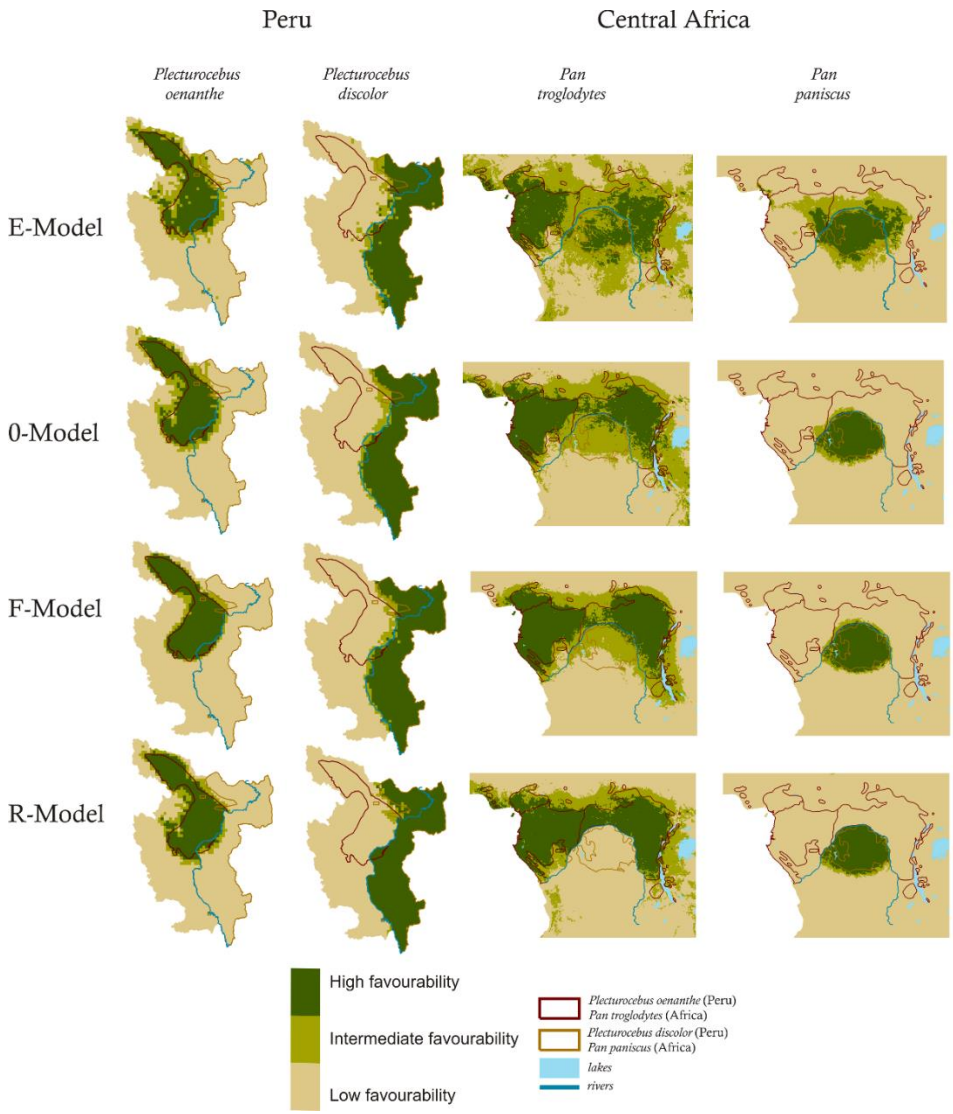

Fig. 4.3 Distribution models for four primate species in two different continents (favourability range, 0 - 1). Four alternative models per species are mapped: *E-Model* (environmental model), *0-Model* (the environmental and spatial null model, lacking specific measures for barrier identification), *F-Model* (flexible model, provided with more flexibility in the spatial component to better fit the curves defined by river meanders), *R-Model* (river model, complementing the *0-Model* with a binary *cis-trans* variable that expresses a position in relation to the river). High favourability: 0 to <0.2; intermediate favourability: 0.2 to <0.8; high favourability: 0.8 to 1.

Thus, adding to the model the location of each geographic unit relative to the river appeared to be the most accurate way to define the presence of a barrier for

dispersal. However, in practice, defining this predictor variable may be a challenging task. Being on the left or right bank of a river implies taking into account a context defined by the river basin. If the study area is higher than the basin, then there is no location on either side of the river. Consequently, the variable *Briv* may lose its effectiveness to define favourable conditions for species presence on a given side of the river. According to the *R-Model*, this situation may hold for some areas with intermediate favourability values for *P. troglodytes* in the south-west of the study area (compare Fig. 4.1 and Fig. 4.3), where this species does not occur. Difficulties in defining the *Briv* variable may increase when a species (e.g., *Cercopithecus cephus* and some *P. troglodytes* subspecies, Butynski *et al.*, 2013) distribution is potentially limited by more than one river, and when these rivers include main water courses and tributaries.

According to the results of our case studies, the flexible trend-surface approach is a better choice when more direct options are unsuitable. It also provides high-quality models under the condition that the exercise is not aimed at exploring the causes of a distribution, or at allowing extrapolations far from the training area (e.g., in scenarios of biological invasion). The spatial structure of a distribution may derive from spatially conditioned factors such as community processes, the species history, and the presence of barriers, or they can derive from the physical forcing of environmental variables that are also spatially structured (Legendre, 1993). Thus (as shown by the variation partitioning analyses conducted, and in contrast to alternatives based on the *Briv* variable), introducing a complex trend surface into ecological models may lead to a decrease in the relevance of the environmental variables in the model equation, because some environmental factors could be non-explicitly represented by the trend-surface itself. Models with a complex trend surface are still valid and useful for descriptive purposes, but they must be subject to deeper analyses if we wish to use them to investigate distribution drivers (e.g., see variation partitioning approaches, Legendre & Legendre, 1998).

In the present study, impermeable barriers were represented by the Congo River. Although the strongest barriers are probably associated with physical environments far outside the tolerance ranges of organisms (Lomolino *et al.*, 2006), areas with suitable conditions for the presence of a species may remain unoccupied because crossing wide aquatic barriers can be very difficult for non-swimming terrestrial taxa (Zunino & Zullini, 2003), as is the case of *P. troglodytes* and *P. paniscus* (Takemoto *et al.*, 2015). The *E-models* suggest that environmental conditions on both sides of the river could mean that *P. troglodytes* and *P. paniscus* are sympatric species, inasmuch as most of the area within the range of *P. paniscus* shows high environmental favourability for the presence of *P. troglodytes*. The Congo River has probably been impermeable to species within the genus *Pan* for the last 34 million years (Takemoto *et al.*, 2015). Until recently, it was believed that the speciation of *Pan* was the result of the formation of the Congo River during early Pleistocene epoch. However, new hypotheses suggest that one or more founder populations of ancestral *P. paniscus* crossed the river to its left bank during the rare times when its discharge decreased during this epoch (Takemoto *et al.*, 2015). According to Gruber & Clay (2016), the speciation of genus *Pan* coincided with a period of pronounced drought in the Congo River basin around 1 million years ago. This does not mean that the possibility of later events of *Pan* individuals dispersal across the barrier should be totally discarded, even if the current features of the Congo River are taken into account. Occasionally, mammal dispersal appears to occur through large water masses, including oceans, and typically over large periods (Ali & Huber, 2010; Gillespie *et al.*, 2012). Nevertheless, the successful establishment of founder populations could be density dependent and restricted by factors such as competitive exclusion (Waters *et al.*, 2013; also see the "Allee effect": Courchamp *et al.*, 1999; Tobin *et al.*, 2007). In the African case study, competition has the potential to be a factor that prevents the establishment of populations on the opposite river bank. Further studies should address the synergy between the barrier effect and

the potential for competitive exclusion. Nevertheless, when tested separately, the current distribution of both *Pan* species appeared to be explained to a greater extent by the presence of a geographical barrier than by the presence of a competing species (compare the *F*- and *R-models* with the *C-model* in Table 4.1).

The River Huallaga in Peru, despite being a clear limit between the populations of *P. discolor* and *P. oenanthe*, is also a permeable barrier for these primates. *P. discolor* has crossed this river westward in the north of San Martin, and *P. oenanthe* has crossed it eastward in the central region (Vermeer *et al.*, 2011). Thus, the River Huallaga is not a closed barrier for these species. However, a permeable barrier can potentially affect coexistence by modulating the balance of competition between animal communities (Cozzi *et al.*, 2013). On the one hand, competing species could coexist in a given area (Krebs, 1985) as a consequence of differences in feeding behaviour (Gause & Witt, 1935) or of the existence of optimally favourable conditions for the two species (Acevedo *et al.*, 2010). On the other hand, such species could compete in other areas where the environment is "suboptimal" for at least one of them (i.e. where resource availability is limited and the two species share environmental requirements).

Competition limits the dispersal of animal species (Lomolino *et al.*, 2006). This constraint could be strengthened by the "rampart effect" resulting from the combination of competition and a physical accident acting as permeable barrier. Favourable conditions for *P. oenanthe* to the east of the River Huallaga in this area are defined by suitable environmental conditions (see the *E-model* for this species in Figure 3), and reinforced through the incorporation of the species' spatial structure in the model (see *0-model* and *F-model* in Fig. 4.3). The tendency of species distributions to adopt the simplest forms was suggested by Rapoport (1975). The simplest distribution form for *P. oenanthe* entails this species being present to the east of the cited meander (i.e. "conquering" the areas immediately behind "the wall"). The *R-model* retains the possibility of favourable conditions in

this area despite the presence of the river (see the *R-model* in Fig. 4.3). Competition in this small area might be compensated by a rescue effect (Brown & Kodric-Brown, 1977) such that eastern populations could be sending propagules from the forests surrounding the meander, thus filling the entire space behind it until a circular pattern is formed. In any case, as observed in Africa, the distribution of both *Plecturocebus* species was explained to a greater extent by the presence of a river than by competition between species (compare the *F-* and *R-models* with the *C-model* in Table 4.1).

The methodological approach proposed in this study can be applied to any species hypothetically subject to dispersal constraints caused by a barrier. Although we cannot ensure that the results of this study can be generalized to other cases, we are confident that the results are sound in that they were derived from case studies conducted on two continents, using several primate groups, and based on different grades of permeability of rivers to species dispersal. Thus, our approach could respond to the need of integrating, in species distribution modelling, factors shaping distribution edges, e.g., the presence of rivers, mountain chains, linear infrastructures, or broad inhospitable areas such as deserts.

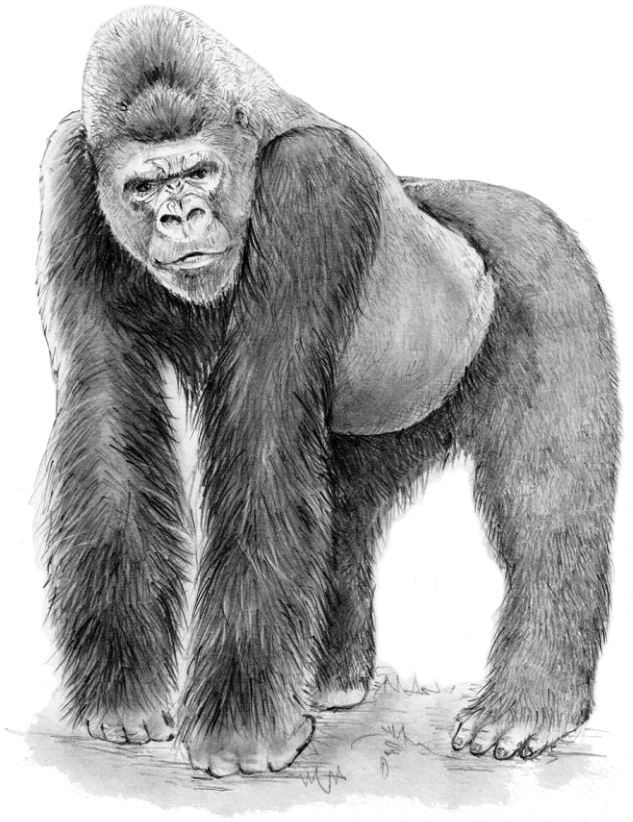

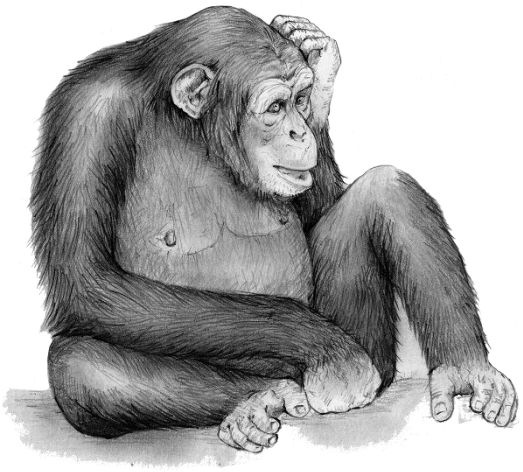

CAPÍTULO 5

Spatial modelling for predicting potential wildlife distributions and human impacts in the Dja Forest Reserve, Cameroon

Modelización espacial para predecir la distribución potencial de la fauna y el impacto humano en la Reserva Forestal del Dja (Camerún)

Este capítulo se basa en/ This chapter is based on:

Farfán, M. A., Aliaga-Samanez, A., Olivero, J., Williams, D., Dupain, J., Guian, Z., & Fa, J. E. (2019). Spatial modelling for predicting potential wildlife distributions and human impacts in the Dja Forest Reserve, Cameroon. Biological Conservation, 230, 104-112. https://doi.org/10.1016/j.biocon.2018.12.015 **(Q1)**.

5 Spatial modelling for predicting potential wildlife distributions and human impacts in the Dja Forest Reserve, Cameroon

5.1. Abstract

Protected areas (PAs) are currently the cornerstones for biodiversity conservation in many regions of the world. Within Africa's moist forest areas, however, numerous PAs are under significant threats from anthropogenic activities. Adequate technical and human resources are required to manage the wildlife within PAs satisfactorily. SMART (Spatial Monitoring And Reporting Tool) software has been developed to aid in fluidly displaying, managing, and reporting on ranger patrol data. These data can be analysed using spatial modelling to inform decision-making. Here we use Favourability Function modelling to generate risk maps from the data gathered on threats (fire, poaching and deforestation) and the presence of Western gorilla (*Gorilla gorilla gorilla*), chimpanzee (*Pan troglodytes*) and African forest elephant (*Loxodonta cyclotis*) in the Dja Forest Reserve (DFR), southern Cameroon. We show that the more favourable areas for the three study species are found within the core of the DFR, particularly for elephant. Favourable areas for fires and deforestation are mostly along the periphery of the reserve, but highly favourable areas for poaching are concentrated in the middle of the reserve, tracking the favourable areas for wildlife. Models such as the ones we use here can provide valuable insights to managers to highlight vulnerable areas within protected areas and guide actions on the ground.

5.2. Introduction

Protected areas (PAs) aim to conserve nature by minimizing human pressures and threats operating within their boundaries. Although PAs are known to perform better than the broader landscape (Barnes *et al.*, 2016; Gray *et al.*, 2016), numerous studies suggest that biodiversity continues to decline within them (Craigie *et al.*, 2010; Geldmann *et al.*, 2013). Numerous PAs within Africa's moist forest regions, often created to safeguard large charismatic fauna and other natural resources, are under significant threats from anthropogenic activities such as deforestation, fires and hunting (Joppa & Pfaff, 2009; Nelson & Chomitz, 2011; Tranquilli *et al.*, 2014). The persistence of wildlife in PAs ultimately depends on increasing conservation efforts to combat such threats (Arcese *et al.*, 1995; Jachmann & Billiouw, 1997; Bruner *et al.*, 2001; De Merode & Cowlishaw, 2006; De Merode *et al.*, 2007).

Law enforcement in PAs in the Congo Basin is notoriously underfinanced (Wilkie *et al.*, 2001). Thus, tools that enable the often, resource-limited (in technology, weapons and personnel) site-based staff, to better patrol more areas with greater regularity, have been developed recently. These have resulted from the increased accessibility of geospatial technologies associated with Global Positioning Satellites (GPS), remote sensing and Geographic Information Systems (GIS) (O'Neil *et al.*, 2005). Two applications, CyberTracker and SMART (Spatial Monitoring And Reporting Tool), are now available to improve the effectiveness of wildlife law enforcement patrols and site-based conservation activities on the ground. SMART contains a suite of programmes that can use mobile data collected with the CyberTracker App (CyberTracker, 2018). CyberTracker operates within a GPS enabled mobile device e.g. smartphone or a Personal Digital Assistant (PDA) to collect observation and GPS data in a single unit. On return from their patrols, data collected by rangers as part of their daily work (e.g. wildlife observations, poaching encounters) can be transferred directly into the SMART database in a semi-automated process. These tools are open source and non-

proprietary and are currently deployed in hundreds of sites around the world (Henson *et al.*, 2016; SMART, 2017, 2018).

Spatial modelling of observation data gathered using CyberTracker and SMART over a relevant period of time can be used to predict significant areas of threats relative to areas of abundance of the target species across a PA including in unpatrolled areas. Increasing the probability of detecting illegal activities improves the efficacy of PA law enforcement (Leader-Williams & Milner-Gulland, 1993), leading managers to target areas where threats are most likely to occur (Campbell & Hofer, 1995). Mapping and predictions of threat occurrence can be effective in helping law enforcement reduce deforestation threats (Linkie *et al.*, 2010) and can result in cost-efficient prevention of illegal activities (Plumptre *et al.*, 2014).

In this paper, we focus attention on understanding the distribution of and threats affecting the Endangered chimpanzee (*Pan troglodytes*), the Critically Endangered Western lowland gorilla (*Gorilla gorilla gorilla*), and the Endangered African forest elephant (*Loxodonta cyclotis*) within the Dja Forest Reserve (DFR) in southern Cameroon. The DFR is a key stronghold for these flagship species and is one of Africa's most biodiverse rainforests. Despite its importance, the state of conservation of the reserve is precarious, due to the continuing impact of uncontrolled commercial hunting and other illegal activities. As a result, the DFR is likely to be inscribed on the List of World Heritage in Danger (UNESCO, 2018). A number of measures have been proposed to strengthen the institutional and operational framework for management of the DFR, including the strengthening of technical and logistical capacities (UNESCO, 2018) .

Adequate law enforcement patrolling within the DFR is restricted by the terrain's inaccessibility and by the small (75-man) ranger force currently in place. Given this situation, timely analyses of data gathered by these patrols can be used to assist the ranger force become more strategic. Here, we utilise patrol data on the distribution of the target species and pressures on these, to generate maps of

high-pressure areas for wildlife. These maps are created using Favourability Function modelling (Real *et al.*, 2006; Acevedo & Real, 2012). Favourability Function is a procedure based on logistic regression that removes the effect of species prevalence from presence probabilities, thus evening out model predictions for different species and factors so that they can be directly combined. Favourability Function modelling has been used to resolve species conservation issues (e.g. Estrada *et al.*, 2008a; Fa *et al.*, 2014). Based on the results of our modelling we discuss possible management and conservations interventions that could be applied to better protect large mammals in protected areas.

5.3. Material and methods

5.3.1. Study area

The DFR (2°50–3°30 N, 12°20–13°40 E) in southeastern Cameroon is bounded on three sides by the Dja River (Fig. 5.1), a major tributary of the Congo River. The DFR was designated as a Biosphere Reserve under the UNESCO Man & Biosphere Programme in 1981 and is classified as an IUCN Management Category VI: Managed Resource Protected Area. At the time of the World Heritage listing, 90% of the area was considered intact and human pressure was low.

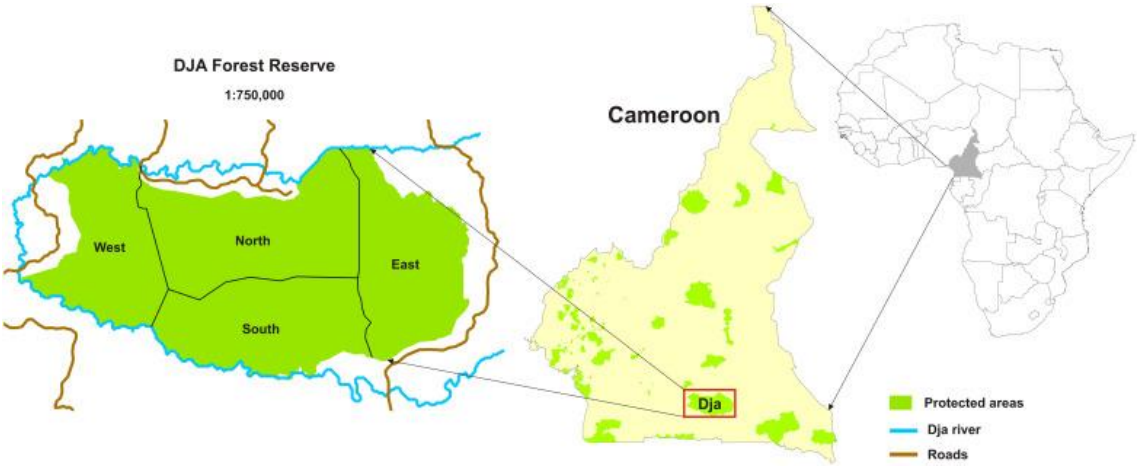

Fig. 5.1. Location of the study area (Dja Forest Reserve), southern Cameroon

Our study area comprised the entire DFR and up to 21 km around the limits of the reserve so as to include the tracks followed by ranger patrols (Fig. 5.2). Covering 5260 km2 and 600–700 m above sea level, the DFR is one of the largest protected areas of lowland rainforest across tropical Africa. Monthly average temperature in the region is 23.5–24.5 °C and annual rainfall 1180–2350 mm. Vegetation in the DFR lies within a transitional zone between the Atlantic equatorial coastal forests of southern Nigeria and western Cameroon, and the evergreen forests of the north-western Congo lowlands. Atlantic, semi-deciduous, Congolese and monospecific forest types are present within the DFR but tree cover is dominated by dense semi-evergreen Congo rainforest.

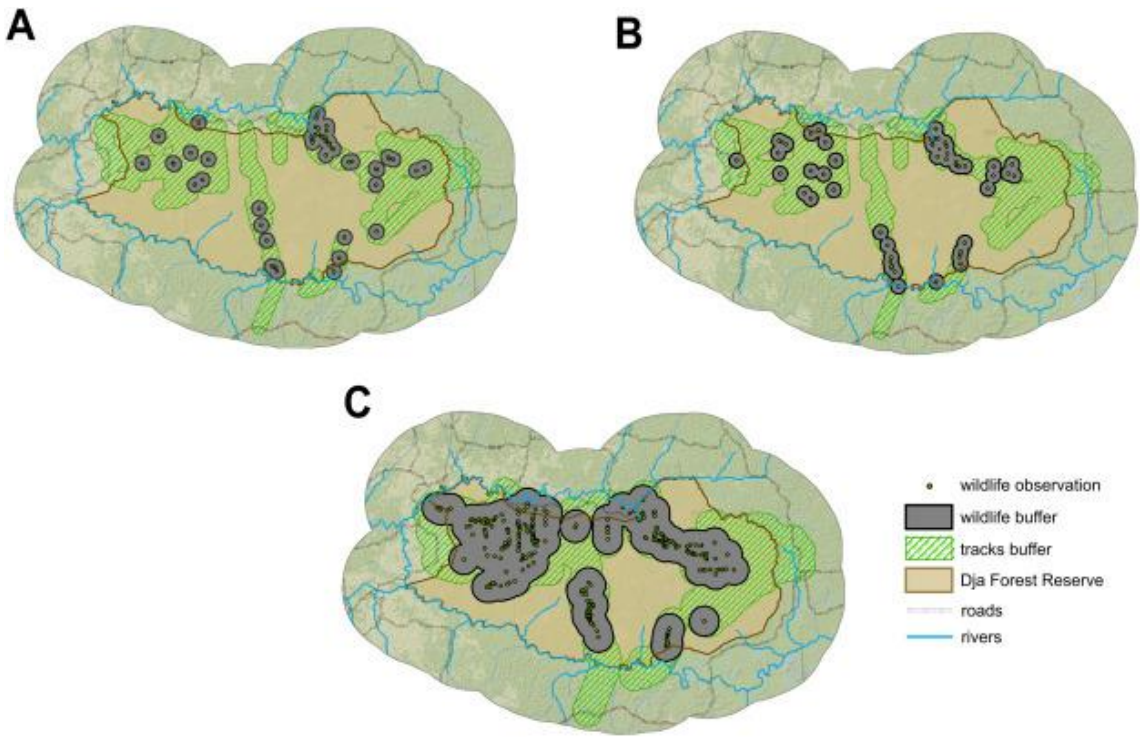

Fig. 5.2. Area for model training (striped plus dark grey area) fixed for a) Western Gorilla, b) Chimpanzee and c) African Forest Elephant, and positive contacts (green points) surrounded by buffer areas suggesting presence of this species (dark grey).

5.3.2. Patrol data

Operating under the auspices of an agreement between The African Ape Initiative (AAI) of the African Wildlife Foundation (AWF) and the Service de Conservation-DFR (SC-DFR), anti-poaching patrols completed pre-identified routes within the

DFR (see routes in Fig. 5.3 and Fig. 5.5). While AAI-supported anti-poaching patrol efforts started in Sept. 2013, here we use data for Feb.–Apr. 2015 and Jan.–Mar. 2016. During this period, a total of 15 patrols were deployed, an average of 2.5 patrols per month (range 1–4), covering a distance of 230.7 km (range 72–458 km) per patrol, and 22.5 days per patrol (range 3–51 days).

In total, patrols covered 1384 km over 192 patrol days (Dupain *et al.*, 2017). Each patrol team undertook 10-day missions within pre-determined itineraries; routes were decided on the basis of knowledge of the terrain, but were not randomly chosen. Data were gathered from 6 h to 17 h during patrol days. Patrols would seize hunting gear and illegally collected products, would destroy traps and camps, collect cartridges and other polluting objects, and be involved in sensitization and eviction of offenders. Tracklogs, photos and observations of mammals and human activities were georeferenced and recorded. For this paper, we used only data of elephant dung, gorilla nests, chimpanzee nests and encounters with hunting camps, poachers, cartridges and snares.

All patrols (each composed of six guards, and four local village porters) carried a PDA equipped with CyberTracker for download to a computer running SMART. A total of 60 out of 75 eco-guards were trained in the use of the PDA and to operate Cyber-Tracker and SMART; all data collection protocols were approved by the Conservation Department in Cameroon.

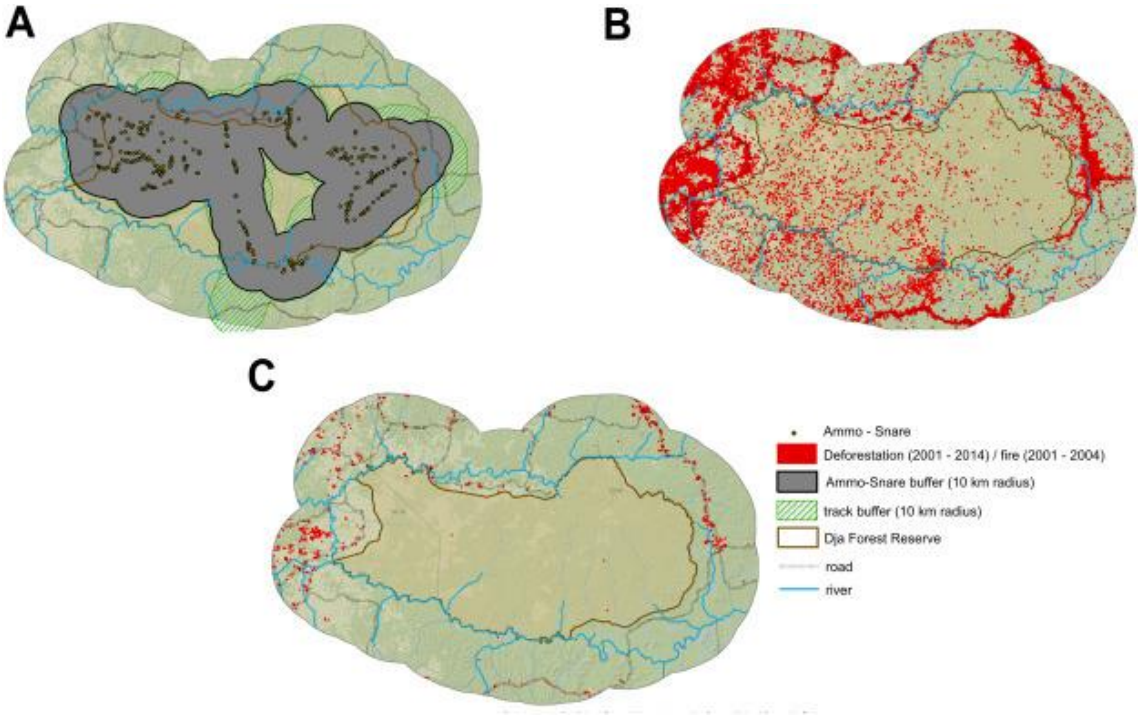

Fig. 5.3. Area for model training fixed for a) poaching (striped plus green area), and observation of traps and ammunition cartridges (black points), surrounded by buffer areas suggesting occurrence of these objects (green); b) distribution of forest loss events in the study area (red squares) and c) distribution of fire events in the study area (red points).

5.3.3. Modelling variables

Patrol observations data of the presence of the three species were used to delimit the distribution of wildlife within the DFR. Threat data based on poaching signs, forest loss and fires, the latter two derived from remote sensing, were dependent variables in our models. Independent variables included spatial data on environmental and anthropogenic factors obtained from non-field based sources. Records for each variable were assigned to 0.5 × 0.5-km grid squares covering the entire study area.

5.3.3.1. Dependent variables

We used presence records of chimpanzees, gorillas and elephants gathered by DFR park personnel during 2015 and 2016. Park personnel employed CyberTracker hand-held devices, allowing them to record observations quickly and easily prior to upload into the fully compatible SMART software. For each positive contact (Fig. 5.2), we fixed a 2.5 km buffer zone for gorillas and

chimpanzees, and 5.0 km for elephants. The size of these buffer zones was based on the average daily distances travelled by each species in Wilson & Mittermeier, (2011) and Mittermeier *et al.* (2013). For modelling purposes, we assumed that the species was present in all the 0.5 × 0.5-km squares included within these buffers.

Data on poaching consisted of geo-referenced records of traps and ammunition cartridges found by the DFR staff during their patrols. We assumed that poachers were active within a maximum of a 10-km radius buffer around each record from data on the area covered by trappers in Equatorial Guinea (Kümpel, 2006).

Forest loss within 0.5 × 0.5-km squares was derived from comparisons of newly deforested areas between 2001 and 2014 (i.e. a 15-year period prior to our wildlife evaluation) available from Hansen *et al.* (2013) and from the Global Forest Change web site (https://earthenginepartners.appspot.com/science-2013-global-forest). Fire presence was defined as all 0.5 × 0.5-km squares containing active fire observations between 2001 and 2014 in NASA's FIRMS database (https://firms.modaps.eosdis.nasa.gov) (Fig. 5.3).

Absences for all variables based on field personnel observations (i.e. wildlife and poaching) were defined as all non-presence in 0.5 × 0.5-km squares within a buffer area around the tracks followed by ranger patrols (Fig. 5.2 and Fig. 5.3a). This minimized bias caused by uneven sampling throughout the study area since models are initially developed within the regions of the study area that were sampled by ranger patrols. Buffer width was specific to every variable, according to the above. Using this criterion, there were 2388 presences and 7994 absences for gorillas, 2630 presences and 7752 absences for chimpanzees, 8542 presences and 6503 absences for elephants as well as 20,858 presences and 3047 absences for poaching. For forest loss and fire, all non-presence 0.5 × 0.5-km squares within the study area were considered as absences, given the unbiased nature of remote sensing observations.

5.3.3.2. Independent variables

Predictors on which the models were based, consisted of 39 variables which described climate, topography, soils, land use and anthropogenic descriptors (Appendix 3). Variable values per 0.5×0.5-km square were calculated using the ZONAL tool of the ArcMap v.10.1 (ESRI©2012) software, starting from 100-m^2 resolution raster layers. We computed average values for each predictor except for the land-use variables, for which square-area proportions covered by each use were considered.

In order to consider autocorrelation resulting from the purely spatial structure of species distributions (Sokal & Oden, 1978), we designed a purely spatial independent variable following the 'trend surface approach' (Legendre & Legendre, 1998). To this end, different combinations of average latitude (Y) and longitude (X) were defined (i.e. X, Y, XY, X^2, Y^2, X^2Y, XY^2, X^3, Y^3), and a backward-stepwise logistic regression of presences/absences was run on these combinations. This modelling method commences with the full combinations of latitude and longitude and then iteratively removes the least significant predictor variable. Because it is based on the location of presences, and not on variables that describe possible causes of distribution, this model is more predictive than explanatory. For that reason, we use backward steps which generates a more conservative model with respect to the number of variables that remain in the model. Then we used the logit of this regression as the spatial independent variable.

5.3.4. Predictive models

5.3.4.1. Model fitting and evaluation

Models defining the distribution of environmentally favourable areas for each species and threat were developed using the Favourability Function, as described by Real *et al.* (2006) and Acevedo & Real (2012):

$$F = \frac{\frac{P}{1-P}}{\frac{n_1}{n_0} + \frac{P}{1-P}}$$

where *F* is environmental favourability (0-1), *P* is the presence probability, and n_1 and n_0 are the numbers of presences and absences, respectively. *P* was calculated using forward-backward stepwise logistic regression, according to the independent variables shown in Appendix 3 and the spatial variables. We have preferred steps forward, against backward steps, to minimize the number of variables in the model, thus favouring its explanatory capacity with respect to the causes of the distribution.

Type I errors, potentially caused by the large number of variables employed in the process, were controlled by using Benjamini and Hochberg's (1995) False Discovery Rate (FDR).

To minimise multicollinearity, we applied a three-step procedure. First, we avoided using variables that had correlation values (Spearman R) greater than 0.8, by removing the least significant within each pair of highly correlated variables. From these, we accepted only significant variables with a FDR of $q < 0.05$. Finally, forward-backward stepwise logistic regression will not consider correlated variables in the final model. Variables enter the equation by forward selection, so that the first variable explains the highest proportion of the variation observed, the second variable explains the highest proportion of the residual variation (i.e. variation not explained by the first variable), and so on. For this reason, the final model does not usually include correlated variables, and if two correlated variables enter it is because one explains part of the variation not explained by the other.

The classification capacity of the models obtained was evaluated using four indices: sensitivity (proportion of correctly classified presences), specificity (proportion of correctly classified absences), correct classification rate (CCR:

proportion of presences and absences correctly classified) and Cohen's Kappa (proportion of specific agreement; Fielding & Bell, 1997). We used the area under the receiver operating characteristic curve (AUC) to assess the discrimination capacity of the models (Lobo *et al.*, 2008). The significance of every independent variable in the model was assessed using the Wald test.

5.3.4.2. Model extrapolation

Wildlife and threat of poaching models, fitted in training areas constrained to buffers around ranger patrol tracks, were extrapolated to the whole of the study area using the following equation (Real *et al.*, 2006):

$$F = \frac{e^{y}}{\left(\frac{n_1}{n_0}\right) + e^{y}}$$

where n_1 and n_0 are presence and absence numbers within the training area, e is the base of the natural logarithms, and y is the linear combination of predictor variables (i.e. the logit) of the logistic regression defining P (see above).

Model extrapolations were made only to the 0.5×0.5-km squares whose variable values were within the dominion of the Favourability Function, i.e. were in the range of values shown by the model variables within the training area. We only accepted a 10% tolerance above and below. This precaution avoided projections to zones that were not environmentally represented in the area used for model training.

5.3.5. Wildlife and risk maps

In this paper we define threat as an action (poaching, fire, forest loss) likely to cause damage, harm or loss. We define risk as the potential or possibility of an adverse consequence resulting from the combined effects of one or more threats. Using the average of favourability models obtained for the three target species we calculated a "Wildlife Index (WI)". A "Threat Index (TI)" was derived from the

average of the three threat models. We employed the average rather than the sum so as to maintain the range of resulting values between 0 and 1. We combined the threat and wildlife indices to derive an overall map (which we call a risk map) to show where wildlife was more likely to be affected by threats either separately or combined. We divided the study area by the following favourability values for each index: High (H): ≥0.8, Intermediate-High (IH): (0.5–0.8), Intermediate-Low (IL): (0.5–0.2), Low (L): ≤0.2.

5.4. Results

5.4.1. Wildlife models

We obtained significant favourability models for all three species (Table 5.1, Fig. 5.4). These models had acceptable values of discrimination capacity (AUC >0.745), and fair classification capacity values (Cohen's Kappa value >0.300) as shown in Table 5.2. All showed a fairly high proportion of correctly classified presences and absences; values being ≥0.635 for sensitivity and specificity. The correct classification rate was always ≥0.670.

Table 5.1. Descriptor variables of environmentally favourable areas for species distribution of the three study species according to the favourability models. **B:** coefficient of variables. **Wald:** Univariate *Wald* test statistic quantifying variable significance in the models. *p*: statistical significance.

Variable	Western Gorilla			Chimpanzee			African Forest Elephant		
	B	Wald	p	B	Wald	P	B	Wald	p
Bio2 (mean diurnal range temp)	-0.478	44.511	0	0.231	44.195	0			
Bio4 (temp seasonality)				0.00608	17.829	0			
Bio5 (max temp warmest month)							0.0933	17.093	0
Bio6 (min temp coldest month)	0.0854	5.871	0.015						
Bio7 (t emp annual range)	0.287	84.163	0						
Bio13 (precip wettest month)	-0.109	5.085	0.024				0.143	29.526	0
Bio16 (precip wettest quarter)							0.127	118.386	0
Bio17 (precip driest quarter)							-0.049	38.032	0
Bio18 (precip warmest quarter)	-0.005	43.035	0	-0.00365	31.273	0	-0.003	32.640	0
Elev (elevation)				-0.00897	42.153	0			
Fire (active fire)				-1.707	2.521	0.112			

Sp-logit (espatial logit)	0.802	141.259	0	0.635	167.396	0	0.375	106.650	0
Loss0105 (forest loss 2001–2005)				-81.022	5.268	0.022			
Loss0609 (forest loss 2006–2009)	-66.509	7.842	0.005	21.373	8.011	0.005			
Loss1314 (forest loss 2013–2014)				-24.284	9.509	0.011	-11.144	4.688	0.030
Lu_agri (agriculture)	-7.553	5.491	0.019						
Lu_wat (water)							-7.075	12.786	0
Lu_degfor (degraded forest)							-6.446	17.963	0
Lu_prifor (primary forest)							2.190	7.357	0.007
Lu_secfor (secondary forest)							12.260	25.201	0
Lu_noforest (non-forest)	2.716	3.960	0.047	4.132	8.368	0.004			
Places_dist (distance from towns)	0.0000712	167.633	0				-0.0000413	74.047	0
Road dist (distance from roads)	0.000142	388.462	0	0.0000788	241.090	0	0.000143	468.565	0
Slope	-0.0735	4.847	0.028	-0.0968	9.731	0			
Soil_org (soil organic carbon)	-0.0392	7.126	0.008	0.0671	24.603	0	-0.0325	7.501	0.006
Soil_pct (soil percent sand)	-0.0794	15.342	0				-0.0376	5.355	0.021
Stream_dist (distance from navigable streams)				0.0000340	35.780	0			
Constant	35.041	2.092	0.148	-19.732	22.778	.000	-144.263	56.195	0

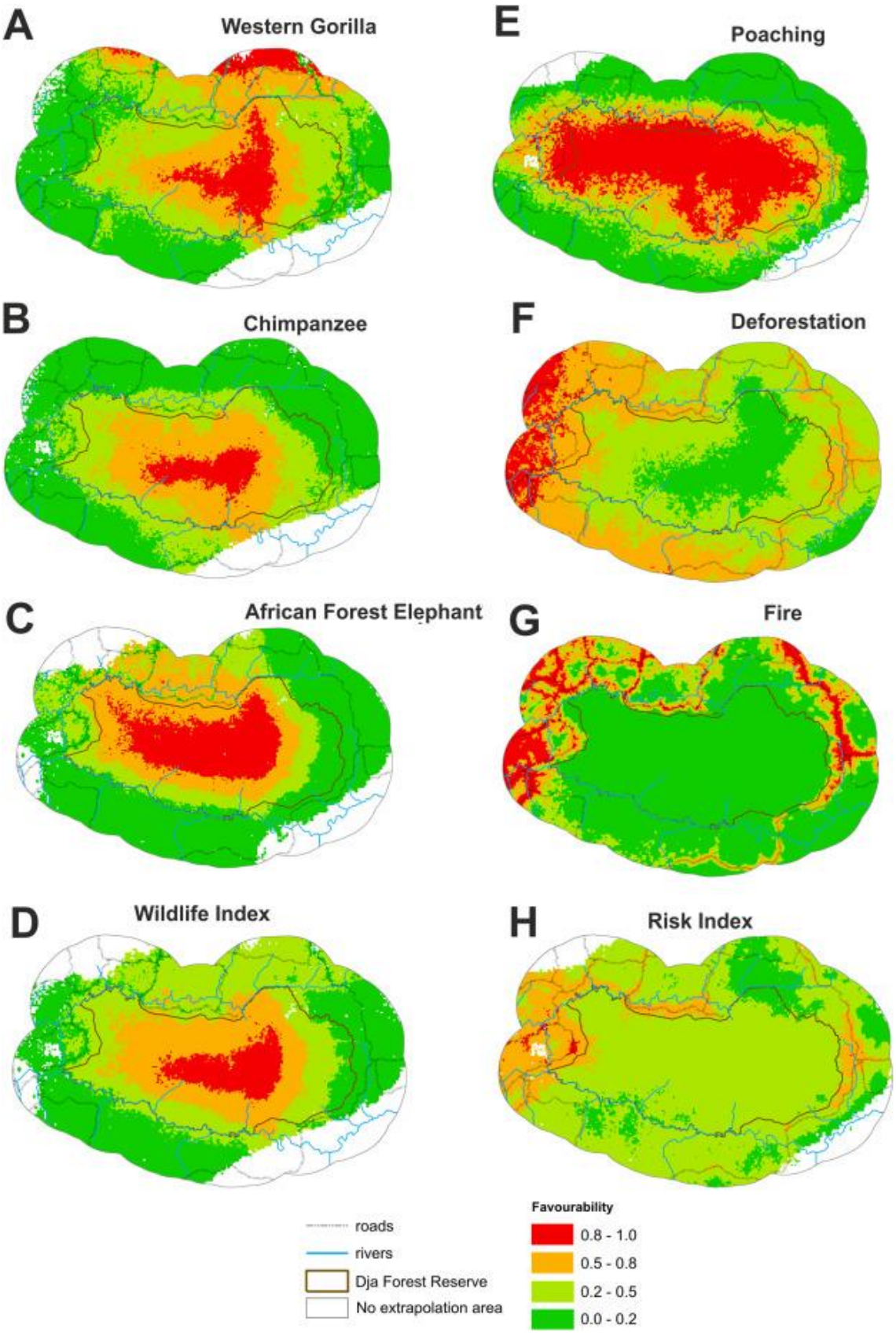

Fig. 5.4. Environmental favourability models projected to the whole study area for species and threats (favourability values: minimum = 0 and maximum = 1). The grey area was not considered for model projection, because the variables values in these squares were not represented in the

model training area. a) Western Gorilla, b) Chimpanzee, c) African Forest Elephant, d) combined species, e) poaching, f) forest loss and g) fire and h) combined threats.

Table 5.2. Classification and discrimination descriptors of the favourability models.

AUC: Area Under the receiver-operating-characteristic Curve**. Kappa:** Cohen's Kappa. **CCR:** Correct classification rate.

Species/Threat	AUC	Kappa	Sensitivity	Specificity	CCR
Western Gorilla	0.764	0.302	0.668	0.704	0.695
Chimpanzee	0.749	0.320	0.775	0.635	0.670
African Forest Elephant	0.833	0.574	0.844	0.726	0.793
Ammunition/snare	0.878	0.422	0.820	0.785	0.816
Deforestation	0.749	0.269	0.688	0.685	0.685
Fire	0.942	0.088	0.949	0.814	0.816

Greater distances to the nearest road were associated with higher favourability for the presence of all species, but larger distances from towns and villages were also significantly related to more favourable areas for gorillas. Maps showed that highly favourable areas within the core of the DFR were typical for all three species. Highly favourable areas for gorillas and elephants were also found along the northern part of the DFR (Fig. 5.4a, c), but not for chimpanzees (Fig. 5.4b). The latter species had highly favourable areas along the south-eastern area of the park as well as in the central region. Overall, larger highly favourable areas within the centre of the DFR were more typical for elephants (Figure 5.4c) than for the other two species. For all three species combined, more favourable areas were within the interior of the DFR (Figure 5.4d), with less favourable areas along a ring from the west to the east of the park.

5.4.2. Threat models

Significant favourability models were also obtained for the three threat variables considered in this study (Table 5.3). Discrimination capacity was acceptable (AUC

>0.749; Table 5.2) but classification capacity was low for fire (Kappa = 0.088), moderate for poaching (Kappa = 0.422) and fair for deforestation (Kappa = 0.269). The three models showed a fairly high proportion of correctly classified presences and absences (sensitivity and specificity values were always ≥0.685).

Table 5.3. Descriptor variables of the environmentally favourable areas for threat factors according to the favourability models.
B: coefficient of variables. **Wald:** Univariate Wald test statistic quantifying variable significance in the models. **p:** statistical significance.

Variable	Poaching			Forest loss			Fire		
	B	**Wald**	**p**	**B**	**Wald**	**p**	**B**	**Wald**	**p**
Bio2 (mean diurnal range temp)							-0.353	28.084	0
Bio4 (temp seasonality)							-0.00472	3.098	0.078
Bio6 (min temp coldest month)	0.560	526.495	0						
Bio7 (temp annual range)	0.278	100.670	0	-0.169	153.871	0			
Bio9 (mean temp driest quarter)				-0.184	107.150	0			
Bio10 (mean temp warmest quarter)							-0.1888	11.457	0.001
Bio11 (mean temp coldest quarter)				0.207	125.598	0			
Bio12 (annual precip)				0.00901	13.920	0			
Bio13 (precip wettest month)	0.0384	159.850	0						
Bio16 (precip wettest quarter)	-0.0822	51.897	0						
Bio17 (precip driest quarter)	0.0638	36.083	0	0.0366	175.189	0	0.0212	5.501	0.019
Bio18 (precip warmest quarter)	-0.0103	141.410	0	0.00091	7.386	0.007	0.00459	12.420	0
Bio19 (precip coldest quarter)	0.00551	56.794	0						
Elev (elevation)							-0.0114	9.755	0
Dist_agri (distance from agriculture)				0.000088	111.345	0	-0.00124	62.872	0
Sp-logit (espatial logit)	0.968	1.438.988	0	0.637	299.954	0	0.528	68.516	0
Loss0105 (forest loss 2001–2005)	20.437	16.251	0						
Loss1314 (forest loss 2013–2014)	-3.832	6.920	0.009						
Lu_wat (water)				4.356	80.704	0			
Places_dist (distance from towns)	-0.00005	91.939	0	-0.00005	211.709	0	-0.000193	57.763	0
Road dist (distance from roads)				-0.00011	270.278	0	-0.000540	46.327	0
Slope				-0.0872	31.106	0			
Soil_org (soil organic carbon)				0.0268	15.003	0			
Soil_pct (soil percent sand)	-0.270	236.970	0	0.138	262.414	0	0.0842	8.889	0.003
Stream_dist (distance from navigable streams)	0.000130	237.187	0	-0.000019	25.809	0	0.000043	8.496	0.004
Surf_rough	-0.0163	27.755	0				-0.0197	5.396	0.020
Constant	-183.082	270.727	0	-10.128	2.038	0.153	81.731	20.636	0

Proximity to roads and to towns and villages were significantly related to high favourability values for forest loss and fire; proximity to agriculture was also relevant. However, environmental variables defining high favourability for poaching were a combination of climatic variables (mainly high precipitation in the wettest month and low precipitation in the warmest quarter), topo-hydrography (high distance from navigable streams) and soil (low sand percentage). Favourable areas for poaching were largely concentrated around the centre of the reserve (Fig. 5.4e), but favourable areas for forest loss and fires were found outside the DFR (Fig. 5.4f, 5.4g). The combined threat index (Fig. 5.4h) indicated that areas that were most favourable for all threats together were along the western boundary and to a lesser extent just outside the eastern border of the DFR.

5.4.3. Combining wildlife and threat models

TI-WI maps for each threat factor indicated that the more favourable areas for poaching actually overlapped considerably with the more favourable areas for wildlife, in fact occupying most of the DFR (Fig. 5a). In contrast, the highest risk from forest loss and fires were concentrated along the western region of the study area, but always outside the DFR (Fig. 5b, c).

The combined TI-WI map showed that the highest levels of risk for wildlife were found along the western and the northern sectors of the DFR (Fig. 5d). Along the east of the DFR, high-risk areas are found just outside the park.

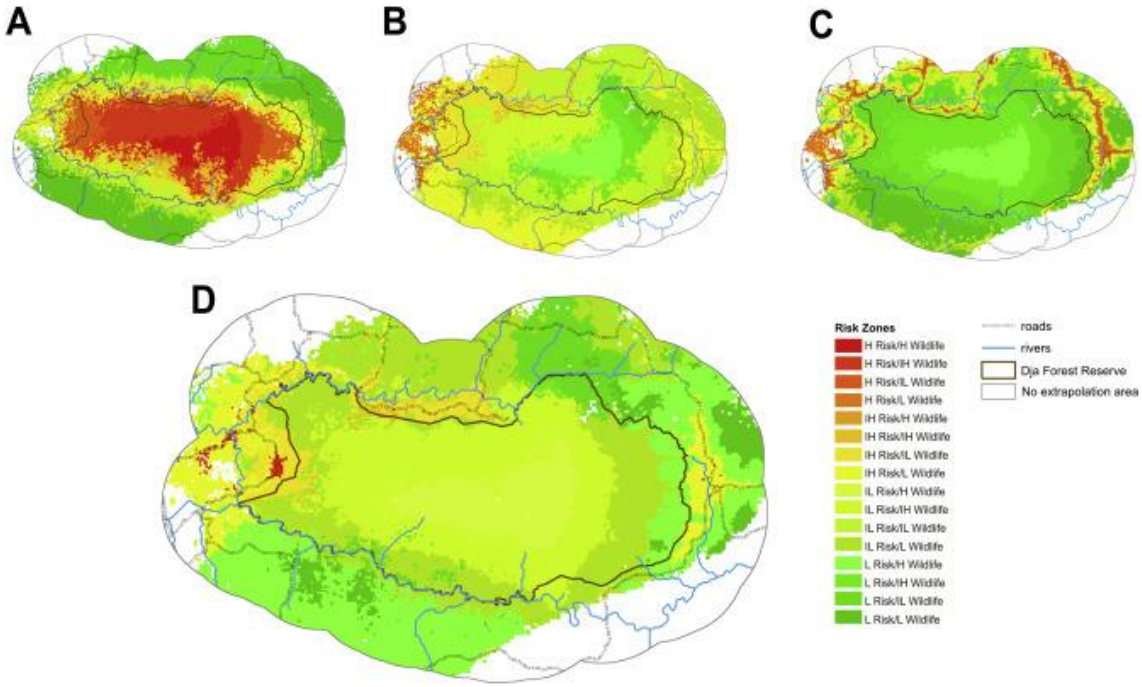

Fig. 5.5. Map of risk for wildlife based on the combination of the Wildlife Index and a) the threat of poaching (represented by favourable areas for ammunition and snare), b) threat of forest loss, c) threat of fire and d) three threats combined. High (H): ≥0.8, Intermediate-High (IH): (0.5–0.8), Intermediate-Low (IL): (0.5–0.2), Low (L): ≤0.2. The grey area was not considered for model projection.

5.5. Discussion

Electronic monitoring tools such as SMART and CyberTracker have been instrumental in empowering protected area managers to record and assess the state of faunal or other elements under their care. Nonetheless, the use of these tools is only effective if the plethora of law enforcement monitoring data that they are able to generate can be analysed promptly to guide management on the ground. Both SMART and CyberTracker, which are free and open-source, are highly configurable and therefore widely accessible to the conservation community, which often has widespread data-management needs. Although SMART is a relatively new piece of software that will no doubt develop further, the conservation community would benefit from parallel initiatives for development of analyses that integrate patrol data with independent data sources to inform more effective targeting of limited management assets.

Together, CyberTracker and SMART provide an integrated and accessible platform for systematic collection and aggregation of structured, actionable wildlife and threat distribution data from protected area patrols and monitoring programmes. Spatial modelling can add value to these data enabling managers to better understand events occurring within the protected areas and facilitate decision-making, whether in response to issues arising or in measuring the impact of new initiatives. Examples of the use of ranger patrol data alongside spatial modelling are still relatively scarce (but see Critchlow *et al.*, 2015 use of Bayesian methods to improve ranger patrols within protected areas).

Species distribution models (SDMs) are widely used in the fields of macroecology, biogeography and biodiversity research for modelling species geographic distributions based on correlations between known occurrence records and the environmental conditions at occurrence localities (Elith & Leathwick, 2009). Although a number of SDMs such as Ecological Niche Factor Analysis (ENFA), Maximum Entropy Approach (MaxEnt) and Favourability Function (Hirzel *et al.*, 2002; Phillips *et al.*, 2006; Real *et al.*, 2006; Elith & Leathwick, 2009) are commonly used, only favourability values for different modeled units (in our case study species and threats) can be compared in absolute terms. Favourability provides commensurate values and is independent from presence prevalence (Acevedo & Real, 2012). Such characteristics are particularly useful in conservation biology such as in defining areas where a group of species may be more vulnerable to different factors (Fa *et al.*, 2014) or when models for a large number of species need to be combined to define relevant areas for conservation (Estrada-Peña *et al.*, 2008). In this paper, we apply Favourability Function modelling which is an approach that has advantages over other more widely used spatial methods (see Acevedo & Real, 2012; Olivero *et al.*, 2016b). Favourability Function like logistic regression relies on assumptions such as the independence of observations, and limited multicollinearty which are not always restricted met. We show how ranger and satellite data can be effectively overlaid to model the distribution of animal

species of conservation interest, to determine areas likely to be more at risk from poaching and other anthropogenic factors.

Scarce technical and human resources and inadequate resource management are among the main reasons for the decline in wild populations of many threatened large mammal species across the Congo Basin, both inside and outside protected areas (Campbell *et al.*, 2008; Kühl *et al.*, 2017). Because of this, the more effective application of existing resources could benefit from the use of suitable tools for wildlife management and conservation. In this study, we propose a conservation biogeography approach to assist in the protection of wild populations of three threatened, iconic African mammal species. Our models clearly suggest that the most favourable areas for gorillas, chimpanzees and elephants are found within the core of the studied protected area, the DFR. According to this, isolation is a highly relevant factor, since the most important variable explaining the presence of the three species in our wildlife models was "distance to roads". This also explains why large areas located within the core of the DFR, at least during our study period, are highly favourable for the three species. These results are corroborated by field work undertaken by one of our authors, (JD) who undertook a transect of 98 km through the middle of the DFR, and who found higher levels of wildlife signs, particularly of elephants, within the core of the reserve (Dupain *et al.*, 2017). Our models clearly suggest that favourable areas for poaching, as expected, correspond with the more favourable areas for wildlife. In both cases, areas that are more distant from roads, from navigable rivers and from human settlements, hence more remote, were more favourable to poaching and wildlife. Also, these areas, primarily along the north-western region of the reserve, are those with a higher proportion of soil. This may point to the fact that more sandy soils are linked to poorer forests, in terms of plant and animal diversity, so naturally poachers are likely to search for animals to hunt in remote forests in deeper soils.

Our results confirm the findings of regional analyses of the spatial relationship between the distribution of gorillas, chimpanzees and elephants and human activities in other parts of the Congo Basin (Stokes *et al.*, 2010; Maisels *et al.*, 2013; Strindberg *et al.*, 2018). In the case of the great apes, Strindberg *et al.* (2018) showed that human-related variables (in particular distance to roads and human population densities) as well as canopy height and Ebola (natural variables) were important predictors of great ape density and distribution. Stokes *et al.* (2010) also indicated that chimpanzees show a clear preference for unlogged or more mature forests and human disturbance had a negative influence on chimpanzee abundance, in spite of anti-poaching interventions. Similarly, proximity to the single integrally protected area in the landscape maintained an overriding positive influence on elephant abundance, and logging roads (exploited by elephant poachers) had a major negative influence on the species' distribution (Stokes *et al.*, 2010).

In our study area (DFR and buffer zone) we show that there are clear spatial differences in the distribution of threats. Areas outside the DFR are mostly affected by forest loss and, secondarily modified by fire. In contrast, wildlife risk areas, due to poaching, are concentrated inside the DFR, where high-diversity areas (according to the WI) overlap with zones where poaching occurs. However, the three threat models combined indicated that the areas outside the DFR (principally in the west but also in the north and the east, see Fig. 5.4h) were the areas with the highest overall risk, with areas within the protected area itself presenting intermediate risk values. This is a consequence of integrating two threat factors that occur principally outside the DFR margins (i.e. forest loss and fire), and only one factor affecting the inside of the DFR (i.e. poaching).

Model-based approaches have clearly demonstrated that in Central Africa poaching and disease are the main threats affecting the survival of great apes, whereas poaching is the prime menace against elephants (Walsh *et al.*, 2003; Stokes *et al.*, 2010; Maisels *et al.*, 2013; Fa *et al.*, 2014; Wich *et al.*, 2014; Critchlow

et al., 2015; Gong *et al.*, 2017; Strindberg *et al.*, 2018). Such models are useful tools for determining the impact of anthropogenic disturbances on protected species on a broad biogeographical scale. However, unlike other commonly used SDM approaches, Favourability Function models and risk maps, as we show in this paper, can provide easily available rapid assessment tools to highlight the most vulnerable regions for species of conservation concern. Conservation managers and planners are able to use these maps to allow a more effective application of human and technical resources and implement more effective conservation measures. Although we have shown that data gathered in the field can be easily analysed beyond the SMART platform, the skills required to undertake modelling such as that performed in this study will require a different staff profile from those involved in the day-to-day running of a protected area. Currently, the application of spatial models to real situations is scarce, but we suggest that this may be possible by finding pragmatic, cost-effective ways in which modelling (and modellers) can be integrated in the team of experts involved with the management wildlife and protected areas. Data input, preparation, and analyses should be planned by modellers who can harness the growing volume of field and satellite-derived data to characterize levels of threat and distribution of wildlife to enable more agile protection of highly threatened species and spaces.

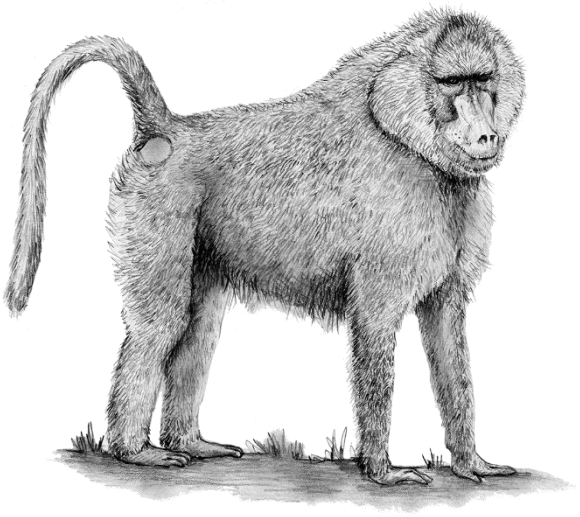

CAPÍTULO 6

Worldwide dynamic biogeography of zoonotic and anthroponotic dengue

Biogeografía dinámica mundial del dengue zoonótico y antroponótico

Este capítulo se basa en/ This chapter is based on:

Aliaga-Samanez A, Cobos-Mayo M, Real R, Segura M, Romero D, Fa JE, et al. (2021) Worldwide dynamic biogeography of zoonotic and anthroponotic dengue. PLoS Negl Trop Dis 15(6): e0009496. https://doi.org/10.1371/journal.pntd.0009496 **(Q1)**.

6 Worldwide dynamic biogeography of zoonotic and anthroponotic dengue

6.1. Abstract

Dengue is a viral disease transmitted by mosquitoes. The rapid spread of dengue could lead to a global pandemic, and so the geographical extent of this spread needs to be assessed and predicted. There are also reasons to suggest that transmission of dengue from non-human primates in tropical forest cycles is being underestimated. We investigate the fine-scale geographic changes in transmission risk since the late 20th century, and take into account for the first time the potential role that primate biogeography and sylvatic vectors play in increasing the disease transmission risk. We apply a biogeographic framework to the most recent global dataset of dengue cases. Temporally stratified models describing favorable areas for vector presence and for disease transmission are combined. Our models were validated for predictive capacity, and point to a significant broadening of vector presence in tropical and non-tropical areas globally. We show that dengue transmission is likely to spread to affected areas in China, Papua New Guinea, Australia, USA, Colombia, Venezuela, Madagascar, as well as to cities in Europe and Japan. These models also suggest that dengue transmission is likely to spread to regions where there are presently no or very few reports of occurrence. According to our results, sylvatic dengue cycles account for a small percentage of the global extent of the human case record, but could be increasing in relevance in Asia, Africa, and South America. The spatial distribution of factors favoring transmission risk in different regions of the world allows for distinct management strategies to be prepared.

6.2. Introduction

Dengue is a viral disease caused by the dengue virus, a group of four Flaviviridae serotypes (Gubler, 2002). The pathogen is principally transmitted by female mosquitoes of the genus *Aedes* to humans. In most cases, the pathogen causes mild illness, but is also known to cause flu-like symptoms, occasionally producing severe complications that are fatal (WHO, 2020a). More than 14,000 annual deaths are reported (Stanaway *et al.*, 2016). Dengue infections occur mainly in the Asian, African, and American tropics, but are being reported in many regions worldwide. The rapid spread of dengue is considered to represent a global pandemic threat (WHO, 2012).

The World Health Organization (WHO) reports that annual dengue cases have increased from approximately 500,000 in 2000 to approximately 4.2 million in 2019 (WHO, 2020a). This is considered an underestimation, however. Some authors have calculated that in 2013 between 58.4 million (Stanaway *et al.*, 2016) and 96 million (Bhatt *et al.*, 2013) yearly cases may have occurred worldwide, with many cases remaining unreported (Grange *et al.*, 2014) and other cases being mistaken for similar pathologies (Potts & Rothman, 2009; Kuno, 2015). This confusion presents serious challenges for assessing the scale and geographic extent of the risk of disease transmission. However, distribution modelling has been used to map the global risk (Bhatt *et al.*, 2013; Messina *et al.*, 2019).

Distribution models are useful not only for locating risk hotspots (Peterson, 2006; Purse & Golding, 2015) but also can be employed to inform prevention and mitigation strategies (Hay *et al.*, 2013; Cattarino *et al.*, 2020) such as vector control measures, large-scale vaccination programmes, and traveller health-care advice. The first global dengue model produced at a high resolution described the geographic distribution of the risk of dengue transmission for the period 1960–2010 (Bhatt *et al.*, 2013). According to this model, as many as 390 million dengue infections in 128 countries were predicted (Brady *et al.*, 2012), in contrast to the

4.2 million cases recorded in 2019 (WHO, 2020a). Annual records of dengue transmission (Messina *et al.*, 2014b) up to 2015 have provided data for the generation of risk models (Messina *et al.*, 2019), which have also considered the environmental suitability for the arbovirus vectors *Aedes aegypti* and *Ae. albopictus* as covariables (Kraemer *et al.*, 2019). The integration of known and potential reservoir species in disease distribution models has already proved invaluable in pathogeography (Pigott *et al.*, 2016; Olivero *et al.*, 2017a) whereas the design of disease models that reflect complex interactions has benefited from biogeographical concepts and tools (Olivero *et al.*, 2011, 2017a; Romero *et al.*, 2019). Thus, determining the distribution of infectious diseases needs to take into account the patterns of distribution of reservoirs and/or vectors (Guernier *et al.*, 2004; Murray *et al.*, 2015) and the ecology of the pathogen itself (Murray *et al.*, 2018), which involves consideration of the environment as well as the human-geography context.

Dengue is principally an indirectly transmitted anthroponosis (Wilson, 2001), humans being the main hosts and *Aedes* mosquitoes the main vectors. However, there are zoonotic "sylvatic" cycles in Africa and Asia where non-human primates are asymptomatically infected by the dengue virus, which is efficiently transmitted by the mosquito fauna in these regions (Rico-Hesse, 1990; Gubler, 1998; Holmes & Twiddy, 2003). There is evidence to suggest that the virus originated in monkeys, and that every one of its four serotypes was independently transmitted to humans in Africa and Asia (Holmes & Twiddy, 2003; Vasilakis *et al.*, 2011). Transmission to humans from other primates appears to be infrequent, but they do occur. The scarcity of records might be a result of inadequate characterization of human exposure to sylvatic viruses (Vasilakis *et al.*, 2011). In Africa and in Asia, there is high potential for the re-emergence of sylvatic dengue in the human transmission cycle as a result of deforestation, climate change, and vector geographic expansion (Vasilakis *et al.*, 2011). While the existence of sylvatic dengue cycles has not been demonstrated in the Neotropical region, there are

reasons to foresee this possibility. This is because enzootic cycles based on American primates are involved in the diversification and transmission to humans of the yellow-fever virus, which shares vectors with the dengue virus (Bryant *et al.*, 2003; Baronti *et al.*, 2011; Auguste *et al.*, 2015).

Sylvatic cycles in South America appear to shape the evolutionary dynamics of recent yellow-fever-virus lineages, and are involved in the current re-emergence of this virus in Brazil (Mir *et al.*, 2017). In this country, dengue-virus-RNA has been found in sylvatic mosquitoes that are vectors of the yellow-fever virus (de Figueiredo *et al.*, 2010). In addition, dengue-virus infections in humans may have occurred in Bolivia in the absence of *Ae. aegypti* and *Ae. albopictus* (Roberts *et al.*, 1984), and different mammalian taxa have been infected with dengue-virus in French Guiana (de Thoisy *et al.*, 2009). In light of these data, the possible presence of sylvatic dengue in the American continent is likely (Marcondes & Tauil, 2011; Vasilakis *et al.*, 2011).

Available models defining the global risk of dengue transmission have not included a zoonotic component. Although likely to be negligible at a global scale, sylvatic-dengue cycles may increase local or regional risk amplification, or represent a threat of dengue re-emergence or diversification. In addition, the global risk of transmission to humans is increasing as a consequence of globalization (Tatem *et al.*, 2006). The pathogen is easily transported by travelers (Leta *et al.*, 2018), and there is a rapid expansion of the main vectors (Kraemer *et al.*, 2015b; Gossner *et al.*, 2018), which also evolve as they spread (Brown *et al.*, 2014). This means that modelling approaches involving temporal stratification are required in the production of dengue-risk maps, as well as a multidisciplinary approach as proposed by the international *One Health* initiative (Gibbs, 2004), to consider a multifactorial dynamic. Hence, evaluations of the current risk should take into account a combination of the inertia of past times, the advent of new factors capable of changing previous expectations, and the zoonotic dimension.

Here, we adopt a multitemporal and multifactorial pathogeographic approach to analyzing the risk of dengue transmission to humans. We produced a risk model for the early 21st century, using available information on dengue cases up to 2019. We achieve this under the assumption that transmission between humans is (1) limited by the vector presence, (2) constrained by environmental conditions favoring vectorial capacity (Gething *et al.*, 2011), (3) could be locally or regionally favored by the occurrence of enzootic cycles in the tropical forests, and (4) are experiencing an inter- and intra-continental spread that is subject to the growth of both virus' and vectors' ranges. Our aim is to contribute to the international health system with reliable forecasts on areas where dengue transmission between humans could increase in the near future, and with quantification and mapping of the contribution of sylvatic cycles.

6.3. Material and methods

6.3.1. Study area and time period

All spatially explicit data (i.e., dengue case records, mosquito occurrences, primate ranges, environmental variables) were projected onto a worldwide grid composed of 18,874 hexagonal units of 7,774 km^2, built using Discrete Global Grids for R (Barnes, 2017). In this way, we prevented autocorrelation that could result from spatial dependence among very close occurrences (Legendre & Legendre, 1998).

As the dengue spatial trends are dynamic, the temporal extent for analysis purposes was divided into three periods: 1970–2000 ("the late 20th century"), 2001–2017 ("the early 21st century"), and 2018–2019. Pre-1970 records were not considered so as to limit our conclusions to a contemporary setting. Some milestones regarding the fight against arboviral diseases occurred circa 1970, such as the re-infestation of Latin America with *Ae. aegypti*, the main vector of the dengue virus, after 50 years of eradication efforts (Soper, 1963). The use of DDT was suspended in the late 1960s in several countries of the Americas due to resistance (Maestre-Serrano *et al.*, 2010). Although the limit between periods at

the turn of the century is arbitrary, it reflects distributional changes in the ranges of the two urban *Aedes* vectors as well as the increase of case reports in sizeable regions all over the world—being, for example, previous to any contemporary record of autochtonous *Aedes*-born disease transmission in Europe and Japan. The bases of the current globalization of international movements were established in the last decade of the 20th century (e.g., with the fall of the Iron Curtain, the advent of the Internet, and the start of low-cost flights); and their full potential was reached just after the start of the 21st century (e.g., with the opening of international borders, the widespread access to the Internet and to cell phones, and the online travel booking generalization). In fact, from 1970 to 2000, global exports nearly doubled to approximately a quarter of global GDP (Mometrix Test Preparation, 2021). The time stratification also provides further opportunities for model validation. Thus, predictions afforded by the late 20th-century models were validated using early 21st-century datasets, and validations of the early 21st-century-model predictions were addressed with post-2017 records. In addition, by performing separate analyses for both centuries, we were able to integrate, in our 21st-century models, social and ecological descriptors that are only available for the last two decades.

6.3.2. Methodological framework

The ultimate objective of our analyses was to build a map that quantified the current level of dengue transmission risk worldwide. This map results from the combination of both a model describing favorable areas for the presence of vectors, and a model describing favorable areas for the occurrence of disease cases. These models were based on the predictive power of macro-environmental and spatial variables that included climate, topo-hydrography, vegetation, human activity, spatial autocorrelation, and potential for enzootic transmission. We first produced models focused on the late 20th century, which were later updated for the early 21st century through a procedure that involved reparameterization and the addition of variables representing changes in the distribution of the modelled

item (i.e., of vector presences and dengue cases). The rationale for this addition is that, when animal and pathogen species spread, their distribution at a given moment is influenced by (1) the inertia of previous situations (i.e., temporal autocorrelation), here represented by the late 20th-century model, and (2) by a multifactorial set of new drivers potentially favoring the spread (i.e., spatial autocorrelation, environmental and socio-economic factors). A schematic description of our methodological framework is represented in Fig 6.1. The outputs of these models were expressed as favorability values (*F*, ranging 0-1) that represent the degree to which environmental conditions, at a particular spatial unit, favor the occurrence of a given event. Thus, favorability is equivalent to a degree of membership in the fuzzy set of environmentally favorable units (Real *et al.*, 2006), so that models based on favorability can be compared and combined through the implementation of fuzzy-sets theory tools (Barbosa & Real, 2012). *F* was calculated according to the Favorability Function (Real *et al.*, 2006; Acevedo & Real, 2012), defined by the following formula:

$$F = \frac{\frac{P}{1-P}}{\frac{n_1}{n_0} + \frac{P}{1-P}}$$

where *P* is the probability of occurrence of the event in question, n_1 is the number of recorded occurrences, and n_0 is the number of units in which occurrences have not been recorded. *P* values were calculated through forward-backward stepwise logistic regression (using IBM SPSS Statistics 23), in which predictor variables were selected according to Rao's score tests (Radhakrishna Rao, 1948), and derived from the formula:

$$P = \frac{e^y}{1 + e^y}$$

where *e* is the basis of Napierian logarithms, and *y* is the "logit equation", i.e. a linear combination of the predictor variables selected. We used iterative log-likelihood maximization for *y*-coefficient parameterization using a gradient

ascent machine learning algorithm, and Wald tests (Wald, 1943) for evaluating the contribution of every variable in a model. The forward-backward stepwise approach prevents redundancy between variables in a model, as variable removal along the stepwise variable selection is allowed. Nevertheless, we strengthened prevention against excessive multicollinearity by preventing variables with Spearman correlation coefficients >0.8 from coinciding in the same model (Olivero *et al.*, 2017a). In case this happened, the least significant variable was deleted and the model was trained again. Benjamini & Hochberg's (1995) procedure for calculating the False Discovery Rate (FDR) was followed to minimise Type I errors that could occur from the consideration of a large number of variables.

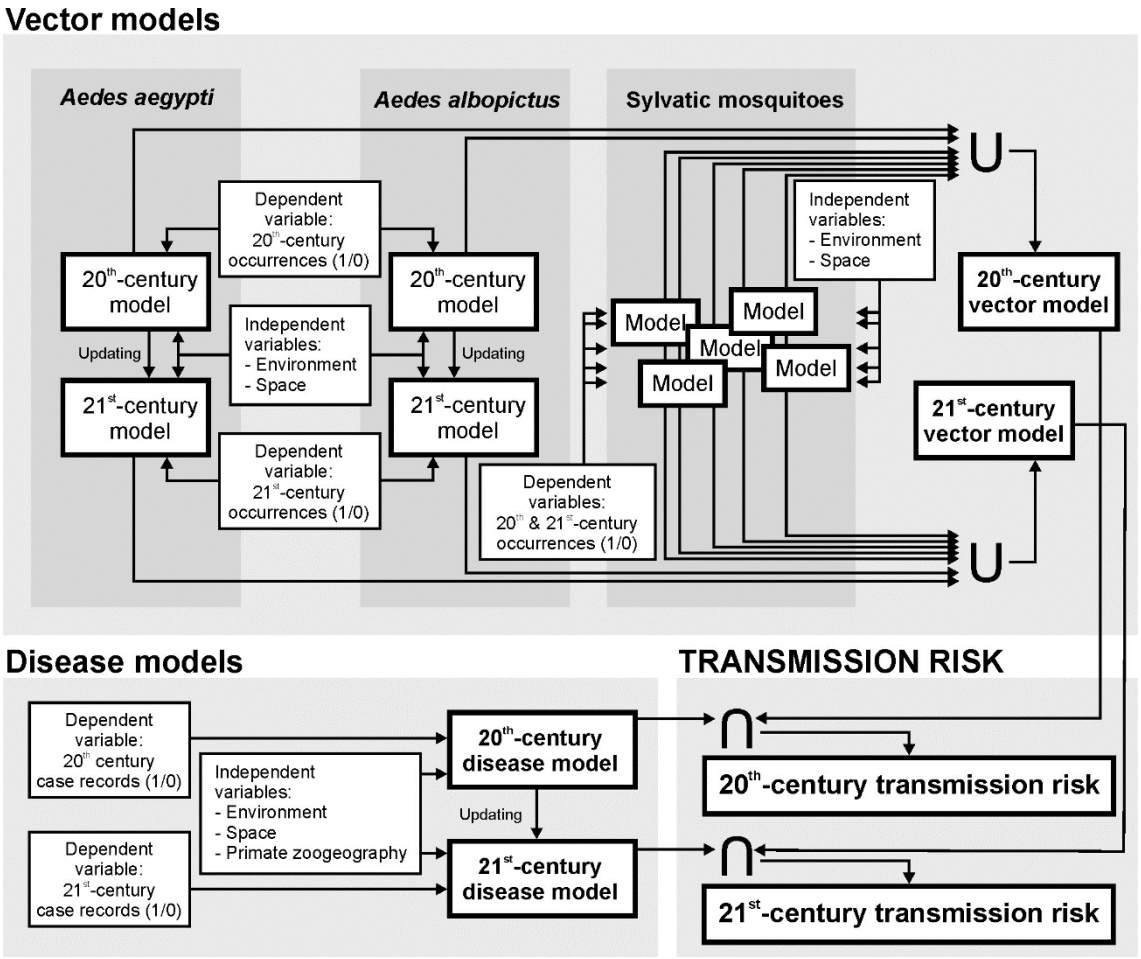

Fig. 6.1. Methodological framework for dengue transmission risk modelling. **Vector models** result from combining, through the fuzzy union (U), favorable areas for the presence of urban and sylvatic vectors, thus denoting that the presence of one vector species already implies some

potential for disease transmission to humans if the pathogen is present. For a given time period and vector species, a vector model is built using mosquito occurrences as dependent variables, and spatial/environmental descriptors as independent predictor variables. **Disease models** describe the areas favorable to the occurrence of dengue cases, using the presence/absence of dengue-case records as dependent variables, and spatial/environmental/zoogeographic descriptors as independent predictor variables. A temporal stratification differentiating between the late 20th century and the early 21st century was applied when the modelled item was subject to a temporally changing dynamic, i.e. to the global distribution of *Ae. aegypti*, *Ae. albopictus*, and dengue cases. 20th-century models were updated by complementing their equations with new variables capable of accounting for the observed changes of distribution. Finally, **transmission-risk models** quantify the level of dengue-transmission risk, according to the fuzzy intersection (∩) between vector and disease models. The intersection reflects that, for dengue to be transmitted in a given location, two elements, acting as limiting factors, must coincide in the area: 1) suitable environmental conditions for disease cases to occur; and 2) suitable conditions for the presence of vectors. Complete methodological descriptions are provided in the main text.

6.3.3. Vector models

We built a global database of dengue vectors on the grid of 7,774-km^2 hexagonal units, through the projection of georeferenced records into hexagons, using ArcGIS 10.3. Records on mosquito species involved in the urban cycle, i.e., *Ae. aegypti* and *Ae. albopictus*, for the period 1970–2014, were taken from "The global compendium of *Aedes aegypti* and *Ae. albopictus occurrence*" (Kraemer *et al.*, 2015a) (Appendix 4). Later occurrences were retrieved from the expert-validated citizen-science platform Mosquito Alert (http://www.mosquitoalert.com/) and from VectorBase (https://www.vectorbase.org/).

Available records on sylvatic vectors (Wang *et al.*, 2000; Vasilakis *et al.*, 2008, 2011; Sudeep & Shil, 2017) (mosquito species *Ae. polynesiensis*, *Ae. luteocephalus, Ae. africanus, Ae. niveus and Ae. vittatus*) were obtained from the literature (Appendix 5), Vectormap (vectormap.si.edu), and Gbif (https://gbif.org) (Appendix 4).

A worldwide favorability model was built for each mosquito species, using presence/absence of occurrence records at each hexagon as dependent variables, and environmental (i.e., climate, topo-hydrography, vegetation, and human-activity) descriptors as independent predictor variables (Appendix 6). Only variables that can be considered reasonably stable in the short term were used at this stage of the analysis, due to the scarcity of high-resolution data for the late

20th century and the changing nature of environments during the study period. Thus, climate was represented by average values for the period 1979–2013 (Karger *et al.*, 2017), vegetation was described using terrestrial ecoregions (Olson *et al.*, 2001), and the human factor was represented by the distance to populated settlements (FAO, 2000) (thus avoiding having to change parameters such as population density, land use, and infrastructure). In addition to environmental variables, we used a trend surface approach (Legendre, 1993) to account for purely spatial factors linked to contagious evolutionary and ecological processes preventing or promoting distribution shifts (Legendre, 1993; Record *et al.*, 2013). The spatial factor could distinguish areas with similar environmental conditions but different probabilities of being reached by a spreading species. This could happen because of spatial autocorrelation (i.e., the species could have nearby populations in some cases); or it could be a result of recent introductions or reintroductions. On every continent that the species occur, we developed a favorability model based on purely spatial descriptors (Legendre & Legendre, 1998) (i.e., 1st to 3rd-degree polynomial combinations of latitude and longitude). Then we added the resulting spatial-model outputs to the set of environmental variables.

In the case of urban-cycle mosquitoes, we generated favorability models based on late 20th-century occurrence records, subsequently updated for the early 21st century. We updated it by developing a model based on early 21st-century occurrence records. This model was completed in two blocks: (1) forcing the entry, as predictor variable, of the late 20th-century-model logit equation; and (2) performing a later stepwise selection in which only variables with the potential to account for changes with respect to the late 20th-century model were selected. This two-block variable selection was implemented using IBM SPSS Statistics 23.

Models for sylvatic-cycle mosquito species were run without temporal considerations, using the above-mentioned set of predictor variables. This is

justified by the scarcity of occurrence records available for these species and by the assumption that their ranges have not changed substantially during the study period, which is based on a comparison of descriptions in the historical literature (Huang, 1977; WHO, 1989; Sudeep & Shil, 2017).

A vector favorability model for the late 20th century was produced using a combination of all individual vector models, including those for the sylvatic vectors and those for the urban vectors. We used the fuzzy union (Zadeh, 1965) for this purpose, which consisted of selecting, for every hexagon, the highest favorability value among those obtained in an individual model. The rationale for this criterion was that, if the pathogen is present in the area, the mere presence of one vector species already implies some potential for disease transmission to humans. Similarly, we created a vector model for the early 21st century.

6.3.4. Disease model

The global record of dengue cases was projected onto 7,774-km^2 hexagons using ArcGIS 10.3. Georeferenced cases for the period 1970–2017 were obtained from the Messina et al.'s database (Messina *et al.*, 2019), and considered only if they matched with the following criteria: (1) they were referred to precise locations, or (2) they were referred to centroids of polygons whose extensions were lower than or similar to the size of the hexagons (Appendix 4). These data were completed with reports from Promedmail.org, using "DENGUE" as the keyword and limiting the search to the period 2013–2019, and with data provided by the epidemiological bulletins and weekly epidemiological surveillance of the Ministries of Health from Brazil, Costa Rica, Colombia, Ecuador, United States of America, Philippines, Honduras, Malaysia, Mexico, Myanmar, Palau, Puerto Rico, Samoa, Sri Lanka, and Thailand. In addition, we carried out searches in reports published by the European Centre for Disease Prevention and Control (ECDC): Communicable disease threats to public health in the European Union—Annual Epidemiological Report; and by the WHO: Dengue Situation Updates. Case

reports for Africa were complemented with the Weekly Bulletin on Outbreaks and Other Emergencies (WHO, African Region), and publications available since 2017. Further information was obtained from the WHO and the Pan American Health Organization (PAHO) websites, and from the Global Infectious Disease and Epidemiology Online Network (GIDEON) (Berger, 2015).

We built a worldwide disease favorability model using presence/absence of case records at each hexagon as the dependent variable, and spatial/environmental descriptors as independent predictor variables (Appendix 6). We used a similar methodological procedure as for vector species, including the performance of a late 20th-century model and its later update based on the early 21st century. The only difference with respect to the vector models was the inclusion of zoogeographical information in the set of predictor variables. This information defined the types of distribution ranges (i.e., chorotypes) of non-human primates, i.e., the most probable dengue reservoirs in the sylvatic cycles. A chorotype is a particular distribution pattern shared by a group of species, and may result from ecological and/or historical causes (Real *et al.*, 2008). When knowledge of the reservoir-species complex is imprecise, the consideration of variables defining chorotypes shared by potential reservoirs helps to improve risk models referred to the distribution of zoonotic disease transmission (Olivero *et al.*, 2017a; Murray *et al.*, 2018). These primate-chorotype variables were defined in six steps:

1. Range maps of the African, Asian, and American primate species were obtained from the the IUCN (IUCN, 2019), and were projected onto the grid of 7,774-km^2 hexagons to produce a presence/absence matrix. The surface area of these units approximates the resolution below which extent-of-occurrence maps provided by the International Union for Conservation of Nature (IUCN) should not be employed for the characterization of macroecological patterns (Hurlbert & Jetz, 2007).
2. Chorotype analyses for each continent were addressed separately.

3. Primate ranges were classified hierarchically according to the Baroni-Urbani & Buser's similarity index (Buser, 1976), using the unweighted pair-group method using arithmetic averages (UPGMA) (Sneath & Sokal, 1973; Kreft & Jetz, 2010).
4. All clusters in the resulting classification dendrogram were assessed for statistical significance using the method proposed by Olivero and colleagues (Olivero *et al.*, 2011), which uses RMacoqui 1.0 software (http://rmacoqui.r-forge.r-project.org/). Groups of distributions that were significantly clustered were considered chorotypes.
5. For each chorotype, a predictor variable was defined using the chorotype species richness (Olivero *et al.*, 2011); that is, in each hexagon, we quantified the number of species whose distributions formed part of the chorotype.
6. We then ran a forward-backward stepwise logistic regression using presence/absence of dengue case records as the dependent variable and chorotype variables as predictors. Only the chorotype-variables selected were considered henceforth.

We did not consider primates to be a limiting factor, since dengue cases among humans could be influenced by, but not depend on the presence of primates in the area (Vasilakis *et al.*, 2011). Guided by this rationale, we produced the disease favorability model for the late 20th-century cases in two blocks: (1) a stepwise selection of environmental and spatial variables; (2) a later stepwise selection of chorotypes that contribute to improve significantly the model likelihood. In turn, the updating of the model based on cases from the early 21st century consisted of three blocks: (1) forcing the entry of the late 20th-century-model logit equation as a predictor variable; (2) making a later stepwise selection of spatial/environmental variables; (3) ending with a stepwise selection of chorotypes contributing to improve model likelihood.

6.3.5. Dengue transmission-risk model

We defined a dengue transmission-risk model according to the intersection between a disease model and a vector model. The fuzzy intersection is used to combine models that represent favorable conditions according to limiting factors (i.e., factors that describe imperative conditions for the modelled item to be present) (Romero *et al.*, 2016). Thus, the transmission-risk model reflected that, for the pathogen to be transmitted in a given hexagon, two elements must coexist: (1) suitable environmental conditions for disease cases to occur; and (2) suitable conditions for the presence of vectors. In operative terms, the intersection consisted of selecting, for every hexagon, the lowest favorability value among those obtained in the different models (Zadeh, 1965). This approach has been used before to reflect the simultaneous need of suitable environments and mammal assemblages for the zoonotic transmission of the Ebola virus to humans (Olivero *et al.*, 2017a). Transmission-risk models were made for both the late 20th and the early 21st centuries. Favorability (F) values were finally reinterpreted as transmission-risk values following this scale: high favorability (i.e., $F > 0.8$ (Muñoz *et al.*, 2005)) was referred as high transmission risk; intermediate-high favorability values ($0.5 \leq F \leq 0.8$) were referred as intermediate-high risk; intermediate-low favorability values ($0.2 \leq F < 0.5$) were referred as intermediate-low risk; and low favorability (i.e. $F < 0.2$ (Muñoz *et al.*, 2005)) was referred as low transmission risk. $F = 0.2$ and $F = 0.8$ match approximately the inflection points in the logistic favorability function, while $F = 0.5$ is the threshold above with the transmission probability defined by spatial and environmental factors is higher than the random transmission probability (Acevedo & Real, 2012).

6.3.6. Transmission-model refinement

The early 21st-century dengue transmission-risk model was refined through model enhancing and downscaling. The models for the 21st century described above, based on variables that are also available for the late 20th century, were useful for risk-map comparisons between periods; however, an enhanced early

21st-century model permitted a more updated representation of factors that could aid in defining the risk of disease transmission. Enhancing was performed through the development of new disease and vector models on the basis of an expanded set of predictors, i.e. complementing the former set of variables with others only available for the early 21st century: human population density, infrastructures, land use, vegetation cover, and forest loss (Appendix 6). Descriptors of livestock density were also considered for the enhancement of vector models. The proximity of human populations and activities not only imply the availability of human potential hosts. Human-modified environments usually provide chances for the local reproduction of urban *Aedes* mosquitoes (e.g. water points) (Overgaard *et al.*, 2017).

The enhanced transmission-risk model was finally downscaled from the initial 7,774-km^2 spatial resolution to a new grid based on 58,612 hexagons of 2,591 km^2 (i.e. to 66.7% smaller units), using the direct downscaling approach (Bombi & D'Amen, 2012). Model predictions should remain meaningful after this downscaling has taken place as, according to Bombi & D'Amen (Bombi & D'Amen, 2012), predictions are not severely affected by a 10-fold shortening of side lengths in the case of squared spatial units, which is equivalent to a 99% decrease of the surface area. The direct downscaling consisted of projecting the favorability equation that defined the original model to a set of variables considered in the finer-resolution grid of hexagons. In order to avoid local artifacts that could result from this downscaling, we excluded from the downscalled outputs all favorable areas that were not highlighted by the pre-downscaling models.

6.3.7. Model assessment and validation

Model goodness-of-fit was evaluated according to Chi-square tests. Discrimination capacity was assessed according to the area under the "receiver operating characteristic (ROC)" curve (AUC) (Lobo *et al.*, 2008). We also assessed

classification capacity based on two favorability thresholds: 0.5, at which probability is equal to the overall prevalence (Acevedo & Real, 2012); and 0.2, below which the risk of disease transmission was considered to be low (see above). The classification indices employed were the sensitivity, the specificity, the correct classification rate (CCR), Cohen's kappa, the under-prediction rate, and the over-prediction rate (Fielding & Bell, 1997; Barbosa & Real, 2012).

We validated the predictive capacity of the late 20th-century disease and transmission-risk models through the evaluation of their discrimination and classification capacities with regard to the 2001–2017 case record. Similarly, the predictive capacity of the early 21st-century model was validated with regard to the dengue cases reported in 2018 and 2019.

6.3.8. Contribution of the zoonotic factor

We used a variation partitioning approach (Borcard *et al.*, 1992) to calculate the relative contribution of non-human primates in determining the environmental favorability for the occurrence of dengue cases. We estimated how much of the variation in favorability for the occurrence of dengue cases was explained by the pure effect of primates (here represented by primate chorotypes), and how much was explained by the pure effect of environmental and spatial constraints. The method used (Muñoz & Real, 2006) also allowed us to calculate how much of the variation in favorability was attributable to both factors (i.e., the shared effect), because primate ranges, in the same way as disease cases, are likely to be influenced by environmental and spatial constraints.

To map the areas in which the sylvatic cycle could have contributed to increase the record of dengue cases in humans, we identified the hexagons in which: 1) favorability values for the presence of dengue cases were ≥0.2; and 2) the difference between favorability values provided by the dengue model, and favorability values provided by a model not considering chorotypes, was positive and ≥0.1.

6.4. Results

6.4.1. Vector models

6.4.1.1. Urban mosquitoes

The global distribution of occurrence records and of favorable areas (as defined by environmental and spatial variables) (F≥0.2) for the presence of *Ae. aegypti* and *Ae. albopictus* in the late 20th and the early 21st centuries can be seen in Appendix 7. *Ae. albopictus* was less widespread but showed a more expansive spatial trend. In the late 20th century, favorable areas for *Ae. aegypti* covered extensive regions in North and South America, but included little of the inner Amazon basin. In contrast, *Ae. albopictus* exhibited highly restricted favorable areas in western USA and in South-Brazil coastal areas. In Africa, *Ae. aegypti* occupied large tropical regions, whereas *Ae. albopictus* only occurred in some areas to the south and the north-west of the continent and in Madagascar. Favorable areas for both species were similar in Asia, although they extended further westward for *Ae. aegypti* and eastward for *Ae. albopictus*. There were more favorable areas for *Ae. aegypti* in Australia than for *Ae. albopictus*, but the opposite was the case in New Zealand. In Europe, only *Ae. albopictus* occurred, with favorable areas extending across the Mediterranean region. These models are strongly characterized by the spatial factor, and highlight the environmental relevance of shorter distances to population centers and high annual precipitation (Appendix 8 and 9). The presence of *Ae. aegypti* was also favored by high summer temperatures though *Ae. albopictus* was favored in the temperate-conifer-forest ecoregion by low elevations and a high temperature annual range.

During the early 21st century (Appendix 7), favorable areas for *Ae. aegypti* in America reached most of the Amazon basin and expanded south to Argentina and Chile, as well as into North-West USA. *Ae. albopictus* occupied new areas in North and South America, and spread radially in Central Africa, northward into East Asia, and east and westward in the Mediterranean region of Europe. The

models show that both species expanded their spatial/environmentally favorable areas into tropical broadleaf forests and temperate grasslands/savannas (Appendix 8 and 9). The range of *Ae. aegypti* also expanded in temperate conifer forests, and was favored by high winter temperatures. *Ae. albopictus* spread in the Mediterranean and in the temperate-broadleaf ecoregions, its presence favored by a high precipitation seasonality. For both species, the refined models outlined the relevance of human presence in explaining the ongoing spread: high human population density, intensive livestock rearing, and, for *Ae. albopictus*, the proximity of railways and roads.

6.4.1.2. Sylvatic mosquitoes

Details of the favorability models generated for the five sylvatic mosquito species are shown in Appendix 10-12. The presence of the four continental species, namely *Ae. africanus*, *Ae. luteocephalus*, *Ae. niveus*, and *Ae. vittatus*, is favored by high minimum temperatures in the coldest months, and in some cases also by high maximum annual temperatures or high precipitation seasonality. *Aedes polynesiensis* was only characterized by its Pacific-insular spatial pattern. Some tropical ecoregions, linked to moist broadleaf forests or to grasslands and savannas, favor the presence of the African and Asian endemics. In contrast, the old-world species *Ae. vittatus* finds suitable habitats in Mediterranean landscapes as well, especially close to human-populated regions. The refined models highlight the relevance of humanized environments including the presence of croplands, areas inhabited by livestock or humans, and human infrastructures.

6.4.1.3. Integrated vector models

Favorable areas for the presence of at least one dengue-vector species, as outlined by the fuzzy union of all the single-species outputs, suggest key differences across the two centuries in South America, where spatial/environmentally favorable areas have spread, and in Australia, where favorability values have decreased (Fig. 6.2). In the Mediterranean basin, favorable

areas have extended to the Maghreb, and are beginning to spread to the European side.

6.4.2. Disease models

The distribution of favorable areas (F ≥ 0.2) for the presence of dengue cases shows that changes have taken place in the continents since the late 20th century (Fig. 6.2). Favorable areas for dengue have spread southward in South America, inland in the Amazon, eastward in Africa, and to the south-west in Asia. Favorability values have also increased in South-East Asia, North Australia, and Papua New Guinea. The refined model also outlined favorable areas in Japan and South Korea (Figs. 6.3 and Appendix 13). Europe, a dengue-free continent in the late 20th century, is currently showing favorable areas in the south, among which are a rising number of urban locations.

The proximity to population centers was the most significant predictor in the model that described areas favorable to the occurrence of dengue cases during the late 20th century (Appendix 14). Dengue was favored in a variety of tropical ecoregions including forests and savannas, mangroves, montane grasslands, and xeric lands, as well as by low elevations and a high minimum temperature in the coldest month (Appendix 14). Increasing favorability during the early 21st century occurred outside the tropical regions in temperate grasslands, and in areas with high maximum annual temperatures and high pluviometric irregularity but low annual temperature ranges and rainfall. As for the vectors, the refined disease model reaffirms the relevance of human presence. Primate chorotypes contributed significantly to all these models (see below).

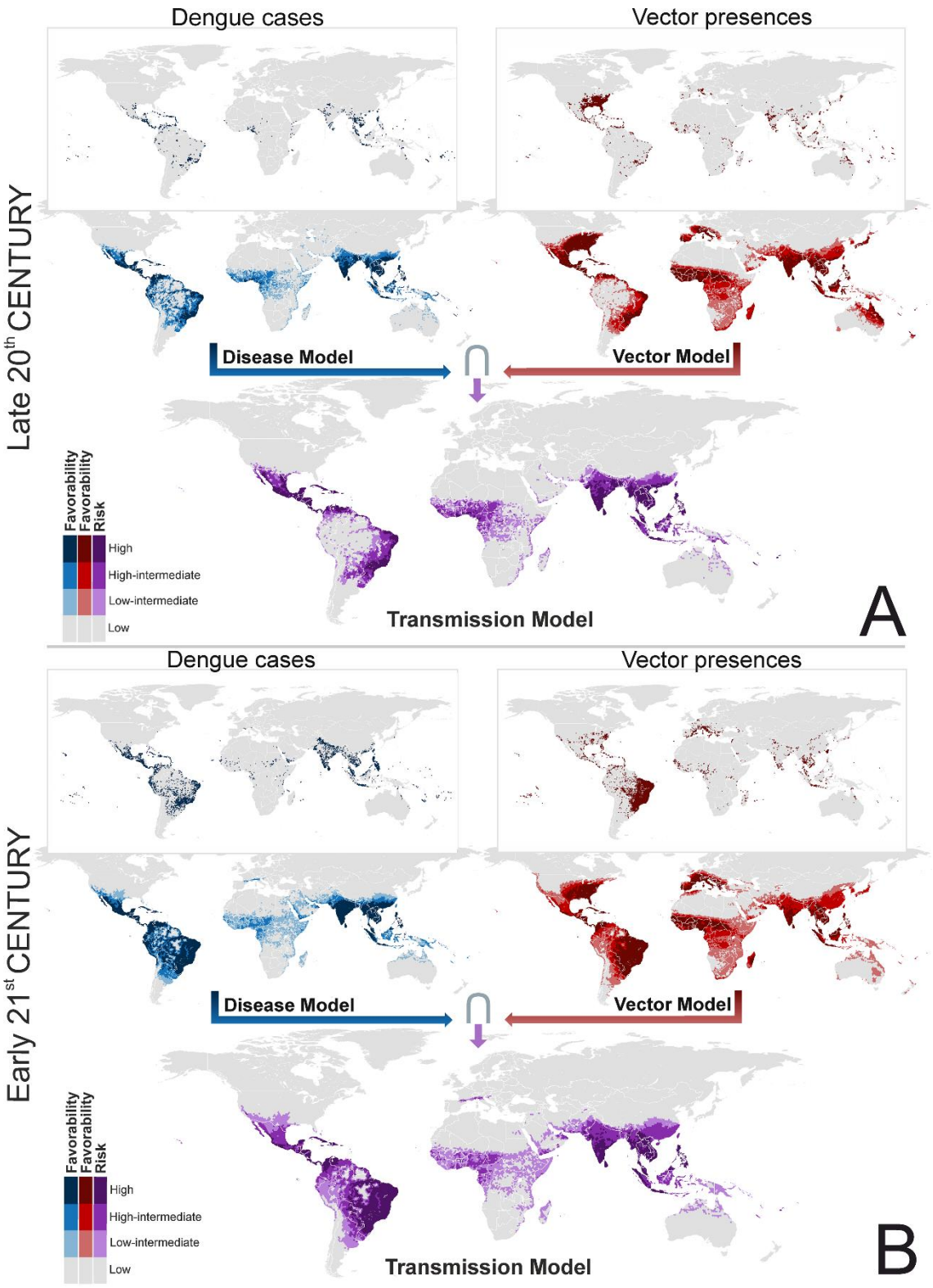

Fig. 6.2. Global disease, vector and transmission-risk models. A: maps for the late 20th century. B: maps for the early 21st century. The risk of transmission is estimated as the intersection (∩) between favorable conditions for the occurrence of dengue cases and favorable conditions for the presence of vector species. The spatial resolution is based on 7,774-km^2 hexagons. Recorded occurrences of dengue cases and vector presences are also mapped. Coast lines source: https://developers.google.com/earth-engine/datasets/catalog/FAO_GAUL_2015_level0.

6.4.3. Dengue transmission-risk models

Differences between the late 20th-century disease and transmission-risk models are most visible in South America (Fig. 6.2A), where a vast area along the north-western coasts, and around rivers crossing the Amazon basin, were favorable for the presence of dengue and unfavorable for the presence of vectors. This was also the case in the Horn of Africa and in the north of Papua New Guinea. In contrast, in the early 21st century, this pattern was only seen in Peru, Bolivia, and Argentina, as well as in Saudi Arabia and Iraq (Fig. 6.2B). The refined transmission-risk model for the early 21st century (Fig. 6.3) still indicated significant risk areas in Japan, South Korea, and some European cities.

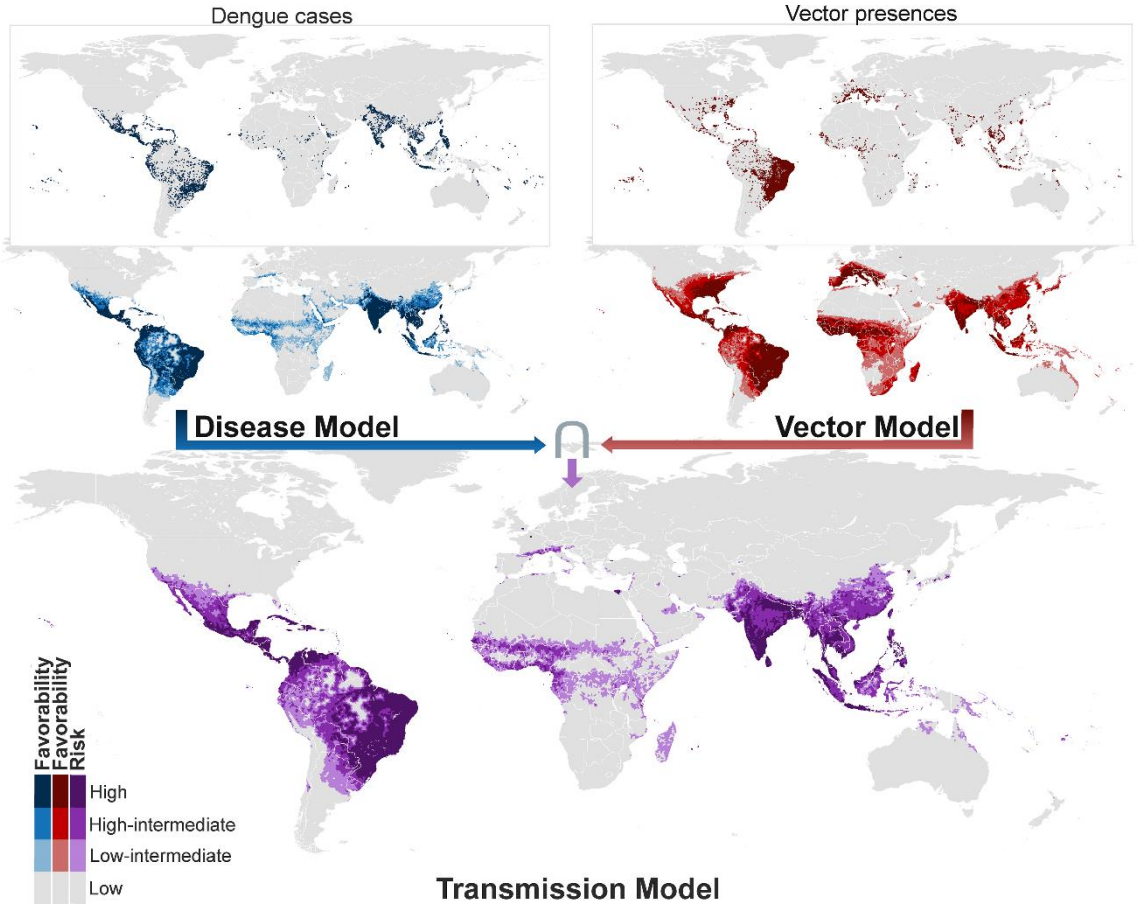

Fig. 6.3. Refined global disease, vector and transmission-risk models for the early 21st century. The risk of transmission is estimated as the intersection (∩) between favorable conditions for the occurrence of dengue cases and favorable conditions for the presence of vector species. Compared to the models in Fig 2, additional predictor variables only available for the 21st century were considered, and the spatial resolution was based on 2,591-km^2 hexagons. Recorded occurrences of dengue cases and of vector presences are also mapped. See pre-downscaled versions of these models in Appendix 15. Coast lines source: https://developers.google.com/earth-engine/datasets/catalog/FAO_GAUL_2015_level0.

6.4.4. Model assessment

6.4.4.1. Model evaluation

The AUC values of all vector, disease, and transmission-risk models were >0.925 (Table 6.1), pointing to "outstanding" discrimination capacities according to Hosmer and Lemeshow (Hosmer & Lemeshow, 2000), although this could be a result of the worldwide geographic extent of the calibration area. For a favorability threshold of 0.5, the CCR ranged between 0.771 and 0.884. Kappa values ranged between 0.228 and 0.252 in all the 20th-century models, and ranged between 0.352 and 0.544 in the early 21st-century models. Nevertheless, in the disease models and transmission-risk models for the 21st century, Kappa was always ≥0.518.

The likelihood of underestimating the degree of favorability in areas where vectors and dengue cases occurred was low, as denoted by sensitivity values >0.800 (i.e., >80% of recorded presences were classified in favorable areas), and by under-prediction values <0.025 (i.e., less than 2.5% of the unfavorable spatial units showed recorded presences).

Compared to the 0.5-favorability threshold, when a 0.2 threshold was adopted, the CCR values of all models decreased by an average 12.67% (SD=3.85), and kappa values decreased by an average 31.04% (SD=4.90), which is related to the average 14.91% (SD=4.25) decrease observed in the specificity values (i.e., some areas without presence records were shown by the models to increase in favorability). Nevertheless, the 0.2-threshold also minimized the likelihood of underestimating the degree of favorability in areas where vectors and dengue cases have occurred, as it produced an approximately 10% increase of the sensitivity values, and an approximately 75% decrease of the under-prediction values.

Table 6.1. Model assessment based on discrimination and classification capacities respect to vector and disease records of the same period. AUC: area under the receiver operator characteristic curve; FCT: favorability classification threshold; Kappa: Cohen's kappa; Sens.: sensitivity; Spec.: specificity; CCR: correct classification rate; Underp.: underprediction rate; Overp.: overprediction rate.

	MODEL	AUC	FCT	Kappa	Sens.	Spec.	CCR	Underp.	Overp.
Late 20th century	Vector	0.935	0.5	0.228	0.936	0.762	0.771	0.005	0.825
			0.2	0.150	0.990	0.637	0.655	0.001	0.872
	Disease	0.934	0.5	0.234	0.893	0.851	0.852	0.004	0.838
			0.2	0.164	0.964	0.767	0.773	0.001	0.882
	Transmission risk	0.927	0.5	0.252	0.822	0.876	0.874	0.007	0.823
			0.2	0.178	0.926	0.794	0.798	0.003	0.873
Early 21st century	Vector	0.926	0.5	0.352	0.925	0.760	0.777	0.011	0.704
			0.2	0.210	0.991	0.580	0.620	0.002	0.795
	Disease	0.948	0.5	0.518	0.903	0.859	0.864	0.013	0.564
			0.2	0.359	0.980	0.730	0.757	0.003	0.696
	Transmission risk	0.939	0.5	0.533	0.822	0.888	0.881	0.024	0.531
			0.2	0.375	0.965	0.749	0.772	0.006	0.684
Early 21st century (refined)	Vector	0.935	0.5	0.369	0.942	0.768	0.785	0.008	0.693
			0.2	0.241	0.991	0.622	0.658	0.002	0.778
	Disease	0.956	0.5	0.531	0.903	0.866	0.870	0.013	0.552
			0.2	0.386	0.981	0.752	0.777	0.003	0.678
	Transmission risk	0.944	0.5	0.544	0.830	0.891	0.884	0.022	0.522
			0.2	0.418	0.955	0.784	0.803	0.007	0.652

6.4.4.2. Predictive capacity

The late 20th-century disease and transmission-risk models demonstrated meaningful predictive capacities with respect to the early 21st-century dengue-case records. In many aspects, the assessments provided better results when the observations compared to the models were "future" cases than when we used for comparison the sets of records employed for model training (see Tables 6.1 and 6.2, and Appendix 16). The AUC values were always >0.910. Considering both the

0.5 and the 0.2-favorability thresholds, and compared to the above model evaluation, the kappa values of the disease and transmission-risk models increased by an average of 59.4% (SD=5.1) when assessed with respect to all dengue cases reported during 1970–2017, which is similar to the 57.6% increase (SD=5.1) when assessed with respect to the 2001–2017 cases alone. The CCR also experienced an average 4.6% increase (SD=1.8) with respect to its evaluation values. This improvement was related to an average 5.8% increase (SD=0.8) in model specificity, which was always >0.900 with the 0.5 favorability threshold (Table 2) and >0.820 with the 0.2 threshold. Sensitivity values experienced an average 14.3% decrease (SD=4.9). Nevertheless, sensitivity was always >0.670 with the 0.5 threshold and >0.820 with the 0.2 threshold. Finally, the underprediction rate decreased by an average of 56.5% (SD=13.8), which indicates that many favorable areas free from disease during the late 20th century experienced outbreaks after 2000.

The early 21st-century (2001–2017) models also showed meaningful predictive capacities (Table 6.2). Compared to the above model assessment (referenced to the 2001–2017 data), when the whole 2001–2019 period was considered, the kappa values increased by an average of 5.6% (SD=1.2), and the CCR values increased by 0.8% (SD=0.3) (Tables 6.1, 6.2 and Appendix 16). When only the 2018 and 2019 data were employed, both kappa and CCR values decreased, but they were always >0.290 and >0.820, respectively, with the 0.5-favorability threshold, and >0.180 and >0.700, respectively, with the 0.2 threshold (Table 6.2).

Table 6.2. Validation of model predictive capacity based on discrimination and classification performance respect to disease records of a later period. AUC: area under the receiver operator characteristic curve; FCT: favorability classification threshold; Kappa: Cohen's kappa; Sens.: sensitivity; Spec.: specificity; CCR: correct classification rate; Underp.: underprediction rate; Overp.: overprediction rate.

	MODEL	Records of reference for validation purposes	AUC	FTC	Kappa	Sens.	Spec.	CCR	Underp.	Overp.
Late 20th century	Disease	1970 to 2017	0.925	0.5	0.558	0.778	0.905	0.891	0.031	0.486
				0.2	0.463	0.888	0.826	0.833	0.017	0.604
	Transmission risk		0.915	0.5	0.535	0.677	0.923	0.895	0.043	0.470
				0.2	0.465	0.821	0.848	0.845	0.026	0.590
	Disease	2001 to 2017	0.923	0.5	0.538	0.781	0.901	0.888	0.028	0.514
				0.2	0.440	0.888	0.820	0.827	0.016	0.627
	Transmission risk		0.914	0.5	0.515	0.678	0.918	0.892	0.040	0.501
				0.2	0.445	0.823	0.843	0.841	0.025	0.614
Early 21st century	Disease	2001 to 2019	0.948	0.5	0.548	0.898	0.867	0.870	0.015	0.530
				0.2	0.385	0.979	0.737	0.765	0.004	0.671
	Transmission risk		0.939	0.5	0.557	0.813	0.894	0.884	0.027	0.498
				0.2	0.402	0.962	0.756	0.780	0.007	0.658
	Disease	2018 and 2019	0.934	0.5	0.296	0.931	0.817	0.823	0.005	0.780
				0.2	0.186	0.987	0.689	0.705	0.001	0.850
	Transmission risk		0.915	0.5	0.305	0.831	0.847	0.846	0.011	0.768
				0.2	0.198	0.978	0.708	0.722	0.002	0.843
Early 21st century (refined)	Disease	2001 to 2019	0.957	0.5	0.561	0.898	0.873	0.876	0.015	0.517
				0.2	0.414	0.979	0.759	0.785	0.004	0.651
	Transmission risk		0.944	0.5	0.564	0.816	0.896	0.887	0.026	0.491
				0.2	0.445	0.95	0.791	0.810	0.008	0.625
	Disease	2018 and 2019	0.945	0.5	0.31	0.943	0.824	0.830	0.004	0.771
				0.2	0.202	0.989	0.710	0.725	0.001	0.841
	Transmission risk		0.924	0.5	0.31	0.834	0.849	0.848	0.011	0.765
				0.2	0.224	0.969	0.742	0.754	0.002	0.827

6.4.5. Contribution of the sylvatic cycle

A total of 51 chorotypes were detected: 24 chorotypes in Asia, 13 in Africa, and 14 in America (Appendix 17-19). Thus the early 21st-century disease model is an update of the late 20th-century disease model (see Fig. 6.1), as all chorotypes in the latter are also included in the former. Taking this into account, Asia contributed to the late 20th-century model with two chorotypes, including species in the following genera: *Hylobates*, *Trachyphitecus*, *Nomascus*, and *Pygathrix* in chorotype AS8; and *Hylobates*, *Presbytis*, *Nycticebus*, and *Trachypithecus* in chorotype AS15. Four additional Asian chorotypes were included in the 21st-century model, with the following species: *Macaca* in chorotype AS5; *Hylobates*, *Presbytis*, *Symphalangus*, and *Nycticebus* in chorotype AS7; *Loris*, *Semnopithecus*, and *Macaca* in chorotype AS9; and *Carlito* in chorotype AS19. The African chorotype AF2, with the genera *Arctocebus*, *Cercopithecus*, *Colobus*, *Euoticus*, *Gorilla*, *Lophocebus*, *Mandrillus*, *Miophitecus*, and *Sciurocheirus*, was included in the 20th-century model, whereas no additional African chorotype was included in the 21st-century model. South America contributed to the 20th-century model with three chorotypes, including species in the following genera: *Alouatta*, *Sapajus*, *Brachyteles*, *Callithrix*, *Callicebus*, and *Leontophitecus* in chorotype SA4; *Aotus*, *Cebus*, *Ateles*, and *Saguinus* in chorotype SA5; and *Aotus*, *Saguinus*, *Oreonax*, and *Callicebus* in chorotype SA14. An additional South-American chorotype, SA2, was included in the 21st-century model, with species of the genera *Alouatta*, *Ateles, Callicebus*, *Chiropotes*, and *Mico* (all the variables included in the disease models can be seen in Appendix 14).

Primate chorotypes contributed to explain a maximum of 16.4% of the variation in favorability for the presence of dengue in the late 20th century (Fig. 6.4A). However, only 0.2% of the variation can be exclusively attributed to these chorotypes. The remaining 16.2% of the variation was indistinguishably attributed to chorotypes and to spatial/environmental factors, as the distribution of primate

ranges is also dependent on the environment. In the early 21st-century model, chorotypes contributed a maximum of 9.8% to explain the variation in favorability, although only 0.7% could be exclusively attributed to them (Fig. 6.4B).

The distribution of areas in which there was a >0.1 favorability increase, as an exclusive effect of primates, is shown in Fig. 6.4. In the late 20th century, these areas were located in Java (Indonesia), in some areas of Cambodia and Vietnam, in northern Colombia, and in southern Brazil (Fig. 6.4A). In the early 21st century, the possible contribution of primate chorotypes expanded to Sumatra in Indonesia, and also involved Asian areas of Afghanistan, Pakistan, India, Nepal, and China in Asia, Amazonian areas of Brazil, and some African countries in the western Congo basin, mainly Cameroon, Gabon, Equatorial Guinea, and the Republic of Congo (Fig. 6. 4B).

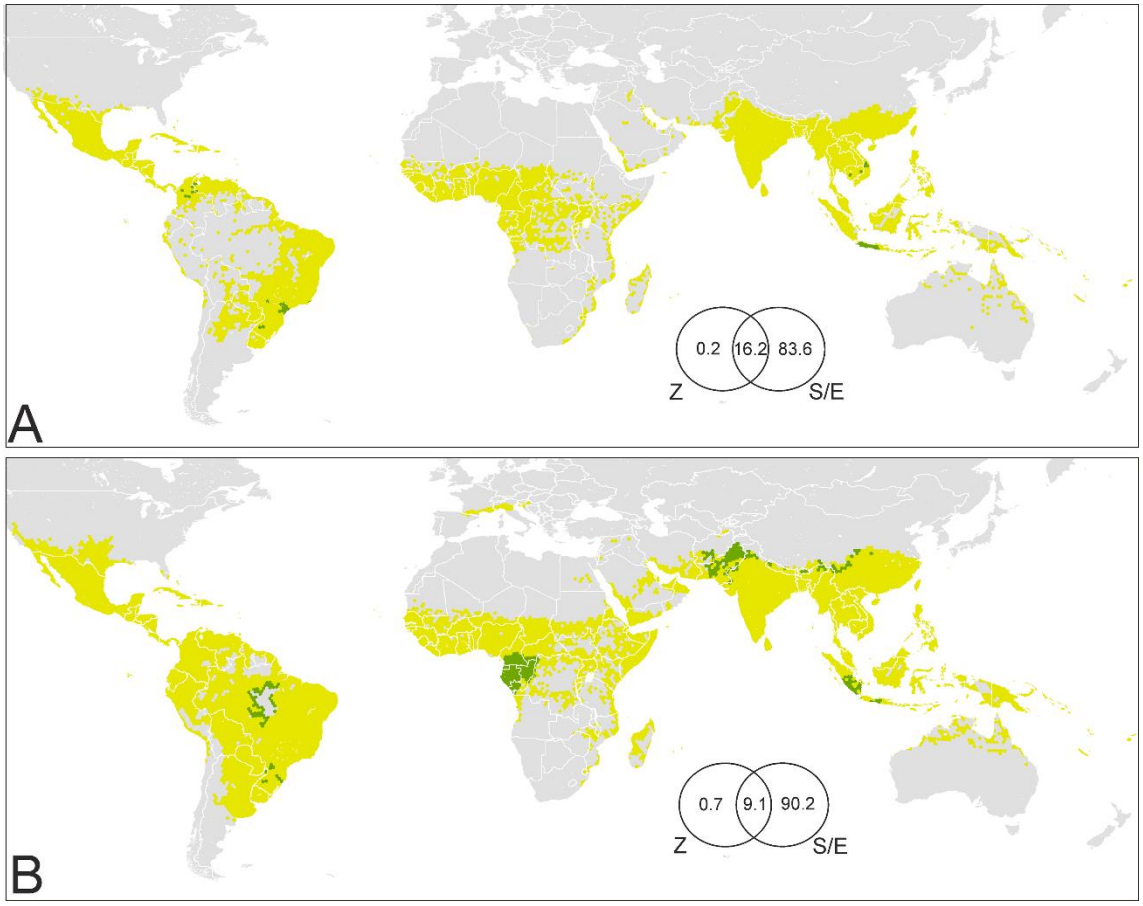

Fig. 6.4. Areas of potential influence of sylvatic cycles on the presence of dengue in humans. (A) Late 20th century; (B) early 21st century. Green: >0.1 increase of favorability values attributed to primate chorotypes; yellow: ≤0.1 increase of favorability values attributed to primate

chorotypes; grey: area with low risk of dengue transmission. Venn diagrams: The numbers are percentages of contribution to the distribution of favorability in the disease models (Z: Zoogeographic factor; S/E: Spatial/Environmental factor). Coast lines source: https://developers.google.com/earth-engine/datasets/catalog/FAO_GAUL_2015_level0.

6.5. Discussion

Our pathogeographic approach is the first to explicitly generate a high-resolution analysis of the geographic changes experienced in the dengue-transmission risk since the late 20th century. During the past century, dengue cases have been reported across a wide range of tropical ecoregions. Based on our research findings, we suggest that areas at risk of dengue transmission included regions in which cases only started being reported after 2000. We show that the distributions of *Aedes aegypti* and *Ae. albopictus* were principally linked to human presence in lowland tropical areas, although *Ae. albopictus* started to occur in some temperate regions as well. In the current century, dengue-risk areas continue to spread, reflecting the fact that both *Aedes* species are expanding their ranges into a number of temperate ecoregions worldwide. Our study is useful as a basis for suggesting specific management strategies according to the spatial distribution of factors favoring risk, and is the first to take into account the potential contribution of primate biogeography and sylvatic vectors in increasing the risk of dengue transmission.

In certain areas in South Asia that were free from dengue two decades ago, such as Pakistan, the presence of dengue and the occurrence of vectors were environmentally favored; thus, we predict the risk of dengue transmission in those areas. The early 21st-century disease reports strongly confirm this forecast (Fig. 6.5A). In contrast, in the Amazon basin, a successful forecast for the near future was provided by the disease model, but the same was not true of the transmission-risk model, which suggested that dengue presence, but not vector presence, was favored by the environment (Fig. 6.5B). Hence, the Pakistani and Amazonian scenarios would require different prevention strategies. The risk in Pakistan was evident, so ensuring a close microbiological and epidemiological

surveillance would have been reasonable (e.g., in the presence of clinically compatible cases, dengue should be suspected and microbiologically confirmed). In the Amazon, meanwhile, the arrival of invasive vectors should have been prevented, but now *Ae. aegypti* and *Ae. albopictus* occur near rivers and tributaries across the basin (Fig. 6.5B). Predicting the establishment of invasive species in new areas is difficult. The dispersal of *Aedes* is strongly influenced by travel and trade routes (Tatem *et al.*, 2006; Kraemer *et al.*, 2015b), as much as by the worldwide propagation of pathogens (Kraemer *et al.*, 2015b; Mas-Coma *et al.*, 2020). The progressive spread of invasive *Aedes* species into temperate ecoregions could also be influenced by climate change (Bouzid *et al.*, 2014; Schaffner & Mathis, 2014; Messina *et al.*, 2019). However, this situation is further aggravated if anthropogenic factors affect their evolutionary and consequently adaptive potential (Brown *et al.*, 2014).

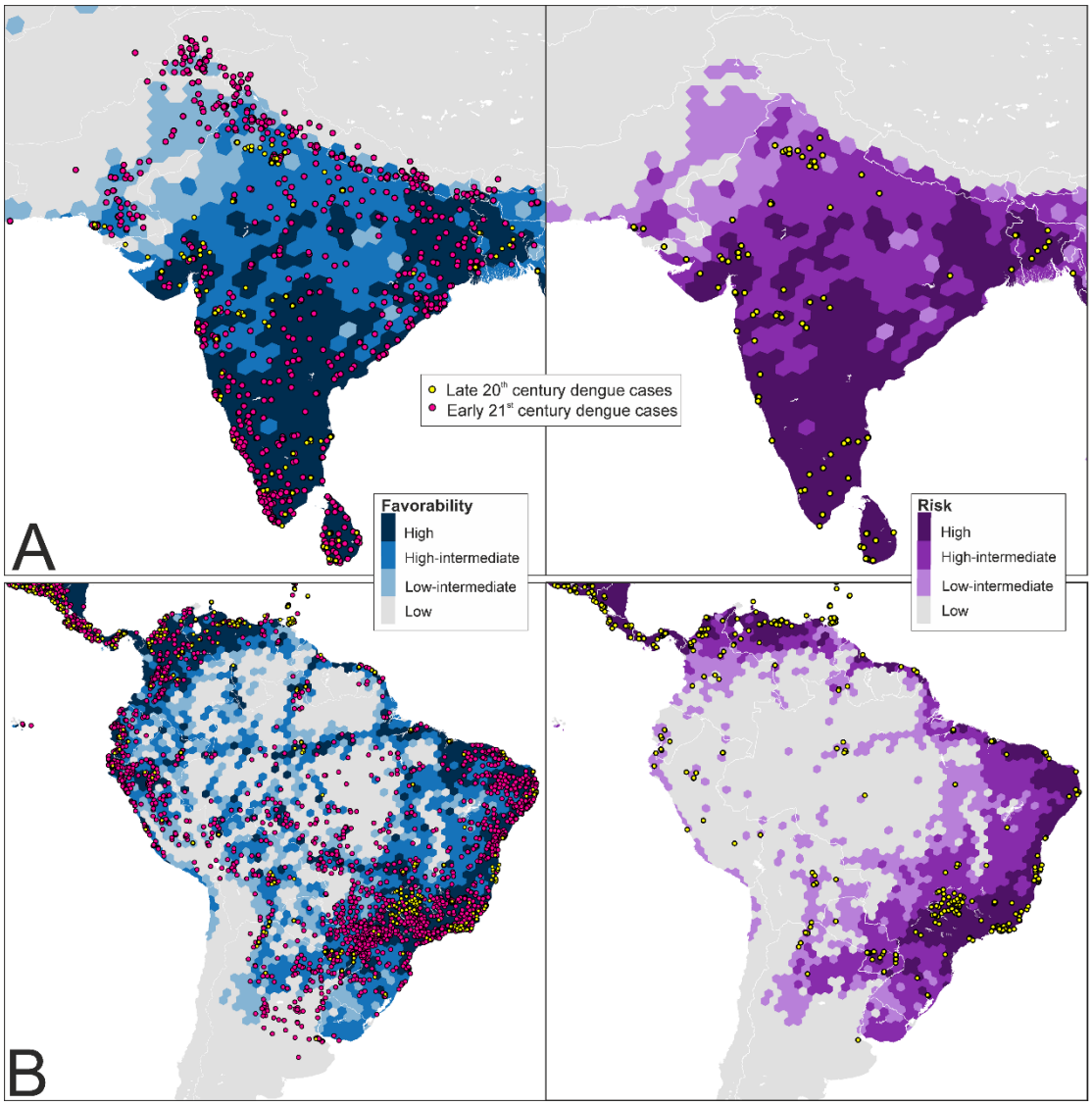

Fig. 6.5. Late 20th century disease and transmission-risk models in the Indian peninsula (A) and South America (B). These models were calibrated according to human-dengue cases from the late 20th century (Fig 2A). The locations of dengue cases recorded in the late 20th and the early 21st centuries are shown in order to illustrate the predictive capacity of these models (see explanations and implications in the main text). See early 21st-century models and data for these areas in S8 Fig. Coast lines source: https://developers.google.com/earth-engine/datasets/catalog/FAO_GAUL_2015_level0.

The predictive power of our late 20th-century models can be assumed for the early 21st-century models as well, as all of them were derived from the same method. The predictive capacity of the 21st-century models has been confirmed by the reported occurrence of autochthonous dengue after 2017 in Muscat (Oman) (Al-Abri *et al.*, 2020), Kyoto, and Nara (Japan) (ECDC, 2019b), and in Spanish coastal cities (ECDC, 2018, 2019a) (Appendix 13). The early 21st-century transmission-risk

models predict a spread of the risk in still barely affected areas exposed to the presence of invasive *Aedes*. This is particularly relevant in South-East China, but also in Papua New Guinea, North Australia, South USA, the interior regions of Colombia and Venezuela, Madagascar, and, according to the refined model, also in Japan and urban areas of South and Central Europe. Our results suggest that dengue could spread into areas of Argentina and South-West Asia (from Pakistan to the Arabian Peninsula) where invasive *Aedes* species occur but are scarcely reported (see Fig. 6.6). In addition, populated areas in Chile, Iran, Iraq, and the Maghreb, still free from invasive *Aedes*, exhibit favorable conditions for the occurrence of vectors and disease. The imminent risk in these locations, despite their distance from the dengue-native regions, should not be discounted given the high level of global connectivity (Kraemer *et al.*, 2015b) and the influence of human-population density on the intensity of dengue transmission (Cattarino *et al.*, 2020). Relevant precedents are the current expansive trend of autochthonous dengue in the Mediterranean cities (ECDC, 2019a), and a local transmission reported in New York (USA) (Rivera *et al.*, 2020) that was predicted two years previously (Shinha & Nautiyal, 2011). The northern coasts of Chile now have a similar situation to what has been seen in the Amazon basin over the past century; vectors have not yet arrived there but the area—which is environmentally similar to the dengue-affected coasts of Peru—is favorable to the presence of dengue cases. Management policies to prevent the arrival of invasive mosquitoes should be strongly encouraged. Finally, the eastern half of the USA and large sections of South-Saharan Africa exhibit unfavorable conditions (in spatial and/or environmental terms) for dengue even though these areas exhibit some limited favorable conditions and are home to *Aedes* mosquitoes. Thus, measures to be taken should depend on the socioeconomic and environmental conditions of the region. In eastern USA, international travellers should be educated about the threat of mosquito-borne diseases and on the importance of using repellents in endemic areas in order to prevent this region from becoming a spatially favorable

zone for local transmission. In Africa, microbiological and epidemiological surveillance should be encouraged and, when needed, internationally supported.

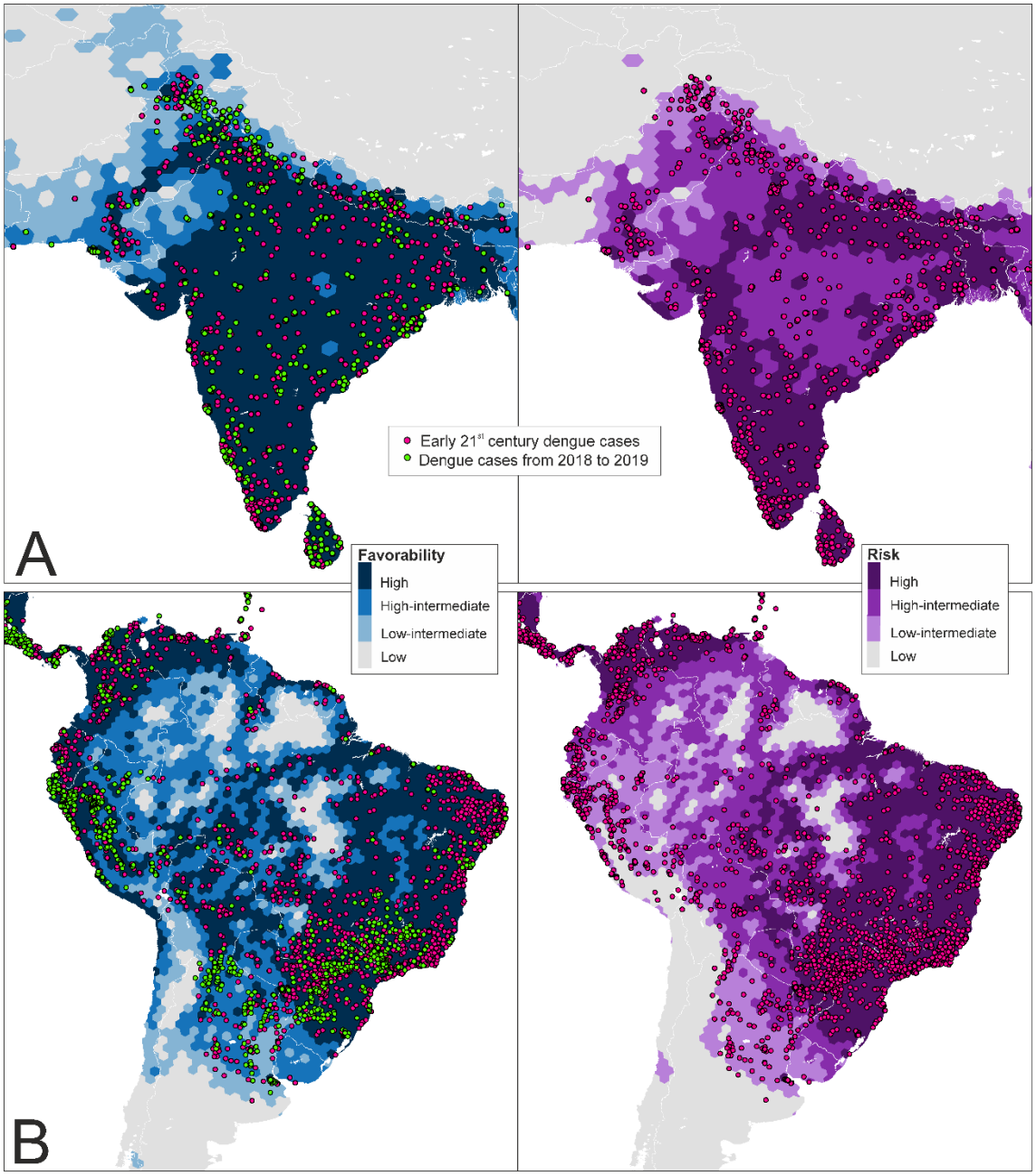

Fig. 6.6 Early 21st century disease and transmission-risk models in the Indian peninsula (A) and South America (B). These models were calibrated according to human-dengue cases from the late 21st century (Fig 3). The locations of dengue cases recorded in the early 21st century and from 2018 to 2019 are shown in order to illustrate the predictive capacity of these models. Coast lines source: https://developers.google.com/earth-engine/datasets/catalog/FAO_GAUL_2015_level0.

Any distribution modelling approach is subject to limitations primarily derived (1) from the spatio-temporal dynamism of the modelled facts, (2) from uncertainties

in the quality of the available information, and (3) from the interpretation of patterns based on correlations between dependent and independent variables (i.e., correlative approaches). First, a high spatio-temporal dynamism affects the distribution of dengue cases and *Aedes* mosquito species. Because of this, the transmission risk in areas that have been favorable for dengue in the past might not always be highlighted by our models. Chances for the disease to reach areas with similar environmental conditions might be different, conditioned by the geographical proximity of vectors and pathogens, i.e. because of the spatio-temporal autocorrelation. We took this autocorrelation into account by considering the spatial factor in the set of predictor variables. Consequently, these models were designed for specific contexts in the spatio-temporal dimension, and so they should be interpreted as focused on the current historical moment. Second, a low quality in the data set might have been a serious drawback in our models if the distribution of false absences were biased with respect to the gradient of environmental conditions, and also if the modelling method used were susceptible to overfitting. One of the methods we employed to addres this problem was the grid approach, as it reduced to a large extent the proportion of area considered to be free from dengue and vectors in the database. In addition, overfitting does not characterize our methodological approach (Olivero *et al.*, 2016b), as was confirmed by the fact that 11–42% of the "absence" hexagons were predicted to be favorable by the models (see specificity in Table 1). In any case, some bias could occur in poorly sampled regions, for example in Africa (Amarasinghe *et al.*, 2011), where model predictions should be interpreted with caution. Finally, a cautiounary approach is always advised when using correlative methods. Measures can be taken to avoid multicollinearity and type I errors, but the link between observed covariances and cause-effect relations always depends on the robustness of the a-priori hypotheses supporting the predictors data set. We were careful in this respect, but we still found a little artifact derived from the model downscaling to smaller hexagons. This procedure led us to estimate a high

risk of dengue transmission in some populated cities that are geographically distant from the areas highlighted by the pre-downscaling model. We corrected this artifact, so that the final output ensured a total correspondence between models before and after the downscaling procedure (see Fig. 6.3 and Appendix 15).

Our model for defining areas at risk of dengue transmission is broadly similar to those produced in previous studies. However, some differences are worth highlighting. We focus on Messina et al.'s research in 2019 (Messina *et al.*, 2019), as it provides an update of previous maps (Simmons *et al.*, 2012; Bhatt *et al.*, 2013) and, as we do here, takes into account the distribution of suitable areas for vectors. There are three main methodological differences that could explain discrepancies between our outputs and previous maps: (1) the treatment given to the temporal dimension, (2) the assumptions made for including vector distributions in the models, and (3) the application of a different modelling method (i.e., the logistic regressions and the Favorability Function).

Our models provide perceptions of current trends such as the spread of dengue in the Amazon basin and southern Asia, resulting from the temporal stratification. In addition, our models were trained with cases reported up to 2017, whereas Messina et al. (Messina *et al.*, 2019) only considered cases up to 2015 and excluded the autochthonous cases that occurred in Europe. This could explain the differences for Europe, Argentina, and Uruguay. We suggest the presence of a high transmission risk in southern France and northern Italy. In South America, as predicted by our models, recent reports demonstrate a significant risk in central Argentina, Peru, Bolivia, Paraguay, and southern and North-West Uruguay (PAHO in www.paho.org; ECDC in ecdc.europa.eu reports), where Messina et al.'s predictions only suggest a modest increase acros the century as a result of climate-warming projections.

The high risk suggested by Messina et al. (Messina *et al.*, 2019) for the eastern half of the USA is a major difference with our transmission-risk map, as risks in that area depend only on the presence of *Aedes* mosquitoes (compare vector and disease models in Fig. 6.3). The way vector species are integrated in a risk model reflects the *a priori* assumptions that are adopted with respect to these vectors' role in the pathogen transmission. In the case of dengue, it depends entirely on mosquitoes, and so it seems reasonable to adopt an intersection approach in which the risk points to areas favorable to both pathogen and vectors. We did this, and Messina et al. also exclude all areas environmentally unsuitable for vectors from their map (Messina *et al.*, 2019). However, their model also considered vectors as part of the predictor-variable ensemble, and this allowed the environment and the vector presence to counter-balance each other with no limiting-factor concerns (Romero *et al.*, 2016). We believe that this is justified, because the mere presence of vectors is a risk factor (May, 2006; Tatem *et al.*, 2006). However, this fact is sufficiently highlighted by a vector model, and the ability to differentiate between factors favoring risk is conductive to evaluating urgency and designing prevention strategies, as seen above. Our approach highlights transmission risks in areas in which both the vector and the disease are environmentally favored, but we also suggest that, regardless of the existence of vector reports, the presence of favorable environments for infections to occur should sound a warning in the event of unprecedented autochthonous cases. These situations, such as that of the Amazon in the late 20th century, are only detected by disease models that are kept "blind" to the vector factor during its training phase.

Lastly, our models show particularities that could result from the performance of the algorithms employed. The most glaring case is related to risk predictions involving the entire Mexican territory, whereas these risks are limited to the coasts in previous models (Messina *et al.*, 2019). The trend of dengue cases reported in Mexico after 2000 suggests an inland-spread of favorable areas.

In Asia, Africa, and South America, the areas prone to risk of zoonotic transmission to humans—according to our models—largely overlap with dengue transmission-intensity hotspots (Cattarino *et al.*, 2020). Although human-to-human transmission in urban contexts represents the most important virus cycle from the epidemic point of view (Gubler, 1998), zoonotic transmission from other primates has also occurred in tropical regions in Asia and Africa (Vasilakis *et al.*, 2011), suggesting that the medical relevance of forest cycles is, perhaps, underestimated. This means that active disease surveillance, such as that employed in Brazil for the yellow fever (Almeida *et al.*, 2014), could be misused. According to our results, sylvatic dengue cycles account for a small percentage of the global extent of the human case record, but could be meaningful in sanitary terms in some tropical areas.

The Asian areas with recorded transmissions of forest-dengue serotypes to humans are located in peninsular Malaysia (Smith, 1958; Cardosa *et al.*, 2009) and Borneo (Liu *et al.*, 2016; Pyke *et al.*, 2016). Besides, positive serological responses to the dengue virus have been detected in non-human primates from Indonesia, the Philippines, Cambodia, Vietnam, Malaysia and Thailand (Rudnick, 1965; Yuwono *et al.*, 1984; Wolfe *et al.*, 2001; Cardosa *et al.*, 2009). The maps presented here suggest that non-human-primate distributions may increase the environmental favorability for the presence of dengue cases in Indonesia (Java and Sumatra), Cambodia, and Vietnam (Fig. 6.4). The fact that these areas overlap with those with seropositivity in non-human primates, and are only approximately 500 km away from locations of confirmed forest dengue in humans, endorses our outputs. Serological surveys and experiments point to the primate genera *Presbytis* and *Macaca*—which are widely represented in the chorotypes involved in our disease models (Appendix 17)—as dengue reservoirs and amplification hosts, suggesting that other areas in Asia could be undiscovered foci of zoonotic dengue transmission (Vasilakis *et al.*, 2011). This could be the case for Pakistan,

Afghanistan, northern India, Nepal, and China, all inhabited by the genus *Macaca* and here outlined as areas of zoonotic transmission risk (Fig. 6.4B).

In Africa, human infections by a forest dengue serotype were detected in 1966 in Ibadan, Nigeria (Vasilakis *et al.*, 2008), approximately 1,000 km from the areas where sylvatic cycles could amplify the risk of dengue transmission according to our models: Cameroon, Equatorial Guinea, Gabon, Congo, and the Democratic Republic of the Congo (Fig. 6.4). The Congo basin, specifically Gabon, could have recently experienced epizootic transmission in non-human primates (Kading *et al.*, 2013). The record of humans affected by sylvatic dengue also points to regions in western Africa such as Senegal (Monlun *et al.*, 1992; Franco *et al.*, 2011); additionally, epizooties in primates could have also occurred in Nigeria (Fagbami *et al.*, 1977), Senegal (Saluzzo *et al.*, 1986; Diallo *et al.*, 2003), and Kenya (Eastwood *et al.*, 2017). Species belonging to the genera *Chlorocebus*, *Erythrocebus*, and *Papio* are considered to be dengue reservoirs or amplification hosts (Vasilakis *et al.*, 2011). Species from these genera help to characterize the distribution of dengue cases in Africa, while close relatives from the same tribe (e.g., *Miopithecus* and *Cercopithecus*) inhabit the Congo-basin areas here suggested to be at risk of zoonotic dengue transmission (Appendix 18).

Forest occupancy by human activities is considered to be a driver of disease emergence (Patz *et al.*, 2004; Allen *et al.*, 2017; Bloomfield *et al.*, 2020; Olivero *et al.*, 2020), increasing the relevance of sylvatic dengue spillover in tropical regions (Young *et al.*, 2017). In Asia and Africa, the real extent of transmission with an enzootic origin could have been neglected due to the impossibility of discerning between forest and urban serotypes (Vasilakis *et al.*, 2011). However, spillback cases with primates acting as reservoirs for urban dengue serotypes could also occur (Valentine *et al.*, 2019), and this might be happening in South America (Roberts *et al.*, 1984; de Figueiredo *et al.*, 2010). Seropositivity to the dengue virus has been documented in species from the genus *Alouatta* in north-eastern

Argentina (Morales *et al.*, 2017) and Costa Rica (Dolz *et al.*, 2019), from *Cebus* in Costa Rica (Dolz *et al.*, 2019), and from *Leontopithecus* in south-eastern Brazil (Catenacci *et al.*, 2018). Precisely, south-eastern Brazil, specifically the Atlantic forests surrounding Bahia, is highlighted by our model as an area at risk of zoonotic transmission to humans (Fig. 6.4). In this region, the yellow-fever virus shows evolutionary dynamics linked to forest primates (Mir *et al.*, 2017), and vectors of this virus have shown positivity to the presence of dengue strains (de Figueiredo *et al.*, 2010). Our model also points to a sylvatic-cycle influence on dengue-case occurrence in the Brazilian Amazon, involving chorotypes that include species of the primate genera *Alouatta* and *Cebus* (Figs. 6.4 and Appendix 19).

In conclusion, the human influence on the dispersal of *Aedes* mosquitoes, as much as the adaptive potential of these animals, make environments currently supporting the presence of dengue vectors not represent the range of conditions that might allow them to establish populations. Our vector model predictions should, therefore, be taken seriously when detecting favorable areas for the presence of invasive *Aedes,* and should be considered to be conservative when neglecting the risk in areas that have already reported pioneer populations. Preventing the arrival of invasive mosquitoes is very important, especially in areas where environmental conditions favor transmission of dengue. If vectors already occur in the area, but virus transmission is not environmentally favored, prevention policies should focus on international-traveller education and microbiological surveillance. Our models are also conservative in mapping the increase of favorability derived from the sylvatic cycle, as we only mapped areas where the contribution of primate chorotypes was not correlated with environmental factors such as presence of tropical forests. Thus, the areas prone to sylvatic dengue transmission could be larger than estimated, mostly in Africa. The concentration of evidence suggests the need for studies that address the occurrence of dengue sylvatic cycles in the Atlantic forest of Brazil and the

Amazon. Besides, we suggest that forests in north-western Colombia be investigated for sylvatic cycles, as a chorotype including a *Cebus* species seems to have contributed to the increased risk of dengue transmission in the recent past.

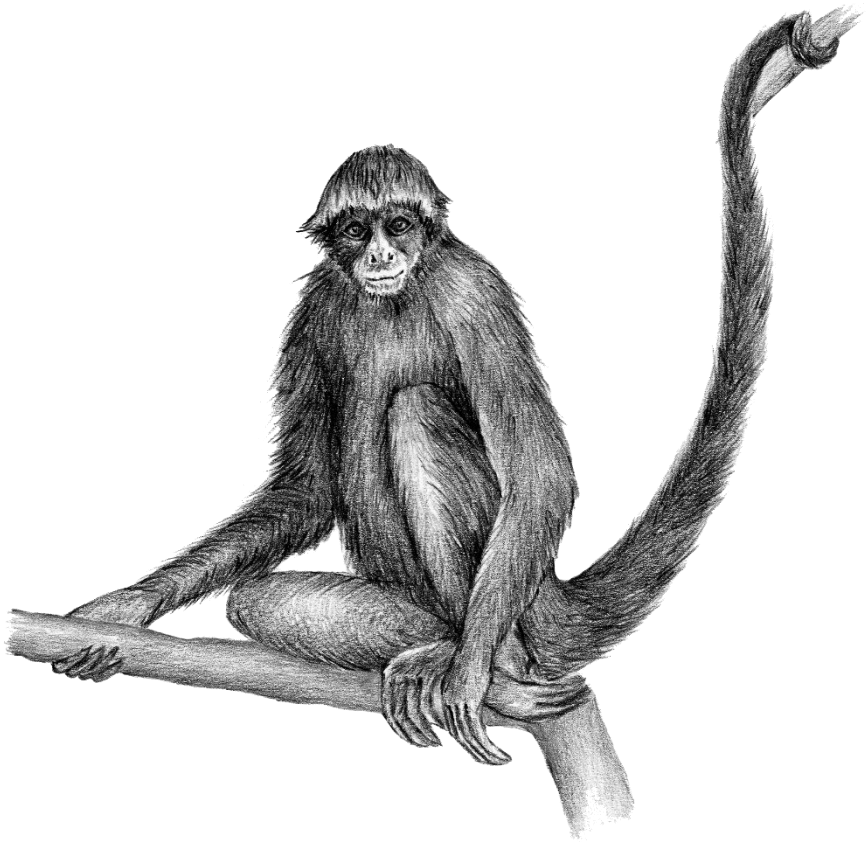

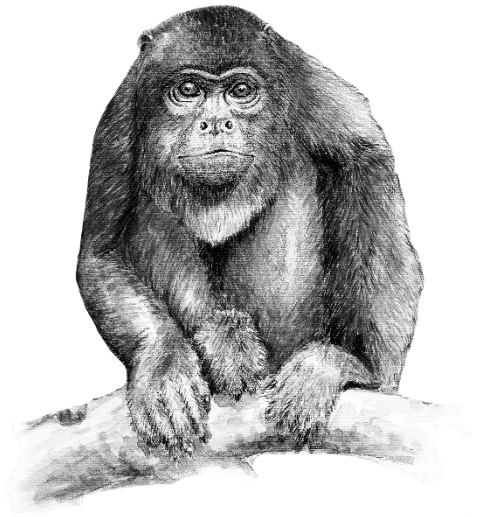

CAPÍTULO 7

Yellow fever surveillance suggests zoonotic and anthroponotic emergent potential

La vigilancia de la fiebre amarilla sugiere un emergente potencial zoonótico y antroponótico

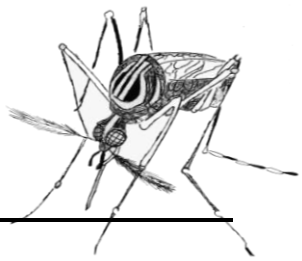

Este capítulo se basa en/ This chapter is based on:

Aliaga-Samanez, A., Real, R., Segura, M., Marfil-Daza, C., & Olivero, J. (2022). Yellow fever surveillance suggests zoonotic and anthroponotic emergent potential. Communications Biology, 5(1), 1-12. https://www.nature.com/articles/s42003-022-03492-9#Sec11 **(Q1)**.

7 Yellow fever surveillance suggests zoonotic and anthroponotic emergent potential

7.1. Abstract

Yellow fever is transmitted by mosquitoes among human and non-human primates. In the last decades, infections are occurring in areas that had been free from yellow fever for decades, probably as a consequence of the rapid spread of mosquito vectors, and of the virus evolutionary dynamic in which non-human primates are involved. This research is a pathogeographic assessment of where enzootic cycles, based on primate assemblages, could be amplifying the risk of yellow fever infections, in the context of spatial changes shown by the disease since the late 20th century. In South America, the most relevant spread of disease cases affects parts of the Amazon basin and a wide area of southern Brazil, where forest fragmentation could be activating enzootic cycles next to urban areas. In Africa, yellow fever transmission is apparently spreading from the west of the continent, and primates could be contributing to this in savannas around rainforests. Our results are useful for identifying new areas that should be prioritised for vaccination, and suggest the need of deep yellow fever surveillance in primates of South America and Africa.

7.2. Introduction

Yellow fever, an acute viral haemorrhagic disease, was the first human pathology to be attributed to a virus, and the first demonstrated to be transmitted by arthropods (Finlay, 1881; Reed *et al.*, 2001). This disease is caused by an arbovirus of the family *Flaviviridae*. This pathogen can be transmitted by mosquitoes of genus *Aedes* in America and Africa, and of genera *Aedes, Sabethes* and *Haemagogus* in America, through three transmission cycle types: the sylvatic cycle (between primates), the urban epidemic cycle (between humans), and the intermediate or savannah cycle in Africa (between humans that live near the jungle) (Cunha *et al.*, 2020). The yellow fever mosquito (*Aedes aegypti*) and the Asian tiger mosquito (*A. albopictus*) represent a major risk for the spread of yellow fever, the former being the main vector in urban areas and the latter a bridge vector between the forest and the urban area (Couto-Lima *et al.*, 2017). The virus is principally maintained by the sylvatic cycle where it evolves (Tatem *et al.*, 2006), and where primate-human zoonotic transmissions through different mosquito species are also possible (Shearer *et al.*, 2018).

The disease has undergone many changes over the past few centuries. The yellow fever virus is native to Africa where it may have emerged around 3,000 years ago (WHO, 2018). The virus was transported by slave-trade ships in the 15th and the 16th centuries from Africa to the Americas (Reed *et al.*, 2001). The later geographical expansion during the 17th and the 18th centuries was closely linked to the spread of *A. aegypti* through the shipping industry and commerce (Gubler, 2004). The number of yellow fever cases decreased in the mid 1900s in Francophone Africa (e.g., most of north-west and central Africa) by vaccination (Smithburn *et al.*, 1956), and in the Americas by effective controls on the principal urban vector, *A. aegypti* (Soper, 1963). Since the late 20th century, however, there has been a resurgence of yellow fever in Africa and America (Shearer *et al.*, 2018). At least 200,000 cases and 30,000 deaths were reported in 1990 worldwide (WHO, 1992). In Africa, virulent outbreaks affected urban areas of Angola and the

Democratic Republic of the Congo (DRC) between December 2015 and July 2016 (Ingelbeen *et al.*, 2018). Shortly after, at the end of 2016, outbreaks started to occur in South Brazil, in areas that had been free from yellow fever cases for decades, probably following a southward path from Trinidad and Tobago (Mir *et al.*, 2017). Since then, new cases have been reported in Surinam, Nigeria and French Guyana, where the last cases dated back to 1971, 1996 and 1998 respectively (Wouthuyzen-Bakker *et al.*, 2017; Sanna *et al.*, 2018; Nwachukwu *et al.*, 2020). Consequently, despite the fact that control policies were able to virtually eliminate yellow fever in wide areas of the globe, the WHO insists in stating that prevention efforts should not be abandoned (WHO, 2016). Instead, in order to prevent and respond efficiently to the occurrence of new outbreaks, risk areas should be delineated according to geographic and environmental factors related to yellow fever (Hamrick *et al.*, 2017; Shearer *et al.*, 2018).

A suitable methodological and conceptual framework for achieving the comprehension and prediction of zoonotic outbreaks is "pathogeography" (Murray *et al.*, 2018), from which the geographic distribution of zoonotic diseases is analyzed on the basis of a multi-level factor approach that considers ecological and human drivers, as well as the biogeography of animal species involving vectors, reservoirs and other roles in the zoonotic cycles (Stephens *et al.*, 2016; Olivero *et al.*, 2017a). The most recent model predicting the risk of infection by the yellow fever virus (Shearer *et al.*, 2018) contemplates all these factors, producing risk maps based on records of infection in humans from 1970 to 2016. The study suggests that the presence of *A. aegypti*, combined with the zoonotic potential for infections (given the presence of potential primate hosts), contributes the receptivity of yellow fever transmission in new regions such as Asia through the spread of the virus or through importation. So, if the current situation points to a yellow fever geographic spread, the forecasting of future trends will need pathogeographical analyses based on the spatio-temporal context.

Sylvatic cycles favour the existence of evolutionary dynamics that have recently led to new yellow fever virus lineages in South America (Mir *et al.*, 2017). These cycles, involving primates and a range of vector species(Roberts *et al.*, 1984), not only are the scenario of the virus diversification, but can also contribute to amplifying the risk of transmission to humans (Bryant *et al.*, 2003; Baronti *et al.*, 2011; Auguste *et al.*, 2015). The globalization of transports, and the expansion of vectors that are themselves evolving, help new virus lineages spread and increase the the risk of transmission to humans (Tatem *et al.*, 2006; Kraemer *et al.*, 2015a). Once the new lineage has arrived in an area, it can enter in the local enzootic cycles and be exposed to selective pressures potentially leading to new viral variants (Hamrick *et al.*, 2017). There are precedents in the analysis of primate influence on infection rates. Hamrick *et al.,* in 2017, considering eight non-human primate genera in South America, calculated that the probability of yellow fever occurrence at the county level doubled with each additional genus. In 2018, Shearer *et al.* carried out a study of the local speed at which human individuals are expected to be infected with the yellow fever virus, for which they included non-human primate distributions as variables in their models. That study was, thus, focused on the virus infection efficiency, whose geographic variation was analized within the area that is already suitable for the occurrence of yellow fever according to risk zones (47 countries of America and Africa) estimated by Jentes *et al.* (2011). Gaythorpe *et al.* (2021), examined the impact of vaccination at the provincial level, taking into account the distribution of three non-human primate families as predictors in their models. Further studies are needed, however, to understand the extent and geography of the non-human primate's influence on the yellow fever transmission to humans (Hamrick *et al.*, 2017).

The main objective of this research is to assess where the risk of yellow fever infections in humans could be being amplified by the contribution of enzootic cycles based on primate assemblages and a pool of sylvatic mosquito vectors. Given the current context of yellow fever geographic spread, we address this

challenge through a temporal stratification of disease cases, thus assuming that the current risk is a combination of past trends and the arrival of new factors.

7.3. Material and Methods

7.3.1. Lattice data geoprocessing and temporal extent

We latticed the data (Cressie, 1993) using a worldwide grid composed of 18,874 hexagonal 7,774 km^2 units, built using Discrete Global for R (https://github.com/r-barnes/dggridR) (Barnes, 2017). All the information we processed on yellow fever cases, on urban and sylvatic vectors presences, and on zoogeographic, spatial and environmental variables (see details on this information below) was aggregated at this spatial resolution. We used zonal statistics to calculate average variable values using ArcMAP 10.7.

The temporal extent for our analysis was divided into three periods: the late 20th century (1970–2000), the early 21st century (2001–2017), and the period 2018–2020. Predictions estimated by the late 20th century models were validated using cases reported in the early 21st century, and predictions from the early 21st century models were validated with records from 2018–2020. Although the limit between periods at the turn of the century is arbitrary, it reflects: 1) Distributional changes in the ranges of the *Ae. aegypti* and *Ae. albopictus* vectors (Liu-Helmersson *et al.*, 2019); 2) after 1999, the yellow fever genotype I has spread outside the endemic regions, and the genotype I modern-lineage has caused all major yellow fever outbreaks detected in non-endemic regions of South America since 2000 (Mir *et al.*, 2017); 3) the maximum potential of globalization was realised at the beginning of the 21st century with the opening of international borders, the widespread access to the Internet and to cell phones, and the generalization of online travel booking and of low-cost flights (Aliaga-Samanez *et al.*, 2021). The end of the second period, 2017, was chosen in order to include three years with occurrence of yellow fever cases in south-western Brazil (and two since its occurrence in

Angola and the DRC), while retaining three later years for predictive testing purposes (details on this testing are given below).

7.3.2. Yellow fever datasets

We used georeferenced cases of yellow fever in humans for a period of 51 years (from 1970 to 2020). This study period starts immediately after the suspension of the use of DDT due to to the appearance of resistance of *Ae. aegypti* in the late 1960s in several countries, after 50 years of eradication efforts (Soper, 1963). We took from Shearer *et al.*, 2018 the distribution of yellow fever cases for the period 1970–2016. We extracted additional cases for the period 1970–2020 from various sources (Supplementary data in the original article), including: ProMED-mail: Program of International society for infectious diseases; World Health Organization (WHO): Yellow fever outbreak weekly situation reports, Rapport de situation fievre jaune en RD Congo and Weekly epidemiological record; Health Ministry of different countries: Epidemiological Bulletins of yellow fever in Brazil, Peru, Colombia, and Paraguay; Pan American Health Organization (PAHO): Epidemiological Update Yellow Fever; European Centre for Disease Prevention and Control (ECDC): Communicable disease threats report and Rapid risk assessment report; Nigeria Centre for Disease Control (NCDC): Situation report, yellow fever outbreak in Nigeria and Global Infectious Disease and Epidemiology Online Network (GIDEON). The reported cases were complemented with publications available since 2016 with geo-referenced information on case location (Supplementary data in the original article). In addition, information was also sought on cases reported in French and Portuguese from local news reports in Africa.

We only represented in the hexagonal lattice the reported cases of yellow fever that had a precise location or that were referred to administrative unit was smaller than or of similar size to the hexagons. This dataset was transformed into a binary variable per study period representing the presence (n = 218 hexagons in the late

20th century; 493 hexagons in the early 21st century) or absence (n = 18,656 hexagons in the late 20th century; 18,381 hexagons in the early 21st century), hereafter the distribution of reported cases of yellow fever.

7.3.3. Vector dataset

The georeferenced presences of vectors involved in the urban cycle of yellow fever (i.e., the mosquitoes *Ae. aegypti* and *Ae. albopictus*) were taken from "The global compendium of the *Ae. aegypti* and *Ae. Albopictus* occurrence"(Kraemer *et al.*, 2015a) for the period 1970–2014. We complemented these records with georeferenced data scientifically validated for the period 2014–2017, taken from VectorBase (https://www.vectorbase.org/) and Mosquito Alert (http://www.mosquitoalert.com/). We included both species because, although *Ae. Aegypti* is the main vector of yellow fever, *Ae. albopictus* can also transmit the yellow fever virus to humans (Couto-Lima *et al.*, 2017; Amraoui *et al.*, 2018).

In addition, we included georeferenced occurrence data of sylvatic vectors (*Haemagogus janthinomys*, *H. leucocelaenus* and *Sabethes chloropterus* in South America; *Ae. africanus* and *Ae. vittatus* in Africa), which were obtained from Vectormap (vectormap.si.edu) and Gbif (https://gbif.org).

We represented in the hexagonal lattice the reported occurrence of mosquitoes that had a precise location or were located in administrative smaller than or of similar size to the hexagons. With this information, we built binary variables representing the presence or absence of each mosquito species in each hexagon. For species involved in the urban cycle, we built two binary variables per species: one for the late 20th century, and another for the early 21st century. For species involved in the sylvatic cycle, we merged the data of late 20th century and early 21st century in order to build a binary variable per species, due the scarcity of data and under the assumption that their distributions have been stable during the four last decades (Huang, 1977; WHO, 1989; Sudeep & Shil, 2017).

7.3.4. Zoogeographic, spatial and environmental variables

We built zoogeographic variables based on chorotypes, or types of distribution ranges, of all non-human primate species, as all are potentially vulnerable to yellow fever (Roig C, Miret J, Rojas A, Guillén Y, Aria L, 2009). A chorotype is a distribution pattern shared by a group of species (IUCN, 2019). For obtaining these zoogeographic variables, we proceeded in 4 steps: (1) Distribution maps of non-human primates were obtained from the IUCN for South-America and Africa; (2) the species ranges were classified hierarchically using the classification algorithm UPGMA according to the Baroni-Urbani & Buser´s similarity index (Buser, 1976); (3) we evaluated the statistical significance of all clusters obtained as a result of the classification using RMacoqui 1.0 software (http://rmacoqui.r-forge.r-project.org/)(Olivero *et al.*, 2011); (4) in each hexagon, the number of species belonging to each chorotype was quantified. We generated a zoogeographic model based on the non-human primates chorotypes by running a forward-backward stepwise logistic regression using presence/absence of yellow fever cases and the number of species of each chorotype as dependent and predictor variables, respectively. This procedure was made for two periods: late 20^{th} century and early 21^{st} century. Henceforth, only the selected chorotype variables were considered in the baseline disease favourability models explained below.

We built a yellow fever spatial variable for each continent (South-America and Africa), which were calculated through the trend surface approach, by performing a backward-stepwise logistic regression of the distribution of yellow fever cases on a ensemble of variables defined for polynomial combinations of longitude (*X*) and latitude (*Y*) up to the third degree: X, Y, XY, X^2, Y^2, X^2Y, XY^2, X^3, and Y^3. We transformed probability values derived from logistic regression into spatial favourability values by applying the Favourability Function (Real *et al.*, 2006; Acevedo & Real, 2012), using the following equation:

$$F = \frac{\frac{P}{1-P}}{\frac{n_1}{n_0} + \frac{P}{1-P}} \quad (1)$$

where *P* is the spatial probability of occurrence of at least a case of yellow fever at each hexagon, and n_1 and n_0 are the numbers of hexagons with presence and absence of yellow fever cases, respectively. We built a different spatial variable for each continent and time period.

We used environmental variables related to the following factors: climate, human activity, topography, hydrography, biome, ecosystem type, and forest loss. For details about the source and description of the environmental variables selected, see Appendix 21.

7.3.5. Pathogeographical approach to transmission risk modelling

Our objectives were to construct a global yellow fever transmission risk map, and to identify areas where primates contribute to increased risk, using the methodology previously used to analyse the worldwide dynamic biogeography of zoonotic and anthroponotic dengue (Aliaga-Samanez *et al.*, 2021) (see flowchart in Fig. 6.1 in the chapter 6 and Appendix 20). We produced a transmission model focused on the late 20th century and another for the early 21st century.

The risk of transmission was assessed by combining a first model describing areas favourable to the presence of yellow fever, i.e., the "baseline disease model"; and another model describing areas favourable to the presence of mosquitoes known to act as vectors, i.e., the "vector model". For this combination, we used the fuzzy intersection (Dubois & Prade, 1979), i.e., the risk of transmission at each hexagon was valued at the minimum between favourability in the baseline disease model and favourability in the vector model.

In this way, we considered that the vectors are a limiting factor, and that the risk of transmission derives from the degree to which the environmental conditions are simultaneously favourable for the presence of vectors and for disease cases to occur (Romero *et al.*, 2016). In order to analyze the spatio-temporal dynamic of yellow fever, we made comparable models for the late 20th century and the early 21st century, using predictor variables that are available for both periods. Later, we made a 21st-century enhanced model that optimized the predictive capacity of availabe information in the search for current risk areas. For this purpose, we included, in the variable set, predictors that are only accessible for the 21st century (e.g., high-resolution population density, livestock, irrigation, infrastructures, intact forest, and GlobCover land cover classes; see Appendix 21).

7.3.6. Baseline disease models

The baseline disease model in the late 20th century was expressed in terms of favourability values, using the equation (1) (see above). This time, *P* was calculated through a multivariable forward-backward stepwise logistic regression of the 20th-century yellow fever presences/absences on a set of zoogeographic, environmental and spatial variables. This was made in two blocks: 1) a stepwise selection of environmental and spatial variables; 2) a later stepwise addition of chorotypes whose presence contribute to improve significantly the likelihood of the model based only on the first block. Variables for each block were preselected using RAO´s score tests (which estimated the significance of its association to the distribution of yellow fever cases), and Benjamini and Hochberg´s (1995) false discovery rate (FDR) to control for Type I errors, which could pass due to the number of variables analysed. We also avoided excesive multicollinearity by preventing that variables with Spearman correlation values >0.8 were included in the same model. In case this happened, only the variable with the most significant RAO´s score-test value was retained, and the multivariable model was re-run. The parameters in the models were estimated using a gradient ascent machine learning algorithm, and the significance of these paremeters was assessed using

the test of Wald. The goodness of fit of the models was established using the test of Hosmer and Lemeshow, which checks the significance of the difference between expected and observed values, so that non significant differences mean that the fit is good. We used IBM-SPSS Statistics 24 software package to perform the models and all the associated tests.

We subsequently updated the baseline disease model to explain the distribution of yellow fever cases in the early 21st century. Compared to the procedure described for the 20th-century model, we included a new block before the two ones mentioned above. Thus, the methodological sequence was as follows: (1) forcing the input, as a predictor variable, of the logit of the late 20th century baseline disease model (the logit being the linear combination of variables in the 20th-century model); (2) making a later stepwise selection of spatial and environmental variables; and (3) a stepwise addition of chorotypes that contribute to improving the model's likelihood. In this way, we took into account that the current spread of yellow fever is influenced by the inertia of previous situations. This is equivalent to assuming that there is temporal autocorrelation (i.e., disease cases in the early 21st century are more probable to occur in areas where they already occurred in the late 20th century). In the 21st-century model, the variables entering in blocks (2) and (3) represent the drivers potentially favouring the spread(Aliaga-Samanez *et al.*, 2021). The preselection of variables for blocks (2) and (3) and the control for excessive multicollinearity between environmental variables were made as explained for the late 20th-century model.

7.3.7. Vector models

We produced a favourabuility model for each vector species for the late 20th century and for the early 21st century separately. We built multivariable favourability models for urban vectors using the distribution of each urban mosquito species in the late 20th century and the spatial and environmental variables for the late 20th century, following the same procedure used for block

(1) in the 20th-century baseline disease model. We also updated each urban vector model for the early 21st century as in the baseline disease model, using the procedure described for blocks (1) and (2).

A single model, referred to both the late 20th and the early 21st centuries, was made for sylvatic vectors, for the reasons explained above. Finally, we built up the vector models for the late 20th century and for the early 21st century by joining all individual vector models of each period using the fuzzy union (Zadeh, 1965) (i.e., considering for each hexagon the maximum value shown by any of the species models). This criterion was taken into account because, if the pathogen were present, the occurrence of a single vector species would involve potential for yellow fever transmission.

7.3.8. Model fit assessment and validation of its predictive capacity

Favourability models were assessed according to their classification and discrimination capacities respect to the training data set (i.e., to the observations used for model training). The classification capacity was based on two classification thresholds: *F*= 0.5, which represents the neutral favourability, and *F*= 0.2, below which the risk of transmission was considered to be low (Acevedo & Real, 2012). Six classification assessment indices were used (Fielding & Bell, 1997): (1) sensitivity (i.e., proportion of presences correctly classified in favourable hexagons), (2) specificity (i.e., proportion of absences correctly classified in unfavourable hexagons), (3) CCR (i.e., proportion of presences and absences correctly classified in favourable hexagons respectively), (4) TSS (that is sensitivity + specifity - 1), (5) underprediction rate (i.e., proportion of favourable areas that are recorded to have presences), and (6) overprediction rate (i.e., proportion of favourable areas that are not recorded to have presences). The discrimination capacity was assessed using the area under the receiver operating characteristic (ROC) curve (AUC) (Lobo *et al.*, 2008).

The validation of the predictive capacity of the late 20th century disease and transmission-risk models was done by evaluating, with the same indices used above, classification and discrimination capacities with respect to the cases of the period 2001–2020. The predictive capacity of the models for the early 21st century was validated with respect to the yellow fever cases reported in the period 2018–2020.

7.3.9. Relative importance of the zoogeographical factor

We estimated the pure contribution of non-human primates to the baseline disease model, i.e., how much of the variation in favourability for yellow fever cases was explained exclusively by the zoogeographical factor, by performing a variation partitioning analysis (Muñoz *et al.*, 2005). This implied the use of the zoogeographic model and a spatio-environmental model constructed with the environmental and spatial variables that entered the baseline disease model. This approach also allowed us to calculate how much is the variation of the baseline disease model attributable simultaneously to the zoogeographical and other factors. We built maps identifying the zones where the non-human primates could increase yellow fever cases in humans, that is, where the presence of primates could favour the occurrence of yellow fever regardless of correlations with other factors. To map these areas we identified the hexagons that fulfilled these conditions: 1) favourability values for the baseline disease model were ≥ 0.2; and 2) the difference between the favourability values provided by the baseline disease model and the spatio-environmental model was positive and ≥ 0.01.

7.4. Results

7.4.1. Zoogeographic Factor

A total of 27 significant primate chorotypes were detected: 13 in Africa and 14 in South America (Appendix 22-23). The distribution of yellow fever cases during the late 20th century was significantly related to three American chorotypes located

in Brazil and Peru and two African chorotypes mostly located south of the Sahara Desert and north of the Equator (Fig. 7.2a). In the case of the early 21st century, the distribution of yellow fever cases was significantly related with chorotypes distributed throughout most of the tropical area of South America and Africa (Fig. 7.2a and Appendix 24).

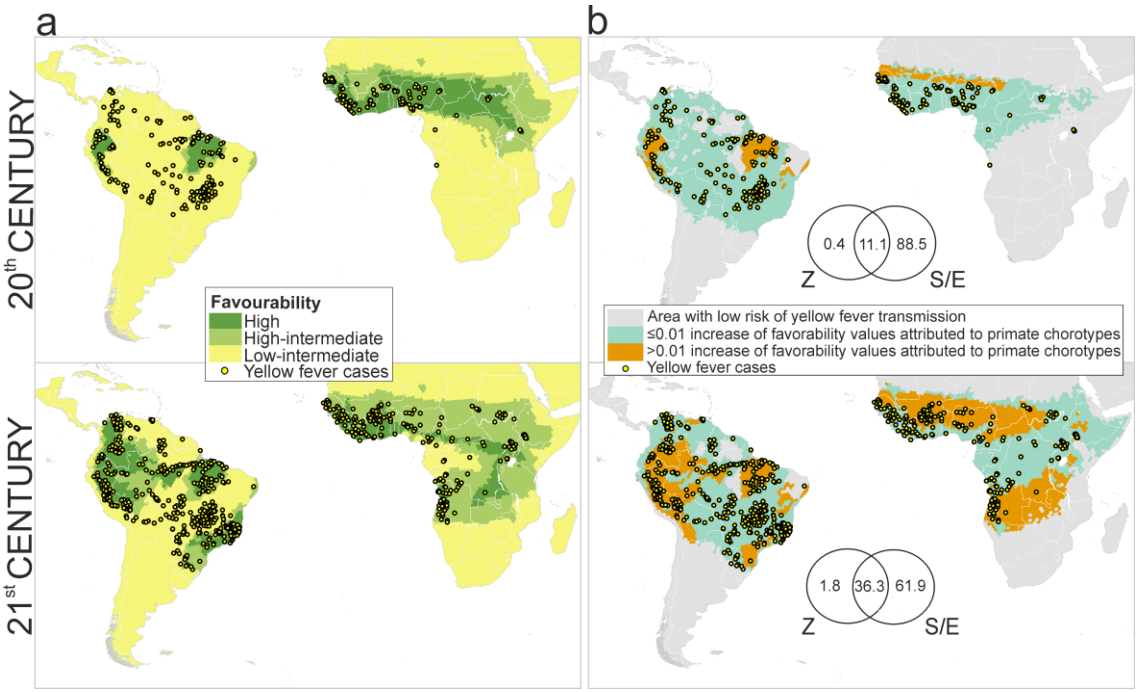

Fig. 2: Contribution of the zoogeographic factor
a Model of favourability for the occurrence of yellow fever cases according to the presence of non-human primate chorotypes (i.e., zoogeographic model) [the scale for favourability values is: high (F > 0.8); high-intermediate (0.5 ≤ F ≤ 0.8); low-intermediate (0.2 ≤ F < 0.5)]. **b** Partial contribution of primates on the presence of yellow fever cases in humans [the numbers are percentages of contribution to the distribution of favourability in the disease models (Z: zoogeographic factor, S/E: spatial/environmental factor)]. The maps in **a** represent the areas where the primate presence could favour the occurrence of disease cases in humans, although correlations with other factors influencing the primate biogeography (such as climate, topography or land cover) might be involved in this relation. Instead, the maps in **b** highlight the areas where the presence of primates could favour the occurrence of yellow fever regardless of correlations with other factors.

7.4.2. Baseline disease models

All the baseline disease favourability models fitted the observed distribution of yellow fever cases, according to Hosmer & Lemeshow's test of goodness of fit (Appendix 25). Trend-surface variables (i.e., the spatial autocorrelation caused by

the historical patterns of the disease) characterized to the highest extent the distribution of yellow fever cases in Africa and America between 1970 and 2000, and also between 2001 and 2017 (Appendix 25). The closeness to population centres was the second most important factor in explaining the distribution of cases in the late 20th century and their spread during the early 21st century. In the late 20th century, the presence of yellow fever cases was also favoured by higher slopes and annual precipitations, whereas high maximum temperatures in the warmest month became significantly relevant during the early 21st century. Among the chorotypes that were significantly related to the distribution of yellow fever cases, three chorotypes from South America were included in the late 20th-century disease model: SA7, SA8, and SA14. Four more chorotypes helped to build the early 21st-century disease model: SA1, SA6, and SA12 from South America, and AF9 from Africa.

Spatial, environmental and zoogeographically favourable areas for the presence of yellow fever cases have spread southward in South America, reaching southern Paraguay, the Misiones province in Argentina, and the Atlantic forests of southern Brazil, locally called "Mata Atlantica"; and south and eastward in Africa, reaching Namibia, Zambia, Tanzania, Kenya and Somalia (Fig. 7.3).

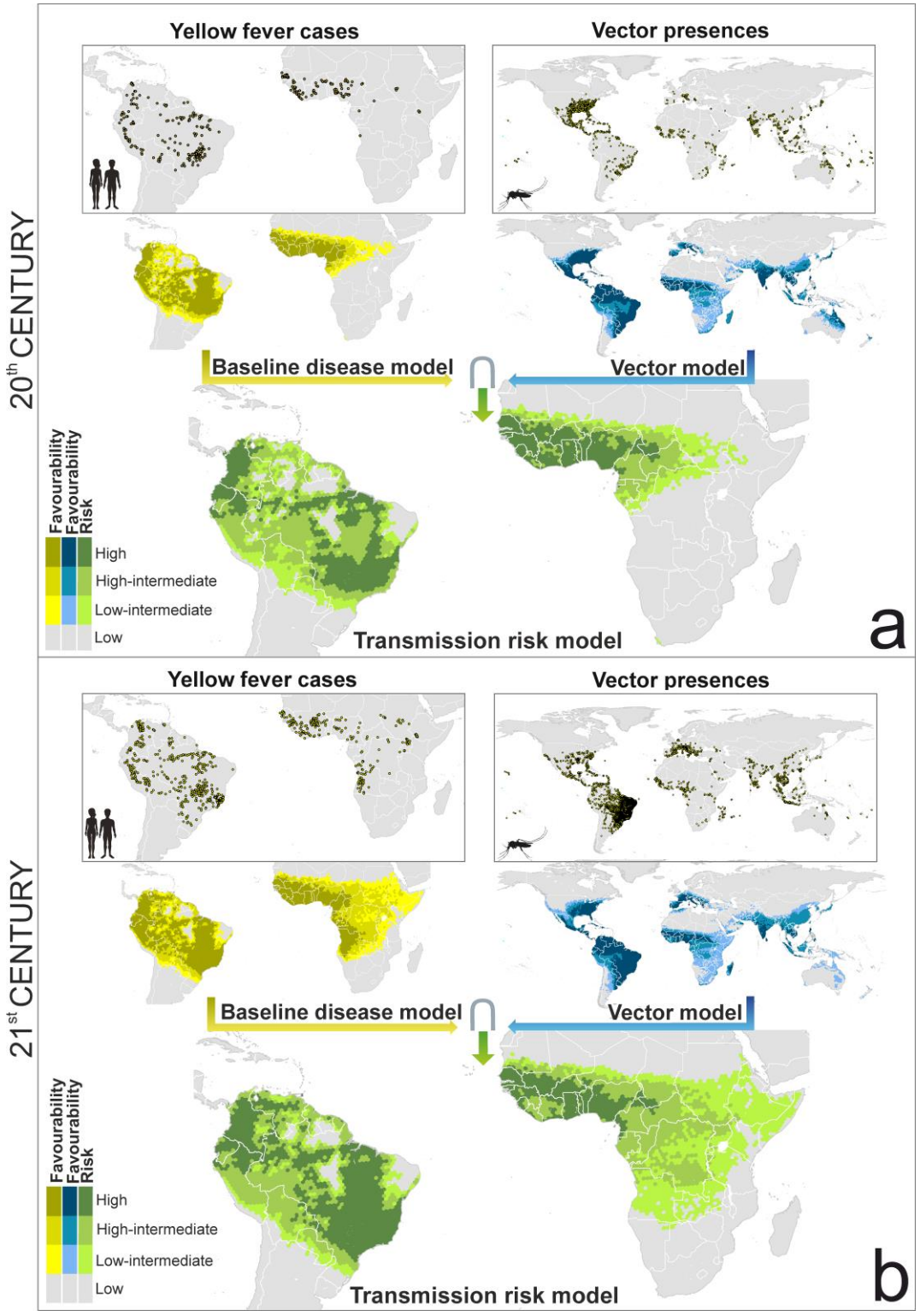

Fig. 7.3: Global baseline disease, vector and transmission-risk model

a maps for the late 20th century. **b** maps for the early 21st century. The risk of transmission is estimated as the fuzzy intersection (∩) between favourable conditions for the occurrence of yellow fever cases, and favourable conditions for the presence of vector species. The Favourability values were considered on the following scale: High ($F > 0.8$); High-Intermediate ($0.5 \leq F \leq 0.8$); Low-Intermediate ($0.2 \leq F < 0.5$); and Low ($F < 0.2$). The spatial resolution is based on 7,774-km2 hexagons. Recorded occurrences of yellow fever cases and of vector presences are also mapped

(see "Yellow fever datasets" and "Vector dataset" in the Methods section for details). Mosquito and humans clip art source: http://www.freepik.com.

7.4.3. Relative importance of the zoogeographical factor

The pure contribution of primate chorotypes to explaining the distribution of yellow fever cases in the late 20th century is 0.4%. Nevertheless, chorotypes could explain up to 11.5%, because 11.1% of the variation in favourability can be as much attributed to the presence of primate chorotypes as to the spatial/environmental factor (Fig. 7.2b). These percentages are higher in the early 21st-century model: 1.8% for the pure contribution of primate chorotypes, and 38.1% for the intersection between chorotypes and the spatial/environmental factor (Fig. 7.2b).

In the late 20th century, primates might have had a relevant role in explaining the occurrence of yellow fever cases in humans in easthern Brazil, northern Peru, and western Sahel (Fig. 7.2b). The area of influence of primates seems to have spread during the early 21st century, expanding northward, eastward and southward in Peru, Colombia, Venezuela, Ecuador and very prominently in Brazil, where it reached the "Mata Atlantica". In Africa, the spread of the primate contribution might have affected most of the tropical regions, only excluding the rainforest domain (Fig. 7.2b). These areas include countries of West Africa, Angola, south of the DRC, and some zones in Tanzania and Kenia.

7.4.4. Vector models

Although the distribution of yellow fever cases is restricted to Africa and South America, there are favourable areas for the presence of vector species in all continents except Antarctica, as outlined by the fuzzy union of all the single-mosquito-species models performed (Fig. 7.3). During the last two decades, spatial and environmentally favourable conditions seem to have spread northward in Europe, USA, and China; eastward in Central Africa; and south and westward in South America. In contrast, favourability has decreased in Oceania and Japan.

7.4.5. Yellow fever transmission-risk model

In the early 21st century, the risk of yellow fever transmission in South America could have increased in Paraguay, in some provinces of northern Argentina (e.g., Misiones and Corrientes), and in the "Mata Atlantica" in the south-east of Brazil (Fig. 7.3). The spread of *Aedes* mosquitoes in central Brazil might have also increased the level of risk in the region between Mato Grosso and Bahia states. Similarly, the increase of the transmission-risk in Africa resembles the south and westward spread of favourable areas for the presence of yellow fever cases (Fig. 7.3).

The enhancement of the early 21th-century transmission-risk model, through the use of variables only available for this period, provided little but meaningful changes compared to the original transmission-risk model (Figs. 7.3 and 7.4). In America, the enhanced model pointed to a moderate level of risk in the north-eastern states of Brazil. In Africa, the highest levels of transmission risk were mostly concentrated in countries of the Atlantic coast extending from the Sahel to the Equator. Here, in contrast to the not-enhanced model, intermediate-risk levels hardly reach the Horn of Africa, which coincides with the record of yellow fever cases and vector presences.

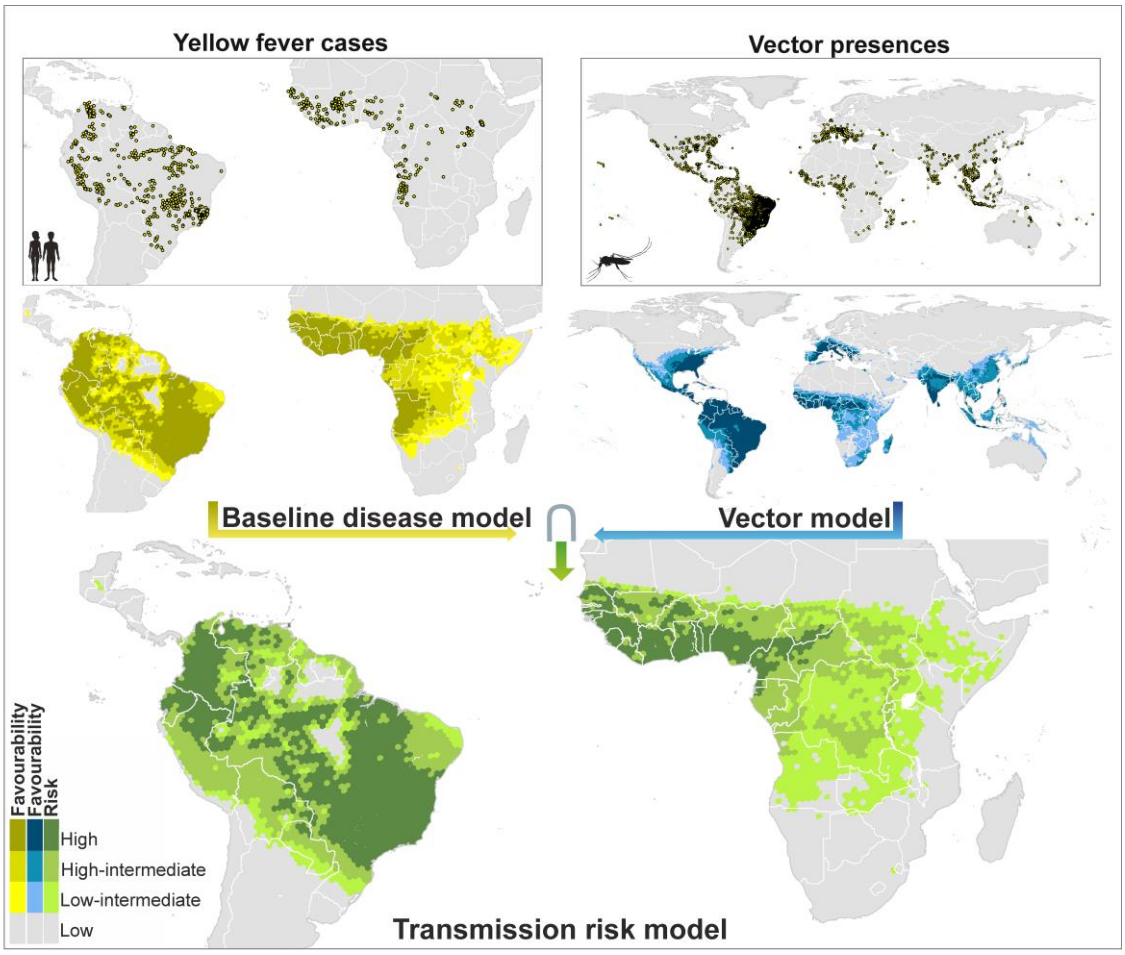

Fig. 7.4: Enhanced global baseline disease, vector and transmission-risk models for the early 21st century.
The risk of transmission is estimated as the fuzzy intersection (∩) between favourable conditions for the occurrence of yellow fever cases, and favourable conditions for the presence of vector species. Compared to the models in Fig. 3, additional predictor variables only available for the 21st century were considered. Recorded occurrences of yellow fever cases and of vector presences are also mapped. The Favourability values were considered on the following scale: High ($F > 0.8$); high-intermediate ($0.5 \leq F \leq 0.8$); Low-Intermediate ($0.2 \leq F < 0.5$); and Low ($F < 0.2$). The spatial resolution is based on 7774- km2 hexagons. Recorded occurrences of yellow fever cases and of vector presences are also mapped (see "Yellow fever datasets" and "Vector dataset" in the Methods section for details). Mosquito and humans clip art source: http://www.freepik.com.

7.4.6. Model fit assessment

Discrimination and classification index values are shown in Table 7.1. All the models showed an outstanding discrimination capacity according to Hosmer and Lemeshow (2000) (i.e., the area under the receiver operator characteristic curve, AUC, was always >0.91). In all models, true skill statistic (TSS) values were positive and >0.582. In the disease and transmission-risk models, correct classification rate

(CCR) values were between 0.83 and 0.91 depending on the favourability threshold considered, and it was between 0.61 and 0.78 in the vector models. Sensitivity values indicate that >85% (and except in two cases, >90%) of hexagons with vector presences and yellow fever cases reported were correctly classified by the models, regardless of the favourability threshold; and underprediction values were never >0.004. So, the occurrence of vectors and yellow fever cases reported, and finally the risk of yellow fever transmission, were rarely underestimated. Specificity values were between 0.82 and 0.91 in the disease and transmission-risk models, and between 0.57 and 0.76 in the vector models. Finally, overprediction values were in the range 0.70–0.92, i.e., a high proportion of hexagons considered favourable for the presence of disease cases or vectors have not been reported to have them. This means that the scattered appearance of presence data did not generate geographically scattered favourability models (see Figs. 7.3 and 7.4), and so that these models were far from overfitting.

Table 7.1. Model fit assessment based on discrimination and classification capacities respect to vector and disease records of the same period. AUC: area under the receiver operator characteristic curve; FCT: favourability classification threshold; Sens.: sensitivity; Spec.: specificity; CCR: correct classification rate TSS: true skill statistic; Underp.: underprediction rate; Overp.: overprediction rate.

	Model	AUC	FCT	Sens.	Spec.	CCR	TSS	Underp.	Overp.
Late 20th century	Disease	0.971	0.5	0.959	0.905	0.905	0.864	0.001	0.895
			0.2	0.982	0.873	0.875	0.855	0.000	0.917
	Vectors	0.919	0.5	0.946	0.705	0.717	0.651	0.004	0.849
			0.2	0.991	0.591	0.612	0.582	0.001	0.881
	Transmission risk	0.962	0.5	0.922	0.909	0.909	0.831	0.001	0.895
			0.2	0.982	0.876	0.877	0.858	0.000	0.915
Early 21st century	Disease	0.963	0.5	0.961	0.872	0.874	0.833	0.001	0.832
			0.2	0.988	0.826	0.830	0.814	0.000	0.868
	Vectors	0.928	0.5	0.947	0.740	0.761	0.687	0.008	0.715
			0.2	0.994	0.576	0.618	0.570	0.001	0.796
		0.951	0.5	0.876	0.889	0.889	0.765	0.004	0.825

	Transmission risk		0.2	0.980	0.833	0.837	0.813	0.001	0.864
Early 21st century (enhanced model)	Disease	0.964	0.5	0.968	0.872	0.875	0.840	0.001	0.831
			0.2	0.994	0.833	0.837	0.827	0.000	0.863
	Vectors	0.932	0.5	0.958	0.752	0.772	0.710	0.006	0.704
			0.2	0.991	0.616	0.653	0.607	0.002	0.780
	Transmission risk	0.954	0.5	0.878	0.894	0.894	0.772	0.004	0.818
			0.2	0.992	0.843	0.847	0.835	0.000	0.855

7.4.7. Validation of model predictive capacity

Model's discrimination and classification capacities remained quite similar or increased, compared to those in table 7.1, when disease cases regarded to "future information" (i.e., data corresponding to time periods later than those considered for model training) were included in the assessment (see Table 7.2). In the late 20th-century transmission-risk models, the use of yellow fever cases from 2001-2020 led to sensitivity values decreased from 0.922–0.982 (Table 7.1) to 0.791–0.864 (Table 7.2) and specificity values increased from 0.876–0.909 (Table 7.1) to 0.885–0.917 (Table 7.2).

Using yellow fever cases from 2018 to 2020 for the assessment of the early 21st-century transmission-risk models, sensitivity values increased from 0.876–0.992 (Table 7.1) to 0.904–1 (Table 7.2) and specificity values decreased from 0.833–0.894 (Table 7.1) to 0.815–0.877 (Table 7.2). The fact that sensitivity of the transmission-risk model increases, only with these "future" values, means that 90–100% of cases recorded after the model-training period were reported in areas predicted to be at risk of yellow fever transmission to humans.

Table 7.2. Validation of model predictive capacity based on discrimination and classification performance respect to yellow fever records of a later period. AUC: area under the receiver operator characteristic curve; FCT: favourability classification threshold; Sens.: sensitivity; Spec.: specificity; CCR: correct classification rate; TSS: true skill statistic; Underp.: underprediction rate; Overp.: overprediction rate.

	Records of reference	Model	AUC	FTC	Sens.	Spec.	CCR	TSS	Under.	Overp.
Late 20th century	2001 to 2020	Disease	0.936	0.5	0.805	0.913	0.911	0.718	0.006	0.800
				0.2	0.864	0.883	0.883	0.747	0.004	0.834
		Transmission risk	0.933	0.5	0.791	0.917	0.914	0.708	0.006	0.795
				0.2	0.864	0.885	0.885	0.749	0.004	0.832
Early 21st century	2018 to 2020	Disease	0.939	0.5	0.932	0.853	0.854	0.785	0.000	0.976
				0.2	1.000	0.808	0.809	0.808	0.000	0.980
		Transmission risk	0.938	0.5	0.932	0.873	0.873	0.805	0.000	0.972
				0.2	1.000	0.815	0.816	0.815	0.000	0.979
Early 21st century (enhanced model)	2018 to 2020	Disease	0.937	0.5	0.904	0.853	0.853	0.757	0.000	0.977
				0.2	0.986	0.814	0.815	0.800	0.000	0.980
		Transmission risk	0.936	0.5	0.904	0.877	0.877	0.781	0.000	0.972
				0.2	0.986	0.825	0.825	0.811	0.000	0.979

7.5. Discussion

The most relevant contribution of our results is the mapping of the areas where zoonotic cycles (involving primates and sylvatic mosquitoes) could be currently favouring the occurrence of yellow fever virus transmission to humans, based on the most updated data-base of humans cases. In South America, these areas include wide regions within the western, eastern and central Amazon basin, and also great part of the "Mata Atlantica", that is the Atlantic forests of Brazil. In Africa, they largely overlap with the open and forested savannas to the north and south of the Central African rainforests. This might be, however, a conservative view of the geographic relevance of the yellow fever zoonotic cycle, as only the areas where the primate contribution to risk was not correlated with

environmental factors were mapped. During the late 20th century, the influence of zoonotic cycles on yellow fever outbreaks could have been restricted to the Peruvian and the easternmost Brazilian Amazon in America, and to the southern limits of the Sahel in Africa. So, the understanding of this dynamic relationship between primates and yellow fever needs to be put in the context of recent changes in the global distribution of reported infection in humans.

Many yellow fever cases have been recorded in the early 21st century in areas that were free from the disease during the late 20th century. For example, disease cases are currently reported in south and southeastern Brazil (Fig. 7.3), where no cases seem to have occurred for decades before 2005 (Mir *et al.*, 2017). According to our baseline disease models, favourability for yellow fever transmission in southeastern Brazil was intermediate ($0.2 \leq F \leq 0.8$) in the late 20th century, and high ($F > 0.8$) in the early 21st century (Fig. 7.3). This increase in favourability could be a consequence of a modern-virus-lineage arrival from the north of South America (Mir *et al.*, 2017), that has caused all major yellow fever outbreaks in the subcontinent since 2000, including those in Brazil in 2008 and 2016 (details are discussed below).

In Africa, the areas favourable to yellow fever transmission are currently spreading from the west of the continent to the south and east, reaching countries such as the DRC, Angola, Namibia, Zambia, Tanzania, and Somalia (Fig. 7.3). In 2015 and 2016, the most widespread outbreaks reported in Africa in more than 20 years took place in Angola and the DRC (Kraemer *et al.*, 2017). Several factors might be responsible for the lower yellow fever activity in East and Central Africa before 2000. According to Mutebi & Barrett, (2002), genetic differences between yellow fever genotypes may play an important role in the distribution pattern of yellow fever outbreaks in Africa, the West African genotypes being associated to more frequent outbreaks. In addition, the ecological diversity and behaviour of vector mosquito species may also influence on the African yellow fever biogeography.

In West Africa, *Ae. Aegypti* populations are responsible for urban outbreaks, whereas no yellow fever cases have been attributed to this species in East Africa (Mutebi & Barrett, 2002). This applies, for example, to the 1992-1993 outbreak happened in Kenya (Mutebi & Barrett, 2002). What is interesting is that *Ae. aegypti* occurs in both East and West Africa, but there are two subspecies: *Ae. ae. aegypti* and *Ae. ae. formosus*. Crawford *et al.* (2017) mentioned that *Ae. ae. aegypti* is a demonstrated vector of yellow fever, whereas the extent to which *Ae. ae. formosus* lives alongside and feeds on humans is unclear (Crawford *et al.*, 2017). These authors suggest that the distribution of *Ae. ae. aegypti* is likely limited to West Africa, eastern populations of the species probably belonging to *Ae. ae. formosus*. So, it is worth investigating whether the distribution of viral and vector genetic variants is currently changing together with the distribution of yellow fever reports, or whether the apparent geographic spread of virus infections is a result of increased reporting efforts.

The interpretation of models based on incomplete information must be made with caution. Sampling bias could lead to interpretation mistakes if the model output maximized the geographic fit between recorded disease cases and the resulting predictions. The combination of logistic regressions and the favourability function, used to get the outputs of our models, do not usually tend to overfitting (Olivero *et al.*, 2016b), hence these models showed high overprediction rates (table 7.1), that is, a high proportion of favourable areas that are not recorded to have had cases. Part of this overprediction might be explained by transmission risks forecasted in areas prone to be endemic in the short term, as shown by the fact that the overprediction rate of the 20th-century model was around 0.9 (table 7.1), but it decreased until about 0.8 when this model's prediction capacity was tested according to the 21st-century cases (table 7.2). However, our model outputs are also consistent with the belief that the reporting of yellow fever cases could underestimate the actual number of cases, this being up to 500 times higher than reported in Africa, and around 10 times higher in

South America (Barrett & Higgs, 2007; Shearer *et al.*, 2018). Anyway, there are limits for any kind of model trying to analyse the geography of infection patterns for a virus showing high spatio-temporal dynamism, that is affected by the emergence of new lineages, by the changing distribution of *Aedes* mosquitoes (Aliaga-Samanez *et al.*, 2021), as much as by revisions of vaccination strategies. So, our models have to be interpreted in the current historical context, as they were designed for this specific spatio-temporal window.

As expected, our 21st-century model outputs resemble the results of recent studies focused on the distribution of yellow fever risk areas. Gaythorpe *et al.* (2021) evaluated the vaccine effectiveness in South America and Africa with a province-level model of the probability of yellow fever case reporting. Compared to this model, our outputs show a similar geographic pattern of yellow fever transmission risk; however, we point to higher risk in South and West Brazil and other South American countries such as Venezuela. Our 21st-century model also outlines the presence of high transmission risk in African countries not highlighted by Gaythorpe *et al.* (2021), such as Zambia and Tanzania. In Tanzania, while no yellow fever cases have been reported for decades (GIDEON, 2021), a study published by Rugarabamu *et al.* (2021) provides evidence of yellow fever exposure, suggesting the need to strengthen the surveillance system. A later research by Shearer *et al.* (2018) assessed the pattern of the speed at which human individuals are expected to acquire yellow fever virus infection in a given location. In principle, Shearer et al.'s results are not comparable to our risk maps because these authors used the estimated area at risk of yellow fever infections (Jentes *et al.*, 2011) as geographic extent for their analyses. Nevertheless, their map of "individual apparent infectious risk" points to areas partially related to those in which non-human primates seem to increase the risk of yellow fever transmission to humans (Fig. 7.2b). This happens, for example, in regions of the Amazon Basin in Peru, Ecuador, Colombia, Venezuela, and North and East Brazil; and of Africa in the southern limits of the Sahel. The overlap could be even higher

because, as mentioned above, we present a conservative view of the zoonotic-cycle influence area. Taking into account that Shearer et al. considered the distribution of primates as predictor variables in their model (together with other environmental factors), we wonder whether, in large regions of South America and Africa, the risk of human individual infection (Shearer *et al.*, 2018) could be linked to the increased risk of transmission favoured by non-human primates (Fig. 7.2). The most relevant difference between Shearer et al.'s maps and ours is located in Southeastern Brazil, probably because they did not considered reports of the most recent yellow fever outbreaks in the area (which happened after 2015).

Deep surveillances should be encouraged in primates of southern Brazil given the active evolutionary dynamism experienced by the yellow fever virus in South America. In this continent, a yellow fever virus "modern lineage" has spread since 1989 out of the endemic areas (Mir *et al.*, 2017). From 1980 to the middle of 2015, 792 sylvatic yellow-fever cases in humans and 421 deaths were reported in Brazil (Silva *et al.*, 2020). The modern lineage has diversified into several sub-lineages, one of which seems to be responsible of the disease re-emergence in 2016–2019 in the "Mata Atlantica" of the southern states of Brazil, causing one of the largest epizootic outbreaks recorded in the country (Mir *et al.*, 2017). The enzootic maintenance in primates is believed to be the background of the yellow-fever virus evolution in America (Mir *et al.*, 2017). However, the modern yellow fever lineage seems to have evolved in Trinidad and Tobago (Auguste *et al.*, 2010), and the "modified" modern lineage, introduced in 2016 in Southern Brazil, was probably a result of human translocations from Venezuela (Mir *et al.*, 2017). Nevertheless, the involvement of primates on transmission to humans in the Mata Atlantica, and the high evolutiounary rate recently shown by the yellow fever virus, might derive in new variants that could reach human populations, taking into account that the zoonotic cycles in Southeastern Brazil are closely connected with urban areas (Cunha *et al.*, 2020).

Forest loss and fragmentation could be increasing the proximity of humans to other primates, enhancing the zoonotic transmission of yellow fever. In fact, our 21st century disease model included forest loss after 2001 as a significant predictor variable (Appendix 25). Habitat destruction affects significantly the ecology of emerging infectious diseases in wildlife and humans (Medina-Vogel, 2010; Mongabay, 2020a). In undisturbed ecosystems, pathogens are diluted in the animal community, whereas some reservoir species and their pathogens may begin to dominate in fragmented forests (Mongabay, 2020a) (for example, Olivero *et al.* (2017b) demonstrated that Ebola outbreaks located along the limits of the African rainforest biome were significantly associated with forest losses that took place within the previous 2 years). A study published by Cunha *et al.* (2020) has proposed a new scenario for the 2016–2019 yellow fever outbreak in São Paulo, indicating that yellow fever sylvatic transmission among primates probably occurs in the city. The virus has been recorded in urban titis (*Callithrix* sp.) and in mosquito species normally inhabiting the forest (e.g., in *Aedes scapularis*). Consequently, the yellow fever pathogeography could be providing a new example of how forest fragmentation could amplify the risk of disease transmission by increasing the proximity of human populations to wildlife, in this case through the occupancy of urban areas by primates and sylvatic mosquitoes.

In case yellow fever surveillances in non-human primates were addressed, we propose to focus on the list of species belonging to chorotypes significantly related to the disease distribution (Appendix 22-23). These chorotypes have represented the diversity of primates reportedly infected by the yellow fever virus so in South America as in Africa. In Brazil, during the period 1996 to 2016, 2,221 deaths in non-human primates caused by yellow fever virus were reported, whereas only in the 2016-2019 outbreak the number of recorded deaths was 3,569 (Silva *et al.*, 2020). In this lastest outbreak, yellow fever virus infections were detected in specimens of genera *Alouatta*, *Brachyteles*, *Callicebus*, *Callithrix, Leontopithecus* and *Sapajus*, all of them inhabiting the Mata Atlantica (WHO,

2014b; Mongabay, 2020b; Silva *et al.*, 2020). All these genera include species whose biogeographic patterns characterize significantly the distribution of humans yellow fever cases in southern Brazil (i.e., species belonging to chorotypes SA4 and SA11, see Appendix 22). Overall in South America, according to the available literatura (WHO, 2014b; Shearer *et al.*, 2018; Mongabay, 2020b; Silva *et al.*, 2020), the yellow fever virus has been detected in 13 non-human primate genera, all of which include species whose biogeography is related to the American distribution of humans cases (see Appendix 22). The same applies in Africa, where the yellow fever virus has been detected in 11 non-human-primate genera (mostly in *Cercocebus*, *Cercopithecus*, *Colobus*, *Erythrocebus*, *Galago*, *Otolemur*, *Papio*, *Perodicticus* and *Pilocolobus*) (WHO, 2014b; Shearer *et al.*, 2018; Mongabay, 2020b; Silva *et al.*, 2020). All these genera include species belonging to the chorotypes that are significantly related to the yellow fever distribution (see Appendix 23).

Our analyses can contribute to identify new areas that should be prioritised for vaccination, for which we propose to take three yellow fever transmission geographic scenarios into account: (1) areas with very favourable conditions ($F \geq 0.5$) for both the presence of the virus and mosquito vectors, in which case the risk of transmission is very high; (2) areas with low but not negligible risk of yellow fever transmission ($0.2 \leq F \leq 0.5$); and (3) areas environmentally favourable to the presence of mosquito vectors, but not to the virus occurrence. In South America, the first and most severe scenario occurs in southern Brazil. Following the 2016–2019 outbreak, the WHO has programmed vaccination in this area (WHO, 2019). Our models provide support for the additional vaccination programme planned by the Brazilian Health Ministry in 2019 (WHO, 2019) in eastern Brazil (involving states such as Pernambuco, Alagoas, Paraíba, Sergipe, and Ceará, see Fig. 7.4), despite vaccination in this area is not yet considered by the WHO (WHO, 2019) and the CDC (CDC, 2018) to be a priority. The African areas included in the most severe scenario are located in west and central countries of the continent, where

the WHO already suggests prescriptive vaccination (WHO, 2015b; CDC, 2017). A set of African areas fits the scenario with low but not negligible risk of yellow fever transmission, but are not yet considered for vaccination by the WHO (WHO, 2015b) and the CDC (CDC, 2018): the north of Namibia, the west of Zambia, the east of Ethiopia, and some areas in Somalia (Fig. 7.4). We propose that active yellow fever surveillance strategies be considered for these areas in order to be alert for outbreaks in the near future. Finally, mosquito vectors already occur or find favourable conditions in many areas in North America, southern Europe, Asia and Oceania that are outside the yellow fever endemic area. The most suitable policies in these cases may involve preventing virus introduction by international travelling. For this reason, there are countries that require the yellow fever vaccination certificate for travellers (WHO, 2021b), although this certificate is not required in some countries with high-risk zones according to our models that also coincide with areas in which vaccination is recommended by the WHO (WHO, 2021b). A global strategy could be designed for granting, with no exceptions, vaccination of third-country citicens entering in countries at high or medium risk of yellow fever transmission (WHO, 2021b). In addition, vaccination should be also considered an option in areas with stable vector-mosquito populations that are close to the endemic areas, as is the case of Uruguay, northern Argentina and the eastern coast of Africa. Vaccination campaings recommended by the WHO in the provinces of Misiones and Corrientes (WHO, 2019), to the north of Argentina, are positive examples of this kind of initiatives.

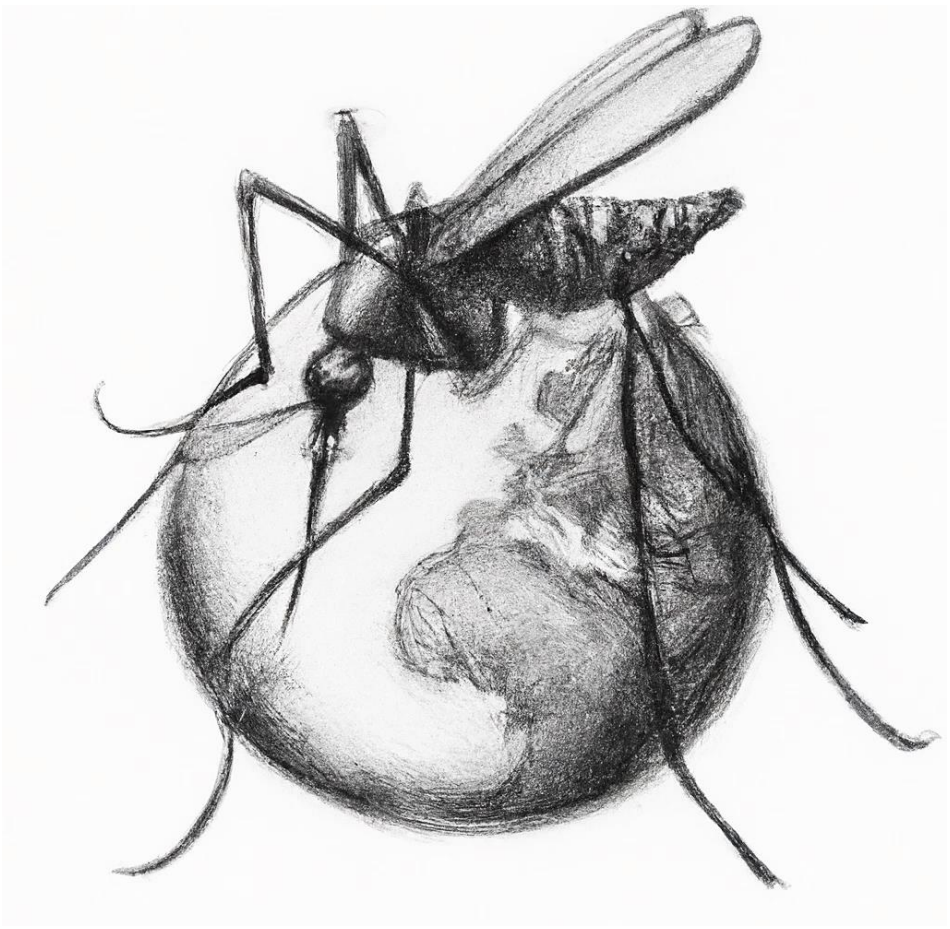

Fuente: Dall-E https://openai.com/research/dall-e

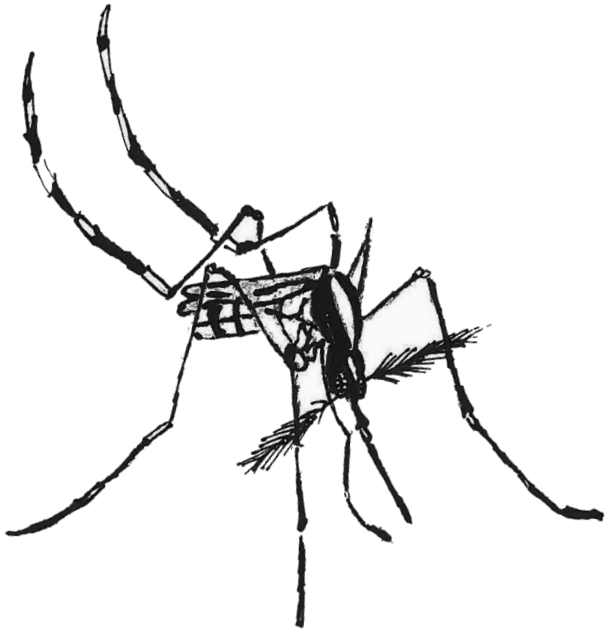

CAPÍTULO 8

Climate change might be aggravating dengue and yellow fever vectors spread

El cambio climático podría agravar la propagación de los vectores del dengue y la fiebre amarilla

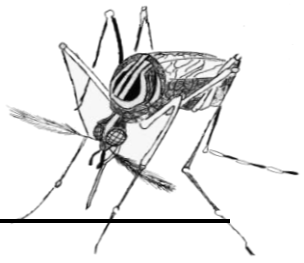

Este capítulo se basa en/ This chapter is based on:

Aliaga-Samanez, A., Romero, D., Murray, K., Cobos-Mayo, M., Segura, M., Real, R. & Olivero, J. (2023). Submitted. Climate change might be aggravating dengue and yellow fever vectors spread.

8 Climate change might be aggravating dengue and yellow fever vectors spread

8.1. Abstract

Climate change could increase the risk of spatial spread of urban and sylvatic mosquito vectors of dengue and yellow fever. Previous studies have focused on developing models to predict the global expansion of *Aedes aegypti* and *Aedes albopictus* due to climate change. However, dengue and yellow fever have complex cycles, involving not only urban mosquitoes but also sylvatic species. We have applied a biogeographical approach to the most recent dataset on the presence of urban and sylvatic vectors, in order to produce models based on individual vectors that are finally combined using fuzzy logic. We mapped areas where favourability may increase, decrease or remain unchanged in the future for the presence of urban and sylvatic vectors in the near (2041-2060) and the distant (2061-2080) future. In addition, we have analysed which species might be implicated in the future spread of favourable areas for vectors to occur. The resulting models suggest that this spread could occur in different regions. So, dengue vectors might find new favourable areas in West and Central Africa and in South-East Asia, reaching Borneo. Yellow fever vectors could spread also in West and Central Africa, as well as in the Amazon basin. In addition, we suggest possible re-infestations by *Ae. aegypti* in Europe, more conditioned by the persistent arrival of individuals to main ports than by climate change; whereas *Ae. albopictus* will continue to find favourable areas in this continent. According to our results, attention should be paid in West and Central sub-Saharan Africa to the three sylvatic vectors: *Ae. vittatus*, *Ae. luteocephalus* and *Ae. africanus*, especially in Cameroon, in Central Africa Republic, and in the north of the Democratic Republic of Congo. This study is the first to analyse the effect of climate change in the distribution of the whole set of mosquito species that are

transmitters of dengue and yellow fever. Detecting which species could find new favourable areas and where the favourability for these species could increase is a relevant tool for the establishment of disease surveillance protocols.

8.2. Introduction

The extent of occurrence of both dengue and yellow fever, the most important arboviral diseases affecting humans worldwide (Kuno, 2015; Colón-González *et al.*, 2021), has been changing due to intensive agriculture, irrigation, deforestation, population movements, rapid unplanned urbanisation, and phenomenal increases in international travel and trade (WHO, 2014a). The "urban" mosquito species *Aedes aegypti* and *Ae. albopictu*s are consider to be main vectors of these diseases, and so the shifting trend of both species' ranges is much of a concern in public health (Rupasinghe *et al.*, 2022). However, these mosquitoes are not the only ones transmitting dengue and yellow fever, as some sylvatic species are also involved in the virus spillover between primates (Hanley *et al.*, 2013).

Rocklöv and Dubrow (Rocklöv & Dubrow, 2020) suggest that global warming could become a driving factor for the future spread of mosquito-borne diseases. So the incidence and distribution of these diseases are often conditioned by the abundance and distribution of their vectors, some studies have developed models to predict range changes for *Ae. aegypti* and *Ae. albopictus* caused by climate change (Campbell *et al.*, 2015; Ryan *et al.*, 2018; Iwamura *et al.*, 2020). *Aedes* mosquito vectors could be currently expanding their distribution to more temperate climates (Aliaga-Samanez *et al.*, 2021; Watts *et al.*, 2021), specifically in North America, Australia, and Europe (Khan *et al.*, 2020; Aliaga-Samanez *et al.*, 2021). Recent research has suggested that, in the last 50 years of the 20th century, the environmental conditions became 1.5% more suitable for *Ae. aegypti* globally, and that suitability could increase by 3.2-4.4% per decade by 2050 (Iwamura *et al.*, 2020). Climate changes could even be forcing vectors to develop adaptation

mechanisms facilitating infection spread (Filho *et al.*, 2022). However, up to now, the effects of climate change on sylvatic vectors have not been taken into account.

Areas prone to sylvatic arboviral transmission to humans from non-human primates may be larger than estimated (Aliaga-Samanez *et al.*, 2021, 2022). Anthropogenic disturbance in forests allows the integration of different mosquito communities at forest edges (Meyer Steiger *et al.*, 2016). So, any attempt to make forecasting of dengue and yellow fever transmission risk, in geographic contexts involving tropical areas, should take both urban and sylvatic vectors into account (Carvalho *et al.*, 2017).

The objectives of this research are to answer the following questions regarding to dengue and yellow fever: (1) Which mosquito species could be implicated in a future increase of the surface of transmission risk areas? (2) Where can be expected those areas to increase.

8.3. Material and Methods

8.3.1. Methodological framework and temporal context

In order to analyse the effect of climate change on dengue and yellow fever vectors distributions, we took into account the favourability models for these species published by Aliaga-Samanez *et al.* (2021, 2022). Favourability models for every single urban vector species (i.e., *Ae. aegypti* and *Ae. albopictus)* and for every single sylvatic vector species (i.e., *Ae. africanus*, *Ae. luteocephalus*, *Ae. niveus*, *Ae. vittatus*, *Sabethes chloropterus*, *Haemagogus leucocelaenus* and *Hg. janthinomys*) were projected to different climate change scenarios over different time periods. The temporal context for Aliaga-Samanez *et al.* 's (2021, 2022) models is 2001-2017. Model projections were made for the period 2041-2060 ("near future"), and 2061-2080 ("distant future"). These projections, representing future forecasts, were mapped in the same grid of 18,874 hexagons of 7,774-km^2 used for the original model, covering the whole world.

8.3.2. Forecasting the future distribution of vectors

In order to make forecasts for a given species, we recalculated favourability values (*F*) using the same equation that defined its original model, replacing the values of climate variables in each hexagon according to predictions by the Intergovernmental Panel on Climate Change (IPCC). This equation is defined as follows:

$$F = \frac{e^{y}}{\left(\frac{n_1}{n_0}\right) + e^{y}}$$

where n_1 and n_0 are, respectively, the number of presences and absences considered as dependent variables for model training, and y is a linear combination of predictor variables. Values for the non-climatic variables forming part of the model were assumed not to change in the future period considered. We used climatic variables from different socioeconomic scenarios and atmosphere–ocean general circulation models to consider uncertainties in our forecasts according to a range of variation in climatic predictions. Five general circulation models (GCM) were selected. They provided predictions available for the whole world and with the lowest detected biases with respect to actual climate data (Mcsweeney *et al.*, 2015; Sanderson *et al.*, 2015): CESM1-CAM5, CNRM-CM5, FIO-ESM, GFDL-CM3, MPI-ESM-LR. We also considered two representative concentration pathway (RCP) scenarios: a stabilised emissions scenario RCP 4.5, and a high emissions scenario RCP 8.5. GCMs and RCP scenarios were got from CHELSA free high resolution climate data (Knutti *et al.*, 2013; Karger *et al.*, 2017, 2021; Nikolaus Karger *et al.*, 2020). So, the model of each single vector species was projected to a total of 10 GCM-RCP scenario combinations per future period. Finally, a climate change forecast consensus was calculated using average favourability values of the 10 projections for a given period.

The forecasts produced for species that are vectors of a same disease were combined with each other using the fuzzy logic operator “fuzzy union” (Estrada

et al., 2008), which is equivalent to assigning the highest favourability value in each hexagonal unit.

8.3.3. Expected rates of change in favourability

We mapped the expected increment of favourability by calculating the difference between forecasted favourability values and those ones in the original model. In order to quantify to what extent the current favourability (F_0) is modified globally in the future forecats (F_f), we calculated the fuzzy parameters of increment and maintenance according to the equations (Kuncheva, 2001; Romero *et al.*, 2014):

$$I = \frac{\mathrm{c}(F_f) - \mathrm{c}(F_0)}{\mathrm{c}(F_0)} \qquad \text{and} \qquad M = \frac{\mathrm{c}(F_f \cap F_0)}{\mathrm{c}(F_0)},$$

where *I* represents the global rate of increment in favourability, and *M* represents the global rate of maintenance of the original values. The factor c(F_x) is the cardinality of the F_x model or model projection –where favourability is treated as a fuzzy set (Estrada *et al.*, 2008)– that is, the sum of all the hexagons' favourability values (which, in turn, are treated as degrees of membership in the fuzzy set of hexagons favourable for the presence of vectors). The intersection between future (F_f) and present (F_0) favourability values is defined as follows:

$$F_f \cap F_0 = \mathrm{Min}\left(F_f, F_0\right).$$

Positive increment values (*I*) indicate a net increase in favourability, that is, a gain of favourable areas; whereas negative values mean a net loss of favourable areas. The maintenance values (*M*) indicate the degree of overlap between present and forecasted favourable areas.

8.3.4. Uncertainty in the forecasts

The local degree of uncertainty of forecasts resulting from a consensus based on averages (see above), was mapped by calculating the standard deviation, for each

spatial unit, of the 10 possible favourability values projected for a given period (5 GCMs x 2 RCP scenarios). This standard deviation was interpreted as a measure of the reliability of forecasts in each hexagonal unit.

8.4. Results

8.4.1. *Ae. aegypti* and *Ae. albopictus* models projected into the future

Favourable areas for *Ae. aegypti*, according to the models projected into the future for periods 2041–2060 and 2061–2080, show little differences compared to the current situation, changes being perceptible only in the regional scales (Fig. 8.1 and Appendix 26). The areas currently favourable to the presence of *Ae. aegypti* are expected to remain that way from now to 2080, the maintenance index value being M ≥ 0,96. In the near future (2041-2060), there could be a very slight global net loss of favourability according to the increment index value being (I = -0,03); whereas a positive increase (I = 0,075) could happen in the distant future (2061-2080) respect to the current situation. This increase would affect some regions of the Amazon basin and of Central Africa where favourability values, currently being intermediate-low, would turn into intermediate-high (Fig. 8.1 and Appendix 26). Extensive areas of the United States, Europe, and Australia could experience a favourability increase of 0,01 to 0,03 points (Appendix 26). Even though, these regions would still keep being unfavourable to the presence of *Ae. aegypti* (Fig. 8.1).

Expected changes for *Ae. albopictus* are much lower (Fig. 8.1). Favourable areas for this species are expected to keep unchanged (M>0,99 in both future periods), while the global net gain in favourability could be slight, and would take place soon in the near future (I=0,019 for the period 2041-2060; I=0,020 for the period 2061-2080) (Appendix 26).

8.4.2. Sylvatic vector models projected into the future

Changes predicted for sylvatic vectors depend on the mosquito species analyzed (Fig. 8.1). In America, favourable areas for *Haemagogus janthinomys* and *H.*

leucocelaenus show not to change apparently with respect to the current time. In contrast, high-favourability areas for *Sabethes chloropterus* in Central and South America seem to increase progressively north and southward. In Africa and Asia, changes could be negligible in the near future, whereas a little increase is expected in the distant future. This would be a north and southward increase in Central Africa for *Ae. luteocephalus* and for *Ae. africanus*; and a south and eastward increase in Asia for *Ae. niveus*. *Ae. vittatus*, which has populations in Europe, Africa and Asia, could experience a slight favourability increase elsewhere in the more distant future (Fig. 8.1).

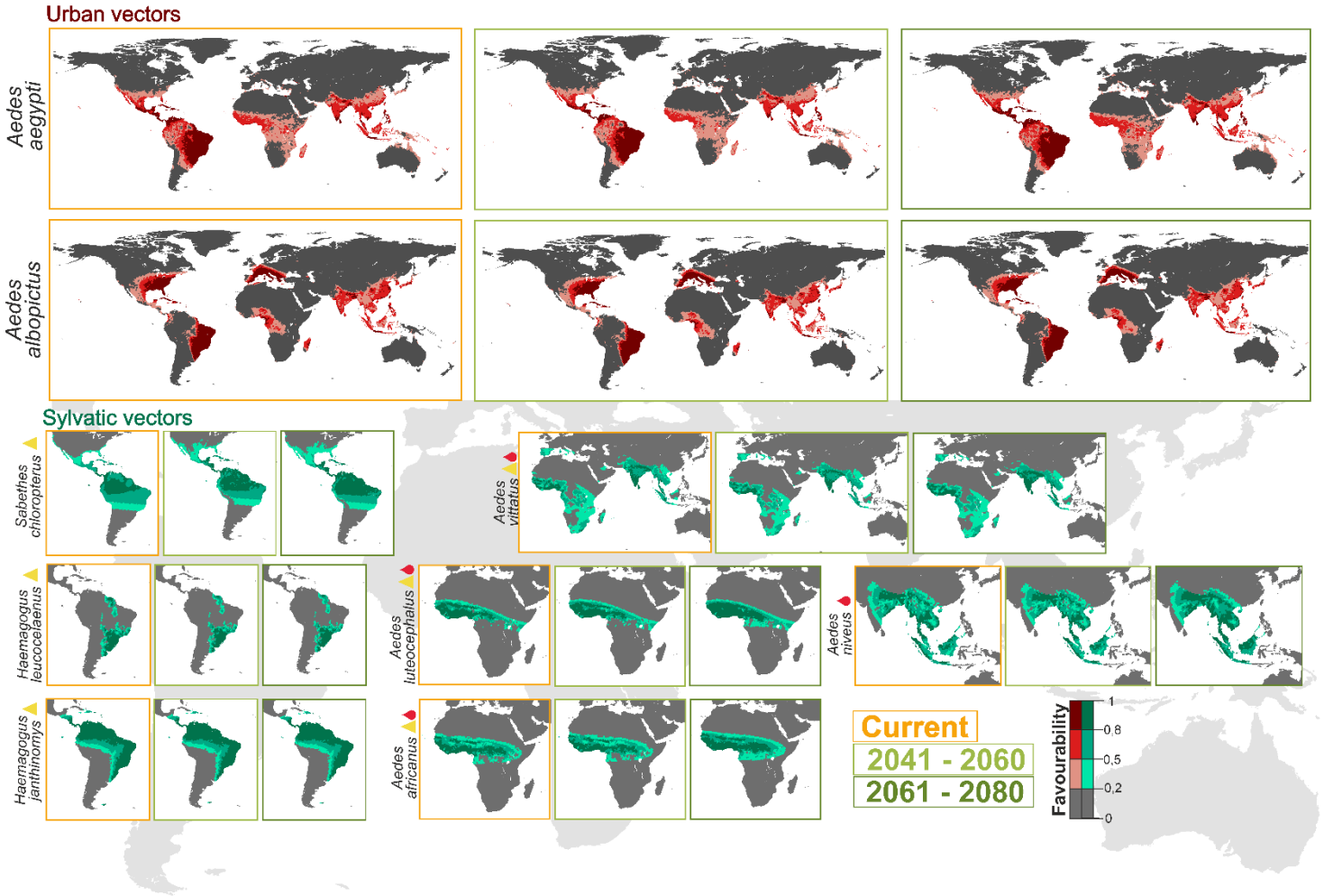

Fig. 8.1. Sylvatic vector models projections into the future for the periods 2041 -2061 and 2061-2080. Models of the sylvatic mosquitoes (*Haemagogus janthinomys*, *Haemagogus leucocelaenus*, *Sabethes chloropterus*, *Aedes luteocephalus*, *Aedes africanus*, *Aedes vittatus*, *Aedes niveus)* for the current time (2001–2017) and average model projections into the future for the periods 2041–2060 and 2061–2080. Yellow triangles represent yellow fever vectors and red drops represent dengue vectors.

8.4.3. Combined (urban and sylvatic) vector models projected into the future

The models combining predictions for all the vectors of dengue show that areas currently favourable to the presence of these species will surely keep this status in the near (2041–2060) and the distant (2061–2080) future (M>0,98). Despite favourability could decrease globally very slightly in the near future (I=-0.006), its values could increase locally more than 7% in the north of West Africa and in the southern limits of the Himalayas (Fig. 8.2C and Appendix 27). However, this increase would not produce a noteworthy enlargement of high-favourability areas (compare Fig. 8.2A and 8.2B). In the more distant future, a 5% favourablity increase is expected (I=0,05), and so new areas could become favourable for the presence of dengue vectors in large areas of West and Central Africa and in South-East Asia, reaching Borneo (Fig. 8.2C and Appendix 27).

Combined predictions for yellow fever vectors (Fig. 8.3) show a similar panorama to that of dengue. Favourable areas will probably keep unchanged in both future periods (M>0,97). Global favourability values could decrease a bit in the near future (I=-0.01), but might increase in the distant future (I=0,03). This increase is expected to affect principally the Amazon basin, West and Central Africa. The models indicate, instead, a regional favourability decrease of more than 0,01 points in coastal areas of Chile and Peru.

According to the uncertainty analysis, variations between scenario-model combinations in the near future mostly occur in the areas where average favourability is predicted to increase. In the more distant future, there is more consistence between projections, and high variations only occur in some areas of West and Central Africa (Fig. 8.2D and 8.3D). Some uncertainty is also found in the southern limits of the Himalayas, in predicted values regarding vectors transmitting the yellow fever virus.

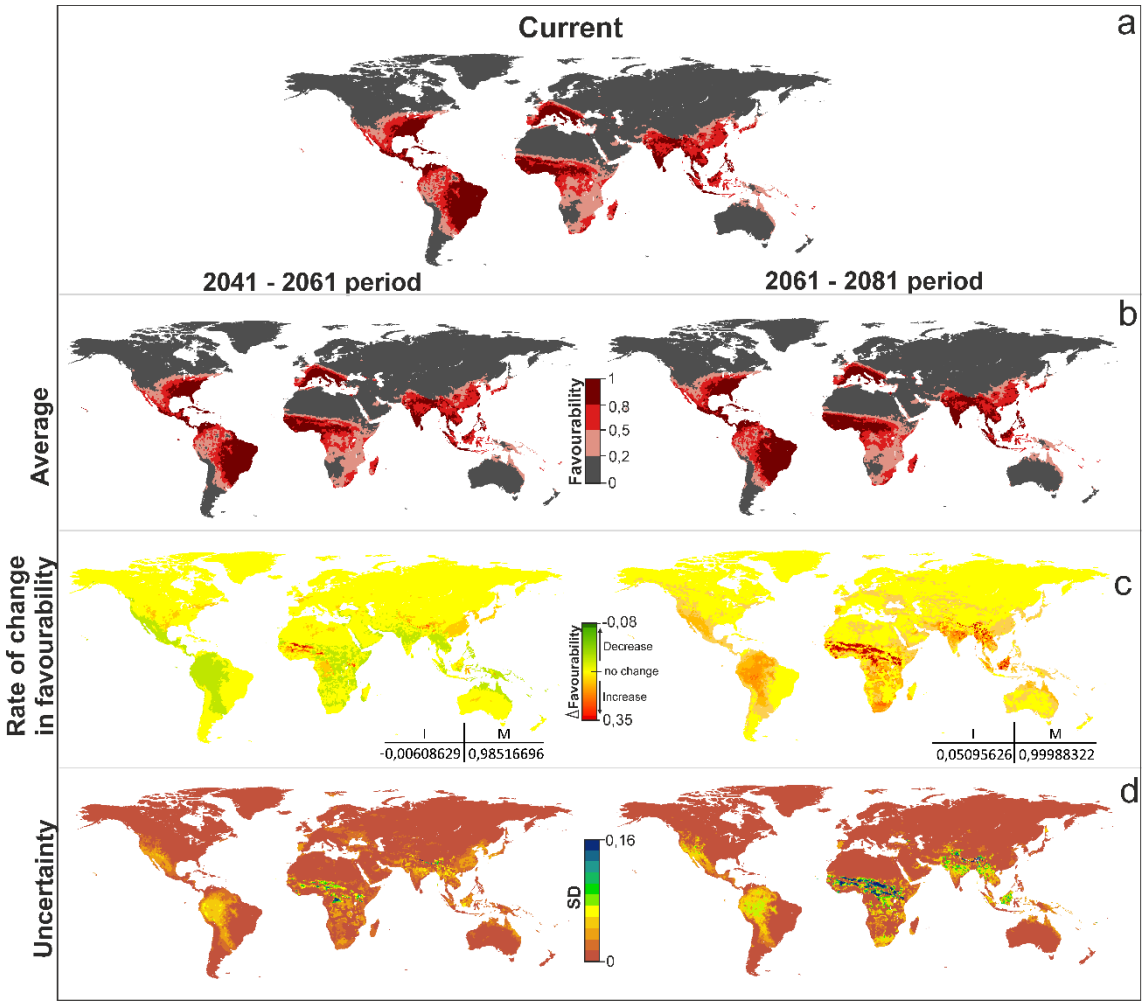

Fig 8.2. Dengue vector model projections into the future for the periods 2041–2060 and 2061–2080. a Vector model for the current time (2001–2017), **b** average model projections into the future for the periods 2041–2060 and 2061–2080, **c** areas where favourability increases and decreases in the future relative to the present**.** Difference between the future projection and the current model. I: increment rate; M: maintenance rate. Positive values of I indicate a net increase in favourability, that is, a gain in favourable areas, whereas negative values of I mean a net loss of favourable areas. M indicates the degree to which the favourable areas in the current model overlap with the favourable forecasted areas. **d** Uncertainty of the vector model in the period 2041-2060 and 2061 – 2080.

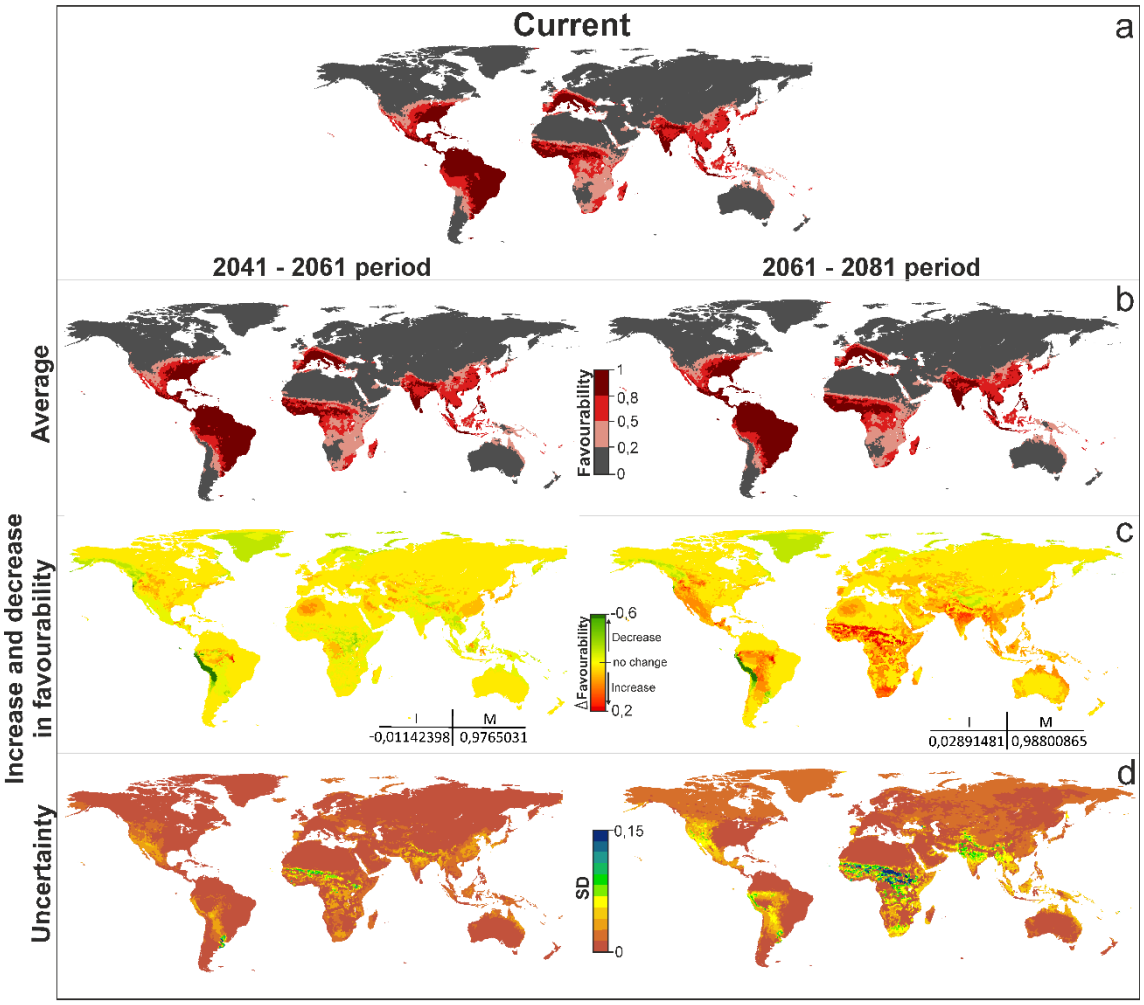

Fig 8.3. Yellow fever vector model projections into the future for the periods 2041–2060 and 2061–2080. a Vector model for the current time (2001–2017), **b** average model projections into the future for the periods 2041–2060 and 2061–2080, **c** areas where favourability increases and decreases in the future relative to the present**.** Difference between the future projection and the current model. I: increment rate; M: maintenance rate. Positive values of I indicate a net increase in favourability, that is, a gain in favourable areas, whereas negative values of I mean a net loss of favourable areas. M indicates the degree to which the favourable areas in the current model overlap with the favourable forecasted areas. **d** Uncertainty of the vector model in the period 2041-2060 and 2061 – 2080. SD: Standard Deviation.

8.5. Discussion

This study is the first to analyze the effect of climate change in the distribution of the whole set of mosquito species transmitting dengue and yellow fever. Based on our results, we suggest that an average global increase in favourable conditions could happen for different species of urban and sylvatic mosquitoes in the future. Regionally, favourability for the presence of these species could increase, decrease or not change.

Climate change is expected to allow *Ae. albopictus* and *Ae. aegypti* to expand into previously unoccupied temperate regions (Ryan *et al.*, 2018; Aliaga-Samanez *et al.*, 2021). Our models for the present time already predict favourable conditions in absence areas for both mosquito species (Fig. 8.1). For example, in Europe, our model suggests that Barcelona, Algeciras, Venice, Sardinia, Antwerp, Naples and the west coast of Portugal are favourable areas (0,2<F<0,5) for the presence of *Ae. aegypti* (Fig. 8.1). In addition, we detect areas with intermediate-high favourability values (0,5<F<0,8) in Valencia, Rotterdam, Istanbul and Naples (Fig. 8.1). Taking into account that some of the most important ports in Europe are located in Barcelona, Rotterdam, Valencia, and Antwerp (Eurostat, 2021), these could be important points for establishment of *Ae. aegypti* in case of accidental entry. Da Re *et al*. (2021) assessed the probability that *Ae. aegypti*, which currently occurs just on the east coast of the Black Sea, Turkey, Bulgaria and Russia (ECDC, 2022), spread through continental Europe. They selected five European ports taking into account environmental conditions and the economic importance of the harbours, and suggested that the city most likely to be at risk of establishment was Barcelona, followed by Algeciras. There is evidence of accidental arrivals of this mosquito species in northern Europe. For example, in 2010, national surveillance in the Netherlands detected the presence of *Ae. aegypti* in a shipment of tires from Miami (Scholte *et al.*, 2010; Brown *et al.*, 2011). Following the discovery, the Dutch government activated control measures that drove to successful elimination (Scholte *et al.*, 2010; Ibañez-Justicia *et al.*, 2017). In 2016,

Ae. aegypti was detected in the Netherlands again, at the Schiphol International airport (Ibañez-Justicia *et al.*, 2017). So, the re-infestation of *Ae. aegypti* in Europe is possible with many pathways and entry points. The question is whether, once the introduction has happened, environmental conditions are suitable for the species to establish successfully in the area. Although Da Re *et al.* (2021) detected that the areas of Genoa, Venice and Rotterdam are not suitable for establishment of *Ae. aegypti* populations now, they suggested that climate change could create conditions for a future invasion. Both Campbell *et al.* (2015) and Ryan *et al.* (2018) sustain that the potential distribution of *Ae. aegypti* under future conditions could increase in most Europe, even reaching the north of the continent as a consequence of climate change. However, our model projections for 2060 and 2080 continue to predict the same favourable areas that are pointed to for the present time. I.e., according to our models, the risk of *Ae. aegypti* new introduction in Europe could keep concentrated in cities that are equipped with large harbours and/or airports, most probably favoured by the chances of arrival than by climate changes. The situation for *Ae. albopictus* in Europe is clearly different. This species established stable populations in this continent since 1979, probably introduced for the Durres Port (Albania) through the entry of goods from China (Adhami & Reiter, 1998). *Ae. albopictus* has been introduced in 33 European countries and is established in 26. This species might have caused dengue outbreaks already in France, Italy and Croatia and autochthonous cases in Spain (Gossner *et al.*, 2018; Centro de Coordinación de Alertas y Emergencias Sanitarias. Ministerio de Sanidad Consumo y Bienestar, 2019). Our models suggest that, currently, *Ae. albopictus* have favourable conditions to occur in the 7 countries where it is not yet established, and will continue to have them in 2080 (Fig. 8.1).

In South America, *Ae. aegypti* has stable populations in all countries. *Ae. albopictus* has not yet been detected in Peru, Ecuador, Chile, Bolivia and Uruguay, but it already occurs in their neighbouring countries. Aliaga-Samanez *et al.* (2021) described an increase in favourable territories, for both *Aedes* species, from the

Brazilian coast to the Amazon basin during the last 20 years. According to our model projections, the Amazon basin could remain favourable for them in the different future periods analysed, and could become even more favourable for *Ae. aegypti*, reaching intermediate-high values in Colombia, Peru and Brazil (Fig. 8.1). This makes us suggest that temperature changes might have already favoured the recent spread of *Aedes* species in the area, in spite of some authors have predicted no new relevant variations in distribution under climate change conditions in South America (Kamal *et al.*, 2018). Good news, in this scenario, are that the Pan American Health Organization (PAHO) has established, since 2019, a manual for indoor residual spraying in urban areas for the control of *Ae. aegypti* in American regions (PAHO, 2019a). In Asia, our models forecast an increase of favourability values for *Ae. aegypti* in territories to the east and south of China (Fig. 8.1), which is consistent with Liu et al. (2019)'s results. According to the WHO, funding is needed in south-eastern Asia for strengthening surveillance, reporting and vector management (Nagpal *et al.*, 2018), as a response to the increased burden of dengue experienced since 2011 (Bangert *et al.*, 2018). Finally, Central Africa could also see a spread of favourable areas for *Ae. aegypti* (Fig. 8.1). Gaythorpe *et al.* (2020) claimed that Central Africa Republic is one of the countries most likely to see an increase in yellow fever transmission. Unfortunately, Africa lacks of uniform surveillance policies (Weetman *et al.*, 2018).

Focusing on the response of sylvatic mosquitoes to climate changes (Figs. 8.1, 8.2 and 8.3), *Ae. niveus* and *Ae. vittatus* should be subject to survey as dengue vectors in Asia, where areas favourable to their presence could spread in the hinterlands of India, in the south-east of China, and in the South-Asian countries, especially in Borneo. In west and central sub-Saharan Africa, according to our results, attention should be paid to the three selvatic vectors of dengue and yellow fever, *Ae. vittatus*, *Ae. luteocephalus* and *Ae. africanus*, especially in Cameroon, Central Africa Republic and north of Democratic Republic of Congo. However, the current entomological capacity in Africa is primarily focused on malaria vectors, and most

of the countries lack routine surveillance programmes, trained personnel and control activities focusing on *Aedes* and the viruses they transmit (Buchwald *et al.*, 2020). As outbreaks of *Aedes*-borne arboviruses continue to increase in Africa, it would be critical to establish a solid public health entomology infrastructure for *Aedes* mosquitoes to contain and prevent further outbreaks (Dadzie *et al.*, 2022).

Both in Africa and in Asia, the most relevant changes are forecasted for the distant future (2061-2080), but in South America, the increase in favourability for the yellow fever vector *Sabetes chloropterus*, forecasted for the jungle areas of Bolivia, Peru and Brazil, could start in the near future (2041-2060). We suggest that the prevention measures planned by the Pan American Health Organization (PAHO) for urban mosquitoes also include specifications and survey planning relative to *S. chloropterus*. In Brazil, sylvatic yellow fever outbreaks that have occurred since 2017 highlight the need to strengthen surveillance for zoonotic yellow fever in non-human primates (PAHO, 2019b; Aliaga-Samanez *et al.*, 2022).

Climate change could modify and make the risk of zoonotic disease increase due to its effects on the configuration and distribution of vectors. The increase in favourability for the presence of urban and sylvatic mosquitoes in the tropics could contribute to the spread of the areas at risk of transmission of dengue and yellow fever. In Europe, some coastal areas are and will remain favourable for the introduction and possible establishment of *Ae. aegypti*. Detecting which mosquito species could find new favourable areas is an important tool to establish a surveillance protocol to prevent new cases of dengue and yellow fever.

CAPÍTULO 9

Discusión general

9. Discusión general

La biodiversidad desempeña un papel fundamental en el funcionamiento de los ecosistemas y en la salud humana. La conservación y el uso sostenible de la biodiversidad podría beneficiar a la salud humana manteniendo los servicios de los ecosistemas y reduciendo el riesgo de enfermedades zoonóticas (Keesing et al., 2010; WHO, 2015). Desde un punto de vista biogeográfico, se puede estudiar y entender la distribución de las especies en el espacio y en el tiempo. La modelación de distribuciones es una herramienta útil para analizar la distribución de las especies desde puntos de vista descriptivo y explicativo, así como para estudiar las relaciones biogeográficas entre taxones muy diferentes (Acevedo *et al.*, 2007), analizar la distribución de una especie que podría estar influida por factores limitantes (Olivero *et al.*, 2017a), e identificar áreas prioritarias para la conservación de especies (Estrada *et al.*, 2008). En los últimos años, la modelación de la distribución de especies se ha convertido en uno de los enfoques biogeográficos con mayor potencial patogeográfico (Guisan & Zimmermann, 2000). Esto se debe a que entender la distribución espacial y temporal de enfermedades infecciosas es importante para entender qué factores condicionan el riesgo de que tengan lugar nuevos brotes (Peterson, 2008; Hay *et al.*, 2013).

En la presente tesis se ha intentado realizar un recorrido por diferentes aspectos biogeográficos teniendo como hilo conductor la distribución de los primates en sus dimensiones espacial y temporal. Se ha hecho con objetivos metodológicos relacionados con la posibilidad de considerar factores históricos concretos en los modelos de distribución **(capítulo 4)**; y también con finalidades vinculadas a la conservación y a la salud humana **(capítulos 5, 6, 7 y 8)**. Se ha comenzado con un enfoque metodológico sobre la posibilidad de incluir información sobre la existencia de barreras a la dispersión en los modelos de distribución **(capítulo 4)**, que ha contribuido a la construcción de los modelos realizados en los siguientes capítulos. Concretamente, se ha tratado de aportar enfoques metodológicos

novedosos que mejoren el rendimiento de los modelos de distribución de especies cuando es necesario tener en cuenta su dinamismo espaciotemporal. La estructura de la distribución de las especies, en este caso de los primates, está influida por diversos factores que pueden alterar su configuración (Wich & Marshall, 2016). Entre estos factores se encuentran las condiciones ambientales que pueden favorecer o desfavorecer la presencia de la especie (Lomolino *et al.*, 2006). Existen también otros factores denominados históricos, difíciles de cuantificar, pero que son capaces de mantener la estructura espacial de una distribución (Rapoport, 1975). Por ejemplo, la capacidad de la especie para ocupar hábitats potencialmente favorables puede estar limitada por barreras a la dispersión, que impactan sobre las poblaciones a largo plazo (Cozzi *et al.*, 2013). Con demasiada frecuencia, en modelación se tienen en cuenta sólo las condiciones ambientales, y en ocasiones sólo el clima (Real *et al.*, 2003; Márquez *et al.*, 2011). Es útil, por tanto, la inclusión de información que permita considerar la existencia de barreras biogeográficas en los modelos de distribución, pues ello permitirá mejorar el rendimiento de los modelos cuando las especies están condicionadas por la historia. Por lo tanto, en los capítulos siguientes, se ha aplicado este enfoque allí donde ha sido necesario.

Los factores antrópicos pueden contribuir a la reducción y alteración de las poblaciones de primates (Estrada *et al.*, 2017). El uso de datos de patrullas de guardabosques, junto con el modelado espacial, permite analizar mejor los eventos antrópicos como la deforestación, la caza furtiva y los incendios, que ocurren dentro de las áreas protegidas, y gestionar la toma de decisiones para la conservación de especies **(capítulo 5**). Estos eventos antrópicos contribuyen a modificar y/o disminuir las áreas de distribución de las especies de primates, y también, son factores que impulsan la aparición de enfermedades zoonóticas (Aliaga-Samanez *et al.*, 2021). Por ejemplo, en la amazonia brasileña y peruana se ha evidenciado que, como consecuencia de la deforestación para agricultura de subsistencia y extracción de recursos, el hábitat del borde del bosque promueve

la transmisión de la malaria debido al aumento de la población de mosquitos y del contacto humano-vector (Vittor *et al.*, 2006; MacDonald & Mordecai, 2019). Podría estar ocurriendo también con la fiebre amarilla, en Sudamérica y África, pues según los análisis biogeográficos realizados en esta tesis doctoral, los casos de esta enfermedad durante inicios del siglo XXI están significativamente relacionados con la pérdida de bosque **(capítulo 7).** También, las poblaciones de primates que son hospedadores de virus pueden perderse cuando sus poblaciones quedan aisladas en pequeños fragmentos, como ocurrió en Brasil, en el estado de Rio Grande do Soul, donde el 80% de las poblaciones de monos aulladores murieron tras un evento epizoótico de fiebre amarilla en 2008 y 2009 (Estrada *et al.*, 2018).

Además, cuando los ecosistemas está perturbados se puede alterar el equilibrio de las poblaciones, aumentando el número de reservorios y de patógenos (por ejemplo, Allan *et al.*, 2003, revelaron un aumento de bacterias que ocasionan la enfermedad de Lyme, en ninfas de garrapatas, debido al aumento de la densidad de ratones ocasionado por la deforestación; y también, Olivero *et al.*, 2017b, revelaron que los brotes ubicados a lo largo de los límites del bioma de la selva tropical se asocian significativamente con pérdidas de bosques en los dos años anteriores). Por todos estos motivos, la conservación de la biodiversidad puede evitar la propagación de enfermedades zoonóticas, debido a que las poblaciones dañadas son más sensibles a enfermar y más susceptibles de generar nuevos brotes (**capítulo 5, 6 y 7**). Por lo tanto, se podría disminuir el riesgo de aparición de nuevos brotes de dengue y de fiebre amarilla en Sudamérica, África y Asia, conservando las poblaciones de primates ya que son hospedadores de estas enfermedades. Los modelos aquí expuestos han detectado que, en el sur de Camerún, los primates podrían contribuir parcialmente a la presencia de casos de dengue en humanos **(capítulo 6).** Además de la deforestación, la caza furtiva también es una amenaza para las poblaciones de primates que puede contribuir a reducir sus poblaciones (**capítulo 5**) y dar comienzo a brotes nuevos. Por

ejemplo, en la reserva del Dja en el sur de Camerún, la fauna protegida se concentra en el núcleo del área protegida coincidiendo con actividades de caza (**capítulo 5**). Esto afecta a primates como el chimpancé y el gorila, especies que según la Lista Roja de la IUCN se encuentran en peligro y en peligro crítico respectivamente **(capítulo 5)**. Los cazadores al adentrarse en la selva, permiten que el contacto entre ellos y especies hospedadoras o vectores de patógenos zoonóticos sea más estrecho, incrementando la posibilidad de contraer enfermedades (Wolfe *et al.*, 2005). Si ocurre esta secuencia de sucesos, los cazadores pueden llegar a ser el "caso cero" y al retornar a sus comunidades puede convertirse en un nuevo brote (Leroy *et al.*, 2004).

Comprender las asociaciones entre los humanos y la vida silvestre permite detectar qué eventos antropogénicos pueden desencadenar que los virus salten a los seres humanos (Olivero *et al.*, 2020). Es importante entender bien las vías que pueden conducir a brotes, porque en muchos casos, la información errónea, por ejemplo sobre los vectores de transmisión, como ocurrió con la fiebre amarilla cuando la población humana local provocó la matanza de poblaciones de monos aulladores (Bicca-Marques *et al.*, 2017; BBC, 2018). Los primates no humanos son hospedadores del virus y, además, especies "centinelas", es decir, especies que advierten de que la enfermedad está presente en la zona, y por tanto con alto valor para la prevención en el contexto de la alerta temprana (Lahm *et al.*, 2007, **capítulo 7)**. También ocurrió con las poblaciones de murciélagos vampiros que disminuyeron a casusa de la matanza descontrolada en América del Sur. La disminución de murciélagos afecta los servicios ecosistémicos que brindan (Kunz *et al.*, 2011). Además, también puede aumentar la prevalencia de patógenos y mejorar la transmisión de enfermedades a los humanos como la rabia (Streicker *et al.*, 2012; Amman *et al.*, 2014).

Las actividades humanas también han permitido que las especies de vectores de enfermedades se adapten y evolucionen en nuevos entornos **(capítulos 6, 7 y 8)**.

Esta dinámica en las distribuciones de mosquitos genera que los patógenos se propaguen a nuevas zonas, por ejemplo, durante el siglo XXI las zonas favorables para los casos de dengue se han extendido por toda la cuenca amazónica **(capítulo 6)** y, en el caso de la fiebre amarilla, se detectaron nuevos casos al sur de Brasil ocasionando un gran brote durante el periodo 2016-2019 **(capítulo 7)**. A su vez, el cambio climático podría modificar y aumentar el riesgo de enfermedades zoonóticas debido a sus efectos sobre la configuración y distribución de los vectores **(capítulo 8)**. En Europa, algunas zonas costeras son, y probablemente seguirán siendo, favorables a la introducción y posible establecimiento de *Aedes aegypti* **(capítulo 8)**. Para evaluar el efecto del cambio climático en el riesgo de transmisión, es necesario tener en cuenta evaluar también cómo va a afectar a la distribución de los primates no humanos. Esta información aún es escasa. Sin embargo, algunas evaluaciones a nivel mundial sugieren que sus distribuciones experimentarán condiciones climáticas cambiantes durante el siglo XXI en el Amazonas, la Mata Atlantica, América Central, y el sureste de Asia (Graham *et al.*, 2016).

Los primates probablemente sean algunos de los mamíferos más vulnerables y menos capaces de seguir el ritmo del cambio climático (Schloss *et al.*, 2012). La presente tesis ha abordado el estudio del posible efecto del cambio climático en los mosquitos vectores de dengue y fiebre amarilla. El siguiente paso a dar es analizar el efecto del cambio climático en la distribución de los primates e integrar esta información con la aquí obtenida sobre los vectores en el capítulo 8. El fin último será proyectar el modelo de riesgo de transmisión de dengue expuesto en el capítulo 6, así como el de la fiebre amarilla descrito en el capítulo 7, a escenarios futuros de cambio climático.

CAPÍTULO 10

Conclusiones

Conclussions

10. Conclusiones

1. La Función de Favorabilidad, al evaluar cómo afecta el ambiente a la distribución de las especies, independientemente de su prevalencia en el área de estudio, ha permitido comparar y combinar diferentes modelos de diferentes especies, integrar factores físicos y factores antrópicos en los modelos, así como combinar factores y agentes a través de la unión y de la intersección difusa.

2. De entre las distintas aproximaciones metodológicas para incorporar las barreras geográficas en los modelos de distribución de primates, la que ha obtenido los mejores valores, según los índices de evaluación utilizados, es aquella que describe la barrera como una entidad física (frente a una entidad ecológica basada en la interacción entre especies). Sin embargo, se ha comprobado que utilizar la superficie de tendencia puramente espacial es, también, una forma efectiva de integrar barreras en un modelo.

3. Los modelos que permiten mayor flexibilidad en el análisis de la estructura espacial describen mejor la forma de la distribución de las especies. En cambio, considerar una estructura espacial menos flexible permite que variables ambientales capaces de explicar la distribución de las especies estén mejor representadas en el modelo matemático.

4. La Función de Favorabilidad brinda herramientas metodológicas aplicables al estudio de otras especies de primates que estén limitadas por barreras geográficas, pues se han obtenido resultados similares con dos casos muy distintos en ubicación, escala, resolución espacial, biología de las especies y características del río.

5. Las zonas más favorables para el chimpancé, el gorila y el elefante, en la Reserva Forestal de Dja en Camerún, se encuentran dentro del núcleo del

área protegida, lo que coincide con las áreas altamente favorables para la caza furtiva. Las áreas favorables para los incendios y la deforestación se encuentran, principalmente, a lo largo de la periferia de la reserva.

6. El modelado espacial puede agregar valor a los datos obtenidos por las herramientas de monitoreo electrónico SMART y CyberTracker. De esta forma, permite a los administradores comprender mejor los eventos que ocurren dentro de las áreas protegidas y puede facilitar la toma de decisiones para mejorar su gestión.

7. Es probable que el dengue y la fiebre amarilla se propaguen a regiones donde actualmente no existen o hay muy pocos casos. El enfoque metodológico propuesto para analizar las zonas de riesgo de ambas enfermedades ha permitido que se pueda sugerir estrategias de vigilancia, y de vacunación en el caso de la fiebre amarilla, considerando tres escenarios geográficos de acuerdo con la distribución espacial de los factores que favorecen el riesgo: (1) áreas con condiciones favorables para los vectores y la presencia del virus, (2) áreas con condiciones favorables solo para los vectores y (3) áreas con condiciones favorables únicamente para la presencia del virus.

8. Se ha identificado las zonas donde los primates no humanos podrían favorecer la aparición de dengue y de fiebre amarilla, independientemente de las correlaciones con otros factores. Además, se aporta un listado de especies de primates no humanos pertenecientes a corotipos significativamente relacionados con la distribución de la fiebre amarilla, con la finalidad de centrar la vigilancia en estas especies, ya que podrían ser el origen de nuevos futuros brotes.

9. Los modelos de enfermedad y riesgo de transmisión de dengue de finales del siglo XX demostraron capacidades predictivas significativas con respecto a los registros de casos de principios del siglo XXI. Los modelos

de principios del siglo XXI también mostraron capacidades predictivas significativas.

10. Se ha detectado áreas que deben ser priorizadas para implementar medidas de vigilancia sanitaria debido a que la transmisión del dengue y de la fiebre amarilla podrían propagarse. Por ejemplo, en el caso del dengue, cabe destacar el sureste de China, Papua Nueva Guinea, el norte de Australia, el sur de EE.UU., Colombia y Venezuela, Madagascar, Japón y áreas urbanas del sur y centro de Europa. En el caso de la fiebre amarilla, se señalan la cuenca del Amazonas y el sur de Brasil, y en África, Namibia, el oeste de Zambia, el este de Etiopía y algunas zonas de Somalia.

11. Los modelos sugieren que los vectores podrían ampliar significativamente su presencia en áreas tropicales y no tropicales a nivel mundial.

12. La pérdida de bosques ha resultado ser una variable significativa en el modelo de enfermedad del siglo XXI de la fiebre amarilla. La deforestación puede favorecer, por tanto, que se desarrollen nuevos brotes de esta enfermedad.

13. Al identificar las zonas en las que la incertidumbre climática para el futuro es menor, se han podido localizar geográficamente las predicciones más fiables.

14. Los resultados sugieren que, debido al cambio climático, las zonas favorables para la presencia de *Ae. niveus* y *Ae. vittatus* podrían extenderse en el interior de la India, en el sureste de China y en los países del sur de Asia, especialmente en Borneo. En África subsahariana occidental y central, habría que centrarse en *Ae. vittatus*, *Ae. luteocephalus* y *Ae. africanus*, especialmente en Camerún, la República Centroafricana y el norte de la República Democrática del Congo. En Europa, algunas zonas

costeras son, y seguirán siendo, propicias para la introducción y el posible establecimiento de *Ae. aegypti*.

10. Conclussions

1. The Favourability Function, by assessing how the environment affects the distribution of species, regardless of their prevalence in the study area, has allowed to compare and combine different models of different species, to integrate physical and anthropogenic factors into the models, as well as to combine factors and agents through fuzzy intersection and the fuzzy union.

2. Among the different methodological approaches to incorporate geographic barriers in primate distribution models, the one that has obtained the best values, according to the evaluation indices used, is the one that describes the barrier as physical (compared to the description of barriers as ecological entities based on between-species interactions). However, using the purely geographical *trend surface* also seems to be an effective way of integrating barriers into a model.

3. Within a model, allowing more flexibility in the analysis of the spatial structure allows better descriptions of the shape of the species distribution. Instead, less flexible descriptions of the spatial structure allow environmental variables capable of explaining species distributions to be better represented in the mathematical model.

4. The Favourability Function provides methodological tools applicable to the study of other primate species that are limited by geographical barriers, as similar results have been obtained with two very different cases in location, scale, spatial resolution, species biology and river characteristics.

5. The most favourable areas for chimpanzees, gorillas and elephants, in the Dja Forest Reserve in Cameroon, are within the core of the protected

reserve, which coincides with areas highly favourable for poaching. Areas favourable for fires and deforestation are found mainly along the periphery of the reserve.

6. Spatial modelling can add value to the data obtained by the SMART and CyberTracker electronic monitoring tools. In this way, it allows managers to better understand events occurring within protected areas and can facilitate decision-making to improve management.

7. Dengue and yellow fever are likely to spread to regions where there are currently no or very few cases. The methodological approach proposed to analyse the risk zones for both diseases has made it possible to suggest surveillance strategies, and vaccination strategies in the case of yellow fever, considering three geographical scenarios according to the spatial distribution of risk factors: (1) areas with favourable conditions for vectors and the presence of the virus, (2) areas with favourable conditions only for vectors, and (3) areas with favourable conditions only for the presence of the virus.

8. Areas where non-human primates may favour the occurrence of dengue and yellow fever have been identified, independently of correlations with other factors. In addition, a list of non-human primate species belonging to chorotypes significantly related to the distribution of yellow fever is provided, with the aim of focusing surveillance on these species, as they could be the source of future outbreaks.

9. Dengue transmission risk and disease models from the late 20th century demonstrated meaningful predictive capacities with respect to early 21st century case records. Early 21st century models also showed significant predictive capacities.

10. Areas have been identified that need to be prioritised for the implementation of health surveillance measures because dengue and yellow fever transmission could spread. For example, in the case of dengue, south-east China, Papua New Guinea, northern Australia, southern USA, Colombia and Venezuela, Madagascar, Japan, and urban areas of southern and central Europe are outlined. For the yellow fever, this research highlights the Amazon basin and southern Brazil, and in Africa, Namibia, western Zambia, eastern Ethiopia, and parts of Somalia.

11. The models suggest that vectors could significantly expand their presence in tropical and non-tropical areas globally.

12. Forest loss resulted to be included, as a significant variable, in the 21st century disease model of yellow fever. Deforestation may, thus, favour the development of new yellow fever outbreaks.

13. By identifying areas where climate uncertainty for the future is lowest, it has been possible to geographically locate the most reliable predictions.

14. The results suggest that, due to climate change, favourable areas for *Ae. niveus* and *Ae. vittatus* may expand in inland India, south-east China and South Asian countries, especially in Borneo. In western and central Sub-Saharan Africa, *Ae. vittatus*, *Ae. luteocephalus* and *Ae. africanus* should be targeted, especially in Cameroon, Central African Republic and northern Democratic Republic of Congo. In Europe, some coastal areas are, and will remain favourable for the introduction and possible establishment of *Ae. aegypti*.

CAPÍTULO 11

Referencias biliográficas

Bibliography

11. Referencias bibliográficas

Acevedo, P., Alzaga, V., Cassinello, J. & Gortázar, C. (2007) Habitat suitability modelling reveals a strong niche overlap between two poorly known species, the broom hare and the Pyrenean grey partridge, in the north of Spain. *Acta Oecologica*, **31**, 174–184.

Acevedo, P. & Real, R. (2012) Favourability: Concept, distinctive characteristics and potential usefulness. *Naturwissenschaften*, **99**, 515–522.

Acevedo, P., Ward, A.I., Real, R. & Smith, G.C. (2010) Assessing biogeographical relationships of ecologically related species using favourability functions: A case study on British deer. *Diversity and Distributions*, **16**, 515–528.

Acevedo-Whitehouse, K. & Duffus, A.L.J. (2009) Effects of environmental change on wildlife health. *Philosophical Transactions of the Royal Society B: Biological Sciences*, **364**, 3429–3438.

Adhami, J. & Reiter, P. (1998) Introduction and establishment of *Aedes* (*Stegomyia*) *albopictus* skuse (Diptera: Culicidae) in Albania. *Journal of the American Mosquito Control Association*, **14**, 340–343.

Akaike, H. (1973) *Information theory and an extension of the maximum likelihood principle*. In: Proceedings of the second international symposium on information theory (ed. by B.N. Petrov & F. Csaki), pp. 267–281. Budapest, Hungary.

Al-Abri, S.S., Kurup, P.J., Al Manji, A., Al Kindi, H., Al Wahaibi, A., Al Jardani, A., Mahmoud, O.A., Al Balushi, L., Al Rawahi, B., Al Fahdi, F., Al Siyabi, H., Al Balushi, Z., Al Mahrooqi, S., Al Manji, A., Al Sharji, A., Al Harthi, K., Al Abri, B., Al-Raidan, A., Al Bahri, Z., Al-Mukhaini, S., Amin, M., Prasanna, A.R., Petersen, E. & Al Ajmi, F. (2020) Control of the 2018–2019 dengue fever outbreak in

Oman: A country previously without local transmission. *International Journal of Infectious Diseases*, **90**, 97–103.

Ali, J.R. & Huber, M. (2010) Mammalian biodiversity on Madagascar controlled by ocean currents. *Nature*, **463**, 653–656.

Aliaga-Samanez, A., Cobos-Mayo, M., Real, R., Segura, M., Romero, D., Fa, J.E. & Olivero, J. (2021) Worldwide dynamic biogeography of zoonotic and anthroponotic dengue. *PLoS Neglected Tropical Diseases*, **15**, e0009496.

Aliaga-Samanez, A., Real, R., Segura, M., Marfil-Daza, C. & Olivero, J. (2022) Yellow fever surveillance suggests zoonotic and anthroponotic emergent potential. *Communications Biology*, **5**, 1–12.

Allan, B.F., Keesing, F. & Ostfeld, R.S. (2003) Effect of forest fragmentation on lyme disease risk. *Conservation Biology*, **17**, 267–272.

Allen, T., Murray, K.A., Zambrana-Torrelio, C., Morse, S.S., Rondinini, C., Di Marco, M., Breit, N., Olival, K.J. & Daszak, P. (2017) Global hotspots and correlates of emerging zoonotic diseases. *Nature Communications*, **8**, 1–10.

Almeida, M.A.B., da Cardoso, J.C., dos Santos, E., da Fonseca, D.F., Cruz, L.L., Faraco, F.J.C., Bercini, M.A., Vettorello, K.C., Porto, M.A., Mohrdieck, R., Ranieri, T.M.S., Schermann, M.T., Sperb, A.F., Paz, F.Z., Nunes, Z.M.A., Romano, A.P.M., Costa, Z.G., Gomes, S.L. & Flannery, B. (2014) Surveillance for Yellow Fever Virus in Non-Human Primates in Southern Brazil, 2001-2011: A Tool for Prioritizing Human Populations for Vaccination. *PLoS Neglected Tropical Diseases*, **8**, e2741.

Amarasinghe, A., Kuritsky, J.N., William Letson, G. & Margolis, H.S. (2011) Dengue virus infection in Africa. *Emerging Infectious Diseases*, **17**, 1349–1354.

Amman, B.R., Nyakarahuka, L., McElroy, A.K., Dodd, K.A., Sealy, T.K., Schuh, A.J., Shoemaker, T.R., Balinandi, S., Atimnedi, P., Kaboyo, W., Nichol, S.T. & Towner,

J.S. (2014) Marburgvirus resurgence in Kitaka mine bat population after extermination attempts, Uganda. *Emerging Infectious Diseases*, **20**, 1761–1764.

Amraoui, F., Pain, A., Piorkowski, G., Vazeille, M., Couto-Lima, D., de Lamballerie, X., Lourenço-de-Oliveira, R. & Failloux, A.B. (2018) Experimental Adaptation of the Yellow Fever Virus to the Mosquito Aedes albopictus and Potential risk of urban epidemics in Brazil, South America. *Scientific reports*, **8**, 14337.

Andrews, P., Harrison, T., Martin, L., Delson, E. & Bernor, R. (1996) *Distribution and biochronology of European and southwest Asian Miocene catarrhines*. In: The Evolution of Western Eurasian Neogene Mammal Faunas (ed. by R. Bernor, V. Fahlbusch & H.W. Mittmann), pp. 168–207. Columbia University Press, New York.

Arcese, P., Hando, J. & Campbell, K. (1995) *Historical and present-day anti-poaching efforts in Serengeti*. In: Serengeti II: Dynamics, Management, and Conservation of an Ecosystem (ed. by A.R.E. Sinclair & P. Arcese), pp. 506–533. University of Chicago Press, Chicago and London.

Auguste, A.J., Lemey, P., Bergren, N.A., Giambalvo, D., Moncada, M., Morón, D., Hernandez, R., Navarro, J.C. & Weaver, S.C. (2015) Enzootic transmission of yellow fever virus, Venezuela. *Emerging Infectious Diseases*, **21**, 99–102.

Auguste, A.J., Lemey, P., Pybus, O.G., Suchard, M.A., Salas, R.A., Adesiyun, A.A., Barrett, A.D., Tesh, R.B., Weaver, S.C. & Carrington, C.V.F. (2010) Yellow Fever Virus Maintenance in Trinidad and Its Dispersal throughout the Americas. *Journal of Virology*, **84**, 9967–9977.

Ayres, J.M. & Clutton-Brock, T.H. (1992) River Boundaries and Species Range Size in Amazonian Primates. *The American Naturalist*, **140**, 531–537.

Ballesta, J.M. (2017) La mona de Gibraltar `*Macaca sylvanus*´: de singularidad zoológica a reclamo turístico. *Almoraima. Revista de Estudios*

Campogibraltareños, **47**, 273–279.

Bangert, M., Latheef, A.T., Dev Pant, S., Nishan Ahmed, I., Saleem, S., Nazla Rafeeq, F., Abdulla, M., Shamah, F., Jamsheed Mohamed, A., Fitzpatrick, C., Velayudhan, R. & Shepard, D.S. (2018) Economic analysis of dengue prevention and case management in the Maldives. *PloS Neglected Tropical Diseases*, **12**, e0006796.

Barbosa, A.M. & Real, R. (2012) Applying fuzzy logic to comparative distribution modelling: a case study with two sympatric amphibians. *The Scientific World Journal*, **2012**, 1–10.

Barbosa, A.M., Raimundo, R., Muñoz, A.R. & Brown, J.A. (2013) New measures for assessing model equilibrium and prediction mismatch in species distribution models. *Diversity and Distributions*, **19**, 1333–1338.

Barnes, M.D., Craigie, I.D., Harrison, L.B., Geldmann, J., Collen, B., Whitmee, S., Balmford, A., Burgess, N.D., Brooks, T., Hockings, M. & Woodley, S. (2016) Wildlife population trends in protected areas predicted by national socio-economic metrics and body size. *Nature Communications*, **7**, 1–9.

Barnes, R. (2017) DggridR: Discrete Global Grids for R. R package version 2.0.4. *https://github.com/r-barnes/dggridR/*.

Baronti, C., Goitia, N.J.V., Cook, S., Roca, Y., Revollo, J., Flores, J.V. & De Lamballerie, X. (2011) Molecular epidemiology of yellow fever in Bolivia from 1999 to 2008. *Vector-Borne and Zoonotic Diseases*, **11**, 277–284.

Barrett, A.D.T. & Higgs, S. (2007) Yellow fever: a disease that has yet to be conquered. *Annual review of entomology*, **52**, 209–229.

BBC (2018) "Se matarem macacos, mosquitos vão atrás de sangue humano": como massacre de primatas é tiro no pé contra febre amarela. *https://www.bbc.com/portuguese/brasil-4*, accessed 2020-07-04.

Benjamini, Y. & Hochberg, Y. (1995) Controlling the False Discovery Rate: a Practical and Powerful Approach to Multiple Testing. *Journal of the Royal Statistical Society*, **57**, 289–300.

Berger, S. (2015) *Dengue: Global Status*, GIDEON Informatics, Inc., Los Angeles, USA.

Berkes, F., Colding, J. & Folke, C. (2000) Rediscovery of Traditional Ecological Knowledge as Adaptive Management. *Ecological Applications*, **10**, 1251–1262.

Bhatt, S., Gething, P.W., Brady, O.J., Messina, J.P., Farlow, A.W., Moyes, C.L., Drake, J.M., Brownstein, J.S., Hoen, A.G., Sankoh, O., Myers, M.F., George, D.B., Jaenisch, T., William Wint, G.R., Simmons, C.P., Scott, T.W., Farrar, J.J. & Hay, S.I. (2013) The global distribution and burden of dengue. *Nature*, **496**, 504–507.

Bicca-Marques, J.C., Calegaro-Marques, C., Rylands, A., Strier, K.B., Mittermeier, R., De Almeida, M.A., De Castro, P.H., Chaves, O.M., Ferraz, L.P., Fortes, V.B., Hirano, Z.M.B., Jerusalinsky, L., Kowalewski, M.M., Martins, W.P., De Melo, F., Mendes, S.L., Neves, L.G., Passos, F.C., Port Carvalho, M., Ribeiro, S., Romano, A., Ruiz Miranda, C., Dos Santos, E.O., De Souza Jr, J.C. & Teixeira, D.S. (2017) Yellow fever threatens Atlantic Forest primates. *Science Advances*, **3**, 1–3.

Bloomfield, L.S.P., McIntosh, T.L. & Lambin, E.F. (2020) Habitat fragmentation, livelihood behaviors, and contact between people and nonhuman primates in Africa. *Landscape Ecology*, **35**, 985–1000.

Bombi, P. & D'Amen, M. (2012) Scaling down distribution maps from atlas data: a test of different approaches with virtual species. *Journal of Biogeography*, **39**, 640–651.

Borcard, D., Legendre, P. & Drapeau, P. (1992) Partialling out the Spatial Component of Ecological Variation. *Ecology*, **73**, 1045–1055.

Bouzid, M., Colón-González, F.J., Lung, T., Lake, I.R. & Hunter, P.R. (2014) Climate change and the emergence of vector-borne diseases in Europe: Case study of dengue fever. *BMC Public Health*, **14**, 1–12.

Bóveda-Penalba, A.J., Vermeer, J., Rodrigo, F. & Guerra-Vásquez, F. (2009) Preliminary report on the distribution of callicebus oenanthe on the eastern feet of the andes. *International Journal of Primatology*, **30**, 467–480.

Braby, M.F., Bertelsmeier, C., Sanderson, C. & Thistleton, B.M. (2014) Spatial distribution and range expansion of the Tawny Coster butterfly, *Acraea terpsicore* (Linnaeus, 1758) (Lepidoptera: Nymphalidae), in South-East Asia and Australia. *Insect Conservation and Diversity*, **7**, 132–143.

Brady, O.J., Gething, P.W., Bhatt, S., Messina, J.P., Brownstein, J.S., Hoen, A.G., Moyes, C.L., Farlow, A.W., Scott, T.W. & Hay, S.I. (2012) Refining the Global Spatial Limits of Dengue Virus Transmission by Evidence-Based Consensus. *PLoS Neglected Tropical Diseases*, **6**, e1760.

Brown, J.E., Evans, B.R., Zheng, W., Obas, V., Barrera-Martinez, L., Egizi, A., Zhao, H., Caccone, A. & Powell, J.R. (2014) Human impacts have shaped historical and recent evolution in *Aedes aegypti*, the dengue and yellow fever mosquito. *Evolution*, **68**, 514–525.

Brown, J.E., Scholte, E.J., Dik, M., den Hartog, W., Beeuwkes, J. & Powell, J.R. (2011) *Aedes aegypti* Mosquitoes Imported into the Netherlands, 2010. *Emerging Infectious Diseases*, **17**, 2335–2337.

Brown, J.H. & Kodric-Brown, A. (1977) Turnover Rates in Insular Biogeography: Effect of Immigration on Extinction. *Ecology*, **58**, 445–449.

Bruner, A.G., Gullison, R.E., Rice, R.E. & Da Fonseca, G.A.B. (2001) Effectiveness of parks in protecting tropical biodiversity. *Science*, **291**, 125–128.

Bryant, J., Wang, H., Cabezas, C., Ramirez, G., Watts, D., Russell, K. & Barrett, A.D.T.

(2003) Enzootic transmission of yellow fever virus in Peru. *Emerging Infectious Diseases*, **9**, 926–933.

Buchwald, A.G., Hayden, M.H., Dadzie, S.K., Paull, S.H. & Carlton, E.J. (2020) *Aedes*-borne disease outbreaks in West Africa: A call for enhanced surveillance. *Acta Tropica*, **209**, 105468.

Burgin, C.J., Wilson, D.E., Mittermeier, R.A., Rylands, A.B., Lacher, T.E. & Sechrest, W. (2020) *Illustrated checklist of the mammals of the world. Volumen 1: Monotremata to Rodentia*, Lynx Edicions, Barcelona, Spain.

Buser, M.W. (1976) Similarity of binary data. *Systematic Zoology*, **25**, 251–259.

Butynski, T.M., Kingdon, J. & Kalina, J. (2013) *Mammals of Africa. Volume II: Primates*, Bloomsbury Publishing, London, United Kingdom.

Campbell, G., Kuehl, H., N'Goran Kouamé, P. & Boesch, C. (2008) Alarming decline of West African chimpanzees in Côte d'Ivoire. *Current Biology*, **18**, R903–R904.

Campbell, K. & Hofer, H. (1995) *People and Wildlife: Spatial Dynamics and Zones of Interaction*. In: Serengeti II: Dynamics, Management, and Conservation of an Ecosystem (ed. by P. Sinclair & A.R.E., Arcese), pp. 534–570. The University of Chicago Press, Chicago and London.

Campbell, L.P., Luther, C., Moo-Llanes, D., Ramsey, J.M., Danis-Lozano, R. & Peterson, A.T. (2015) Climate change influences on global distributions of dengue and chikungunya virus vectors. *Philosophical Transactions of the Royal Society B: Biological Sciences*, **370**, 1–9.

Cardosa, J., Ooi, M.H., Tio, P.H., Perera, D., Holmes, E.C., Bibi, K. & Manap, Z.A. (2009) Dengue Virus Serotype 2 from a Sylvatic Lineage Isolated from a Patient with Dengue Hemorrhagic Fever. *PLoS Neglected Tropical Diseases*, **3**, e423.

Carvalho, B.M., Rangel, E.F. & Vale, M.M. (2017) Evaluation of the impacts of climate change on disease vectors through ecological niche modelling. *Bulletin of Entomological Research*, **107**, 419–430.

Castro, M.C., Baeza, A., Codeço, C.T., Cucunubá, Z.M., Dal'Asta, A.P., De Leo, G.A., Dobson, A.P., Carrasco-Escobar, G., Lana, R.M., Lowe, R., Monteiro, A.M.V., Pascual, M. & Santos-Vega, M. (2019) Development, environmental degradation, and disease spread in the Brazilian Amazon. *PLoS Biology*, **17**, e3000526.

Catenacci, L.S., Ferreira, M., Martins, L.C., De Vleeschouwer, K.M., Cassano, C.R., Oliveira, L.C., Canale, G., Deem, S.L., Tello, J.S., Parker, P., Vasconcelos, P.F.C. & Travassos da Rosa, E.S. (2018) Surveillance of Arboviruses in Primates and Sloths in the Atlantic Forest, Bahia, Brazil. *EcoHealth*, **15**, 777–791.

Cattarino, L., Rodriguez-Barraquer, I., Imai, N., Cummings, D.A.T. & Ferguson, N.M. (2020) Mapping global variation in dengue transmission intensity. *Science Translational Medicine*, **12**, eaax4144.

CDC (2017) Areas with Risk of Yellow Fever Virus Transmission in Africa. *https://www.cdc.gov/yellowfever/maps/africa.html*, accessed 2021-05-27.

CDC (2018) Yellow Fever Maps. *https://www.cdc.gov/yellowfever/maps/index.html*, accessed 2021-04-19.

Centro de Coordinación de Alertas y Emergencias Sanitarias. Ministerio de Sanidad Consumo y Bienestar (2019) *Dengue autóctono en España 2ª actualización. Evaluación rápida de riesgo*, España.

Chala, B. & Hamde, F. (2021) Emerging and Re-emerging Vector-Borne Infectious Diseases and the Challenges for Control: A Review. *Frontiers in Public Health*, **9**, 1466.

Chomel, B.B. (2009) *Zoonoses*. In: Encyclopedia of Microbiology, 3rd edn (ed. by

M. Schaechter), pp. 820–829. Elsevier Inc., Amsterdam, The Netherlands.

Colón-González, F.J., Sewe, M.O., Tompkins, A.M., Sjödin, H., Casallas, A., Rocklöv, J., Caminade, C. & Lowe, R. (2021) Projecting the risk of mosquito-borne diseases in a warmer and more populated world: a multi-model, multi-scenario intercomparison modelling study. *The Lancet Planetary Health*, **5**, e404–e414.

Courchamp, F., Clutton-Brock, T. & Grenfell, B. (1999) Inverse density dependence and the Allee effect. *Trends in Ecology & Evolution*, **14**, 405–410.

Couto-Lima, Di., Madec, Y., Bersot, M.I., Campos, S.S., Motta, M.D.A., Dos Santos, F.B., Vazeille, M., Da Costa Vasconcelos, P.F., Lourenço-De-Oliveira, R. & Failloux, A.B. (2017) Potential risk of re-emergence of urban transmission of Yellow Fever virus in Brazil facilitated by competent *Aedes* populations. *Scientific Reports*, **7**, 1–12.

Cowlishaw, G. & Dunbar, R. (2000) *Primate conservation biology*, University of Chicago Press, Chicago.

Cozzi, G., Broekhuis, F., Mcnutt, J.W. & Schmid, B. (2013) Comparison of the effects of artificial and natural barriers on large African carnivores: Implications for interspecific relationships and connectivity. *Journal of Animal Ecology*, **82**, 707–715.

Craigie, I.D., Baillie, J.E.M., Balmford, A., Carbone, C., Collen, B., Green, R.E. & Hutton, J.M. (2010) Large mammal population declines in Africa's protected areas. *Biological Conservation*, **143**, 2221–2228.

Crawford, J.E., Alves, J.M., Palmer, W.J., Day, J.P., Sylla, M., Ramasamy, R., Surendran, S.N., Black, W.C., Pain, A. & Jiggins, F.M. (2017) Population genomics reveals that an anthropophilic population of *Aedes aegypti* mosquitoes in West Africa recently gave rise to American and Asian populations of this major disease vector. *BMC Biology*, **15**, 1–16.

Cressie, N.A.C. (1993) *Statistics for spatial data*, John Wiley & Sons, Inc., New York.

Critchlow, R., Plumptre, A.J., Driciru, M., Rwetsiba, A., Stokes, E.J., Tumwesigye, C., Wanyama, F. & Beale, C.M. (2015) Spatiotemporal trends of illegal activities from ranger-collected data in a Ugandan national park. *Conservation Biology*, **29**, 1458–1470.

Cunha, M.S., Tubaki, R.M., de Menezes, R.M.T., Pereira, M., Caleiro, G.S., Coelho, E., Saad, L. del C., Fernandes, N.C.C. de A., Guerra, J.M., Nogueira, J.S., Summa, J.L., Coimbra, A.A.C., Zwarg, T., Witkin, S.S., Mucci, L.F., Timenetsky, M. do C.S.T., Sabino, E.C. & de Deus, J.T. (2020) Possible non-sylvatic transmission of yellow fever between non-human primates in São Paulo city, Brazil, 2017–2018. *Scientific Reports*, **10**, 1–8.

CyberTracker (2018) CyberTracker: discover, explore and protect our planet. *https://cybertracker.org/*, accessed 2018-09-22.

Dadzie, S.K., Akorli, J., Coulibaly, M.B., Ahadji-Dabla, K.M., Baber, I., Bobanga, T., Boukhary, A.O.M.S., Canelas, T., Facchinelli, L., Gonçalves, A., Guelbeogo, M., Kamgang, B., Keita, I.K., Konan, L., Levine, R., Dzuris, N., Lenhart, A., Appawu, M., Ayorinde, D.F., Boakye, D., Diallo, M., Dinis, J., Fayiah, J.S., Hamani, B., Idam, E.E., Jorge, C.P., Kandeh, B., Kanmi, O.A., N'Guessan, R., Pi-Bansa, S., Salem, S.M., Sillah, A., Smith, S., Toé, H., Williams, C., Wilson, M. & Yadouleton, A. (2022) Building the capacity of West African countries in *Aedes* surveillance: inaugural meeting of the West African *Aedes* Surveillance Network (WAASuN). *Parasites & Vectors*, **15**, 381.

Diallo, M., Ba, Y., Sall, A.A., Diop, O.M., Ndione, J.A., Mondo, M., Girault, L. & Mathiot, C. (2003) Amplification of the sylvatic cycle of dengue virus type 2, Senegal, 1999-2000: Entomologic findings and epidemiologic considerations. *Emerging Infectious Diseases*, **9**, 362–367.

Dolz, G., Chaves, A., Gutiérrez-Espeleta, G.A., Ortiz-Malavasi, E., Bernal-Valle, S. &

Herrero, M.V. (2019) Detection of antibodies against flavivirus over time in wild non-human primates from the lowlands of Costa Rica. *PLoS ONE*, **14**, 1–12.

Dubois, D. & Prade, H. (1979) Operations in a Fuzzy-Valued Logic. *Information and Control*, **43**, 224–240.

Dupain, J., Guian, Z., Epanda, M.A. & Williams, D. (2017) The "Walk through the Dja." *https://www.berggorilla.org/en/gorillas/species/western-gorillas/articles-western-gorillas/the-walk-through-the-dja/*, accessed 2018-09-11.

Eastwood, G., Sang, R.C., Guerbois, M., Taracha, E.L.N. & Weaver, S.C. (2017) Enzootic circulation of chikungunya virus in East Africa: Serological evidence in non-human Kenyan primates. *American Journal of Tropical Medicine and Hygiene*, **97**, 1399–1404.

Ebi, K.L. & Nealon, J. (2016) Dengue in a changing climate. *Environmental Research*, **151**, 115–123.

ECDC (2018) *Communicable disease threats report CDTR Week 41, 7-13 October 2018*, Solna, Sweden.

ECDC (2019a) *Communicable disease threats report CDTR Week 38, 15-21 September 2019*, Solna, Sweden.

ECDC (2019b) *Communicable disease threats report CDTR Week 42, 13-19 October 2019*, Solna, Sweden.

ECDC (2022) *Aedes aegypti* - current known distribution: March 2022. *https://www.ecdc.europa.eu/en/publications-data/aedes-aegypti-current-known-distribution-march-2022*, accessed 2022-05-07.

Elith, J. & Leathwick, J.R. (2009) Species Distribution Models: Ecological Explanation and Prediction Across Space and Time. *Annual Review of Ecology,*

Evolution, and Systematics, **40**, 677–697.

Estrada, A., Garber, P.A., Gouveia, S., Fernandez-Llamazares, A., Ascensao, F., Fuentes, A., Garnett, S.T., Shaffer, C., Bicca-Marques, J., Fa, J.E., Hockings, K., Shanee, S., Johnson, S., Shepard, G.H., Shanee, N., Golden, C.D., Cardenas-Navarrete, A., Levey, D.R., Boonratana, R., Dobrovolski, R., Chaudhary, A., Ratsimbazafy, J., Supriatna, J., Kone, I. & Volampeno, S. (2022) Global importance of Indigenous Peoples, their lands, and knowledge systems for saving the world's primates from extinction. *Science Advances*, **8**, 1–19.

Estrada, A., Garber, P.A., Mittermeier, R.A., Wich, S., Gouveia, S., Dobrovolski, R., Nekaris, K.A.I., Nijman, V., Rylands, A.B., Maisels, F., Williamson, E.A., Bicca-Marques, J., Fuentes, A., Jerusalinsky, L., Johnson, S., de Melo, F.R., Oliveira, L., Schwitzer, C., Roos, C., Cheyne, S.M., Kierulff, M.C.M., Raharivololona, B., Talebi, M., Ratsimbazafy, J., Supriatna, J., Boonratana, R., Wedana, M. & Setiawan, A. (2018) Primates in peril: The significance of Brazil, Madagascar, Indonesia and the Democratic Republic of the Congo for global primate conservation. *PeerJ*, **6**, e4869.

Estrada, A., Garber, P.A., Rylands, A.B., Roos, C., Fernandez-Duque, E., Di Fiore, A., Nekaris, K.A.-I., Nijman, V., Heymann, E.W., Lambert, J.E., Rovero, F., Barelli, C., Setchell, J.M., Gillespie, T.R., Mittermeier, R.A., Arregoitia, L.V., de Guinea, M., Gouveia, S., Dobrovolski, R., Shanee, S., Shanee, N., Boyle, S.A., Fuentes, A., MacKinnon, K.C., Amato, K.R., Meyer, A.L.S., Wich, S., Sussman, R.W., Pan, R., Kone, I. & Li, B. (2017) Impending extinction crisis of the world's primates: Why primates matter. *Science Advances*, **3**, e1600946.

Estrada, A., Real, R. & Vargas, J.M. (2008) Using crisp and fuzzy modelling to identify favourability hotspots useful to perform gap analysis. *Biodiversity and Conservation*, **17**, 857–871.

Estrada-Peña, A., Acevedo, P., Ruiz-Fons, F., Gortázar, C. & de la Fuente, J. (2008)

Evidence of the Importance of Host Habitat Use in Predicting the Dilution Effect of Wild Boar for Deer Exposure to *Anaplasma* spp. *PLoS ONE*, **3**, e2999.

Eurostat (2021) Top 20 EU ports handling containers, 2010, 2019 and 2020 (million TEUs). *https://ec.europa.eu/eurostat/statistics-explained/index.php?title=File:Top_20_EU_ports_handling_containers,_2010,_2019_and_2020_(million_TEUs)_V2.png*, Accessed 2022-06-28.

Fa, J.E. & Brown, D. (2009) Impacts of hunting on mammals in African tropical moist forests: a review and synthesis. *Mammal Review*, **39**, 231–264.

Fa, J.E., Olivero, J., Farfán, M.Á., Márquez, A.L., Vargas, J.M., Real, R. & Nasi, R. (2014) Integrating sustainable hunting in biodiversity protection in central Africa: Hot spots, weak spots, and strong spots. *PLoS ONE*, **9**, e112367.

Fagbami, A.H., Fabiyi, A. & Monath, T.P. (1977) Dengue virus infections in nigeria: A survey for antibodies in monkeys and humans. *Transactions of the Royal Society of Tropical Medicine and Hygiene*, **71**, 60–65.

FAO (2000) GeoNetwork: Administrative Centres & Populated Places shapefile at the Relational World Database II (RWDB2). *http://www.fao.org/geonetwork/srv/en/main.home*, Accessed: 2018-07-11.

Farfán, M.A., Aliaga-Samanez, A., Olivero, J., Williams, D., Dupain, J., Guian, Z. & Fa, J.E. (2019) Spatial modelling for predicting potential wildlife distributions and human impacts in the Dja Forest Reserve, Cameroon. *Biological Conservation*, **230**, 104–112.

Fielding, A.H. & Bell, J.F. (1997) A review of methods for the assessment of prediction errors in conservation presence/absence models. *Environmental Conservation*, **24**, 38–49.

de Figueiredo, M.L., De C Gomes, A., Amarilla, A.A., de S Leandro, A., de S Orrico, A., de Araujo, R.F., Do Sm Castro, J., Durigon, E.L., Aquino, V.H. & Figueiredo,

L.T. (2010) Mosquitoes infected with dengue viruses in Brazil. *Virology Journal*, **7**, 152.

Filho, W.L., Ternova, L., Parasnis, S.A., Kovaleva, M. & Nagy, G.J. (2022) Climate Change and Zoonoses: A Review of Concepts, Definitions, and Bibliometrics. *International Journal of Environmental Research and Public Health*, **19**, 893.

Finlay, C.J. (1881) El mosquito hipotéticamente considerado como agente de transmisión de la fiebre amarilla. *Anales de la Real Academia de Ciencias Médicas, Físicas y Naturales de la Habana*, **18**, 147–169.

Fleagle, J.G. & Gilbert, C.C. (2006) *The Biogeography of Primate Evolution: The Role of Plate Tectonics, Climate and Chance*. In: Primate Biogeography (ed. by S.M. Lehman & J.G. Fleagle), pp. 375–418. Springer, Boston, Massachusetts.

Franco, L., Palacios, G., Martinez, J.A., Vázquez, A., Savji, N., de Ory, F., Sanchez-Seco, M.P., Martín, D., Lipkin, W.I. & Tenorio, A. (2011) First report of sylvatic DENV-2-associated dengue hemorrhagic fever in West Africa. *PLoS Neglected Tropical Diseases*, **5**, e1251.

Gause, G.F. & Witt, A.A. (1935) Behavior of Mixed Populations and the Problem of Natural Selection. *The American Naturalist*, **69**, 596–609.

Gaythorpe, K.A.M., Hamlet, A., Cibrelus, L., Garske, T. & Ferguson, N.M. (2020) The effect of climate change on yellow fever disease burden in Africa. *eLife*, **9**, 1–27.

Gaythorpe, K.A.M., Hamlet, A., Jean, K., Garkauskas Ramos, D., Cibrelus, L., Garske, T. & Ferguson, N. (2021) The global burden of yellow fever. *eLife*, **10**, e64670.

Geist, H. & Lambin, E.F. (2022) Proximate Causes and Underlying Driving Forces of Tropical Deforestation: Tropical forests are disappearing as the result of many pressures, both local and regional, acting in various combinations in different geographical locations. *BioScience*, **52**, 143–150.

Geldmann, J., Barnes, M., Coad, L., Craigie, I.D., Hockings, M. & Burgess, N.D. (2013) Effectiveness of terrestrial protected areas in reducing habitat loss and population declines. *Biological Conservation*, **161**, 230–238.

Gething, P.W., Van Boeckel, T.P., Smith, D.L., Guerra, C.A., Patil, A.P., Snow, R.W. & Hay, S.I. (2011) Modelling the global constraints of temperature on transmission of *Plasmodium falciparum* and *P. vivax*. *Parasites and Vectors*, **4**, 1–11.

Gibbs, E.P.J. (2004) The evolution of One Health: a decade of progress and challenges for the future. *Veterinary Record*, **174**, 85–91.

Gibbs, H.K., Ruesch, A.S., Achard, F., Clayton, M.K., Holmgren, P., Ramankutty, N. & Foley, J.A. (2010) Tropical forests were the primary sources of new agricultural land in the 1980s and 1990s. *Proceedings of the National Academy of Sciences*, **107**, 16732–16737.

GIDEON (2021) Yellow fever cases in Tanzania. *https://app.gideononline.com/explore/diseases/yellow-fever-12650/tanzania-G278*, accessed 2021-02-01.

Gillespie, R.G., Baldwin, B.G., Waters, J.M., Fraser, C.I., Nikula, R. & Roderick, G.K. (2012) Long-distance dispersal: a framework for hypothesis testing. *Trends in Ecology & Evolution*, **27**, 47–56.

Gong, M., Fan, Z., Zhang, X., Liu, G., Wen, W. & Zhang, L. (2017) Measuring the effectiveness of protected area management by comparing habitat utilization and threat dynamics. *Biological Conservation*, **210**, 253–260.

Gossner, C.M., Ducheyne, E. & Schaffner, F. (2018) Increased risk for autochthonous vector-borne infections transmitted by *Aedes albopictus* in continental Europe. *Eurosurveillance*, **23**, 2–7.

Gould, E., Pettersson, J., Higgs, S., Charrel, R. & de Lamballerie, X. (2017) Emerging

arboviruses: Why today? *One Health*, **4**, 1–13.

Graham, T., Matthews, H. & Turner, S. (2016) A global-scale evaluation of primate exposure and vulnerability to climate change. *Springer*, **37**, 158–174.

Grange, L., Simon-Loriere, E., Sakuntabhai, A., Gresh, L., Paul, R. & Harris, E. (2014) Epidemiological risk factors associated with high global frequency of inapparent dengue virus infections. *Frontiers in Immunology*, **5**, 1–10.

Gray, C.L., Hill, S.L.L., Newbold, T., Hudson, L.N., Boïrger, L., Contu, S., Hoskins, A.J., Ferrier, S., Purvis, A. & Scharlemann, J.P.W. (2016) Local biodiversity is higher inside than outside terrestrial protected areas worldwide. *Nature Communications*, **7**, 1–7.

Gruber, T. & Clay, Z. (2016) A Comparison Between Bonobos and Chimpanzees: A Review and Update. *Evolutionary Anthropology*, **25**, 239–252.

Gubler, D.J. (1998) Dengue and dengue hemorrhagic fever. *Clinical Microbiology Reviews*, **11**, 480–496.

Gubler, D.J. (2002) Epidemic dengue/dengue hemorrhagic fever as a public health, social and economic problem in the 21st century. *Trends in Microbiology*, **10**, 100–103.

Gubler, D.J. (2004) The changing epidemiology of yellow fever and dengue, 1900 to 2003: Full circle? *Comparative Immunology, Microbiology and Infectious Diseases*, **27**, 319–330.

Guernier, V., Hochberg, M.E. & Guégan, J.F. (2004) Ecology drives the worldwide distribution of human diseases. *PLoS Biology*, **2**, 740–746.

Guisan, A. & Zimmermann, N.E. (2000) Predictive habitat distribution models in ecology. *Ecological Modelling*, **135**, 147–186.

Hamrick, P.N., Aldighieri, S., Machado, G., Leonel, D.G., Vilca, L.M., Uriona, S. & Schneider, M.C. (2017) Geographic patterns and environmental factors

associated with human yellow fever presence in the Americas. *PLoS Neglected Tropical Diseases*, **11**, 1–27.

Hanley, K.A., Monath, T.P., Weaver, S.C., Rossi, S.L., Richman, R.L. & Vasilakis, N. (2013) Fever versus Fever: the role of host and vector susceptibility and interspecific competition in shaping the current and future distributions of the sylvatic cycles of dengue virus and yellow fever virus. *Infection, genetics and evolution*, **19**, 292–311.

Hansen, M.C., Potapov, P. V., Moore, R., Hancher, M., Turubanova, S.A., Tyukavina, A., Thau, D., Stehman, S. V., Goetz, S.J., Loveland, T.R., Kommareddy, A., Egorov, A., Chini, L., Justice, C.O. & Townshend, J.R.G. (2013) High-resolution global maps of 21st-century forest cover change. *Science*, **342**, 850–853.

Harcourt, A.H. & Wood, M.A. (2012) Rivers as Barriers to Primate Distributions in Africa. *International Journal of Primatology*, **33**, 168–183.

Harrison, T. (2016) *Miocene Primates*. In: The International Encyclopedia of Primatology (ed. by A. Fuentes), pp. 1–5. John Wiley & Sons, Inc., Hoboken, New York.

Hay, S.I., Battle, K.E., Pigott, D.M., Smith, D.L., Moyes, C.L., Bhatt, S., Brownstein, J.S., Collier, N., Myers, M.F., George, D.B. & Gething, P.W. (2013) Global mapping of infectious disease. *Philosophical Transactions of the Royal Society B: Biological Sciences*, **368**, 20120250.

Henson, D.W., Malpas, R.C. & D'Udine, A.C. (2016) *Wildlife Law Enforcement in Sub-Saharan African Protected Areas A Review of Best Practices*, IUCN Species Survival Commission No. 58, Cambridge, UK and Gland, Switzerland.

Hirzel, A.H., Hausser, J., Chessel, D. & Perrin, N. (2002) Ecological-Niche Factor Analysis: How to Compute Habitat-Suitability Maps without Absence Data? *Ecology*, **83**, 2027–2036.

Holmes, E.C. & Twiddy, S.S. (2003) The origin, emergence and evolutionary genetics of dengue virus. *Infection, Genetics and Evolution*, **3**, 19–28.

Hoskins, H.M.J., McCann, N.P., Jocque, M. & Reid, N. (2020) Rapid defaunation of terrestrial mammals in a protected Neotropical cloud forest remnant. *Journal for Nature Conservation*, **56**, 125861.

Hosmer, D.W. & Lemeshow, S. (2000) *Applied Logistic Regression*, John Wiley & Sons, Inc., Hoboken, New York.

Howe, H.F. (1986) *Seed dispersal by fruit-eating birds and mammals*. In: Seed Dispersal (ed. by D.R. Murray), pp. 123–189. Academic Press, Wollongong.

Huang, Y.M. (1977) Medical entomology studies - VIII. Notes on the taxonomic status of *Aedes vittatus* (Diptera: Culicidae). *American Entomological Institute*, **14**, 113–132.

Hubálek, Z. (2003) Emerging Human Infectious Diseases: Anthroponoses, Zoonoses, and Sapronoses. *Emerging Infectious Diseases*, **9**, 403–404.

Hurlbert, A.H. & Jetz, W. (2007) Species richness, hotspots, and the scale dependence of range maps in ecology and conservation. *Proceedings of the National Academy of Sciences of the United States of America*, **104**, 13384–13389.

Ibañez-Justicia, A., Gloria-Soria, A., Den Hartog, W., Dik, M., Jacobs, F. & Stroo, A. (2017) The first detected airline introductions of yellow fever mosquitoes (*Aedes aegypti*) to Europe, at Schiphol International airport, the Netherlands. *Parasites and Vectors*, **10**, 1–9.

Ingelbeen, B., Weregemere, N.A., Noel, H., Tshapenda, G.P., Mossoko, M., Nsio, J., Ronsse, A., Ahuka-Mundeke, S., Cohuet, S. & Kebela, B.I. (2018) Urban yellow fever outbreak—Democratic Republic of the Congo, 2016: Towards more rapid case detection. *PLoS Neglected Tropical Diseases*, **12**, e0007029.

IPCC (2014) *Climate Change 2014 Synthesis Report Summary Chapter for Policymakers*, New York, USA.

IUCN (2017) The IUCN Red List of Threatened Species. Version 2017–3. *https://www.iucnredlist.org/*, accessed 2017-11-04.

IUCN (2019) IUCN Red List of Threatened Species. Version 2019-2. *https://www.iucnredlist.org/*, accessed 2019-07-02.

IUCN (2022) IUCN Red List of Threatened Species. Version 2022-2. *https://www.iucnredlist.org/search/grid?query=primates&searchType=species*, accessed 2022-09-28.

Iwamura, T., Guzman-Holst, A. & Murray, K.A. (2020) Accelerating invasion potential of disease vector *Aedes aegypti* under climate change. *Nature Communications*, **11**, 1–10.

Jachmann, H. & Billiouw, M. (1997) Elephant Poaching and Law Enforcement in the Central Luangwa Valley, Zambia. *The Journal of Applied Ecology*, **34**, 233–244.

Jentes, E.S., Poumerol, G., Gershman, M.D., Hill, D.R., Lemarchand, J., Lewis, R.F., Staples, J.E., Tomori, O., Wilder-Smith, A. & Monath, T.P. (2011) The revised global yellow fever risk map and recommendations for vaccination, 2010: Consensus of the Informal WHO Working Group on Geographic Risk for Yellow Fever. *The Lancet Infectious Diseases*, **11**, 622–632.

Joppa, L.N. & Pfaff, A. (2009) High and Far: Biases in the Location of Protected Areas. *PLoS ONE*, **4**, e8273.

Junker, J., Petrovan, S.O., Arroyo-Rodríguez, V., Boonratana, R., Byler, D., Chapman, C.A., Chetry, D., Cheyne, S.M., Cornejo, F.M., Cortés-Ortiz, L., Cowlishaw, G., Christie, A.P., Crockford, C., Torre, S.D. La, De Melo, F.R., Fan, P., Grueter, C.C., Guzmán-Caro, D.C., Heymann, E.W., Herbinger, I., Hoang,

M.D., Horwich, R.H., Humle, T., Ikemeh, R.A., Imong, I.S., Jerusalinsky, L., Johnson, S.E., Kappeler, P.M., Kierulff, M.C.M., Koné, I., Kormos, R., Le, K.Q., Li, B., Marshall, A.J., Meijaard, E., Mittermeier, R.A., Muroyama, Y., Neugebauer, E., Orth, L., Palacios, E., Papworth, S.K., Plumptre, A.J., Rawson, B.M., Refisch, J., Ratsimbazafy, J., Roos, C., Setchell, J.M., Smith, R.K., Sop, T., Schwitzer, C., Slater, K., Strum, S.C., Sutherland, W.J., Talebi, M., Wallis, J., Wich, S., Williamson, E.A., Wittig, R.M. & Kühl, H.S. (2020) A Severe Lack of Evidence Limits Effective Conservation of the World's Primates. *BioScience*, **70**, 794–803.

Kading, R.C., Borland, E.M., Cranfield, M. & Powers, A.M. (2013) Prevalence of antibodies to alphaviruses and flaviviruses in free-ranging game animals and nonhuman primates in the greater Congo basin. *Journal of Wildlife Diseases*, **49**, 587–599.

Kamal, M., Kenawy, M.A., Rady, M.H., Khaled, A.S. & Samy, A.M. (2018) Mapping the global potential distributions of two arboviral vectors *Aedes aegypti* and *Ae. albopictus* under changing climate. *PLOS ONE*, **13**, e0210122.

Kamilar, J.M. (2017) *Biogeography and Primate Biogeography*. In: The International Encyclopedia of Primatology (ed. by A. Fuentes), pp. 1–4. John Wiley & Sons, Ltd, Hoboken, New York.

Karger, D.N., Conrad, O., Böhner, J., Kawohl, T., Kreft, H., Soria-Auza, R.W., Zimmermann, N.E., Linder, H.P. & Kessler, M. (2017) Climatologies at high resolution for the earth's land surface areas. *Scientific Data*, **4**, 1–20.

Karger, D.N., Wilson, A.M., Mahony, C., Zimmermann, N.E. & Jetz, W. (2021) Global daily 1 km land surface precipitation based on cloud cover-informed downscaling. *Scientific data*, **8**, 307.

Keesing, F., Belden, L.K., Daszak, P., Dobson, A., Harvell, C.D., Holt, R.D., Hudson, P., Jolles, A., Jones, K.E., Mitchell, C.E., Myers, S.S., Bogich, T. & Ostfeld, R.S.

(2010) Impacts of biodiversity on the emergence and transmission of infectious diseases. *Nature*, **468**, 647–652.

Khan, S.U., Ogden, N.H., Fazil, A.A., Gachon, P.H., Dueymes, G.U., Greer, A.L. & Ng, V. (2020) Current and Projected Distributions of *Aedes aegypti* and *Ae. albopictus* in Canada and the U.S. *Environmental Health Perspectives*, **128**, 057007.

Knutti, R., Masson, D. & Gettelman, A. (2013) Climate model genealogy: Generation CMIP5 and how we got there. *Geophysical Research Letters*, **40**, 1194–1199.

Kosko, B. (1986) Fuzzy entropy and conditioning. *Information Sciences*, **40**, 165–174.

Kraemer, M.U.G., Faria, N.R., Reiner, R.C., Golding, N., Nikolay, B., Stasse, S., Johansson, M.A., Salje, H., Faye, O., Wint, G.R.W., Niedrig, M., Shearer, F.M., Hill, S.C., Thompson, R.N., Bisanzio, D., Taveira, N., Nax, H.H., Pradelski, B.S.R., Nsoesie, E.O., Murphy, N.R., Bogoch, I.I., Khan, K., Brownstein, J.S., Tatem, A.J., de Oliveira, T., Smith, D.L., Sall, A.A., Pybus, O.G., Hay, S.I. & Cauchemez, S. (2017) Spread of yellow fever virus outbreak in Angola and the Democratic Republic of the Congo 2015–16: a modelling study. *The Lancet Infectious Diseases*, **17**, 330–338.

Kraemer, M.U.G., Hay, S.I., Pigott, D.M., Smith, D.L., Wint, G.R.W. & Golding, N. (2016) Progress and Challenges in Infectious Disease Cartography. *Trends in Parasitology*, **32**, 19–29.

Kraemer, M.U.G., Reiner, R.C., Brady, O.J., Messina, J.P., Gilbert, M., Pigott, D.M., Yi, D., Johnson, K., Earl, L., Marczak, L.B., Shirude, S., Davis Weaver, N., Bisanzio, D., Perkins, T.A., Lai, S., Lu, X., Jones, P., Coelho, G.E., Carvalho, R.G., Van Bortel, W., Marsboom, C., Hendrickx, G., Schaffner, F., Moore, C.G., Nax, H.H., Bengtsson, L., Wetter, E., Tatem, A.J., Brownstein, J.S., Smith, D.L., Lambrechts,

L., Cauchemez, S., Linard, C., Faria, N.R., Pybus, O.G., Scott, T.W., Liu, Q., Yu, H., Wint, G.R.W., Hay, S.I. & Golding, N. (2019) Past and future spread of the arbovirus vectors *Aedes aegypti* and *Aedes albopictus*. *Nature Microbiology*, **4**, 854–863.

Kraemer, M.U.G., Sinka, M.E., Duda, K.A., Mylne, A., Shearer, F.M., Brady, O.J., Messina, J.P., Barker, C.M., Moore, C.G., Carvalho, R.G., Coelho, G.E., Van Bortel, W., Hendrickx, G., Schaffner, F., Wint, G.R.W., Elyazar, I.R.F., Teng, H.J. & Hay, S.I. (2015a) The global compendium of *Aedes aegypti* and *Ae. albopictus* occurrence. *Scientific Data*, **2**, 1–8.

Kraemer, M.U.G., Sinka, M.E., Duda, K.A., Mylne, A., Shearer, F.M., Barker, C.M., Moore, C.G., Carvalho, R.G., Coelho, G.E., Van Bortel, W., Hendrickx, G., Schaffner, F., Elyazar, I.R., Teng, H.J., Brady, O.J., Messina, J.P., Pigott, D.M., Scott, T.W., Smith, D.L., William Wint, G.R., Golding, N. & Hay, S.I. (2015b) The global distribution of the arbovirus vectors *Aedes aegypti* and *Ae. albopictus*. *eLife*, **4**, e08347.

Krebs, C.J. (1985) *Ecología, estudio de la distribución y la abundancia*, Harla. México.

Kreft, H. & Jetz, W. (2010) A framework for delineating biogeographical regions based on species distributions. *Journal of Biogeography*, **37**, 2029–2053.

Kühl, H.S., Sop, T., Williamson, E.A., Mundry, R., Brugière, D., Campbell, G., Cohen, H., Danquah, E., Ginn, L., Herbinger, I., Jones, S., Junker, J., Kormos, R., Kouakou, C.Y., N'Goran, P.K., Normand, E., Shutt-Phillips, K., Tickle, A., Vendras, E., Welsh, A., Wessling, E.G. & Boesch, C. (2017) The critically endangered western chimpanzee declines by 80%. *American Journal of Primatology*, **79**, e22681.

Kümpel, N.F. (2006) Incentives for sustainable hunting of bushmeat in Río Muni, Equatorial Guinea. *PhD. thesis*, Imperial College London, United kingdom.

Kuncheva, L.I. (2001) Using measures of similarity and inclusion for multiple classiÿer fusion by decision templates. *Fuzzy Sets and Systems*, **122**, 401–407.

Kuno, G. (2015) A Re-Examination of the History of Etiologic Confusion between Dengue and Chikungunya. *PLoS Neglected Tropical Diseases*, **9**, 1–11.

Kunz, T.H., de Torrez, E.B., Bauer, D., Lobova, T. & Fleming, T.H. (2011) Ecosystem services provided by bats. *Annals of the New York Academy of Sciences*, **1223**, 1–38.

Lahm, S.A., Kombila, M., Swanepoel, R. & Barnes, R.F.W. (2007) Morbidity and mortality of wild animals in relationto outbreaks of Ebola haemorrhagic fever in Gabon, 1994—2003. *Transactions of the Royal Society of Tropical Medicine and Hygiene*, **101**, 64–78.

Leader-Williams, N. & Milner-Gulland, E.J. (1993) Policies for the Enforcement of Wildlife Laws: The Balance between Detection and Penalties in Luangwa Valley, Zambia. *Conservation Biology*, **7**, 611–617.

Legendre, P. (1993) Spatial Autocorrelation: Trouble or New Paradigm? *Ecology*, **74**, 1659–1673.

Legendre, P. & Legendre, L. (1998) *Numerical ecology (2nd English edition)*, Elsevier Science, Amsterdam, The Netherlands.

Leroy, E.M., Rouquet, P., Formenty, P., Souquière, S., Kilbourne, A., Froment, J.M., Bermejo, M., Smit, S., Karesh, W., Swanepoel, R., Zaki, S.R. & Rollin, P.E. (2004) Multiple Ebola virus transmission events and rapid decline of central African wildlife. *Science*, **303**, 387–390.

Leta, S., Beyene, T.J., De Clercq, E.M., Amenu, K., Kraemer, M.U.G. & Revie, C.W. (2018) Global risk mapping for major diseases transmitted by *Aedes aegypti* and *Aedes albopictus*. *International Journal of Infectious Diseases*, **67**, 25–35.

Linkie, M., Rood, E. & Smith, R.J. (2010) Modelling the effectiveness of

enforcement strategies for avoiding tropical deforestation in Kerinci Seblat National Park, Sumatra. *Biodiversity and Conservation*, **19**, 973–984.

Liu-Helmersson, J., Brännström, Å., Sewe, M.O., Semenza, J.C. & Rocklöv, J. (2019) Estimating past, present, and future trends in the global distribution and abundance of the arbovirus vector *Aedes aegypti* under climate change scenarios. *Frontiers in Public Health*, **7**, 148.

Liu, B., Gao, X., Ma, J., Jiao, Z., Xiao, J., Hayat, M.A. & Wang, H. (2019) Modeling the present and future distribution of arbovirus vectors *Aedes aegypti* and *Aedes albopictus* under climate change scenarios in Mainland China. *Science of the Total Environment*, **664**, 203–214.

Liu, W., Pickering, P., Duchêne, S., Holmes, E.C. & Aaskov, J.G. (2016) Highly Divergent Dengue Virus Type 2 in Traveler Returning from Borneo to Australia. *Emerging Infectious Diseases*, **22**, 2146–2148.

Lobo, J.M., Jiménez-Valverde, A. & Real, R. (2008) AUC: A misleading measure of the performance of predictive distribution models. *Global Ecology and Biogeography*, **17**, 145–151.

Lomolino, M., Riddle, B. & Brown, J. (2006) *Biogeography, Third edition*, Sinauer Associates, Inc. Sunderland, Massachusetts.

MacDonald, A.J. & Mordecai, E.A. (2019) Amazon deforestation drives malaria transmission, and malaria burden reduces forest clearing. *Proceedings of the National Academy of Sciences of the United States of America*, **116**, 22212–22218.

Maestre-Serrano, R., Rey, G., De las salas, J., Vergara, C., Santacoloma, L., Goenaga, S. & Carrasquilla, M.C. (2010) Estado de la susceptibilidad de *Aedes aegypti* a insecticidas en Atlántico (Colombia). *Revista Colombiana de Entomología*, **36**, 242–248.

Maisels, F., Strindberg, S., Blake, S., Wittemyer, G., Hart, J., Williamson, E.A., Aba'a, R., Abitsi, G., Ambahe, R.D., Amsini, F., Bakabana, P.C., Hicks, T.C., Bayogo, R.E., Bechem, M., Beyers, R.L., Bezangoye, A.N., Boundja, P., Bout, N., Akou, M.E., Bene, L.B., Fosso, B., Greengrass, E., Grossmann, F., Ikamba-Nkulu, C., Ilambu, O., Inogwabini, B.I., Iyenguet, F., Kiminou, F., Kokangoye, M., Kujirakwinja, D., Latour, S., Liengola, I., Mackaya, Q., Madidi, J., Madzoke, B., Makoumbou, C., Malanda, G.A., Malonga, R., Mbani, O., Mbendzo, V.A., Ambassa, E., Ekinde, A., Mihindou, Y., Morgan, B.J., Motsaba, P., Moukala, G., Mounguengui, A., Mowawa, B.S., Ndzai, C., Nixon, S., Nkumu, P., Nzolani, F., Pintea, L., Plumptre, A., Rainey, H., de Semboli, B.B., Serckx, A., Stokes, E., Turkalo, A., Vanleeuwe, H., Vosper, A. & Warren, Y. (2013) Devastating Decline of Forest Elephants in Central Africa. *PloS ONE*, **8**, e59469.

Marcondes, C.B. & Tauil, P.L. (2011) Dengue silvestre: Devemos nos preocupar? *Revista da Sociedade Brasileira de Medicina Tropical*, **44**, 263–264.

Márquez, A.L., Real, R., Olivero, J. & Estrada, A. (2011) Combining climate with other influential factors for modelling the impact of climate change on species distribution. *Climatic Change*, **108**, 135–157.

Márquez, A.L., Real, R. & Vargas, J.M. (2004) Dependence of broad-scale geographical variation in fleshy-fruited plant species richness on disperser bird species richness. *Global Ecology and Biogeography*, **13**, 295–304.

Marshall, A.J. & Wich, S.A. (2016) *Why conserve primates?* In: An Introduction to Primate Conservation (ed. by W. Serge & A.J. Marshall), pp. 13–30. Oxford University Press, Oxford, United Kingdom.

Mas-Coma, S., Jones, M.K. & Marty, A.M. (2020) COVID-19 and globalization. *One Health*, **9**, 100132.

May, R. (2006) Plagues and peoples. *IUBMB Life*, **58**, 119–121.

McMichael, A.J. (2013) Globalization, Climate Change, and Human Health. *New*

England Journal of Medicine, **368**, 1335–1343.

Mcsweeney, C.F., Jones, R G, Lee, R W & Rowell, D P (2015) Selecting CMIP5 GCMs for downscaling over multiple regions. *Climate Dynamics*, **44**, 3237–3260.

Medina-Vogel, G. (2010) Ecología de enfermedades infecciosas emergentes y conservación de especies silvestres. *Archivos de Medicina Veterinaria*, **42**, 11–24.

Meijaard, E., Buchori, D., Hadiprakarsa, Y., Utami-Atmoko, S.S., Nurcahyo, A., Tjiu, A., Prasetyo, D., Nardiyono, Christie, L., Ancrenaz, M., Abadi, F., Antoni, I.N.G., Armayadi, D., Dinato, A., Ella, Gumelar, P., Indrawan, T.P., Kussaritano, Munajat, C., Priyono, C.W.P., Purwanto, Y., Puspitasari, D., Putra, M.S.W., Rahmat, A., Ramadani, H., Sammy, J., Siswanto, D., Syamsuri, M., Andayani, N., Wu, H., Wells, J.A. & Mengersen, K. (2011) Quantifying Killing of Orangutans and Human-Orangutan Conflict in Kalimantan, Indonesia. *PLoS ONE*, **6**, e27491.

De Merode, E. & Cowlishaw, G. (2006) Species Protection, the Changing Informal Economy, and the Politics of Access to the Bushmeat Trade in the Democratic Republic of Congo. *Conservation Biology*, **20**, 1262–1271.

De Merode, E., Smith, K.H., Homewood, K., Pettifor, R., Rowcliffe, M. & Cowlishaw, G. (2007) The impact of armed conflict on protected-area efficacy in Central Africa. *Biology Letters*, **3**, 299–301.

Messina, J.P., Brady, O.J., Golding, N., Kraemer, M.U.G., Wint, G.R.W., Ray, S.E., Pigott, D.M., Shearer, F.M., Johnson, K., Earl, L., Marczak, L.B., Shirude, S., Davis Weaver, N., Gilbert, M., Velayudhan, R., Jones, P., Jaenisch, T., Scott, T.W., Reiner, R.C. & Hay, S.I. (2019) The current and future global distribution and population at risk of dengue. *Nature Microbiology*, **4**, 1508–1515.

Messina, J.P., Brady, O.J., Pigott, D.M., Brownstein, J.S., Hoen, A.G. & Hay, S.I. (2014a) A global compendium of human dengue virus occurrence. *Scientific*

Data, **1**, 1–6.

Messina, J.P., Brady, O.J., Scott, T.W., Zou, C., Pigott, D.M., Duda, K.A., Bhatt, S., Katzelnick, L., Howes, R.E., Battle, K.E., Simmons, C.P. & Hay, S.I. (2014b) Global spread of dengue virus types: mapping the 70 year history. *Trends in microbiology*, **22**, 138–146.

Meyer Steiger, D.B., Ritchie, S.A. & Laurance, S.G.W. (2016) Mosquito communities and disease risk influenced by land use change and seasonality in the Australian tropics. *Parasites and Vectors*, **9**, 1–13.

Mills, J.N., Gage, K.L. & Khan, A.S. (2010) Potential Influence of Climate Change on Vector-Borne and Zoonotic Diseases: A Review and Proposed Research Plan. *Environmental Health Perspectives*, **118**, 1507–1514.

Mir, D., Delatorre, E., Bonaldo, M., Lourenço-De-Oliveira, R., Vicente, A.C. & Bello, G. (2017) Phylodynamics of Yellow Fever Virus in the Americas: New insights into the origin of the 2017 Brazilian outbreak. *Scientific Reports*, **7**, 1–9.

Mittermeier, R.A., Rylands, A.B. & Wilson, D.E. (2013) *Handbook of the Mammals of the World. Vol. 3. Primates*, Lynx Edicions, Barcelona, Spain.

Mometrix Test Preparation (2021) Millennium Milestones of Globalization. *https://www.mometrix.com/academy/globalization-millennium-milestones/*, accessed 2021-04-05.

Mongabay (2020a) ¿Por qué la deforestación y la pérdida de especies abren la puerta a nuevas enfermedades? *https://es.mongabay.com/2020/04/covid-19-deforestacion-y-la-perdida-de-especies/*, accessed 2021-04-20.

Mongabay (2020b) The next great threat to Brazil's golden lion tamarin: Yellow fever. *https://news.mongabay.com/2020/03/the-next-great-threat-to-brazils-golden-lion-tamarin-yellow-fever/*, accessed 2021-01-14.

Monlun, E., Zeller, H., Traore-Lamizana, M., Hervy, J.P., Adam, E., Mondo', M. &

Digouttet, J.P. (1992) Caractères cliniques et épidémiologiques de la dengue 2 au Sénégal. *Médecine et Maladies Infectieuses*, **22**, 718–721.

Morales, M.A., Fabbri, C.M., Zunino, G.E., Kowalewski, M.M., Luppo, V.C., Enría, D.A., Levis, S.C. & Calderón, G.E. (2017) Detection of the mosquito-borne flaviviruses, West Nile, Dengue, Saint Louis Encephalitis, Ilheus, Bussuquara, and Yellow Fever in free-ranging black howlers (*Alouatta caraya*) of Northeastern Argentina. *PloS Neglected Tropical Diseases*, **11**, e0005351.

Mott, C.L. (2010) Environmental Constraints to the Geographic Expansion of Plant and Animal Species. *Nature Education Knowledge*, **3**, 72.

Mpakairi, K.S., Ndaimani, H., Tagwireyi, P., Gara, T.W., Zvidzai, M. & Madhlamoto, D. (2017) Missing in action: Species competition is a neglected predictor variable in species distribution modelling. *PloS ONE*, **12**, e0181088.

Muñoz, A.R. & Real, R. (2006) Assessing the potential range expansion of the exotic monk parakeet in Spain. *Diversity and Distributions*, **12**, 656–665.

Muñoz, A.-R. & Real, R. (2013) Distribution of Bonelli's Eagle Aquila fasciata in Southern Spain: Scale May Matter. *Acta Ornithologica*, **48**, 93–101.

Muñoz, A.R., Real, R., Barbosa, A.M. & Vargas, J.M. (2005) Modelling the distribution of Bonelli's eagle in Spain: implications for conservation planning. *Diversity and Distributions*, **11**, 477–486.

Murai, M., Ruffler, H., Berlemont, A., Campbell, G., Esono, F., Agbor, A., Mbomio, D., Ebana, A., Nze, A. & Kühl, H.S. (2013) Priority Areas for Large Mammal Conservation in Equatorial Guinea. *PloS ONE*, **8**, e75024.

Murray, K.A., Olivero, J., Roche, B., Tiedt, S. & Guégan, J.F. (2018) Pathogeography: leveraging the biogeography of human infectious diseases for global health management. *Ecography*, **41**, 1411–1427.

Murray, K.A., Preston, N., Allen, T., Zambrana-Torrelio, C., Hosseini, P.R. & Daszak,

P. (2015) Global biogeography of human infectious diseases. *Proceedings of the National Academy of Sciences of the United States of America*, **112**, 12746–12751.

Mutebi, J.P. & Barrett, A.D.T. (2002) The epidemiology of yellow fever in Africa. *Microbes and Infection*, **4**, 1459–1468.

Nagpal, B., Knox, T., Risintha, P., Yadav, R., Ghosh, S., Uragayala, S., Valecha, N., Christophel, E.M. & Jamsheed, M. (2018) Strengthening of vector control in South-East Asia: Outcomes from a WHO regional workshop. *Journal of Vector Borne Diseases*, **55**, 247.

Narat, V., Kampo, M., Heyer, T., Rupp, S., Ambata, P., Njouom, R. & Giles-Vernick, T. (2018) Using physical contact heterogeneity and frequency to characterize dynamics of human exposure to nonhuman primate bodily fluids in central Africa. *PLoS Neglected Tropical Diseases*, **12**, e0006976.

Nelson, A. & Chomitz, K.M. (2011) Effectiveness of Strict vs. Multiple Use Protected Areas in Reducing Tropical Forest Fires: A Global Analysis Using Matching Methods. *PLoS ONE*, **6**, e22722.

Nijman, V., Nekaris, K., Donati, G., Bruford, M. & Fa, J. (2011) Primate conservation: measuring and mitigating trade in primates. *Endangered Species Research*, **13**, 159–161.

Nikolaus Karger, D., Schmatz, D.R., Dettling, G. & Zimmermann, N.E. (2020) High-resolution monthly precipitation and temperature time series from 2006 to 2100. *Scientific Data*, **7**, 248.

Nunn, C.L. & Altizer, S.M. (2006) *Infectious diseases in primates: Behavior, Ecology and Evolution*, Oxford University Press, Oxford, United Kingdom.

Nwachukwu, W.E., Yusuff, H., Nwangwu, U., Okon, A., Ogunniyi, A., Imuetinyan-Clement, J., Besong, M., Ayo-Ajayi, P., Nikau, J., Baba, A., Dogunro, F.,

Akintunde, B., Oguntoye, M., Kamaldeen, K., Fakayode, O., Oyebanji, O., Emelife, O., Oteri, J., Aruna, O., Ilori, E., Ojo, O., Mba, N., Nguku, P. & Ihekweazu, C. (2020) The response to re-emergence of yellow fever in Nigeria, 2017. *International Journal of Infectious Diseases*, **92**, 189–196.

O'Neil, T.A., Bettinger, P., Marcot, B.G., Luscombe, B.W., Koeln, G.T., Bruner, H.J., Barrett, C., Pollock, J.A. & Bernatas, S. (2005) *Application of spatial technologies in wildlife biology*. In: Techniques for Wildlife Investigations and Management (ed. by C. Braun), pp. 418–447. Grouse Inc., Maryland, USA.

Olivero, J. (2021) *Biogeography of Diseases*. In: Biogeography: An Integrative Approach of the Evolution of Living (ed. by E. Guilbert), pp. 275–301. John Wiley & Sons, Inc., Hoboken, New York.

Olivero, J., Fa, J.E., Farfán, M., Márquez, A.L., Real, R., Juste, F.J., Leendertz, S.A. & Nasi, R. (2020) Human activities link fruit bat presence to Ebola virus disease outbreaks. *Mammal Review*, **50**, 1–10.

Olivero, J., Fa, J.E., Real, R., Farfán, M.Á., Márquez, A.L., Vargas, J.M., Gonzalez, J.P., Cunningham, A.A. & Nasi, R. (2017a) Mammalian biogeography and the Ebola virus in Africa. *Mammal Review*, **47**, 24–37.

Olivero, J., Fa, J.E., Real, R., Márquez, A.L., Farfán, M.A., Vargas, J.M., Gaveau, D., Salim, M.A., Park, D., Suter, J., King, S., Leendertz, S.A., Sheil, D. & Nasi, R. (2017b) Recent loss of closed forests is associated with Ebola virus disease outbreaks. *Scientific Reports*, **7**, 1–9.

Olivero, J., Ferri, F., Acevedo, P., Lobo, J.M., Fa, J.E., Farfán, M.Á., Romero, D., Blanco, G. & Real, R. (2016a) Using indigenous knowledge to link hyper-temporal land cover mapping with land use in the Venezuelan Amazon: "The Forest Pulse." *Revista de Biología Tropical*, **64**, 1661–1682.

Olivero, J., Real, R. & Márquez, A.L. (2011) Fuzzy chorotypes as a conceptual tool to improve insight into biogeographic patterns. *Systematic Biology*, **60**, 645–

660.

Olivero, J., Toxopeus, A.G., Skidmore, A.K. & Real, R. (2016b) Testing the efficacy of downscaling in species distribution modelling: a comparison between MaxEnt and Favourability Function models. *Animal Biodiversity and Conservation*, **39**, 99–114.

Olson, D.M., Dinerstein, E., Wikramanayake, E.D., Burgess, N.D., Powell, G.V.N., Underwood, E.C., D'amico, J.A., Itoua, I., Strand, H.E., Morrison, J.C., Loucks, C.J., Allnutt, T.F., Ricketts, T.H., Kura, Y., Lamoreux, J.F., Wettengel, W.W., Hedao, P. & Kassem, K.R. (2001) Terrestrial Ecoregions of the World: A New Map of Life on Earth: A new global map of terrestrial ecoregions provides an innovative tool for conserving biodiversity. *BioScience*, **51**, 933–938.

Omotayo, A. & Musa, M.W. (2008) The Role of Indigenous Land Classification and Management Practices in Sustaining Land Use System in the Semi-Arid Zone of Nigeria. *Journal of Sustainable Agriculture*, **14**, 49–58.

Overgaard, H.J., Olano, V.A., Jaramillo, J.F., Matiz, M.I., Sarmiento, D., Stenström, T.A. & Alexander, N. (2017) A cross-sectional survey of *Aedes aegypti* immature abundance in urban and rural household containers in central Colombia. *Parasites and Vectors*, **10**, 356.

PAHO (2011) Enfermedades Desatendidas, Tropicales y Transmitidas por Vectores. *https://www.paho.org/es/temas/enfermedades-desatendidas-tropicales-transmitidas-por-vectores*, accessed 2023-01-18.

PAHO (2014) 10 vector-borne diseases that put the population of the Americas at risk. *https://www.paho.org/en/news/7-4-2014-10-vector-borne-diseases-put-population-americas-risk*, accessed 2020-11-16.

PAHO (2019a) *Manual for Indoor Residual Spraying in Urban Areas for* Aedes aegypti *Control*, Washington, USA.

PAHO (2019b) *Plan de acción sobre entomología y control de vectores 2018-2023 (56 Consejo Directivo)*, Washington, USA.

PAHO (2022) Vectores: Manejo integrado y entomología en salud pública. *https://www.paho.org/es/temas/vectores-manejo-integrado-entomologia-salud-publica*, accessed 2022-11-16.

Patz, J.A., Daszak, P., Tabor, G.M., Aguirre, A.A., Pearl, M., Epstein, J., Wolfe, N.D., Kilpatrick, A.M., Foufopoulos, J., Molyneux, D., Bradley, D.J., Amerasinghe, F.P., Ashford, R.W., Barthelemy, D., Bos, R., Bradley, D.J., Buck, A., Butler, C., Chivian, E.S., Chua, K.B., Clark, G., Colwell, R., Confalonieri, U.E., Corvalan, C., Cunningham, A.A., Dein, J., Dobson, A.P., Else, J.G., Epstein, J., Field, H., Furu, P., Gascon, C., Graham, D., Haines, A., Hyatt, A.D., Jamaluddin, A., Kleinau, E.F., Koontz, F., Koren, H.S., LeBlancq, S., Lele, S., Lindsay, S., Maynard, N., McLean, R.G., McMichael, T., Molyneux, D., Morse, S.S., Norris, D.E., Ostfeld, R.S., Pearl, M.C., Pimentel, D., Rakototiana, L., Randriamanajara, O., Riach, J., Rosenthal, J.P., Salazar-Sanchez, E., Silbergeld, E., Thomson, M., Vittor, A.Y., Yameogo, L. & Zakarov, V. (2004) Unhealthy landscapes: Policy recommendations on land use change and infectious disease emergence. *Environmental Health Perspectives*, **112**, 1092–1098.

Patz, J.A. & Hahn, M.B. (2012) *Climate Change and Human Health: A One Health Approach*. In: One Health: The Human-Animal-Environment Interfaces in Emerging Infectious Diseases (ed. by J. Mackenzie, J., Jeggo, M., Daszak & P., Richt), pp. 141–171. Springer, Berlin, Germany.

Peterson, A.T. (2006) Ecologic niche modeling and spatial patterns of disease transmission. *Emerging Infectious Diseases*, **12**, 1822–1826.

Peterson, A.T. (2008) Biogeography of diseases: A framework for analysis. *Naturwissenschaften*, **95**, 483–491.

Peterson, A.T. (2015) Mapping Disease Transmission Risk: Enriching Models Using

Biogeography and Ecology. *Emerging Infectious Diseases*, **21**, 1489.

Peterson, A.T. & Cohoon, K.P. (1999) Sensitivity of distributional prediction algorithms to geographic data completeness. *Ecological Modelling*, **117**, 159–164.

Phillips, S.B., Aneja, V.P., Kang, D. & Arya, S.P. (2006) Maximum entropy modeling of species geographic distributions. *Ecological Modelling*, **190**, 231–259.

Pigott, D.M., Golding, N., Mylne, A., Huang, Z., Henry, A.J., Weiss, D.J., Brady, O.J., Kraemer, M.U.G., Smith, D.L., Moyes, C.L., Bhatt, S., Gething, P.W., Horby, P.W., Bogoch, I.I., Brownstein, J.S., Mekaru, S.R., Tatem, A.J., Khan, K. & Hay, S.I. (2014) Mapping the zoonotic niche of Ebola virus disease in Africa. *eLife*, **3**, e04395.

Pigott, D.M., Millear, A.I., Earl, L., Morozoff, C., Han, B.A., Shearer, F.M., Weiss, D.J., Brady, O.J., Kraemer, M.U.G., Moyes, C.L., Bhatt, S., Gething, P.W., Golding, N. & Hay, S.I. (2016) Updates to the zoonotic niche map of Ebola virus disease in Africa. *eLife*, **5**, e16412.

Pilbrow, V. & Groves, C. (2013) Evidence for Divergence in Populations of Bonobos (*Pan paniscus*) in the Lomami-Lualaba and Kasai-Sankuru Regions Based on Preliminary Analysis of Craniodental Variation. *International Journal of Primatology*, **34**, 1244–1260.

Plumptre, A.J., Fuller, R.A., Rwetsiba, A., Wanyama, F., Kujirakwinja, D., Driciru, M., Nangendo, G., Watson, J.E.M. & Possingham, H.P. (2014) Efficiently targeting resources to deter illegal activities in protected areas. *Journal of Applied Ecology*, **51**, 714–725.

Potts, J.A. & Rothman, A.L. (2009) Clinical and laboratory features that distinguish dengue from other febrile illnesses in endemic populations. *Tropical Medicine and International Health*, **13**, 1328–1340.

Purse, B.V. & Golding, N. (2015) Tracking the distribution and impacts of diseases with biological records and distribution modelling. *Biological Journal of the Linnean Society*, **115**, 664–677.

Pyke, A.T., Moore, P.R., Taylor, C.T., Hall-Mendelin, S., Cameron, J.N., Hewitson, G.R., Pukallus, D.S., Huang, B., Warrilow, D. & Van Den Hurk, A.F. (2016) Highly divergent dengue virus type 1 genotype sets a new distance record. *Scientific Reports*, **6**, 22356.

Queenborough, S.A., Mazer, S.J., Vamosi, S.M., Garwood, N.C., Valencia, R. & Freckleton, R.P. (2009) Seed mass, abundance and breeding system among tropical forest species: do dioecious species exhibit compensatory reproduction or abundances? *Journal of Ecology*, **97**, 555–566.

Radhakrishna Rao, C. (1948) Large sample tests of statistical hypotheses concerning several parameters with applications to problems of estimation. *Mathematical Proceedings of the Cambridge Philosophical Society*, **44**, 50–57.

Ramette, A. & Tiedje, J.M. (2007) Biogeography: An emerging cornerstone for understanding prokaryotic diversity, ecology, and evolution. *Microbial Ecology*, **53**, 197–207.

Rapoport, E. (1975) *Areografía: estrategias geográficas de las especies*, Fondo de Cultura Económica, México.

Da Re, D., Montecino-Latorre, D., Vanwambeke, S.O. & Marcantonio, M. (2021) Will the yellow fever mosquito colonise Europe? Assessing the re-introduction of *Aedes aegypti* using a process-based population dynamical model. *Ecological Informatics*, **61**, 101180.

Real, R., Barbosa, A.M., Porras, D., Kin, M.S., Márquez, A.L., Guerrero, J.C., Javier Palomo, L., Justo, E.R. & Mario Vargas, J. (2003) Relative importance of environment, human activity and spatial situation in determining the distribution of terrestrial mammal diversity in Argentina. *Journal of*

Biogeography, **30**, 939–947.

Real, R., Barbosa, A.M., Rodríguez, A., García, F.J., Vargas, J.M., Palomo, L.J. & Delibes, M. (2009) Conservation biogeography of ecologically interacting species: the case of the Iberian lynx and the European rabbit. *Diversity and Distributions*, **15**, 390–400.

Real, R., Barbosa, A.M. & Vargas, J.M. (2006) Obtaining environmental favourability functions from logistic regression. *Environmental and Ecological Statistics*, **13**, 237–245.

Real, R., Olivero, J. & Vargas, J.M. (2008) Using chorotypes to deconstruct biogeographical and biodiversity patterns: the case of breeding waterbirds in Europe. *Global Ecology and Biogeography*, **17**, 735–746.

Record, S., Fitzpatrick, M.C., Finley, A.O., Veloz, S. & Ellison, A.M. (2013) Should species distribution models account for spatial autocorrelation? A test of model projections across eight millennia of climate change. *Global Ecology and Biogeography*, **22**, 760–771.

Reed, W., Carroll, J. & Agramonte, A. (2001) Experimental Yellow Fever. *Military Medicine*, **166**, 55–60.

Rico-Hesse, R. (1990) Molecular evolution and distribution of dengue viruses type 1 and 2 in nature. *Virology*, **174**, 479–493.

Rivera, A., Adams, L.E., Sharp, T.M., Lehman, J.A., Waterman, S.H. & Paz-Bailey, G. (2020) Travel-associated and locally acquired dengue cases - United States, 2010-2017. *Morbidity and Mortality Weekly Report*, **69**, 149–154.

Roberts, D.R., Peyton, E.L., Pinheiro, F.P., Balderrama, F. & Vargas, R. (1984) Associations of arbovirus vectors with gallery forests and domestic environments in southeastern Bolivia. *Bulletin of the Pan American Health Organization*, **18**, 337–350.

Rocklöv, J. & Dubrow, R. (2020) Climate change: an enduring challenge for vector-borne disease prevention and control. *Nature Immunology*, **21**, 479–483.

Roig C, Miret J, Rojas A, Guillén Y, Aria L, M.L. et al (2009) Study of Yellow Fever in primates in outbreaks areas of the departments of San Pedro and Central in Paraguay. *Memorias del Instituto de Investigaciones en Ciencias de la Salud*, **7**, 40–45.

Romero, D., Olivero, J., Brito, J.C. & Real, R. (2016) Comparison of approaches to combine species distribution models based on different sets of predictors. *Ecography*, **39**, 561–571.

Romero, D., Olivero, J., Márquez, A.L., Báez, J.C. & Real, R. (2014) Uncertainty in distribution forecasts caused by taxonomic ambiguity under climate change scenarios: a case study with two newt species in mainland Spain. *Journal of Biogeography*, **41**, 111–121.

Romero, D., Olivero, J., Real, R. & Guerrero, J.C. (2019) Applying fuzzy logic to assess the biogeographical risk of dengue in South America. *Parasites and Vectors*, **12**, 1–13.

Rudnick, A. (1965) Studies of the Ecology of Dengue in Malaysia: A Preliminary Report. *Journal of Medical Entomology*, **2**, 203–208.

Rugarabamu, S., Mwanyika, G.O., Rumisha, S.F., Sindato, C., Lim, H.Y., Misinzo, G. & Mboera, L.E.G. (2021) Seroprevalence and associated risk factors of selected zoonotic viral hemorrhagic fevers in Tanzania. *International Journal of Infectious Diseases*, **109**, 174–181.

Rupasinghe, R., Chomel, B.B. & Martínez-López, B. (2022) Climate change and zoonoses: A review of the current status, knowledge gaps, and future trends. *Acta Tropica*, **226**, 106225.

Ryan, S.J., Carlson, C.J., Mordecai, E.A. & Johnson, L.R. (2018) Global expansion

and redistribution of *Aedes*-borne virus transmission risk with climate change. *PLoS Neglected Tropical Diseases*, **13**, e0007213.

Saluzzo, J.F., Cornet, M., Adam, C., Eyraud, M. & Digoutte, J.P. (1986) Dengue 2 in eastern Senegal: serologic survey in simian and human populations. 1974-85. *Bulletin de la Société de Pathologie Exotique*, **79**, 313–322.

Sanderson, B.M., Knutti, R. & Caldwell, P. (2015) A representative democracy to reduce interdependency in a multimodel ensemble. *Journal of Climate*, **28**, 5171–5194.

Sanna, A., Andrieu, A., Carvalho, L., Mayence, C., Tabard, P., Hachouf, M., Cazaux, C.M., Enfissi, A., Rousset, D. & Kallel, H. (2018) Yellow fever cases in French Guiana, evidence of an active circulation in the Guiana shield, 2017 and 2018. *Eurosurveillance*, **23**, 1800471.

Schaffner, F. & Mathis, A. (2014) Dengue and dengue vectors in the WHO European region: Past, present, and scenarios for the future. *The Lancet Infectious Diseases*, **14**, 1271–1280.

Schloss, C.A., Nuñez, T.A. & Lawler, J.J. (2012) Dispersal will limit ability of mammals to track climate change in the Western Hemisphere. *Proceedings of the National Academy of Sciences*, **109**, 8606–8611.

Scholte, E.J., den Hartog, W., Dik, M., Schoelitsz, B., Brooks, M., Schaffner, F., Foussadier, R., Braks, M. & Beeuwkes, J. (2010) Introduction and control of three invasive mosquito species in the Netherlands, July-OctOber 2010. *Eurosurveillance*, **15**, 1–4.

Shearer, F.M., Longbottom, J., Browne, A.J., Pigott, D.M., Brady, O.J., Kraemer, M.U.G., Marinho, F., Yactayo, S., de Araújo, V.E.M., da Nóbrega, A.A., Fullman, N., Ray, S.E., Mosser, J.F., Stanaway, J.D., Lim, S.S., Reiner, R.C., Moyes, C.L., Hay, S.I. & Golding, N. (2018) Existing and potential infection risk zones of yellow fever worldwide: a modelling analysis. *The Lancet Global Health*, **6**,

e270–e278.

Shinha, T. & Nautiyal, P. (2011) Emerging Dengue Fever in New York City. *Journal of Hospital Medicine*, **6**, 2.

Silva, N.I.O., Sacchetto, L., De Rezende, I.M., Trindade, G.D.S., Labeaud, A.D., De Thoisy, B. & Drumond, B.P. (2020) Recent sylvatic yellow fever virus transmission in Brazil: The news from an old disease. *Virology Journal*, **17**, 9.

Silveira, J.M., Louzada, J., Barlow, J., Andrade, R., Mestre, L., Solar, R., Lacau, S. & Cochrane, M.A. (2016) A Multi-Taxa Assessment of Biodiversity Change After Single and Recurrent Wildfires in a Brazilian Amazon Forest. *Biotropica*, **48**, 170–180.

Simmons, C.P., Farrar, J.J., Van Vinh Chau, N. & Wills, B. (2012) Dengue. *The New England Journal of Medicine*, **366**, 1423–1432.

SMART (2018) Spatial Monitoring And Reporting Tool: measure, evaluate and improve the effectiveness of your wildlife law enforcement patrols and site-based conservation activities. *https://smartconservationtools.org/*, accessed 2018-06-25.

SMART (2017) *Spatial Monitoring And Reporting Tool partnership annual report 2017*, Rotterdam, The Netherlands.

Smith, C.E.G. (1958) The distribution of antibodies to Japanese encephalitis, dengue, and yellow fever viruses in five rural communities in Malaya. *Transactions of the Royal Society of Tropical Medicine and Hygiene*, **52**, 237–252.

Smith, T.D. & Burrows, A.M. (2004) *Primate Studies, Ecology and Behavior*. In: Encyclopedia of Social Measurement (ed. by K. Kempf-Leonard), pp. 149–160. Elsevier Inc., Amsterdam, The Netherlands.

Smithburn, K.C., Durieux, C., Koerber, E., Penna, H.A., Dick, G.W.A., Courtois, G. &

Bonnel, P.H. (1956) *Yellow Fever Vaccination*, World Health Organization, Geneva, Switzerland.

Sneath, P.H.A. & Sokal, R.R. (1973) *Numerical Taxonomy The principles and practice of numerical classification*, W. H. Freeman and Company, San Francisco, California.

Sokal, R.R. & Oden, N.L. (1978) Spatial autocorrelation in biology: 1. Methodology. *Biological Journal of the Linnean Society*, **10**, 199–228.

Soper, F.L. (1963) The elimination of urban yellow fever in the Americas through the eradication of *Aedes aegypti*. *American journal of public health*, **53**, 7–16.

Stanaway, J.D., Shepard, D.S., Undurraga, E.A., Halasa, Y.A., Coffeng, L.E., Brady, O.J., Hay, S.I., Bedi, N., Bensenor, I.M., Castañeda-Orjuela, C.A., Chuang, T.W., Gibney, K.B., Memish, Z.A., Rafay, A., Ukwaja, K.N., Yonemoto, N. & Murray, C.J.L. (2016) The global burden of dengue: an analysis from the Global Burden of Disease Study 2013. *The Lancet Infectious Diseases*, **16**, 712–723.

Stephens, P.R., Altizer, S., Smith, K.F., Alonso Aguirre, A., Brown, J.H., Budischak, S.A., Byers, J.E., Dallas, T.A., Jonathan Davies, T., Drake, J.M., Ezenwa, V.O., Farrell, M.J., Gittleman, J.L., Han, B.A., Huang, S., Hutchinson, R.A., Johnson, P., Nunn, C.L., Onstad, D., Park, A., Vazquez-Prokopec, G.M., Schmidt, J.P. & Poulin, R. (2016) The macroecology of infectious diseases: a new perspective on global-scale drivers of pathogen distributions and impacts. *Ecology letters*, **19**, 1159–1171.

Stokes, E.J., Strindberg, S., Bakabana, P.C., Elkan, P.W., Iyenguet, F.C., Madzoké, B., Malanda, G.A.F., Mowawa, B.S., Moukoumbou, C., Ouakabadio, F.K. & Rainey, H.J. (2010) Monitoring Great Ape and Elephant Abundance at Large Spatial Scales: Measuring Effectiveness of a Conservation Landscape. *PLOS ONE*, **5**, e10294.

Streicker, D.G., Recuenco, S., Valderrama, W., Benavides, J.G., Vargas, I., Pacheco,

V., Condori Condori, R.E., Montgomery, J., Rupprecht, C.E., Rohani, P. & Altizer, S. (2012) Ecological and anthropogenic drivers of rabies exposure in vampire bats: Implications for transmission and control. *Proceedings of the Royal Society B: Biological Sciences*, **279**, 3384–3392.

Strindberg, S., Maisels, F., Williamson, E.A., Blake, S., Stokes, E.J., Aba'a, R., Abitsi, G., Agbor, A., Ambahe, R.D., Bakabana, P.C., Bechem, M., Berlemont, A., De Semboli, B.B., Boundja, P.R., Bout, N., Breuer, T., Campbell, G., De Wachter, P., Akou, M.E., Mba, F.E., Feistner, A.T.C., Fosso, B., Fotso, R., Greer, D., Inkamba-Nkulu, C., Iyenguet, C.F., Jeffery, K.J., Kokangoye, M., Kühl, H.S., Latour, S., Madzoke, B., Makoumbou, C., Malanda, G.A.F., Malonga, R., Mbolo, V., Morgan, D.B., Motsaba, P., Moukala, G., Mowawa, B.S., Murai, M., Ndzai, C., Nishihara, T., Nzooh, Z., Pintea, L., Pokempner, A., Rainey, H.J., Rayden, T., Ruffler, H., Sanz, C.M., Todd, A., Vanleeuwe, H., Vosper, A., Warren, Y. & Wilkie, D.S. (2018) Guns, germs, and trees determine density and distribution of gorillas and chimpanzees in Western Equatorial Africa. *Science Advances*, **4**, eaar2964.

Sudeep, A.B. & Shil, P. (2017) *Aedes vittatus* (Bigot) mosquito: An emerging threat to public health. *Journal of Vector Borne Diseases*, **54**, 295–300.

Takemoto, H., Kawamoto, Y. & Furuichi, T. (2015) How did bonobos come to range south of the congo river? Reconsideration of the divergence of *Pan paniscus* from other *Pan* populations. *Evolutionary Anthropology: Issues, News, and Reviews*, **24**, 170–184.

Tatem, A.J., Hay, S.I. & Rogers, D.J. (2006) Global traffic and disease vector dispersal. *Proceedings of the National Academy of Sciences of the United States of America*, **103**, 6242–6247.

Tavaré, S., Marshall, C.R., Will, O., Soligo, C. & Martin, R.D. (2002) Using the fossil record to estimate the age of the last common ancestor of extant primates.

Nature, **416**, 726–729.

Taylor, L.H., Latham, S.M. & Woolhouse, M.E.J. (2001) Risk factors for human disease emergence. *Philosophical Transactions of the Royal Society B: Biological Sciences*, **356**, 983–989.

de Thoisy, B., Lacoste, V., Germain, A., Muñoz-Jordán, J., Colón, C., Mauffrey, J.F., Delaval, M., Catzeflis, F., Kazanji, M., Matheus, S., Dussart, P., Morvan, J., Setién, A.A., Deparis, X. & Lavergne, A. (2009) Dengue infection in neotropical forest mammals. *Vector-Borne and Zoonotic Diseases*, **9**, 157–169.

Tobin, P.C., Whitmire, S.L., Johnson, D.M., Bjørnstad, O.N. & Liebhold, A.M. (2007) Invasion speed is affected by geographical variation in the strength of Allee effects. *Ecology Letters*, **10**, 36–43.

Tobler, M.W., Kéry, M., Hui, F.K.C., Guillera-Arroita, G., Knaus, P. & Sattler, T. (2019) Joint species distribution models with species correlations and imperfect detection. *Ecology*, **100**, e02754.

Tranquilli, S., Abedi-Lartey, M., Abernethy, K., Amsini, F., Asamoah, A., Balangtaa, C., Blake, S., Bouanga, E., Breuer, T., Brncic, T.M., Campbell, G., Chancellor, R., Chapman, C.A., Davenport, T.R.B., Dunn, A., Dupain, J., Ekobo, A., Eno-Nku, M., Etoga, G., Furuichi, T., Gatti, S., Ghiurghi, A., Hashimoto, C., Hart, J.A., Head, J., Hega, M., Herbinger, I., Hicks, T.C., Holbech, L.H., Huijbregts, B., Kühl, H.S., Imong, I., Yeno, S.L.D., Linder, J., Marshall, P., Lero, P.M., Morgan, D., Mubalama, L., N'Goran, P.K., Nicholas, A., Nixon, S., Normand, E., Nziguyimpa, L., Nzooh-Dongmo, Z., Ofori-Amanfo, R., Ogunjemite, B.G., Petre, C.A., Rainey, H.J., Regnaut, S., Robinson, O., Rundus, A., Sanz, C.M., Okon, D.T., Todd, A., Warren, Y. & Sommer, V. (2014) Protected Areas in Tropical Africa: Assessing Threats and Conservation Activities. *PloS ONE*, **9**, e114154.

UNESCO (2018) State of conservation. Dja Faunal Reserve (Cameroon). *https://whc.unesco.org/en/soc/3654*, accessed 2018-10-04.

Valentine, M.J., Murdock, C.C. & Kelly, P.J. (2019) Sylvatic cycles of arboviruses in non-human primates. *Parasites and Vectors*, **12**, 1–18.

Vasilakis, N., Cardosa, J., Hanley, K.A., Holmes, E.C. & Weaver, S.C. (2011) Fever from the forest: Prospects for the continued emergence of sylvatic dengue virus and its impact on public health. *Nature Reviews Microbiology*, **9**, 532–541.

Vasilakis, N., Tesh, R.B. & Weaver, S.C. (2008) Sylvatic dengue virus type 2 activity in humans, Nigeria, 1966. *Emerging Infectious Diseases*, **14**, 502–504.

Vermeer, J., Tello-Alvarado, J.C., Moreno-Moreno, S. & Guerra-Vásquez, F. (2011) Extension of the Geographical Range of White-browed Titi Monkeys (*Callicebus discolor*) and Evidence for Sympatry with San Martin Titi Monkeys (*Callicebus oenanthe*). *International Journal of Primatology*, **32**, 924–930.

Virchow, R. (1855) *Handbuch per Spezielle Pathologie und Therapie*, Verlag Von Ferdinand Enke, Erlangen, Germany.

Virginia Department of Health (2011) Guidelines for Investigating Bites and Other Exposures from Nonhuman Primates. *https://www.vdh.virginia.gov/environmental-epidemiology/zoonoses/guidelines-for-investigating-bites-and-other-exposures-from-nonhuman-primates/*, accessed 2023-01-09.

Vittor, A.Y., Gilman, R.H., Tielsch, J., Glass, G., Shields, T., Lozano, W.S., Pinedo-Cancino, V. & Patz, J.A. (2006) The effect of deforestation on the human-biting rate of *Anopheles darlingi*, the primary vector of Falciparum malaria in the Peruvian Amazon. *The American Journal of Tropical Medicine and Hygiene*, **74**, 3–11.

Wald, A. (1943) Tests of Statistical Hypotheses Concerning Several Parameters When the Number of Observations is Large. *Transactions of the American Mathematical Society*, **54**, 426.

Wallace, R. (1852) On the monkeys of the Amazon. *Proceedings Zoological Society of London*, **20**, 107–110.

Wallace, R.G., Gilbert, M., Wallace, R., Pittiglio, C., Mattioli, R. & Kock, R. (2014) Did Ebola emerge in West Africa by a policy-driven phase change in agroecology? Ebola's social context. *Environment and Planning A*, **46**, 2533–2542.

Walsh, P.D., Abernethy, K.A., Bermejo, M., Beyers, R., De Wachter, P., Akou, M.E., Huljbregts, B., Mambounga, D.I., Toham, A.K., Kilbourn, A.M., Lahm, S.A., Latour, S., Maisels, F., Mbina, C., Mihindou, Y., Ndong Obiang, S., Effa, E.N., Starkey, M.P., Teifer, P., Thibault, M., Tutin, C.E.G., White, L.J.T. & Wilkie, D.S. (2003) Catastrophic ape decline in western equatorial Africa. *Nature*, **422**, 611–614.

Wang, E., Ni, H., Xu, R., Barrett, A.D.T., Watowich, S.J., Gubler, D.J. & Weaver, S.C. (2000) Evolutionary Relationships of Endemic/Epidemic and Sylvatic Dengue Viruses. *Journal of Virology*, **74**, 3227–3234.

Waters, J.M., Fraser, C.I. & Hewitt, G.M. (2013) Founder takes all: density-dependent processes structure biodiversity. *Trends in Ecology & Evolution*, **28**, 78–85.

Watts, N., Amann, M., Arnell, N., Ayeb-Karlsson, S., Beagley, J., Belesova, K., Boykoff, M., Byass, P., Cai, W., Campbell-Lendrum, D., Capstick, S., Chambers, J., Coleman, S., Dalin, C., Daly, M., Dasandi, N., Dasgupta, S., Davies, M., Di Napoli, C., Dominguez-Salas, P., Drummond, P., Dubrow, R., Ebi, K.L., Eckelman, M., Ekins, P., Escobar, L.E., Georgeson, L., Golder, S., Grace, D., Graham, H., Haggar, P., Hamilton, I., Hartinger, S., Hess, J., Hsu, S.C., Hughes, N., Jankin Mikhaylov, S., Jimenez, M.P., Kelman, I., Kennard, H., Kiesewetter, G., Kinney, P.L., Kjellstrom, T., Kniveton, D., Lampard, P., Lemke, B., Liu, Y., Liu, Z., Lott, M., Lowe, R., Martinez-Urtaza, J., Maslin, M., McAllister, L., McGushin,

A., McMichael, C., Milner, J., Moradi-Lakeh, M., Morrissey, K., Munzert, S., Murray, K.A., Neville, T., Nilsson, M., Sewe, M.O., Oreszczyn, T., Otto, M., Owfi, F., Pearman, O., Pencheon, D., Quinn, R., Rabbaniha, M., Robinson, E., Rocklöv, J., Romanello, M., Semenza, J.C., Sherman, J., Shi, L., Springmann, M., Tabatabaei, M., Taylor, J., Triñanes, J., Shumake-Guillemot, J., Vu, B., Wilkinson, P., Winning, M., Gong, P., Montgomery, H. & Costello, A. (2021) The 2020 report of The Lancet Countdown on health and climate change: responding to converging crises. *The Lancet*, **397**, 129–170.

Weetman, D., Kamgang, B., Badolo, A., Moyes, C.L., Shearer, F.M., Coulibaly, M., Pinto, J., Lambrechts, L. & McCall, P.J. (2018) *Aedes* Mosquitoes and *Aedes*-Borne Arboviruses in Africa: Current and Future Threats. *International Journal of Environmental Research and Public Health*, **15**, 220.

van der Werf, G.R., Morton, D.C., Defries, R.S., Olivier, J.G.J., Kasibhatla, P.S., Jackson, R.B., Collatz, G.J. & Randerson, J.T. (2009) CO2 emissions from forest loss. *Nature Geoscience*, **2**, 737–738.

Whitaker, R.J., Grogan, D.W. & Taylor, J.W. (2003) Geographic Barriers Isolate Endemic Populations of Hyperthermophilic Archaea. *Science*, **301**, 976–978.

WHO & FAO (1959) *Comité mixto OMS/FAO de expertos en zoonosis*, World Health Organization Press, Ginebra, Italia.

WHO (1989) *Geographical distribution of arthropod-borne diseases and their principal vectors*, World Health Organization Press, Geneva, Switzerland.

WHO (1992) *Global health situation and projections*, World Health Organization Press, Geneva, Switzerland.

WHO (2012) *Global strategy for dengue prevention and control 2012-2020*, World Health Organization Press, Geneva, Switzerland.

WHO (2014a) *A global brief on vector-borne diseases*, World Health Organization

Press, Geneva, Switzerland.

WHO (2014b) *Risk assessment on yellow fever virus circulation in endemic countries: working document from an informal consultation of experts: a protocol risk assessment at the field level*, Biotext Pty Ltd, Bruce, Australia.

WHO (2015a) *Connecting global priorities: biodiversity and human health: a state of knowledge review*, World Health Organization Press, Geneva, Switzerland.

WHO (2015b) Yellow Fever Vaccination Recommendations in Africa, 2015. *http://gamapserver.who.int/mapLibrary/Files/Maps/ITH_YF_vaccination_africa.png?ua=1*, accessed 2021-04-19.

WHO (2016) Yellow fever: the resurgence of a forgotten disease. *https://apps.who.int/mediacentre/commentaries/yellow-fever/en/index.html*, accessed 2021-01-07.

WHO (2018) Yellow fever in Africa and the Americas, 2017. *Weekly epidemiological record*, **93**, 409–416.

WHO (2019) Yellow Fever Vaccination Recommendations in the Americas, 2013-2020. *https://who.maps.arcgis.com/apps/webappviewer/index.html?id=7f2ecf3d51c244ba8694c3bf725a7601*, accessed 2021-04-19.

WHO (2020a) Dengue and severe dengue. *https://www.who.int/news-room/fact-sheets/detail/dengue-and-severe-dengue*, accessed 2020-09-10.

WHO (2020b) Vector-borne diseases. *https://www.who.int/news-room/fact-sheets/detail/vector-borne-diseases*, accessed 2022-11-16.

WHO (2021a) Enfermedades tropicales desatendidas. *https://www.who.int/es/news-room/questions-and-answers/item/neglected-tropical-diseases*, accessed 2022-12-29.

WHO (2021b) Vaccination requirements and recommendations for international

travellers; and malaria situation per country – 2021 edition. *https://www.who.int/publications/m/item/vaccination-requirements-and-recommendations-for-international-travellers-and-malaria-situation-per-country-2021-edition*, accessed 2021-08-04.

WHO (2022) New report highlights the impact of changes in environment on One Health. *https://www.who.int/europe/news/item/01-07-2022-new-report-highlights-the-impact-of-changes-in-environment-on-one-health*, accessed 2022-11-11.

WHO Regional Office for Europe (2022) *A health perspective on the role of the environment in One Health*, Copenhagen, Denmark.

Wich, S.A., Garcia-Ulloa, J., Kühl, H.S., Humle, T., Lee, J.S.H. & Koh, L.P. (2014) Will Oil Palm's Homecoming Spell Doom for Africa's Great Apes? *Current Biology*, **24**, 1659–1663.

Wich, S.A. & Marshall, A.J. (2016) *An introduction to primate conservation*, Oxford University Press, Oxford, United Kingdom.

Wilkie, D.S., Carpenter, J.F. & Zhang, Q. (2001) The under-financing of protected areas in the Congo Basin: so many parks and so little willingness-to-pay. *Biodiversity and Conservation*, **10**, 691–709.

Wilkinson, D.P., Golding, N., Guillera-Arroita, G., Tingley, R. & McCarthy, M.A. (2018) A comparison of joint species distribution models for presence–absence data. *Methods in Ecology and Evolution*, **10**, 198–211.

Wilson, D.E. & Mittermeier, R.A. (2011) *Handbook of the Mammals of the World. Volume 2. Hoofed Mammals*, Lynx Edicions, Barcelona, Spain.

Wilson, M.L. (2001) *Ecology and infectious disease*. In: Ecosystem Change and Public Health: A Global Perspective (ed. by J.L. Aron & J.A. Patz), pp. 283–324. Johns Hopkins University Press, Baltimore, Maryland.

Wolfe, N.D., Daszak, P., Kilpatrick, A.M. & Burke, D.S. (2005) Bushmeat Hunting, Deforestation, and Prediction of Zoonotic Disease. *Emerging Infectious Diseases*, **11**, 1822–1827.

Wolfe, N.D., Kilbourn, A.M., Karesh, W.B., Rahman, H.A., Bosi, E.J., Cropp, B.C., Andau, M., Spielman, A. & Gubler, D.J. (2001) Sylvatic transmission of arboviruses among Bornean orangutans. *American Journal of Tropical Medicine and Hygiene*, **64**, 310–316.

Wouthuyzen-Bakker, M., Knoester, M., van den Berg, A.P., GeurtsvanKessel, C.H., Koopmans, M.P., Van Leer-Buter, C., Oude Velthuis, B., Pas, S.D., Ruijs, W.L., Schmidt-Chanasit, J., Vreden, S.G., van der Werf, T.S., Reusken, C.B. & Bierman, W.F.W. (2017) Yellow fever in a traveller returning from Suriname to the Netherlands, March 2017. *Eurosurveillance*, **22**, 30488.

Young, K.I., Mundis, S., Widen, S.G., Wood, T.G., Tesh, R.B., Cardosa, J., Vasilakis, N., Perera, D. & Hanley, K.A. (2017) Abundance and distribution of sylvatic dengue virus vectors in three different land cover types in Sarawak, Malaysian Borneo. *Parasites and Vectors*, **10**, 1–14.

Yuwono, J., Suharyono, W., Koiman, I., Tsuchiya, Y. & Tagaya, I. (1984) Seroepidemiological survey on dengue and Japanese encephalitis virus infections in Asian monkeys. *The Southeast Asian Journal of Topical Medicine and Public Health*, **15**, 194–200.

Zadeh, L.A. (1965) Fuzzy sets. *Information and Control*, **8**, 338–353.

Zunino, M. & Zullini, A. (2003) *Biogeografía, la dimensión espacial de la evolución*, Fondo de Cultura Económica, México.

CAPÍTULO 12

Apéndices

Appendixes

12. Apéndices

Appendix 1. Predictor variables considered for distribution modelling of primate species in Peru and Africa.

Factor	Code	Variable
Spatial	*Spay*[3]	Combinations of: X = longitude (degrees) + 78 (Peru)[1] Y = latitude (degrees) + 9 (Peru)[1] X = longitude (degrees) + 0 (Africa)[1] Y = latitude (degrees) + 14 (Africa)[1]
	Spay[4]	
Types of Ecosystems	*Besr*	Broadleaf evergreen/semideciduous rainforests (class 40 GC)[2]
	Swf	Swamp forest (class 160 GC)[2]
	Decf	Deciduous forests (class 50 GC)[2]
	Wosa	Woody savannas (class 60/120 GC)[2]
	Shru	Shrublands (class 110/130 GC)[2**]
	Sveg	Sparse vegetation (class 150 GC)*
	Rfv	Regularly flooded closed to open vegetation (class 180 GC)*
	Grass	Grassland (class 140 GC)[2]
	Desr	Deserts (class 200 GC)[2]
	Crop	Croplands (class 14 GC)[2]
	Cropm	Cropland (>50%)/vegetation mosaics (class 20 GC)[2]
	Vegm	Vegetation (>50%)/cropland mosaics (class 30 GC)[2]
	Hags	High Andean grasslands with shrubs[3*]
	Haco	High Andean communities of low and wide trees, grasslands with shrubs and dispersed trees[3*]
	Hamf	High-Andean mountain forests with medium-sized trees[3*]
	Subfh	Sub-Andean forests of high steep mountains with large and vigorous trees[3*]
	Subms	Sub-Andean mountain communities with medium and scattered trees and dense shrubs[3*]
	Subfl	Sub-Andean forests of low steep mountains with medium and large trees[3*]
	Hhf	High-hill forests[3*]
	Samf	Savannah-type mountain forests[3 *]
	Lhf	Low-hill forests[3*]
	Mxfp	Mixed forests with palms[3*]
	Var	*Varillales* (forest on white sand)[3*]
	Areva	Association of arboreal swamps (*renacales*) with forest on white sand (*varillales*), composed by Myristicaceae plants[3*]
	Ren	*Renacal* (arboreal swamps)[3*]
	Agu	*Aguajal* (permanently flooded swamps where *Mauritia flexuosa* palms predominate)[3*]
	Dryf	Dry forests with scrubland on low hills[3*]
	Fterr	Forest of high, medium and low terraces[3*]
	Hswa	Herbaceous swamps[3*]
	Ori	*Orillares* complex (land forms caused by the temporary flow of sediments from river waters)[3*]
Topography	*Elev*	Elevation[4]
	Slope	Slope[4]
Hydrography	*Dma*	Distance to water masses (i. e., lakes and main river courses with water flow accumulation > 106 cells)[5]

	Driv	Distance to minor rivers (with water flow accumulation between 104 and 106 cells)[5]
Climate	*Bio1*	Annual mean temperature[6]
	Bio2	Mean diurnal range (Mean of monthly (max temp – min temp)[6]
	Bio3	Isothermality (Bio2/Bio7) (× 100)[6]
	Bio4	Temperature seasonality (standard deviation × 100)[6]
	Bio5	Max temperature of warmest month[6]
	Bio6	Min temperature of coldest month[6]
	Bio7	Temperature annual range (Bio5-Bio6)[6]
	Bio12	Annual precipitation[6]
	Bio13	Precipitation of wettest month[6]
	Bio14	Precipitation of driest month[6]
	Bio15	Precipitation seasonality (coefficient of variation)[6]
Human concentration	*Popd*	Population density[7]
Infrastructures	*Droad*	Distance to roads[8]
Competence	*SpD(x)*	Species distribution (x), where (x) = *P. oenanthe* o *P. discolor* o *P. paniscus* o *P. troglodytes*[9]
Barrier	*Briv(x)*	Binary *cis-trans* variable that took value 0 for squares located on the same side of the river where the species x occurs, and value 1 on the opposite side of the river.

[1]These two variables were combined following a trend surface approach (Legendre 1993)
[2]GlobCover (GC) Land Cover version 2.3 database for 2009 (Bontemps et al., 2011)
[3]San Martín Regional Environmental Authority Database (intersected with the *Besr* (class 40 GC) variable)
[4]GTOPO30 (US Geological Survey 1996)
[5]Hydrologically conditioned DEM de HydroSHEDS (http://hydrosheds.cr.usgs.gov)
[6]WorldClim (http://www.worldclim.org)
[7]LandScan™ 2008 High Resolution Global Population Data Set (copyrighted by UT-Battelle, LLC, operator of Oak Ridge National Laboratory)
[8]Vector Map Level 0 at the Digital Chart of the World (DCW, http://worldmap.harvard.edu), updated in 2002
[9]African distribution data: IUCN (http://www.iucnredlist.org). Peruvian distribution data: presence points (see Vermeer et al., 2011) modified according to data provided by Proyecto Mono Tocon (http://www.monotocon.org/ and Primate of Peru, Pocket Identification Guide by Conservation International)
*Variables only used for Peru
**Variables that were used for Peru divided (*Mofsg* - Mosaic forest / shrubland (50-70%) / grassland (class 110 GC) and *Cshr* – Closed to open (>15%) shrubland (<5m) (class 130 GC))

References:

Bontemps, S., Defourny, P., Van Bogaert, E., Arino, O., Kalogirou, V. & Perez, J. R. (2011). GlobCover 2009: Products Description and Validation Report. http://due.esrin.esa.int/page_globcover.php (accessed 04/07/2018).

US Geological Survey (1996). GTOPO30. Land processes distributed active archive center (LP DAAC), EROS data center. https://lta.cr.usgs.gov/GTOPO30 (accessed 11/08/2018).

Appendix 2. Variables included in the models: coefficients (*B*), Wald parameter values (*Wald*) and significance (*P*).

Models for *Plecturocebus oenanthe*															
	E-Model			0-Model			F-Model			R-Model			C-Model		
	B	*Wald*	*P*	*B*	*Wald*	*P*	*B*	*Wald*	*P*	*B*	*Wald*	*P*	*B*	*Wald*	*P*
Driv	-8,273	36,364	0,000	-9,860	34,932	0,000	-	-	-	-12,080	36,244	0,000	-9,298	31,170	0,000
Ren	-17,893	3,998	0,046	-	-	-	-46,207	0,290	0,590	-	-	-	-	-	-
Lhf	-4,978	10,780	0,001	-4,814	6,319	0,012	-10,332	6,283	0,012	-	-	-	-	-	-
Subfh	-1,287	11,426	0,001	-1,127	7,797	0,005	-	-	-	-1,395	9,212	0,002	-1,178	7,972	0,005
Hamf	-4,525	48,465	0,000	-	-	-	-	-	-	-	-	-	-	-	-
Mofsg	77,975	13,660	0,000	70,380	9,966	0,002	-	-	-	-	-	-	57,741	6,146	0,013
Crop	17,138	47,291	0,000	14,912	7,860	0,005	-	-	-	15,863	6,840	0,009	14,558	7,459	0,006
Rfv	-9,199	29,183	0,000	-	-	-	-	-	-	-5,000	6,405	0,011	-	-	-
Bio12	-	-	-	-	-	-	-	-	-	-	-	-	-0,007	58,810	0,000
Bio13	-0,084	193,897	0,000	-0,044	37,587	0,000	-	-	-	-,088	78,607	0,000	-	-	-
Bio15	0,306	90,279	0,000	0,197	33,012	0,000	0,098	4,442	0,035	0,151	16,506	0,000	-	-	-
Bio2	-0,477	125,456	0,000	-0,386	68,307	0,000	-0,076	18,168	0,000	-0,239	18,819	0,000	-0,228	20,823	0,000
Bio3	0,775	74,488	0,000	0,641	40,964	0,000	-	-	-	0,391	10,760	0,001	0,408	13,907	0,000
Bio6	0,067	46,922	0,000	0,061	43,184	0,000	0,063	27,552	0,000	0,129	82,218	0,000	0,099	65,946	0,000
Slope	0,027	4,076	0,043	-	-	-	-	-	-	-	-	-	-	-	-
Popd	0,009	3,012	0,083	0,012	3,138	0,076	-	-	-	-	-	-	-	-	-
Spay^3	N/A	N/A	N/A	1,044	126,261	0,000	N/A	N/A	N/A	0,983	81,916	0,000	0,849	76,045	0,000
Spay^4	N/A	N/A	N/A	N/A	N/A	N/A	0,974	121,076	0,000	N/A	N/A	N/A	N/A	N/A	N/A
Briv(Poenanthe)	N/A	N/A	N/A	N/A	N/A	N/A	N/A	N/A	N/A	-5,964	84,546	0,000	N/A	N/A	N/A
SpD(Pdiscolor)	N/A	N/A	N/A	N/A	N/A	N/A	N/A	N/A	N/A	N/A	N/A	N/A	-3,601	50,412	0,000
Constant	-13,182	32,979	0,000	-15,058	28,154	0,000	-4,007	5,337	0,021	-12,322	13,759	0,000	-12,531	18,208	0,000

Models for *Plecturocebus discolor*															
	E-Model			0-Model			F-Model			R-Model			C-Model		
	B	*Wald*	*P*	*B*	*Wald*	*P*	*B*	*Wald*	*P*	*B*	*Wald*	*P*	*B*	*Wald*	*P*
Dryf	16,996	8,509	0,004	-	-	-	8,288	2,601	0,107	-	-	-	-	-	-
Ren	8,226	5,857	0,016	-6,830	7,378	0,007	-6,165	4,556	0,033	-	-	-	-6,830	7,378	0,007
Lhf	5,126	16,147	0,000	-	-	-	-	-	-	-	-	-	-	-	-
Subms	5,149	53,174	0,000	-	-	-	-	-	-	7,027	34,596	0,000	-	-	-
Subfh	5,357	56,547	0,000	-	-	-	1,943	5,251	0,022	5,133	21,479	0,000	-	-	-
Hamf	-30,302	1,629	0,202	-	-	-	-	-	-	-	-	-	-	-	-
Mofsg	-47,385	15,589	0,000	-	-	-	-23,625	4,197	0,041	-	-	-	-	-	-
Cshr	-23,518	21,528	0,000	-19,320	15,498	0,000	-19,451	16,373	0,000	-	-	-	-19,320	15,498	0,000
Crop	-9,133	11,597	0,001	-	-	-	-	-	-	-	-	-	-	-	-
Vegm	-38,934	23,925	0,000	-21,980	7,349	0,007	-23,801	8,001	0,005	-	-	-	-21,980	7,349	0,007
Besr	-4,995	16,860	0,000	-	-	-	-	-	-	-	-	-	-	-	-
Bio12	0,005	137,590	0,000	-	-	-	-	-	-	-	-	-	-	-	-
Bio14	-	-	-	-	-	-	-	-	-	0,082	28,380	0,000	-	-	-
Bio15	-0,227	22,349	0,000	-	-	-	-	-	-	-	-	-	-	-	-
Bio2	0,506	185,013	0,000	-	-	-	0,078	4,251	0,039	0,413	27,297	0,000	-	-	-
Bio3	-1,244	104,864	0,000	-	-	-	-0,246	5,016	0,025	-1,676	33,235	0,000	-	-	-
Bio4	-0,037	62,497	0,000	-0,017	9,334	0,002	-0,025	14,781	0,000	-0,125	45,003	0,000	-0,017	9,334	0,002
Bio5	0,163	85,328	0,000	-	-	-	-	-	-	0,166	32,690	0,000	-	-	-
Driv	-	-	-	-11,262	16,372	0,000	-17,064	20,073	0,000	-	-	-	-11,262	16,372	0,000
Spay³	N/A	N/A	N/A	1,090	131,475	0,000	N/A	N/A	N/A	-	-	-	1,090	131,475	0,000
Spay⁴	N/A	N/A	N/A	N/A	N/A	N/A	1,008	99,812	0,000	N/A	N/A	N/A	N/A	N/A	N/A
Briv(Pdiscolor)	N/A	N/A	N/A	N/A	N/A	N/A	N/A	N/A	N/A	-14,455	53,711	0,000	N/A	N/A	N/A
SpD(Poenanthe)	N/A	N/A	N/A	N/A	N/A	N/A	N/A	N/A	N/A	N/A	N/A	N/A	-	-	-
Constant	12,640	3,331	0,068	9,580	11,189	0,001	25,209	8,047	0,005	104,565	21,058	0,000	9,580	11,189	0,001

Models for *Pan troglodytes*															
	E-Model			0-Model			F-Model			R-Model			C-Model		
	B	*Wald*	*P*	*B*	*Wald*	*P*	*B*	*Wald*	*P*	*B*	*Wald*	*P*	*B*	*Wald*	*P*
Bio12	-0,003	584,152	0,000	-	-	-	0,000	4,664	0,031	0,003	187,853	0,000	0,001	64,629	0,000
Bio1	-	-	-	-	-	-	-	-	-	-0,031	211,493	0,000	-0,082	344,633	0,000
Bio13	0,023	909,167	0,000	-0,008	444,019	0,000	-0,006	25,949	0,000	-0,018	255,017	0,000	-0,014	170,791	0,000
Bio15	-0,038	359,187	0,000	0,047	1198,818	0,000	0,031	114,172	0,000	0,007	6,100	0,014	0,029	122,593	0,000
Bio6	-	-	-	0,023	227,732	0,000	-0,003	6,278	0,012	0,031	355,344	0,000	0,048	494,514	0,000
Bio5	0,035	760,025	0,000	-	-	-	0,012	94,092	0,000	-	-	-	0,028	134,732	0,000
Bio7	-0,028	743,067	0,000	-0,003	7,822	0,005	-	-	-	-	-	-	-	-	-
Elev	0,002	644,716	0,000	0,001	228,525	0,000	-	-	-	-	-	-	-	-	-
Crop	1,372	7,284	0,007	-2,762	15,011	0,000	-	-	-	-2,007	10,965	0,001	-2,879	19,638	0,000
Grass	-1,097	10,886	0,001	-1,859	28,764	0,000	-	-	-	-2,254	56,805	0,000	-1,913	44,486	0,000
Swf	2,625	667,363	0,000	2,304	168,461	0,000	3,365	906,308	0,000	4,802	346,815	0,000	1,871	307,790	0,000
Cropm	-4,625	142,270	0,000	-	-	-	-	-	-	-2,550	49,581	0,000	-2,008	29,497	0,000
Shru	-	-	-	0,736	15,346	0,000	-0,602	29,621	0,000	-	-	-	-	-	-
Desr	-	-	-	11,646	17,636	0,000	18,320	6,326	0,012	-	-	-	5,754	4,405	0,036
Vegm	1,601	354,526	0,000	0,970	32,270	0,000	1,040	129,098	0,000	-	-	-	-	-	-
Besr	3,788	2284,453	0,000	3,352	408,455	0,000	2,747	1152,926	0,000	4,275	2038,639	0,000	3,335	1901,150	0,000
Decf	-0,302	5,947	0,015	2,977	210,348	0,000	1,369	93,160	0,000	2,729	438,307	0,000	2,665	418,113	0,000
Wosa	1,073	165,974	0,000	0,999	34,640	0,000	-	-	-	0,760	101,230	0,000	0,349	21,987	0,000
Dma	0,106	96,063	0,000	0,385	533,650	0,000	0,138	42,447	0,000	0,395	511,565	0,000	0,463	627,251	0,000
Slope	0,252	594,294	0,000	0,473	1317,115	0,000	0,281	405,051	0,000	0,270	444,311	0,000	0,360	764,431	0,000
Popd	-0,001	51,432	0,000	-0,001	70,449	0,000	0,000	16,713	0,000	-0,001	78,422	0,000	-0,001	75,299	0,000
Spay^3	N/A	N/A	N/A	1,282	6177,449	0,000	N/A	N/A	N/A	0,479	957,795	0,000	0,919	3653,805	0,000
Spay^4	N/A	N/A	N/A	N/A	N/A	N/A	1,047	6701,866	0,000	N/A	N/A	N/A	N/A	N/A	N/A
Briv(Ptroglodytes)	N/A	N/A	N/A	N/A	N/A	N/A	N/A	N/A	N/A	-23,780	0,007	0,933	N/A	N/A	N/A
SpD(Ppaniscus)	N/A	N/A	N/A	N/A	N/A	N/A	N/A	N/A	N/A	N/A	N/A	N/A	-22,651	0,001	0,971
Constant	-9,786	582,527	0,000	-7,964	281,336	0,000	-4,332	144,505	0,000	0,179	0,303	0,582	0,336	1,090	0,297

Models for *Pan paniscus*															
	E-Model			**0-Model**			**F-Model**			**R-Model**			**C-Model**		
	B	*Wald*	*P*	*B*	*Wald*	*P*	*B*	*Wald*	*P*	*B*	*Wald*	*P*	*B*	*Wald*	*P*
Bio12	0,006	236,349	0,000	-0,007	98,559	0,000	-0,006	105,035	0,000	-0,006	104,417	0,000	-0,006	106,544	0,000
Bio13	-0,031	220,779	0,000	-	-	-	-	-	-	0,011	7,438	0,006	0,010	6,128	0,013
Bio14	0,002	127,892	0,000	-0,013	25,527	0,000	-	-	-	-	-	-	-	-	-
Bio4	-0,011	485,376	0,000	-	-	-	-0,003	19,168	0,000	-0,006	58,965	0,000	-0,006	51,226	0,000
Bio2	-	-	-	0,282	115,246	0,000	-	-	-	-	-	-	-	-	-
Bio5	-0,022	8,863	0,003	-0,120	52,300	0,000	-	-	-	0,091	44,700	0,000	0,087	39,889	0,000
Bio6	-	-	-	0,201	81,954	0,000	-	-	-	-	-	-	-	-	-
Bio7	-0,040	53,224	0,000	-	-	-	0,016	6,462	0,011	-	-	-	-	-	-
Elev	-0,009	603,437	0,000	-0,009	127,552	0,000	-0,005	39,584	0,000	-0,006	74,072	0,000	-0,006	76,751	0,000
Shru	-12,222	54,377	0,000	-6,267	8,558	0,003	-8,532	19,516	0,000	-5,009	6,524	0,011	-4,995	6,734	0,009
Swf	1,139	10,428	0,001	1,250	12,209	0,000	0,906	8,012	0,005	0,970	6,745	0,009	1,428	15,629	0,000
Vegm	2,069	29,910	0,000	-0,993	5,127	0,024	-2,386	35,095	0,000	-1,633	14,174	0,000	-1,134	7,228	0,007
Besr	2,092	35,776	0,000	2,530	47,251	0,000	1,337	17,966	0,000	2,000	29,348	0,000	2,457	47,144	0,000
Decf	2,193	14,165	0,000	-2,724	12,495	0,000	-4,524	41,285	0,000	-4,499	34,777	0,000	-4,059	28,668	0,000
Wosa	1,702	5,136	0,023	6,152	24,455	0,000	-	-	-	2,646	5,453	0,020	3,024	7,458	0,006
Dma	0,722	255,890	0,000	-0,263	5,696	0,017	-	-	-	-	-	-	-	-	-
Slope	-0,675	111,171	0,000	-	-	-	-	-	-	-	-	-	-	-	-
Popd	-0,005	11,332	0,001	-	-	-	-	-	-	-	-	-	-	-	-
Droad	0,000	38,411	0,000	0,000	247,641	0,000	0,000	132,580	0,000	0,000	244,570	0,000	0,000	241,388	0,000
Driv	1,234	26,493	0,000	-	-	-	-	-	-	-	-	-	-	-	-
Spay^3	N/A	N/A	N/A	1,607	829,629	0,000	N/A	N/A	N/A	1,262	631,209	0,000	1,268	629,420	0,000
Spay^4	N/A	N/A	N/A	N/A	N/A	N/A	1,329	994,373	0,000	N/A	N/A	N/A	N/A	N/A	N/A
Briv(Ppaniscus)	N/A	N/A	N/A	N/A	N/A	N/A	N/A	N/A	N/A	-15,495	0,015	0,904	N/A	N/A	N/A
SpD(Ptroglodyt	N/A	N/A	N/A	N/A	N/A	N/A	N/A	N/A	N/A	N/A	N/A	N/A	-14,923	0,021	0,884
Constant	13,641	45,536	0,000	-12,758	9,018	0,003	11,639	127,184	0,000	-14,728	13,860	0,000	-13,647	11,851	0,001

Appendix 3. Independent-variable descriptions and sources of the 39 variables considered for building the environmental favourability models for wildlife (W = Wildlife) and threats (TP = poaching; TFL = forest loss; TF: TF).

Abbreviation	Description	Source	Model
Topography			
Elev	Elevation from Digital Elevation Model (DEM)	SRTM v 4.1, provided by AWF	W, TP, TFL and TF
Surf_rough	Surface roughness: Focal statistics that calculates the range of DEM values within a 5-cell rectangle	SRTM v 4.1, provided by AWF	W, TP, TFL and TF
Slope	Slope (degrees) calculated from DEM	SRTM v 4.1, provided by AWF	W, TP, TFL and TF
Ecosystem types			
Lu_agri	Agriculture and settlement, Land use/cover, dja_lulc2015 class 10	dja_lulc2015_alb.img, provided by AWF	W and TP
Lu_noforest	Non-forest, Land use/cover, dja_lulc2015 class 8	dja_lulc2015_alb.img, provided by AWF	W and TP
Lu_degfor	Degraded forest to shrub, Land use/cover, dja_lulc2015 class 5	dja_lulc2015_alb.img, provided by AWF	W and TP
Lu_secfor	Secondary forest, Land use/cover, dja_lulc2015 class 4	dja_lulc2015_alb.img, provided by AWF	W and TP
Lu_prifor	Primary forest, Land use/cover,	dja_lulc2015_alb.img, provided by AWF	W and TP

	dja_lulc2015 class 3		
Lu_wat	Water, Land use/cover, dja_lulc2015 class 1	dja_lulc2015_alb.img, provided by AWF	W, TP, TFL and TF
Climate			
BIO1	Annual Mean Temperature	WorldClim, provided by AWF	W, TP, TFL and TF
BIO2	Mean Diurnal Range (Mean of monthly (max temp - min temp))	WorldClim, provided by AWF	W, TP, TFL and TF
BIO3	Isothermality (BIO2/BIO7) (* 100)	WorldClim, provided by AWF	W, TP, TFL and TF
BIO4	Temperature Seasonality (standard deviation *100)	WorldClim, provided by AWF	W, TP, TFL and TF
BIO5	Max Temperature of Warmest Month	WorldClim, provided by AWF	W, TP, TFL and TF
BIO6	Min Temperature of Coldest Month	WorldClim, provided by AWF	W, TP, TFL and TF
BIO7	Temperature Annual Range (BIO5-BIO6)	WorldClim, provided by AWF	W, TP, TFL and TF
BIO8	Mean Temperature of Wettest Quarter	WorldClim, provided by AWF	W, TP, TFL and TF
BIO9	Mean Temperature of Driest Quarter	WorldClim, provided by AWF	W, TP, TFL and TF
BIO10	Mean Temperature of Warmest Quarter	WorldClim, provided by AWF	W, TP, TFL and TF
BIO11	Mean Temperature of Coldest Quarter	WorldClim, provided by AWF	W, TP, TFL and TF
BIO12	Annual Precipitation	WorldClim, provided by AWF	W, TP, TFL and TF
BIO13	Precipitation of Wettest Month	WorldClim, provided by AWF	W, TP, TFL and TF
BIO14	Precipitation of Driest Month	WorldClim, provided by AWF	W, TP, TFL and TF
BIO15	Precipitation Seasonality (Coefficient of Variation)	WorldClim, provided by AWF	W, TP, TFL and TF
BIO16	Precipitation of Wettest Quarter	WorldClim, provided by AWF	W, TP, TFL and TF

BIO17	Precipitation of Driest Quarter	WorldClim, provided by AWF	W, TP, TFL and TF
BIO18	Precipitation of Warmest Quarter	WorldClim, provided by AWF	W, TP, TFL and TF
BIO19	Precipitation of Coldest Quarter	WorldClim, provided by AWF	W, TP, TFL and TF
Infrastructures			
Road dist	Distance from roads calculated using ArcMap v.10.1	Open Street Maps (dja_roads_2015_2.shp), provided by AWF	W, TP, TFL and TF
Anthropogenic impact			
Loss0105	Proportion of forest loss area between 2001 and 2005	Global Forest Change (Hansen *et al.* (2013)	W and TP
Loss0609	Proportion of forest loss area between 2006 and 2009	Global Forest Change (Hansen *et al.* (2013)	W and TP
Loss1012	Proportion of forest loss area between 2010 and 2012	Global Forest Change (Hansen *et al.* (2013)	W and TP
Loss1314	Proportion of forest loss area between 2013 and 2014	Global Forest Change (Hansen *et al.* (2013)	W and TP
Fire	Active Fire observations from 2001-2014	Fire Information for Resource Management System (FIRMS) (https://firms.modaps.eosdis.nasa.gov)	W and TP
Places_dist	Distance from towns, villages, etc	Open Street Maps, provided by AWF	W, TP, TFL and TF

Dist_agri	Distance from agriculture areas, calculated using ArcMap v.10.1	dja_lulc2015_alb.img, provided by AWF	W, TP, TFL and TF
Hydrography			
Stream_dist	Distance from navigable streams.	USGS hydrosheds, provided by AWF	W, TP, TFL and TF
Soil			
Soil_pct	Soil percent sand, 0-5cm layer	Africa Soil covariates (250 m), provided by AWF	W, TP, TFL and TF
Soil_org	Soil organic carbon concentration, 0-5cm layer	Africa Soil covariates (250 m), provided by AWF	W, TP, TFL and TF
Spatial descriptors			
LA	Geographical latitude (LA) and longitude (LO) These two variables were combined following the trend surface approach (esp-logit)	-	W, TP, TFL and TF
LO		-	W, TP, TFL and TF

Appendix 4. Number of dengue case reports and vector occurrences considered in the analyses; and number of presences after point transference to a 7,774-km² hexagons grid. See source references in the maintext.

	Points		Hexagons
Dengue cases			
	Messina *et al.* (2019)	Various sources	Presences
Late 20th-century reports	3923	0	556
Early 21st-century reports	6993	4495	2027
2018 -2019 validation data set	0	3996	992
Aedes aegypti			
	Kraemer *et al.* (2015)	Various sources	Presences
Late 20th-century occurrences	3385	0	585
Early 21st-century occurrences	16739	6117	1376
Aedes albopictus			
	Kraemer *et al.* (2015)	Various sources	Presences
Late 20th-century occurrences	1886	0	477
Early 21st-century occurrences	19892	2757	1007
Sylvatic vectors			
	Various sources		Presences
Aedes niveus	29		16
Aedes luteocephalus	76		18
Aedes africanus	71		27
Aedes vittatus	74		41
Aedes polynisiensis	69		2

Appendix 5. Literature used for georeferencing the presence of sylvatic dengue vectors

Sylvatic vectors	Sources
Aedes polynesiensis	*[1][2][3][4][5][6][7][8][9][10]*
Aedes luteocephalus	*[11][12][13][14][15][16][17][18][19][20][20][21][22][23][24]*
Aedes africanus	*[25][13][26][15][16][27][19][20][22][23][24]*
Aedes vittatus	*[11][12][13][27][19][28][22][24][29]*
Aedes niveus	*[30][31][32][33][34][35][36][37][38][39][40][41][29]*

References:

1. Lardeux F, Cheffort J. Ambient temperature effects on the extrinsic incubation period of *Wuchereria bancrofti* in *Aedes polynesiensis*: Implications for filariasis transmission dynamics and distribution in French Polynesia. Med Vet Entomol. 2001;15: 167–176. doi:10.1046/j.0269-283X.2001.00305.x
2. Chambers EW, Bossin HC, Ritchie SA, Russell RC, Dobson SL. Landing response of *Aedes (Stegomyia) polynesiensis* mosquitoes to coloured targets. Med Vet Entomol. 2013;27: 332–338. doi:10.1111/j.1365-2915.2012.01065.x
3. Richard V, Paoaafaite T, Cao-Lormeau VM. Vector Competence of *Aedes aegypti* and *Aedes polynesiensis* Populations from French Polynesia for Chikungunya Virus. PLoS Negl Trop Dis. 2016;10: 1–9. doi:10.1371/journal.pntd.0004694
4. Mercer DR, Bossin H, Sang MC, O'Connor L, Dobson SL. Monitoring Temporal Abundance and Spatial Distribution of *Aedes polynesiensis* Using BG-Sentinel Traps in Neighboring Habitats on Raiatea, Society Archipelago, French Polynesia .J Med Entomol. 2012;49: 51–60. doi:10.1603/me11087
5. Bett B. Agriculture-associated diseases research at ILRI: Emerging infectious diseases. Exch Organ Behav Teach J. 2011;12: 1–4. Available: http://www.ilri.cgiar.org/handle/10568/10627
6. Hapairai LK, Sang MAC, Sinkins SP, Bossin HC. Population Studies of the Filarial Vector *Aedes polynesiensis* (Diptera: Culicidae) in Two Island Settings of French Polynesia J Med Entomol. 2013;50: 965–976. doi:10.1603/me12246
7. Russell RC, Webb CE, Davies N. *Aedes aegypti* (L.) and *Aedes polynesiensis* Marks (Diptera: Culicidae) in Moorea, French Polynesia: A Study of Adult Population Structures and Pathogen (*Wuchereria bancrofti* and *Dirofilaria immitis*) Infection Rates to Indicate Regional and Seasonal Epidemi. J Med Entomol. 2005;42: 1045–1056. doi:10.1093/jmedent/42.6.1045
8. Samarawickrema WA, Sone F, Kimura E, Self RF, Cummings FR, Paulson SG. The relative importance and distribution of *Aedes polynesiensis* and *Ae. aegypti* larval habitats in Samoa. Med Vet Entomol. 1993;7: 27–36.
9. Riviere F. Ecologie de *Aedes (Stegomyia) polynesiensis*, Marks, 1951 et transmission de la filariose de Bancroft en Polynésie. Universite de Paris-Sud Centre d'Orsay. 1988.
10. Suzuki T, Kutsuna S, Taniguchi S, Tajima S, Maeki T, Kato F, et al. Dengue virus exported from côte d'ivoire to Japan, June 2017. Emerg Infect Dis. 2017;23: 1758–1760. doi:10.3201/eid2310.171132
11. Diagne CT, Diallo D, Faye O, Ba Y, Faye O, Gaye A, et al. Potential of selected Senegalese *Aedes spp*. mosquitoes (Diptera: Culicidae) to transmit Zika virus. BMC Infect Dis. 2015;15: 2–7. doi:10.1186/s12879-015-1231-2
12. Joseph AO, Adepeju S-OI, Omosalewa OB. Distribution, abundance and diversity of mosquitoes in Akure, Ondo State, Nigeria. J Parasitol Vector Biol. 2013;5: 132–136. doi:10.5897/JPVB2013.0133
13. Diallo D, Sall AA, Buenemann M, Chen R, Faye O, Diagne CT, et al. Landscape Ecology of Sylvatic Chikungunya Virus and Mosquito Vectors in Southeastern Senegal. PLoS Negl Trop Dis. 2012;6: 1–14. doi:10.1371/journal.pntd.0001649
14. Diallo M, Thonnon J, Traore-Lamizana M, Fontenille D. Vectors of Chikungunya virus in Senegal: Current data and transmission cycles. Am J Trop Med Hyg. 1999;60: 281–286. doi:10.4269/ajtmh.1999.60.281
15. Bang YH, Bown DN, Arata AA. Ecological studies on *Aedes Africanus* (Diptera: Culicidae) and associated species in Southeastern Nigeria. J Med Entomol. 1980;17: 411–416. doi:10.1093/jmedent/17.5.411

16. Hervy JP, Legros F, Roche JC, Monteny N, Diaco B. Circulation du virus Dengue 2 dans plusieurs milieux boisés des savanes soudaniennes de la région de Bobo-Dioulasso (Burkina Faso). Cah ORSTOM Ser Ent Med Parasitol. 1984;22: 135–143.
17. Roche JC, Cordellier R, Hervy JP. Ninety-six strains of dengue 2 virus isolated from mosquitoes collected in Ivory Coast and Upper Volta. Ann Virol. 1983;134: 233–244. Available: http://www.embase.com/search/results?subaction=viewrecord&from=export&id=L13088076%5Cnhttp://sfx.hul.harvard.edu/sfx_local?sid=EMBASE&issn=02425017&id=doi:&atitle=Ninety-six+strains+of+dengue+2+virus+isolated+from+mosquitoes+collected+in+Ivory+Coast+and+U
18. Onyido A, Ezike V, Ozumba N, Nwosu E, Ikpeze O, Obiukwu M, et al. Crepuscular Man-Biting Mosquitoes Of A Tropical Zoological Garden In Enugu, South-Eastern Nigeria. Internet J Parasit Dis. 2012;4: 4–9. doi:10.5580/11a2
19. Agwu EJ, Igbinosa IB, Isaac C. Entomological assessment of yellow fever-epidemic risk indices in Benue State, Nigeria, 2010-2011. Acta Trop. 2016;161: 18–25. doi:10.1016/j.actatropica.2016.05.005
20. Ahmed UA, Sani Z. Studies of mosquitoes in Hadejia Emirate, Jigawa state, Nigeria. Book of Proceedings of the Academic Conference on Positioning Sub-Sahara Africa for Development in the new Development. 2016. pp. 1–6.
21. Bang YH, Bown DN, Onwubiko AO. Prevalence of larvae of potential yellow fever vectors in domestic water containers in south-east Nigeria. Bull World Health Organ. 1981;59: 107–114.
22. Diallo M, Ba Y, Sall AA, Diop OM, Ndione JA, Mondo M, et al. Amplification of the sylvatic cycle of dengue virus type 2, Senegal, 1999-2000: Entomologic findings and epidemiologic considerations. Emerg Infect Dis. 2003;9: 362–367. doi:10.3201/eid0903.020219
23. Anosike JC, Nwoke BEB, Okere AN, Oku EE, Asor JE, Emmy-Egbe IO, et al. Epidemiology of tree-hole breeding mosquitoes in the tropical rainforest of Imo State, South-East Nigeria. Pediatr Dev Pathol. 1998;1: 200–209. doi:10.1007/s100249900027
24. Guindo-Coulibaly N, Adja AM, Koudou BG, Konan YL, Diallo M, Koné AB, et al. Distribution and seasonal variation of *Aedes aegypti* in the health district of Abidjan (Côte d'Ivoire). Eur J Sci Res. 2010;40: 522–530.
25. Bang YH, Knudsen AB, Onwubiko AO, Bown DN. Seasonal survival of *Aedes africanus* (Diptera: Culicidae) in Nigeria. J Med Entomol. 1983;20: 128–133. doi:10.1093/jmedent/20.2.128
26. McCrae AWR, Kirya BG. Yellow fever and Zika virus epizootics and enzootics in Uganda. Trans R Soc Trop Med Hyg. 1982;76: 552–562.
27. Cordellier R, Botjchité B, Roche J-C, Monteny N. Circulation selvatique du virus dengue 2 en 1980, dans les savanes sub-soudaniennes de Côte d'Ivoire. Ent med Parasitol. 1983;21: 165–179. Available: https://core.ac.uk/download/pdf/39874081.pdf
28. Darsie F., Richard Pradhan SP, Vaidya RG. Notes on the Mosquitoes of Nepal I . New Country Records and Revised *Aedes* Keys (Diptera, Culicidae). Seta. 1991;23: 39–45.
29. Harinasuta C, Sucharit S, Deesin T, Surathin K, Vutikes S. Bancroftian filariasis in Thailand, a new endemic area. J Trop Med Pub Hlth Seas. 1970;1: 233–245.
30. Young KI, Mundis S, Widen SG, Wood TG, Tesh RB, Cardosa J, et al. Abundance and distribution of sylvatic dengue virus vectors in three different land cover types in Sarawak, Malaysian Borneo. Parasites and Vectors. 2017;10: 1–14. doi:10.1186/s13071-017-2341-z
31. Wiwatanaratanabutr I. Geographic distribution of wolbachial infections in mosquitoes from Thailand. J Invertebr Pathol. 2013;114: 337–340. doi:10.1016/j.jip.2013.04.011
32. Santiago ATA, Claveria FG. Medically important mosquitoes (Diptera: Culicidae) identified in rural Barangay Binubusan, Lian, Batangas Province, Philippines. Philipp J Sci. 2012;141: 103–109.
33. Rogozi E, Ahmad RB, Ismail Z. Distribution and species composition of mosquitoes in three malay recreational parks. Burazeri G, Kakarriqi E, editors. Albanian Med J. 2012;4: 42–55. Available: http://www.ishp.gov.al/wp-content/uploads/2012/12/revista_nr_4_2012.pdf#page=30
34. Parker OS, Chaney AH. *Liomys irroratus* (Rodentia: Heteromyidae), a new host for *Cuterebra fontinella* (Diptera: Cuterebridae). J Med Entomol. 1979;15: 573–576. doi:10.1093/jmedent/15.5-6.573
35. Harrison BA, Rattanarithikul R, Peyton EL, Mongkolpanya K. Taxonomic changes, revised occurrence records and notes on the Culicidae of Thailand and neighboring countries. Mosq Syst. 1990;22: 196–227. Available: http://oai.dtic.mil/oai/oai?verb=getRecord&metadataPrefix=html&identifier=ADA512869
36. Chen CD, Lee HL, Stella-Wong SP, Lau KW, Sofian-Azirun M. Container survey of mosquito breeding sites in a university campus in Kuala Lumpur, Malaysia. Dengue Bull. 2009;33: 187–193.

37. Azmi NNM, Saad AR. Spatial distribution and habitat characterization of aedes mosquito larvae in Dengue hotspot areas on Penang Island. The 3rd International PSU-UNS Conferences on Bioscience. 2010. pp. 134–136.
38. Gould DJ, Bailey CL, Vongpradist S. Implication of forest mosquitoes in the transmission of *Wuchereria Bancrofti* in Thailand. Mosq News. 1982;42: 560–563.
39. Darsie F. Richard J, Gregory WC, Shreedhar PP. Notes on the mosquitoes of Nepal: III. Additional New Records in 1992 (Diptera: Culicidae). Mosq Syst. 1993;25: 186–191.
40. Richard, F. Dardsie J, Pradhan PP, Riddhi VG. Notes on the Mosquitoes of Nepal: II. New Species records from 1991 collections. Mosq Syst. 1992;24: 23–28.
41. Sucharit S, Rongsriyam Y, Deesin V, Komalamisra N, Apiwathnasorn C, Surathint K. Biology of Dengue Vectors and Their Control in Thailand. Trop Med. 1993;35: 253–257.

Appendix 6. Independent predictor variables considered for disease, vector, and transmission-risk modelling. Some variables were used only in specific models: *20th century models; **refined 21st century models; ***refined 21st century vector models; ****disease models.

Factor	Code	Variable	Source
Climate	*Bio1*	Annual Mean Temperature	Chelsa (http://chelsa-climate.org)
	Bio5	Max Temperature of Warmest Month	
	Bio6	Min Temperature of Coldest Month	
	Bio7	Temperature Annual Range (Bio5-Bio6)	
	Bio12	Annual Precipitation	
	Bio15	Precipitation Seasonality (Coefficient of Variation)	
Human Concentration	*Pop_den*	Population density**	Administrative Centres & Populated Places shapefile at the Relational World Database II (RWDB2) updated in 2000 (http://www.fao.org/geonetwork)
	Dist_pop	Distance to populated places	
Infrastructures**	*Dist_road*	Distance to roads	Vector Map Level 0 at the Digital Chart of the World (DCW,http://worldmap.harvard.edu), updated in 2002
	Dist_rail	Distance to rail-roads	
Livestock***	*Buffaloes*	Density of buffaloes	FAO 2010(http://www.fao.org/livestock-systems/en/)
	Poultry	Density of poultry	
	Goats	Density of small ruminants (goats)	
	Pigs	Density of pigs	
	Sheep	Density of small ruminants (sheep)	
	Cattle	Density of cattle	
Topography	*Slope*	slope	From GTOPO30 (US Geological Survey 1996), using ArcGIS Desktop 10.3.
	Elev	Elevation	GTOPO30 (US Geological Survey 1996).
Hydrography	*Dist_riv*	Distance to rivers	Global Drainage Basin Database GDBD. Released Version 1.0: May 29, 2007 (http://www.cger.nies.go.jp/db/gdbd/gdbd_index_e.html).
Ecoregions*	*MedFWS*	Mediterranean Forest, Woodlands and Scrub	Terrestrial Ecoregions of the World: A New Map of Life on Earth: A new global map of terrestrial ecoregions provides an innovative tool for conserving biodiversity [42]
	TrosubDBF	Tropical and Subtropical Dry Broadleaf Forest	
	TempCF	Temperate Coniferous Forests	
	TempBMF	Temperate Broadleaf and Mixed Forests	
	TrosubCF	Tropical and Subtropical Coniferous Forests	
	DeXS	Deserts and Xeric Shrublands	
	Mangro	Mangroves	
	TrosubMBF	Tropical and Subtropical Moist Broadleaf Forest	
	BorFT	Boreal Forests/Taiga	
	TrosubGSS	Tropical and Subtropical Grasslands, Savannas and Shrublands	
	TempGSS	Temperate Grasslands, Savannas and Shrublands	
	FloGS	Flooded Grassland and Savannas	
	MonGS	Montane Grasslands and Shrublands	
	Tundra	Tundra	

Agriculture	*Class 11-14*	Croplands	GlobCover (GC) Land Cover version 2.3 database for 2009 [43]
	Class 20	Mosaic Cropland (50-70%) / Vegetation (grassland, shrubland, forest) (20-50%)**	
	Class 30	Mosaic Vegetation (grassland, shrubland, forest) (50-70%) / Cropland (20-50%)**	
	Equi_irrig	Percentage of area equipped for irrigation***	Global Map of Irrigation Areas (version 4.0.1) around the year 2000 (http://www.fao.org/nr/water)
Ecosystem Types**	*Class 40*	Closed to open (>15%) broadleaved evergreen and/or semi-deciduous forest (>5m)	GlobCover (GC) Land Cover version 2.3 database for 2009 [43]
	Class 50	Closed (>40%) broadleaved deciduous forest (>5m)	
	Class 60	Open (15-40%) broadleaved deciduous forest (>5m)	
	Class 70	Closed (>40%) needleleaved evergreen forest (>5m)	
	Class 90	Open (15-40%) needleleaved deciduous or evergreen forest (>5m)	
	Class 100	Closed to open (>15%) mixed broadleaved and needleleaved forest (>5m)	
	Class 110	Mosaic Forest/Shrubland (50-70%) / Grassland (20-50%)	
	Class 120	Mosaic Grassland (50-70%) / Forest/Shrubland (20-50%)	
	Class 130	Closed to open (>15%) shrubland (<5m)	
	Class 140	Closed to open (>15%) grassland	
	Class 150	Sparse (>15%) vegetation (woody vegetation, shrubs, grassland)	
	Class 160	Closed (>40%) broadleaved semi-deciduous and/or evergreen forest regularly flooded - Saline water	
	Class 170	Closed (>40%) broadleaved semi-deciduous and/or evergreen forest regularly flooded - Saline water	
	Class 180	Closed to open (>15%) vegetation (grassland, shrubland, woody vegetation) on regularly flooded or waterlogged soil - Fresh, brackish or saline water	
	Class 200	Bare areas	
	Class 220	Permanent snow and ice	
Forest loss**	*Forest loss*	Non intact forest	High-Resolution Global Maps of 21st-Century Forest Cover Change [44]
Logit equation	*Y-20th century*	20th-century-model logit equation	Linear combinations of predictor variables that form part of the logistic-regression equations
Spatial descriptors	*Fx*	Spatial trend, where "x" represents a continent	Linear combination of spatial variables derived from continental-scale trend surface analyses [45]
Primate chorotypes**	*ASx, AFy and SAz*	Chorotype species richness. *ASx*: Asian chorotype "x"; *AFy*: African chorotype "y"; *SAz*: South-American chorotype "z"	Supplementary Figs. 5-7 [46]

References:

[42] Olson DM, Dinerstein E, Wikramanayake E, Burgess ND, Powell G, Underwood E, et al. Terrestrial Ecoregions of the World: A New Map of Life on Earth: A new global map of terrestrial ecoregions provides an innovative tool for conserving biodiversity. Bioscience. 2001; 51: 933–938.

[43] Bontemps S. GLOBCOVER 2009 Products Description and Validation Report. 2011.

[44] Hansen MC. High-resolution global maps of 21st-century forest cover change. Science. 2013;342: 850–853

[45] Legendre P. Spatial autocorrelation: Trouble or New Paradigm? Ecology. 1993;74: 1659–1673

[46] Olivero J, Real R, Márquez AL. Fuzzy chorotypes as a conceptual tool to improve insight into biogeographic patterns. Syst Biol. 2011;60: 645–660. doi:10.1093/sysbio/syr026

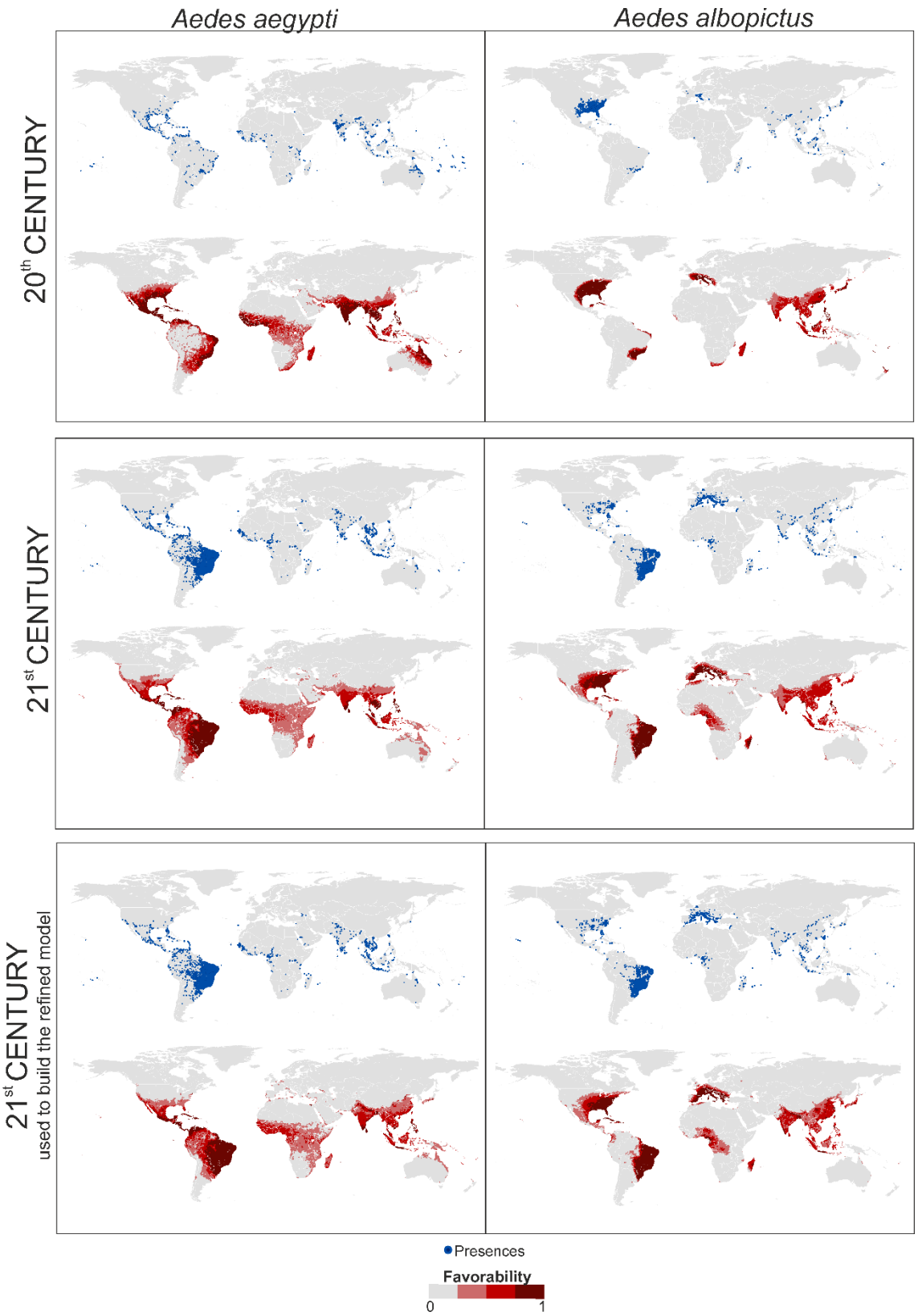

Appendix 7. Urban-vector presence records and favorability models. Coast lines source: https://developers.google.com/earth-engine/datasets/catalog/FAO_GAUL_2015_level0.

Appendix 8. Vector-model (*Aedes aegypti*) logit equations (i.e., linear combinations of predictor variables that form part of the logistic-regression equations). Variables in bold letters are mentioned in the results section of the main text. B: variable coefficient; SE: standard error; W: Wald parameter; DF: degrees of freedom; S: statistical significance. Variable codes as in Supplementary Table 3.

20th-century model					
Model goodness of fit	χ^2 = 1772.271; p<0.05				
Variable	**B**	**SE**	**W**	**DF**	**S**
Bio12	0.215×10^{-3}	0.723×10^{-4}	8.854	1	0.003
Bio5	0.568×10^{-2}	0.002	13.581	1	0.228×10^{-3}
Dist_pop	-0.483×10^{-4}	0.476×10^{-5}	103.018	1	0.332×10^{-23}
Elev	-0.342×10^{-3}	0.122×10^{-3}	7.828	1	0.005
FAmericanorth	5.103	0.233	478.237	1	0.517×10^{-105}
FAmericasouth	4.765	0.293	264.171	1	0.211×10^{-58}
FAfrica	4.230	0.284	222.491	1	0.259×10^{-49}
FAsia	3.953	0.262	228.428	1	0.131×10^{-50}
FOceania	5.543	0.310	318.722	1	0.275×10^{-70}
Constant	-6.277	0.539	135.832	1	0.217×10^{-30}
21st-century model					
Model goodness of fit	χ^2 = 5016.603; p<0.05				
Variable	**B**	**SE**	**W**	**DF**	**S**
Y-20th century	0.056	0.053	1.126	1	0.289
Dist_pop	-0.150×10^{-4}	0.339×10^{-5}	19.530	1	0.100×10^{-4}
Bio6	0.008	0.001	146.720	1	0.904×10^{-33}
Slope	0.092	0.024	14.573	1	0.135×10^{-3}
TempGSS	1.293	0.262	24.291	1	0.828×10^{-6}
TempCF	1.163	0.313	13.854	1	0.198×10^{-3}
TrosubDBF	0.636	0.154	17.078	1	0.36×10^{-4}
Fafrica	1.760	0.280	39.436	1	0.339×10^{-9}
FAsia	2.262	0.247	83.926	1	0.514×10^{-19}
FOceania	0.966	0.383	6.343	1	0.012
FAmericanorth	2.485	0.293	71.934	1	0.223×10^{-16}
FAmericasouth	6.991	0.263	706.823	1	0.982×10^{-155}
FEurope	6.334	2.431	6.789	1	0.009
Constant	-4.725	0.253	348.718	1	0.806×10^{-77}
21st-century refined model					
Model goodness of fit	χ^2 = 5227.031; p<0.05				

Variable	B	SE	W	DF	S
Y-20th century	0.096	0.048	3.949	1	0.047
Bio12	-0.207×10^{-3}	0.65×10^{-4}	10.235	1	0.001
Bio6	0.010	0.001	137.132	1	0.113×10^{-30}
Class 110	-2.715	0.922	8.678	1	0.003
Class 150	-2.273	0.994	5.228	1	0.022
Class 160	-2.690	0.886	9.211	1	0.002
Class 200	-1.483	0.389	14.538	1	0.137×10^{-3}
Class 50	-1.271	0.404	9.899	1	0.002
Class 70	1.336	0.573	5.442	1	0.020
Dist_pop	-0.1×10^{-4}	0.315×10^{-5}	10.161	1	0.001
Equi_irrig	0.015	0.005	9.578	1	0.002
Pop_den	0.001	0.158×10^{-3}	69.113	1	0.929×10^{-16}
Poultry	0.72×10^{-4}	0.627×10^{-4}	8.694	1	0.003
Sheep	-0.008	0.003	6.286	1	0.012
Slope	0.111	0.026	18.056	1	0.214×10^{-4}
FAfrica	1.071	0.241	19.747	1	0.884×10^{-5}
FAsia	1.016	0.209	23.579	1	0.112×10^{-5}
FAmericanorth	1.838	0.251	53.673	1	0.237×10^{-12}
FAmericasouth	6.222	0.223	780.911	1	0.763×10^{-171}
FEurope	6.601	2.613	6.380	1	0.012
Constant	-4.034	0.248	263.853	1	0.248×10^{-58}

Appendix 9. Vector-model (*Aedes albopictus*) logit equations (i.e., linear combinations of predictor variables that form part of the logistic-regression equations). Variables in bold letters are mentioned in the results section of the main text. B: variable coefficient; SE: standard error; W: Wald parameter; DF: degrees of freedom; S: statistical significance. Variable codes as in Supplementary Table 3.

20th-century model					
Model goodness of fit	χ^2 =2714.105; p<0.05				
Variable	**B**	**SE**	**W**	**DF**	**S**
Bio12	0.001	0.117×10^{-3}	20.335	1	0.650×10^{-5}
Bio7	0.003	0.001	8.958	1	0.276×10^{-2}
Dist_pop	-0.334×10^{-4}	0.653×10^{-5}	26.154	1	0.315×10^{-6}
Elev	-0.001	0.220×10^{-3}	13.598	1	0.226×10^{-3}
TempCF	1.242	0.378	10.801	1	0.001
FAmericanorth	8.533	0.371	529.728	1	0.324×10^{-116}
FAmericasouth	6.204	0.451	189.334	1	0.444×10^{-42}
FEurope	6.186	0.442	195.751	1	0.176×10^{-43}
FAfrica	5.366	0.533	101.278	1	0.799×10^{-23}
FAsia	5.429	0.458	140.438	1	0.213×10^{-31}
FOceania	6.235	0.538	134.205	1	0.493×10^{-30}
Constant	-7.590	0.479	250.819	1	0.172×10^{-56}
21st-century model					
Model goodness of fit	χ^2 = 4356.324; p<0.05				
Variable	**B**	**SE**	**W**	**DF**	**S**
Y-20th century	0.140	0.029	22.978	1	0.164×10^{-5}
Dist_pop	-0.242×10^{-4}	0.351×10^{-5}	47.670	1	0.504×10^{-11}
Bio15	0.010	0.002	26.120	1	0.321×10^{-6}
Bio12	0.208×10^{-3}	0.946×10^{-4}	4.849	1	0.028
Bio7	-0.003	0.001	8.259	1	0.004
MedFWS	1.807	0.269	45.225	1	0.176×10^{-10}
TempBMF	1.100	0.204	29.149	1	0.673×10^{-7}
TempGSS	1.175	0.280	17.566	1	0.278×10^{-5}
TrosubMBF	0.848	0.168	25.577	1	0.425×10^{-7}
FAfrica	3.225	0.282	130.421	1	0.332×10^{-29}
FAsia	2.785	0.303	84.235	1	0.439×10^{-19}
FOceania	2.168	0.506	18.350	1	0.184×10^{-4}
FAmericanorth	4.372	0.358	148.809	1	0.316×10^{-33}
FAmericasouth	7.702	0.248	962.278	1	0.284×10^{-210}

FEurope	5.198	0.321	261.777	1	$0.703x10^{-58}$
Constant	-4.843	0.416	135.328	1	$0.280x10^{-30}$
21st-century refined model					
Model goodness of fit	$\chi^2 = 4520.879$; $p<0.05$				
Variable	**B**	**SE**	**W**	**DF**	**S**
Y-20th century	0.089	0.029	9.124	1	0.003
Bio15	0.009	0.002	20.732	1	$0.528x10^{-5}$
Bio12	$0.341x10^{-3}$	$0.909x10^{-4}$	14.081	1	$0.175x10^{-3}$
Class 130	-1.526	0.413	13.672	1	$0.218x10^{-3}$
Class 200	-7.853	2.891	7.382	1	0.007
Class 40	1.118	0.275	16.548	1	$0.474x10^{-4}$
Dist_rail	$-0.108x10^{-5}$	$0.465x10^{-6}$	5.387	1	$0.203x10^{-1}$
Dist_road	$-0.406x10^{-5}$	$0.169x10^{-5}$	5.743	1	$0.166x10^{-1}$
Dist_pop	$-0.135x10^{-4}$	$0.359x10^{-5}$	14.144	1	$0.169x10^{-3}$
Pop_den	0.002	$0.163x10^{-3}$	107.589	1	$0.331x10^{-24}$
Pigs	0.002	0.001	4.435	1	0.035
FAfrica	3.219	0.281	131.037	1	$0.243x10^{-29}$
FAsia	2.350	0.325	52.336	1	0.468x10-12
FOceania	3.215	0.569	31.875	1	$0.164x10^{-7}$
FAmericanorth	4.532	0.360	158.799	1	$0.207x10^{-35}$
FAmericasouth	7.891	0.251	985.359	1	$0.273x10^{-215}$
FEurope	6.099	0.291	440.676	1	$0.771x10^{-97}$
Constant	-5.497	0.339	263.690	1	$0.268x10^{-58}$

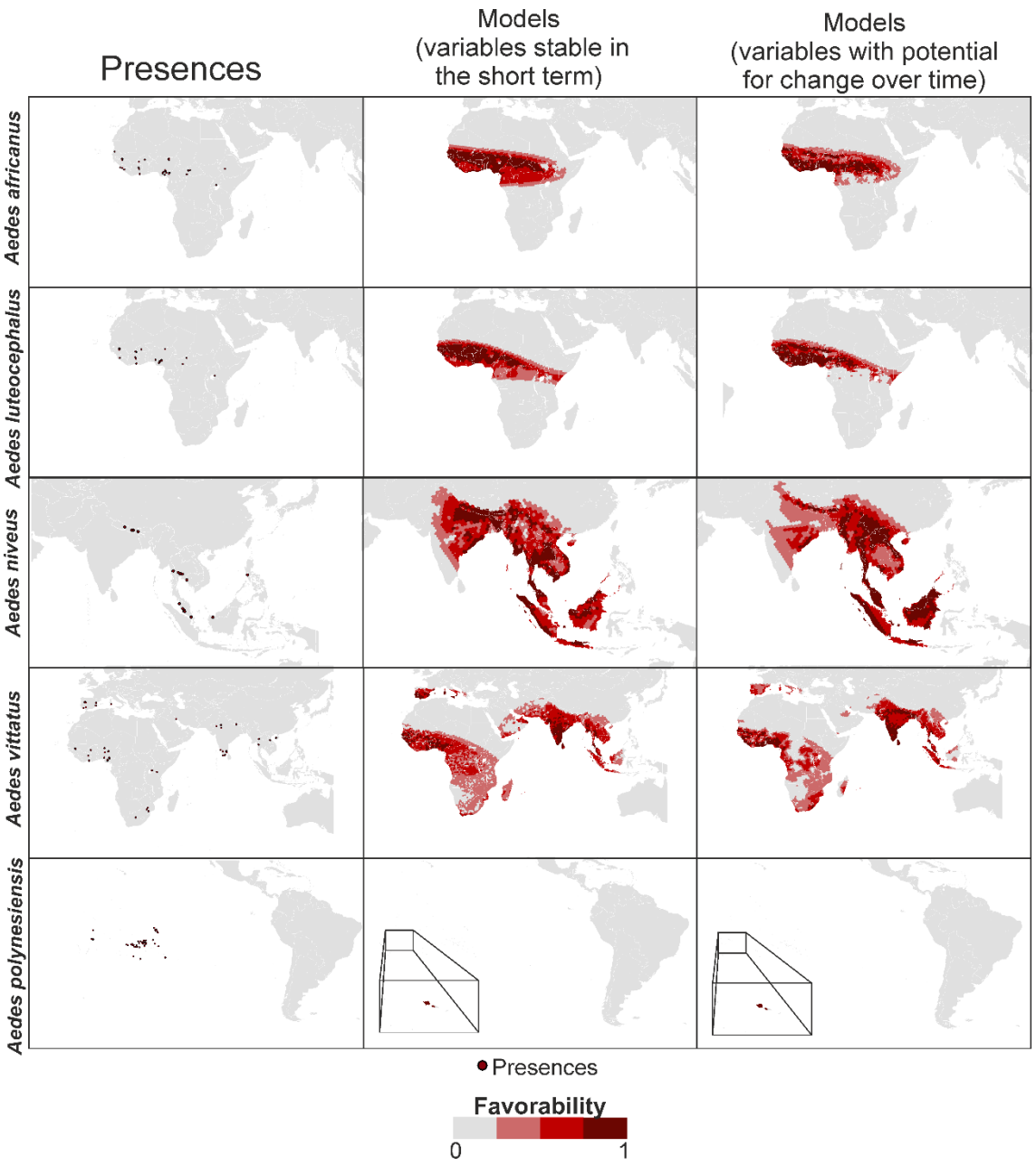

Appendix 10. Sylvatic-vector presence records and favorability models. Models with temporally stable variables in the short term were used for building models shown in main text Fig 2. Models with variables subject to potential change over time in the short term were used for building models shown in main text Fig 3. Coast lines source: https://developers.google.com/earth-engine/datasets/catalog/FAO_GAUL_2015_level0.

Appendix 11. Sylvatic-vector-model logit equations (i.e., linear combinations of predictor variables that form part of the logistic-regression equations). The *Aedes polynesiensis* model was only based on the spatial factor. For the rest of species, an environmental model and a spatial model were intersected. These decisions responded to the geographically restricted character of these species distributions. Variables in bold letters are mentioned in the results section of the main text. B: variable coefficient; SE: standard error; W: Wald parameter; DF: degrees of freedom; S: statistical significance. Variable codes as in Supplementary Table 3.

Aedes africanus					
Model goodness of fit	χ^2 =78.913; p<0.05				
Variable	**B**	**SE**	**W**	**DF**	**S**
TrosubGSS	3.921	1.581	6.149	1	0.013
Bio6	0.019	0.007	8.364	1	0.004
TrosubMBF	3.593	1.709	4.42	1	0.036
Bio15	0.017	0.007	6.285	1	0.012
Mangro	4.342	2.368	3.363	1	0.067
Constant	-13.889	2.192	40.148	1	$0.235X10^{-9}$
Aedes luteocephalus					
Model goodness of fit	χ^2 = 60.025; p<0.05				
Variable	**B**	**SE**	**W**	**DF**	**S**
Bio6	0.032	0.009	13.419	1	$0.249X10^{-3}$
TrosubGSS	1.763	0.607	8.43	1	0.004
Bio5	0.014	0.007	3.787	1	0.052
Constant	-17.481	3.542	24.351	1	$0.803X10^{-6}$
Aedes niveus					
Model goodness of fit	χ^2 = 47.551; p<0.05				
Variable	**B**	**SE**	**W**	**DF**	**S**
Bio6	0.011	0.004	6.228	1	0.013
Slope	0.438	0.103	18.231	1	$0.2X10^{-4}$
TrosubMBF	1.568	0.773	4.116	1	0.042
Constant	-10.039	0.892	126.606	1	$0.227X10^{-28}$
Aedes vittatus					
Model goodness of fit	χ^2 = 91.570; p<0.05				
Variable	**B**	**SE**	**W**	**DF**	**S**
Bio6	0.009	0.002	15.015	1	$0.107X10^{-3}$
Bio5	0.014	0.003	15.855	1	$0.68X10^{-4}$
Dist_pop	$-0.58X10^{-4}$	$0.15X10^{-4}$	15.095	1	$0.102X10^{-3}$

MedFWS	2.089	0.561	13.852	1	$0.198X10^{-3}$
Constant	-9.991	1.283	60.658	1	$0.679X10^{-14}$
Aedes polynesiensis					
Model goodness of fit	χ^2 = 30.295; p<0.05				
Variable	**B**	**SE**	**W**	**DF**	**S**
Lat	-0.842	48.929	$0.296X10^{-3}$	1.000	0.986
Long	-0.175	8.291	$0.447X10^{-3}$	1.000	0.983
Constant	-26.676	1143.681	0.001	1.000	0.981

Appendix 12. Sylvatic-vector refined-model logit equations (i.e., linear combinations of predictor variables that form part of the logistic-regression equations). The *Aedes polynesiensis* model was only based on the spatial factor. For the rest of species, an environmental model and a spatial model were intersected. These decisions responded to the geographically restricted character of these species distributions. Variables in bold letters are mentioned in the results section of the main text. B: variable coefficient; SE: standard error; W: Wald parameter; DF: degrees of freedom; S: statistical significance. Variable codes as in Supplementary Table 3.

Aedes africanus					
Model goodness of fit	χ^2 = 130.737 ; p<0.05				
Variable	**B**	**SE**	**W**	**DF**	**S**
Bio15	0.024	0.006	14.666	1	$0.128X10^{-3}$
Bio12	0.001	$0.249X10^{-3}$	8.88	1	0.003
Bio6	0.024	0.006	13.762	1	$0.207X10^{-3}$
Class 130	2.731	1.19	5.266	1	0.022
Class 30	5.707	0.898	40.344	1	$0.213X10^{-9}$
Class 60	6.077	1.053	33.303	1	$0.789X10^{-8}$
Pop_den	0.001	$0.337X10^{-3}$	3.035	1	0.081
Goats	0.012	0.004	8.971	1	0.003
Sheep	0.016	0.004	13.398	1	$0.252X10^{-3}$
Constant	-15.508	1.751	78.463	1	$0.815X10^{-18}$
Aedes luteocephalus					
Model goodness of fit	χ^2 = 105.707; p<0.05				
Variable	**B**	**SE**	**W**	**DF**	**S**
Bio6	0.035	0.010	12.199	1	$0.478X10^{-3}$
Bio5	0.031	0.009	12.264	1	$0.462X10^{-3}$
Class 130	3.806	1.355	7.889	1	0.005
Class 30	6.752	1.236	29.838	1	$0.470X10^{-7}$
Class 60	6.486	1.299	24.931	1	$0.594X10^{-6}$
Goats	0.017	0.004	20.117	1	$0.7X10^{-5}$
Pop_den	0.001	$0.362X10^{-3}$	7.270	1	0.007
Constant	-25.799	4.553	32.113	1	$0.145X10^{-7}$
Aedes niveus					
Model goodness of fit	χ^2 = 88.027; p<0.05				
Variable	**B**	**SE**	**W**	**DF**	**S**
Bio12	0.001	$0.259X10^{-3}$	7.818	1	0.005
Bio6	0.017	0.004	14.87	1	$0.115X10^{-3}$
Class 11-14	4.736	1.483	10.204	1	0.001
Equi_irrig	0.054	0.019	8.377	1	0.004

Slope	0.687	0.128	28.791	1	$0.806X10^{-7}$
Constant	-13.729	1.485	85.494	1	$0.232X10^{-19}$
Aedes vittatus					
Model goodness of fit	$\chi^2 = 122.41$; $p<0.05$				
Variable	**B**	**SE**	**W**	**DF**	**S**
Bio6	0.012	0.002	28.833	1	$0.789X10^{-7}$
Buffaloes	0.021	0.006	12.646	1	$0.376X10^{-3}$
Class 130	2.513	0.754	11.117	1	0.001
Class 30	2.428	0.815	8.864	1	0.003
Dist_rail	$-0.13X10^{-4}$	$0.4X10^{-5}$	12.845	1	$0.338X10^{-3}$
Goats	0.007	0.003	7.229	1	0.007
Sheep	0.008	0.003	7.472	1	0.006
Constant	-7.24	0.465	242.182	1	$0.131X10^{-53}$
Aedes polynesiensis					
Model goodness of fit	$\chi^2 = 30.295$; $p<0.05$				
Variable	**B**	**SE**	**W**	**DF**	**S**
Lat	-0.842	48.929	$0.296X10^{-3}$	1	0.986
Long	-0.175	8.291	$0.447X10^{-3}$	1	0.983
Constant	-26.676	1143.681	0.001	1	0.981

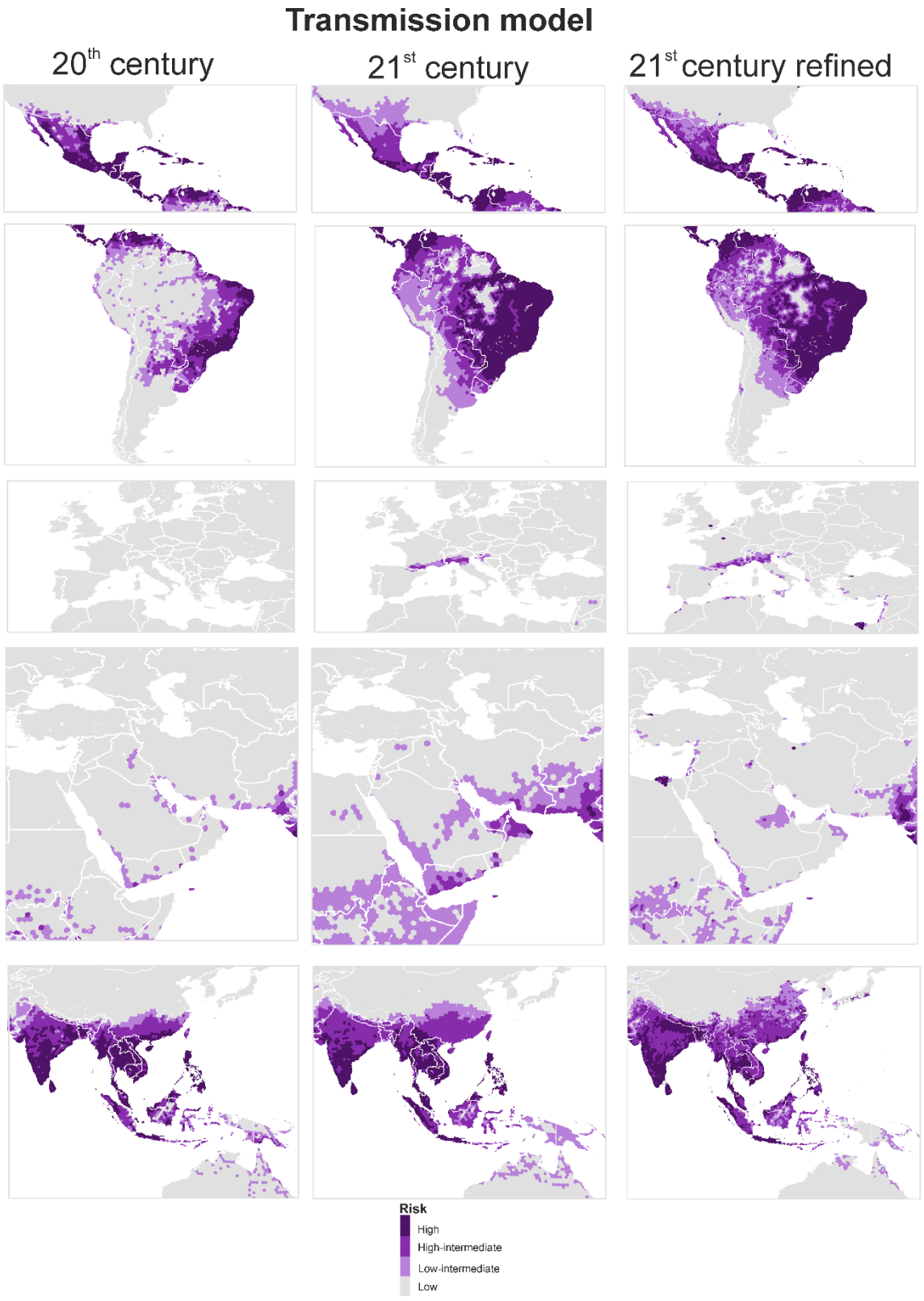

Appendix 13. **Zoomed details of dengue transmission-risk models shown in main text Fig 2 (late 20th and 21st century) and 3 (early 21st century refined)**. Coast lines source: https://developers.google.com/earth-engine/datasets/catalog/FAO_GAUL_2015_level0.

Appendix 14. Disease-model logit equations (i.e., linear combinations of predictor variables that form part of the logistic-regression equations). Variables in bold letters are mentioned in the results section of the main text. B: variable coefficient; SE: standard error; W: Wald parameter; DF: degrees of freedom; S: statistical significance. Variable codes as in Appendix 6.

20th-century model					
Model goodness of fit	χ^2 = 2133.082; p<0.05				
Variable	**B**	**SE**	**W**	**DF**	**S**
Bio6	0.001	0.001	0.238	1	0.626
Dist_pop	-0.828×10^{-4}	5.73×10^{-5}	209.014	1	0.225×10^{-46}
Elev	-0.001	1.66×10^{-3}	32.365	1	0.128×10^{-7}
FAmerica	4.157	0.453	84.376	1	0.409×10^{-19}
FAfrica	2.363	0.452	27.283	1	0.176×10^{-6}
FAsia-Oceania	3.372	0.382	78.125	1	0.967×10^{-18}
DeXS	2.920	0.605	23.262	1	0.141×10^{-5}
Mangro	3.229	0.817	15.608	1	0.779×10^{-4}
MonGS	3.141	1.209	6.757	1	0.009
TrosubGSS	2.950	0.613	23.196	1	0.146×10^{-5}
TrosubCF	4.381	0.779	31.594	1	0.190×10^{-7}
TrosubMBF	3.065	0.609	25.301	1	0.491×10^{-6}
TrosubDBF	3.580	0.620	33.339	1	0.774×10^{-8}
SA4	0.268	0.073	13.409	1	0.250×10^{-3}
SA5	0.279	0.093	9.018	1	0.003
SA14	0.519	0.227	5.225	1	0.022
AS8	0.430	0.112	14.723	1	0.125×10^{-3}
AS15	0.570	0.135	17.896	1	0.233×10^{-4}
Constant	-5.668	0.545	107.989	1	0.270×10^{-24}
21st-century model					
Model goodness of fit	χ^2 = 6443.0004; p<0.05				
Variable	**B**	**SE**	**W**	**DF**	**S**
Y-20th century	0.466	0.021	501.666	1	0.413×10^{-110}
Bio15	0.005	0.001	13.397	1	0.252×10^{-3}
Bio12	-0.276×10^{-3}	0.571×10^{-4}	23.468	1	0.127×10^{-5}
Bio5	0.008	0.001	41.104	1	0.144×10^{-9}
Bio7	-0.004	0.001	22.930	1	0.168×10^{-5}
Slope	0.188	0.023	66.532	1	0.344×10^{-15}
DeXS	-0.259	0.126	4.211	1	0.040
MedFWS	-1.690	0.777	4.728	1	0.030
TempGSS	1.363	0.270	25.479	1	0.447×10^{-6}
FAmerica	3.591	0.239	226.400	1	0.363×10^{-50}

FAfrica	0.500	0.305	2.688	1	0.101
FEurope	4.346	0.737	34.770	1	0.371×10^{-8}
FAsia-Oceania	1.853	0.247	56.112	1	0.685×10^{-13}
SA2	0.295	0.083	12.514	1	0.404×10^{-3}
SA4	0.631	0.105	36.019	1	0.195×10^{-8}
AF2	0.112	0.035	10.125	1	0.001
AS5	0.748	0.138	29.352	1	0.603×10^{-7}
AS7	0.255	0.070	13.246	1	0.273×10^{-3}
AS8	0.352	0.135	6.818	1	0.009
AS9	0.430	0.100	18.342	1	0.185×10^{-4}
AS15	0.681	0.223	9.298	1	0.002
AS19	2.134	0.616	11.994	1	0.001
Constant	-3.332	0.396	70.638	1	0.429×10^{-16}
21st-century refined model					
Model goodness of fit	χ^2 = 6932.184; p<0.05				
Variable	**B**	**SE**	**W**	**DF**	**S**
Y-20th century	0.339	0.021	257.529	1	0.593×10^{-57}
Bio12	-0.240×10^{-3}	0.520×10^{-4}	21.235	1	0.406×10^{-5}
Bio5	0.005	0.001	20.916	1	0.408×10^{-5}
Bio6	0.007	0.001	83.845	1	0.535×10^{-19}
Class 11-14	1.924	0.203	89.857	1	0.256×10^{-20}
Class 150	-1.674	0.766	4.781	1	0.029
Class 220	5.099	1.387	13.523	1	0.236×10^{-3}
Class 60	-5.482	1.111	24.349	1	0.804×10^{-6}
Class 70	-1.247	0.502	6.169	1	0.013
Dist_rail	-0.167×10^{-5}	1.83×10^{-6}	83.486	1	0.642×10^{-19}
Pop_den	0.002	1.62×10^{-3}	116.075	1	0.458×10^{-26}
Slope	0.318	0.024	168.400	1	0.165×10^{-37}
FAmerica	3.888	0.251	240.155	1	0.364×10^{-53}
FAfrica	1.072	0.303	12.530	1	0.401×10^{-3}
FEurope	2.453	0.666	13.562	1	0.231×10^{-3}
FAsia-Oceania	1.777	0.240	54.843	1	0.131×10^{-12}
SA2	0.381	0.080	22.737	1	0.186×10^{-5}
SA4	0.496	0.102	23.505	1	0.125×10^{-5}
AF2	0.111	0.035	9.867	1	0.002
AS8	0.388	0.133	8.483	1	0.004
AS19	1.430	0.618	5.349	1	0.021
Constant	-4.537	0.415	119.611	1	0.770×10^{-27}

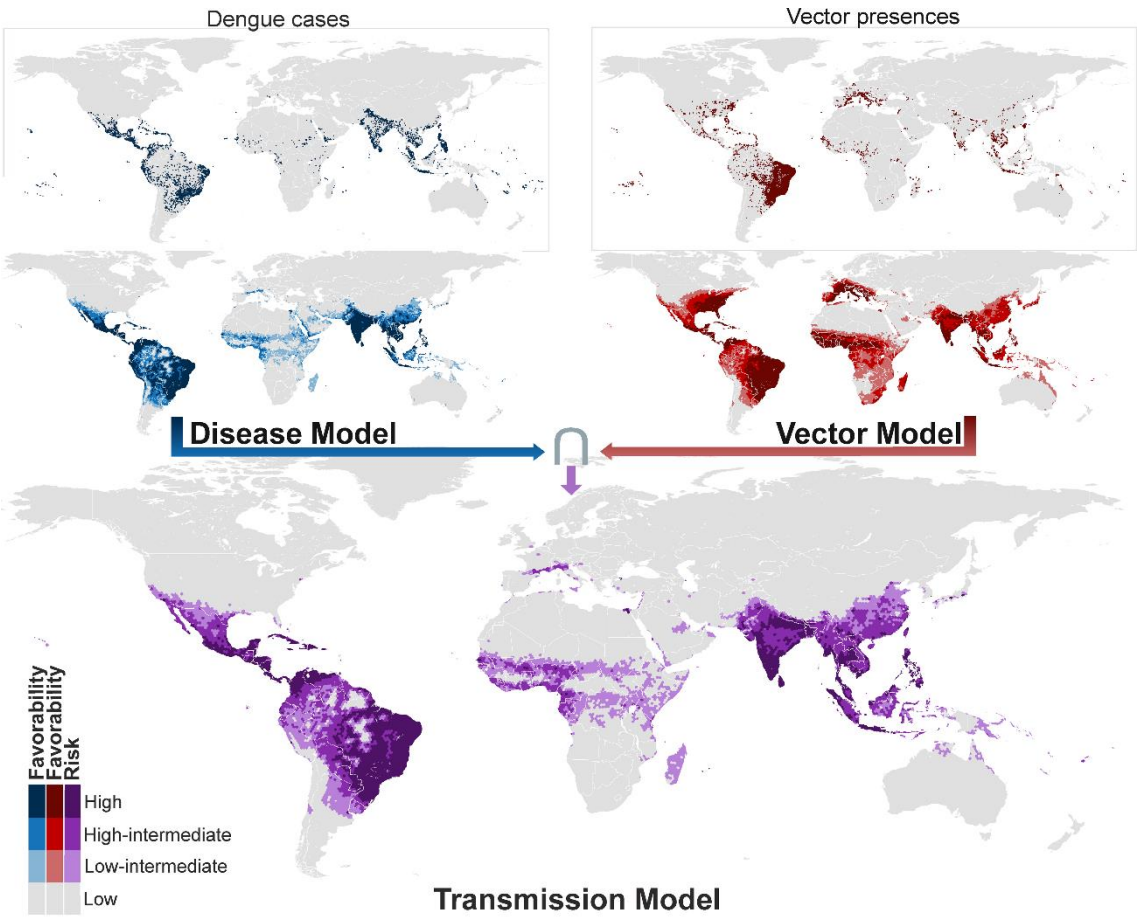

Appendix 15. Pre-downscaling refined global disease, vector, and transmission-risk models for the early 21st century. The risk of transmission is estimated as the intersection (∩) between favorable conditions for the occurrence of dengue cases and favorable conditions for the presence of vector species. Coast lines source: https://developers.google.com/earth-engine/datasets/catalog/FAO_GAUL_2015_level0.

Appendix 16. Percentage of increase in values of the model predictive-capacity assessment (i.e., discrimination and classification performance with respect to disease records of a later period) compared to the descriptive-capacity assessment (i.e., discrimination and classification performance with respect to disease records of the same period). AUC: area under the receiver operator characteristic curve; FCT: favorability classification threshold; Kappa: Cohen's kappa; Sens.: sensitivity; Spec.: specificity; CCR: correct classification rate; Underp.: underprediction rate; Overp.: overprediction rate.

	MODEL	Records of reference	AUC	FTC	Kappa	Sens.	Spec.	CCR	Underp.	Overp.
20th century	Disease	1970 to 2017	-1.0	0.5	58.1	-14.9	6.0	4.3	86.9	-72.4
				0.2	64.6	-8.7	7.1	7.1	91.3	-46.0
	Transmission risk		-1.3	0.5	529	-21.5	5.0	2.3	84.9	-75.1
				0.2	61.8	-12.7	6.3	5.5	88.6	-48.0
	Disease	2001 to 2017	-1.2	0.5	56.6	-14.4	5.5	4.0	85.8	-62.9
				0.2	62.8	-8.6	6.5	6.6	90.8	-40.6
	Transmission risk		-1.4	0.5	51.1	-21.2	4.6	2.0	83.9	-64.5
				0.2	60.1	-12.5	5.8	5.1	87.7	-42.3
21st century	Disease	2001 to 2019	0.0	0.5	5.5	-0.5	0.8	0.7	12.1	-6.5
				0.2	6.9	-0.2	1.0	1.1	14.9	-3.7
	Transmission risk		0.0	0.5	4.3	-1.2	0.7	0.4	12.6	-6.7
				0.2	6.6	-0.3	0.9	1.0	14.5	-3.9
	Disease	2018 and 2019	-1.5	0.5	-74.9	3.1	-5.2	-5.0	-190.0	27.7
				0.2	-93.2	0.7	-5.9	-7.4	-208.0	18.1
	Transmission risk		-2.6	0.5	-74.7	1.0	-4.8	-4.1	-114.0	30.8
				0.2	-89.9	1.3	-5.7	-6.9	-223.0	18.9
21st century (refined)	Disease	2001 to 2019	0.1	0.5	5.4	-0.6	0.8	0.7	12.5	-6.8
				0.2	6.7	-0.2	1.0	1.0	17.0	-4.1
	Transmission risk		0.0	0.5	3.5	-1.8	0.6	0.3	15.1	-6.4
				0.2	6.1	-0.5	0.9	0.9	16.4	-4.4
	Disease	2018 and 2019	-1.2	0.5	-71.7	4.2	-5.1	-4.8	-243.9	28.4
				0.2	-91.3	0.8	-5.9	-7.2	-254.6	19.4
	Transmission risk		-2.2	0.5	-75.8	0.4	-4.9	-4.2	-108.5	31.7
				0.2	-86.8	1.5	-5.7	-6.4	-196.8	21.1

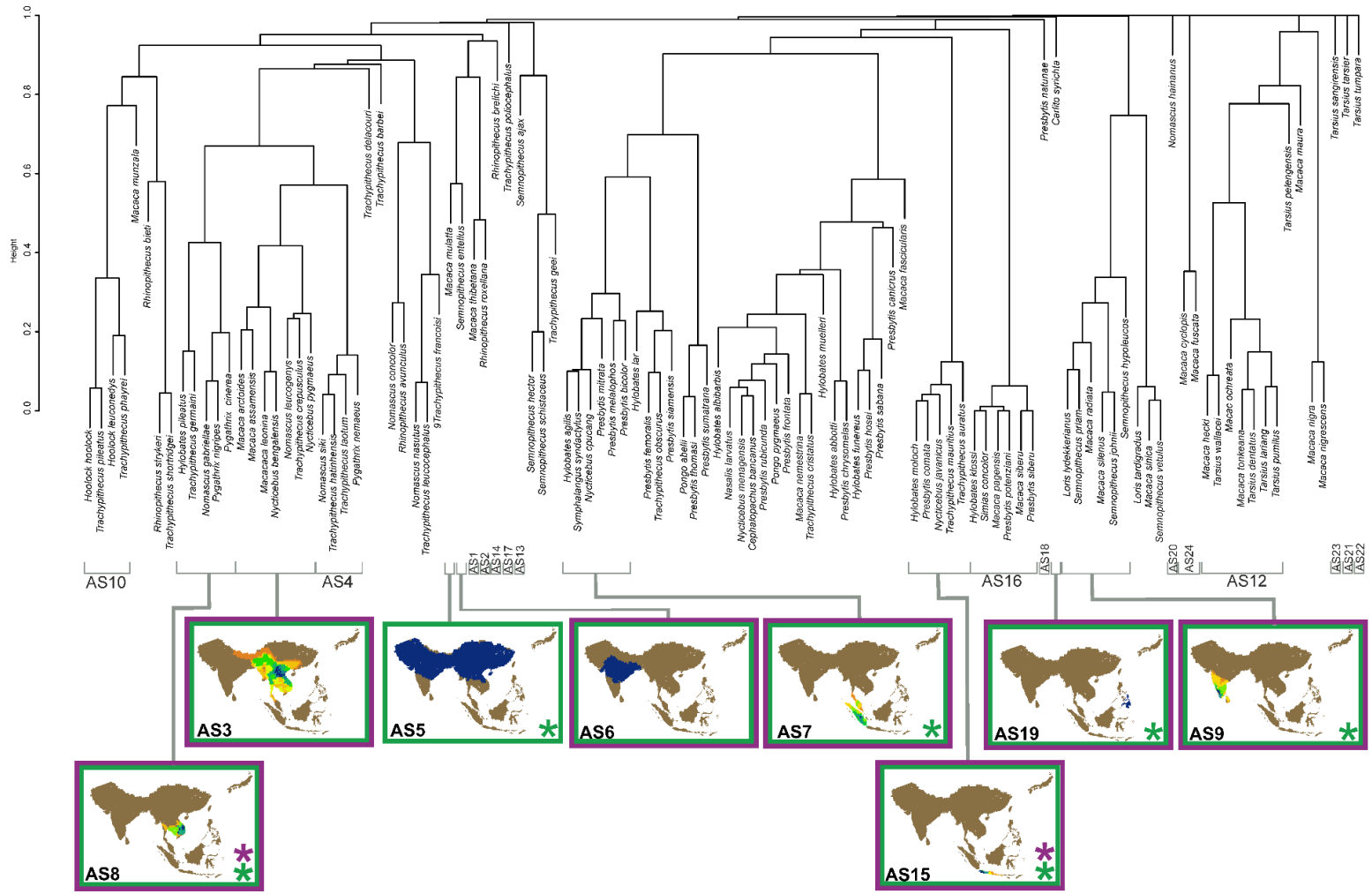

Appendix 17. Classification dendrograms of primate distributions in Asia. Violet rectangles: chorotypes significantly related to the distribution of the late 20th-century dengue cases according to a forward-stepwise logistic regression. Green rectangles: chorotypes significantly related only to the distribution of the 21st-century cases. Chorotypes that were finally included in disease models are highlighted with a violet asterisk for the late 20th century, and with a green asterisk for the 21st century. Asian chorotype names are coded as AS1 to AS24. Coast lines source: https://developers.google.com/earth-engine/datasets/catalog/FAO_GAUL_2015_level0.

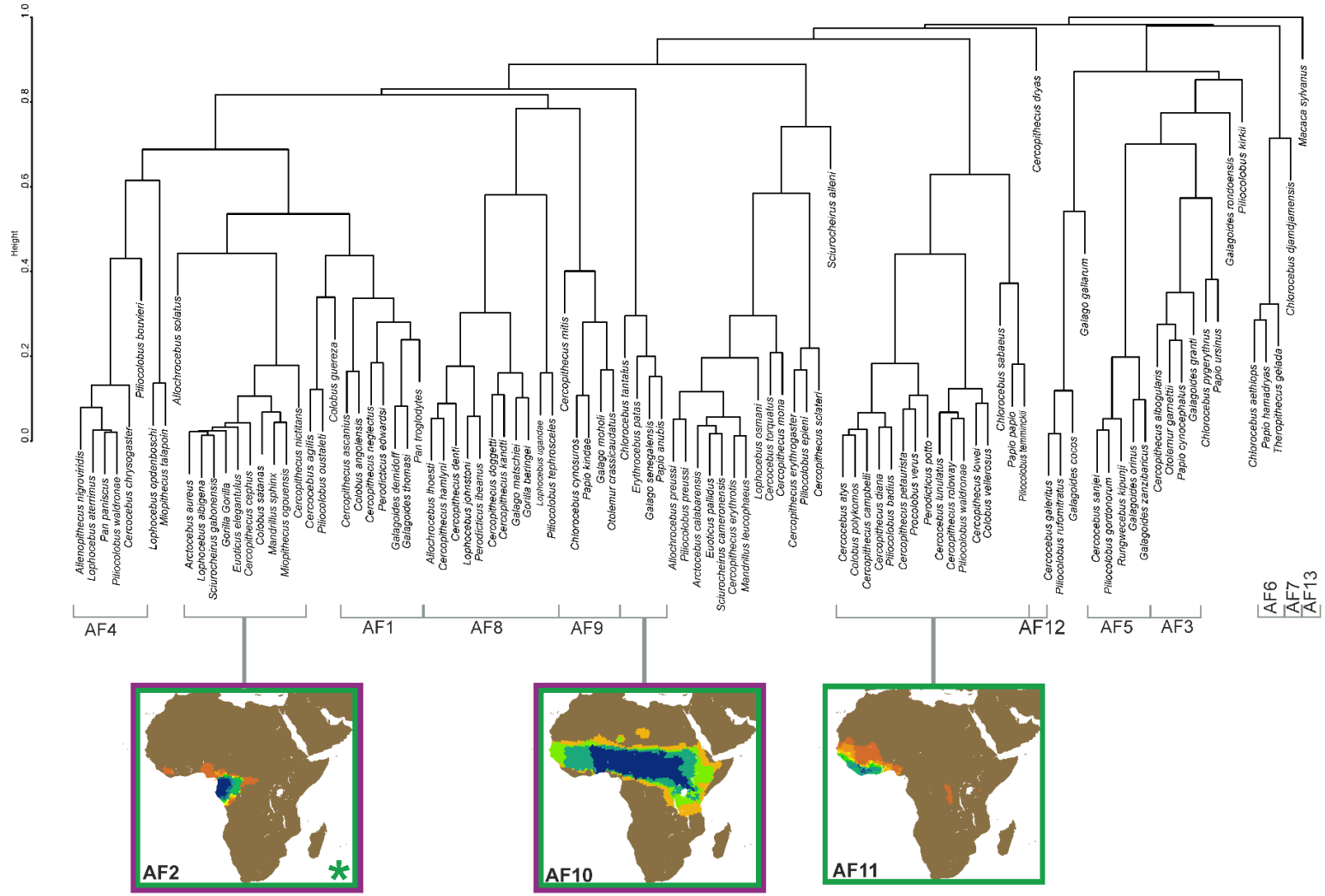

Appendix 18. Classification dendrograms of primate distributions in Africa. Violet rectangles: chorotypes significantly related to the distribution of the late 20th-century dengue cases according to a forward-stepwise logistic regression. Green rectangles: chorotypes significantly related only to the distribution of the 21st-century cases. Chorotypes that were finally included in disease models are highlighted with a violet asterisk for the late 20th century, and with a green asterisk for the 21st century. African chorotype names are coded as AF1 to AF13. Coast lines source: https://developers.google.com/earth-engine/datasets/catalog/FAO_GAUL_2015_level0.

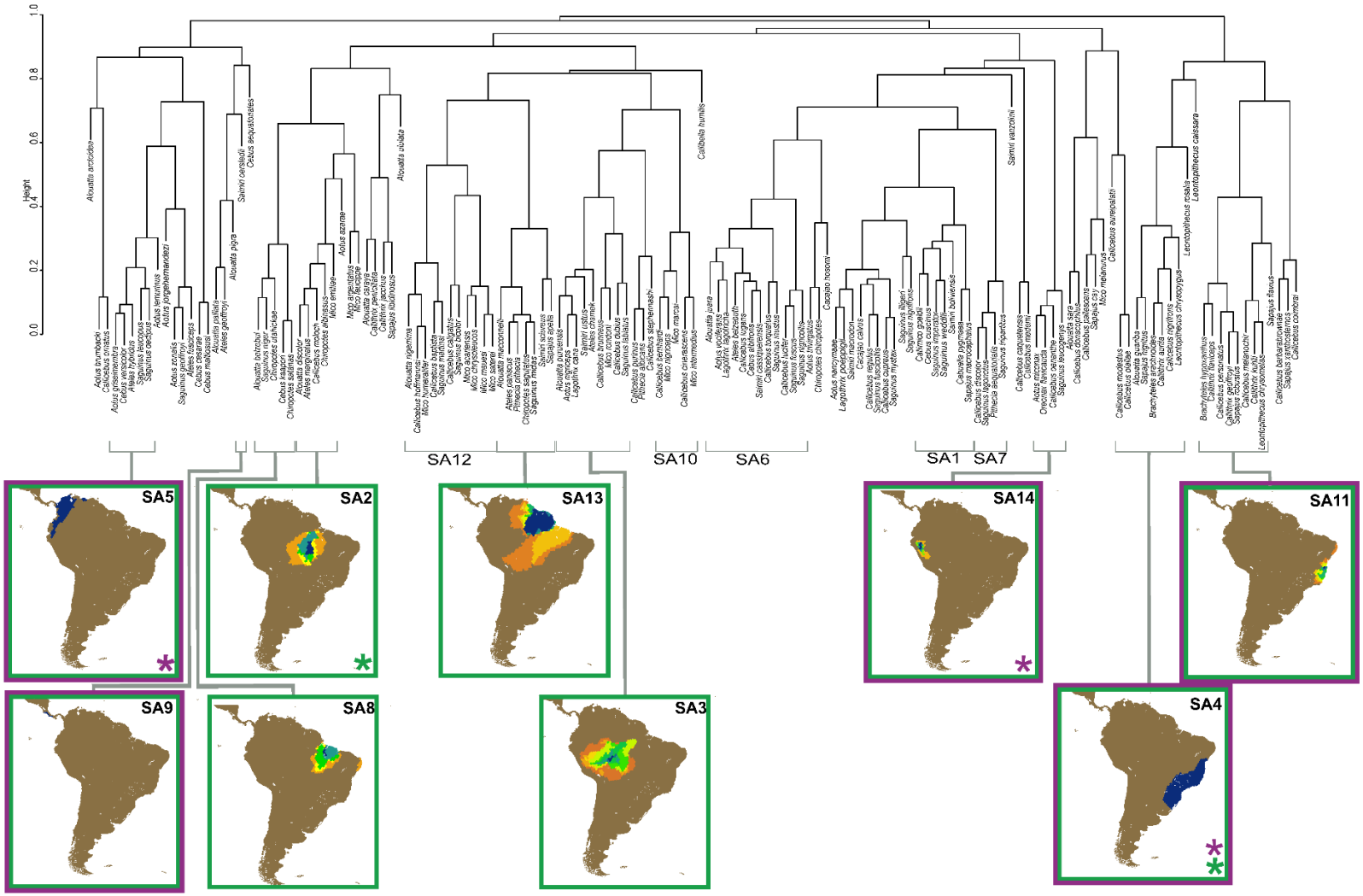

Appendix 19. Classification dendrograms of primate distributions in America. Violet rectangles: chorotypes significantly related to the distribution of the late 20th-century dengue cases according to a forward-stepwise logistic regression. Green rectangles: chorotypes significantly related only to the distribution of the 21st-century cases. Chorotypes that were finally included in disease models are highlighted with a violet asterisk for the late 20th century, and with a green asterisk for the 21st century. American chorotype names are coded as SA1 to SA14. Coast lines source: https://developers.google.com/earth-engine/datasets/catalog/FAO_GAUL_2015_level0.

Appendix 20. Supplementary methods

Methodological explanations for the variables and outputs shown in Fig. 4 of the main text. These variables and outputs are related to the following sections through letter codes (A – F).

A. Independent variables: Environment

1. Preselection of environmental variables potentially influencing the distribution of the item to be modelled (i.e., a mosquito species, yellow fever cases). Variable sources and descriptions are shown in Supplementary Table 3.

B. Independent variables: Space

1. Selection of the geographic context: A spatial independent variable was made for each continent (*x*).
2. Logistic regression: It provides a probability value (P_x), based on spatial descriptors, of the analysed item to occur in each hexagon:
   a. Dependent variable: Presences (1) and absences (0) of the item to be modelled.
   b. Initial independent variables: Spatial descriptors consisting on polynomial combinations of longitude (X) and latitude (Y) up to the third degree: X, Y, XY, X^2, Y^2, X^2Y, XY^2, X^3, and Y^3.
   c. Selection of independent variables: Conditional backward-stepwise procedure.
   d. Estimation of variable coefficients: machine-learning iterative process based on the maximum log-likelihood criterion.
   e. Model evaluation: Hosmer & Lemeshow's goodness of fit.

SPSS syntax for the logistic regression

```
LOGISTIC REGRESSION VARIABLES Dependent_variable
  /METHOD=BSTEP(COND) List_of_spatial_descriptors
  /SAVE=PRED
  /CRITERIA=PIN(.05) POUT(.10) ITERATE(20) CUT(.5).
```

3. A spatial independent variable is defined by the spatial favourability (F_x), where *x* represents a continent. F_x provides a value of the degree to which spatial descriptors favour the occurrence of the analysed item in each hexagon.

$$F_x = \frac{P_x}{1 - P_x} / \left(\frac{n_1}{n_0} + \frac{P_x}{1 - P_x}\right)$$

where n_1 = number of presences, and n_0 = number of absences of the item to be modelled.

C. Independent variables: Primate zoogeography

1. Initial data: IUCN range maps of the American and African non-human primates.
2. For every continent, building of a matrix of presence (1) / absence (0) of every primate species (columns) in every hexagon (rows): "primate_data"
3. Hierarchical classification of the species ranges, separately for every continent, through the analysis of the 1/0 matrix using the Baroni-Urbani & Buser´s similarity index and the UPGMA classification method.
4. Chorotype variables: Definition of chorotypes through the evaluation of the statistical significance of all clusters in the hierarchical classification using RMacoqui 1.0 software (http://rmacoqui.r-forge.r-project.org/). For every chorotype, quantification, in each hexagon, of the number of species belonging to each chorotype.

R script for the package "RMacoqui" (https://rmacoqui.r-forge.r-project.org/)

```
## The data set was a presences/absences matrix for primates of a continent.

data(primate_data)
macoquires <- macoqui(primate_data)

## Friendly 'macoqui' results. Output of interest: "Chorotype Report".

ver.matRmacoqui(macoquires)

## Parameters for chorotype variable quantification. Output of interest: "Chorotypes in
Localities". The SR (species richness) result was used.

locs <- locCorot(macoquires)
ver.matRmacoqui(locs)
```

5. Logistic regression: The objective is to choose the set of chorotype variables to be considered henceforth. The study area is global, and so both African and American chorotypes are included in the analysis.
    a. Dependent variable: Presences (1) and absences (0) of yellow fever cases
    b. Independent variables: African and American chorotype variables.
    c. Selection of independent variables: Conditional forward-backward stepwise procedure.
    d. Estimation of variable coefficients: machine-learning iterative process based on the maximum log-likelihood criterion.
    e. Only the chorotype variables selected by the stepwise logistic regression were considered to be "primate zoogeography" variables henceforth.

SPSS syntax for the logistic regression

```
LOGISTIC REGRESSION VARIABLES Dependent_variable
  /METHOD=FSTEP(COND) List_of_chorotype_variables
  /SAVE=PRED
  /CRITERIA=PIN(.05) POUT(.10) ITERATE(20) CUT(.5).
```

D. Vector models

D1. 20th-century model for urban vector species *Aedes aegypti* and *Ae. albopictus*

1. Control of the Type I error using the False Discovery Rate (FDR):
    a. RAO´s score test of all environmental variables (respect to the presences and absences of the mosquito species between 1970 and 2000) to get the *p* values.
    b. Pre-selection of variables for which $p < i \times q/v$ [i = position of the variable, arranged in increasing p order; q = 0.05; v = total number of environmental variables]. Only these pre-selected variables are considered henceforth.
2. Logistic regression: It provides a probability value (P_{um20}), based on environment and space variables, of the urban mosquito (*um*) species to occur in each hexagon during the late 20th century.
    a. Dependent variable: Presences (1) and absences (0) of the mosquito species between 1970 and 2000. *Ae. aegypti* and *Ae. albopictus* are modelled separately.
    b. Independent variables: environment (**A**) and space (**B**) variables.
    c. Selection of independent variables: Conditional forward-backward stepwise procedure.
    d. Estimation of variable coefficients: machine-learning iterative process based on the maximum log-likelihood criterion.
    e. Model evaluation: Hosmer & Lemeshow's goodness of fit.

SPSS syntax for the logistic regression
LOGISTIC REGRESSION VARIABLES *Dependent_variable*
/METHOD=FSTEP(COND) *List_of_environment_and_space_variables*
/SAVE=PRED
/CRITERIA=PIN(.05) POUT(.10) ITERATE(20) CUT(.5).

3. Control for excessive multicollinearity:
   a. Identification of variables with Spearman correlation coefficient > 0.8 among the variables selected by the logistic regression.
   b. This being the case, deletion of the least significant correlated variable according to the RAO´s score test, and repetition of the logistic regression.
4. Favourability (F_{um20}) values are calculated, based on the probability (P_{um20}) values provided by the logistic regression:

$$F_{um20} = \frac{P_{um20}}{1 - P_{um20}} \Big/ \left(\frac{n_1}{n_0} + \frac{P_{um20}}{1 - P_{um20}}\right)$$

where n_1 = number of presences, and n_0 = number of absences of the modelled mosquito species

D2. 21st-century model for urban vector species *Aedes aegypti* and *Ae. albopictus*

1. Control of the Type I error using the False Discovery Rate (FDR):
   a. RAO´s score test of all environmental variables (respect to the presences and absences of the mosquito species between 2001 and 2017) to get the *p* values.
   b. Pre-selection of variables for which $p < i \times q/v$ [i = position of the variable, when arranged in increasing p order; q = 0.05; v = total number of environmental variables]. Only these pre-selected variables are considered henceforth.
2. Logistic regression: It provides a probability value (P_{um21}), based on environmental and spatial variables, of the urban mosquito (*um*) species to occur in each hexagon during the early 21st century.
   a. Dependent variable: Presences (1) and absences (0) of the mosquito species between 2001 and 2017. *Ae. aegypti* and *Ae. albopictus* are modelled separately.
   b. Independent variables: environment (**A**) and space (**B**) variables, and the "updating variable", that is the value for the logit equation of this mosquito's 20th-century model (**D1**). The logit equation is the linear combination of variables selected in section D1.2c (see above).
   c. Selection of independent variables: A two-blocks approach is employed. The updating variable is forced to enter in the model in the first block; environment and space variables are selected in the second block using a conditional forward-backward stepwise procedure.
   d. Estimation of variable coefficients: machine-learning iterative process based on the maximum log-likelihood criterion.
   e. Model evaluation: Hosmer & Lemeshow's goodness of fit.

SPSS syntax for the logistic regression
LOGISTIC REGRESSION VARIABLES *Dependent_variable*
/METHOD=ENTER *20th-century_model_logit*
/METHOD=FSTEP(COND) *List_of_environment_and_space_variables*
/SAVE=PRED
/CRITERIA=PIN(.05) POUT(.10) ITERATE(20) CUT(.5).

3. Control for excessive multicollinearity:
   a. Identification of variables with Spearman correlation coefficient > 0.8 among the variables selected.
   b. This being the case, deletion of the least significant correlated variable according to the RAO´s score test, and repetition of the logistic regression.
4. Favourability (F_{um21}) values are calculated, based on the probability (P_{um21}) values provided by the logistic regression:

$$F_{um21} = \frac{P_{um21}}{1 - P_{um21}} / \left(\frac{n_1}{n_0} + \frac{P_{um21}}{1 - P_{um21}}\right)$$

where n_1 = number of presences, and n_0 = number of absences of the modelled mosquito species.

D3. Model for every sylvatic vector species

1. Control of the Type I error using the False Discovery Rate (FDR):
   a. RAO´s score test of all environmental variables (respect to the presences and absences of the mosquito species between 1970 and 2017) to get the *p* values.
   b. Pre-selection of variables for which $p < i \times q/v$ [*i* = position of the variable, when arranged in increasing *p* order; *q* = 0.05; *v* = total number of environmental variables]. Only these pre-selected variables are considered henceforth.
3. Logistic regression: It provides a probability value (P_{sm}), based on environmental and spatial variables, of the sylvatic mosquito (*sm*) species to occur in each hexagon
   a. Dependent variable: Presences (1) and absences (0) of the mosquito species between 1970 and 2017. *Haemagogus janthinomys*, *H. leucocelaenus, Sabethes chloropterus*, *Ae. africanus*, and *Ae. vittatus* are modelled separately.
   b. Independent variables: environment (**A**) and space (**B**) variables.
   c. Selection of independent variables: Conditional forward-backward stepwise procedure.
   d. Estimation of variable coefficients: machine-learning iterative process based on the maximum log-likelihood criterion.
   e. Model evaluation: Hosmer & Lemeshow's goodness of fit.

SPSS syntax for the logistic regression
LOGISTIC REGRESSION VARIABLES *Dependent_variable*
/METHOD=FSTEP(COND) *List_of_environment_and_space_variables*
/SAVE=PRED
/CRITERIA=PIN(.05) POUT(.10) ITERATE(20) CUT(.5).

4. Control for excessive multicollinearity:
   a. Identification of variables with Spearman correlation coefficient > 0.8 among the variables selected.
   b. This being the case, deletion of the least significant correlated variable according to the RAO´s score test, and repetition of the logistic regression.
5. Favourability (F_{sm}) values are calculated, based on the probability (P_{sm}) values provided by the logistic regression:

$$F_{\mathrm{sm}} = \frac{P_{sm}}{1 - P_{sm}} / \left(\frac{n_1}{n_0} + \frac{P_{sm}}{1 - P_{sm}} \right)$$

where n_1 = number of presences, and n_0 = number of absences of the modelled mosquito species.

D4. Integration of individual vector models using fuzzy logic

1. **20th-century vector model:** Application of the fuzzy union (U) between the models of the seven mosquito species considered (**D1** and **D3**); i.e., in each hexagon, the maximum value shown by any of the mosquito species models is selected. The 20th-century models are used for *Ae. aegypti* and *Ae albopictus*.

> **SPSS syntax for fuzzy union between mosquito models, late 20th century**
> COMPUTE 20_century_vector_model =MAX(Fum20_Ae_aegypti, Fum20_Ae_albopictus, Fsm_H_janthinomys, Fsm_H_leucocelaenus, Fsm_S_chloropterus, Fsm_Ae_africanus, Fsm_Ae_vittatus).
> EXECUTE.

2. **21st-century vector model:** Application of the fuzzy union (U) between the models of the seven mosquito species considered (**D2** and **D3**); i.e., in each hexagon, the maximum value shown by any of the mosquito species models is selected. The 21st-century models are used for *Ae. aegypti* and *Ae albopictus*.

> **SPSS syntax for fuzzy union between mosquito models, early 21st century**
> COMPUTE 21_century_vector_model =MAX(Fum21_Ae_aegypti, Fum21_Ae_albopictus, Fsm_H_janthinomys, Fsm_H_leucocelaenus, Fsm_S_chloropterus, Fsm_Ae_africanus, Fsm_Ae_vittatus).
> EXECUTE.

E. Baseline disease models:

E.1. 20th-century disease model

1. Control of the Type I error using the False Discovery Rate (FDR):
   a. RAO´s score test of all environmental variables (respect to the presences and absences of yellow fever cases between 1970 and 2000) to get the *p* values.
   b. Pre-selection of variables for which $p < i \times q/v$ [i = position of the variable, when arranged in increasing p order; q = 0.05; v = total number of environmental variables]. Only these pre-selected variables are considered henceforth.
2. Logistic regression: It provides a probability value (P_{dis20}) based on environmental and spatial variables, of yellow fever disease cases (*dis*) to occur in each hexagon during the late 20th century.
   a. Dependent variable: Presences (1) and absences (0) of yellow fever cases between 1970 and 2000.
   b. Independent variables: environment (**A**), space (**B**) and primate zoogeography (**C**) variables.
   c. Selection of independent variables: A two-blocks approach is employed. Environment and space variables are selected the first block; primate zoogeography variables are selected the second block. For this selection, a conditional forward-backward stepwise procedure is used.
   d. Estimation of variable coefficients: machine-learning iterative process based on the maximum log-likelihood criterion.
   e. Model evaluation: Hosmer & Lemeshow's goodness of fit.

SPSS syntax for the logistic regression
LOGISTIC REGRESSION VARIABLES *Dependent_variable*
/METHOD=FSTEP(COND) *List_of_environment_and_space_variables*
/METHOD=FSTEP(COND) *Primate_zoogeography_variables*
/SAVE=PRED
/CRITERIA=PIN(.05) POUT(.10) ITERATE(20) CUT(.5).

3. Control for excessive multicollinearity:
   a. Identification of variables with Spearman correlation coefficient > 0.8 among the variables selected.
   b. This being the case, deletion of the least significant correlated variable according to the RAO´s score test, and repetition of the logistic regression.
4. Favourability (F_{dis20}) values are calculated, based on the probability (P_{dis20}) values provided by the logistic regression:

$$F_{dis20} = \frac{P_{dis20}}{1 - P_{dis20}} \Big/ \left(\frac{n_1}{n_0} + \frac{P_{dis20}}{1 - P_{dis20}}\right)$$

where n_1 = number of presences, and n_0 = number of absences of yellow fever cases during the late 20th century.

E.2. 21st-century disease model

1. Control of the Type I error using the False Discovery Rate (FDR):
   a. RAO´s score test of all environmental variables (respect to the presences and absences of yellow fever cases between 2001 and 2017) to get the *p* values.
   b. Pre-selection of variables for which $p < i \times q/v$ [*i* = position of the variable, when arranged in increasing *p* order; *q* = 0.05; *v* = total number of environmental variables]. Only these pre-selected variables are considered henceforth.
2. Logistic regression: It provides a probability value (P_{dis21}) based on environmental and spatial variables, of yellow fever disease cases (*dis*) to occur in each hexagon during the late 21st century.
   a. Dependent variable: Presences (1) and absences (0) of yellow fever cases between 2001 and 2017.
   b. Independent variables: environmental variables (**A**), spatial variables (**B**), primate zoogeography (**C**) variables, and the "updating variable", that is the value for the logit equation of the 20th-century disease model (**E1**). The logit equation is the linear combination of variables selected in section E1.2c (see above).
   c. Selection of independent variables: A three-blocks approach is employed. The updating variable is forced to enter in the model in the first block; environment and space variables are selected in the second block; primate zoogeography variables are selected in the third block. For this selection, a conditional forward-backward stepwise procedure is used.
   d. Estimation of variable coefficients: machine-learning iterative process based on the maximum log-likelihood criterion.
   e. Model evaluation: Hosmer & Lemeshow's goodness of fit.

SPSS syntax for the logistic regression
LOGISTIC REGRESSION VARIABLES *Dependent_variable*
/METHOD=ENTER *20_century_disease_model_logit*
/METHOD=FSTEP(COND) *List_of_environment_and_space_variables*
/METHOD=FSTEP(COND) *Primate_zoogeography_variables*
/SAVE=PRED
/CRITERIA=PIN(.05) POUT(.10) ITERATE(20) CUT(.5).

5. Control for excessive multicollinearity:
   a. Identification of variables with Spearman correlation coefficient > 0.8 among the variables selected.
   b. This being the case, deletion of the least significant correlated variable according to the RAO´s score test, and repetition of the logistic regression.
6. Computation of favourability (F_{dis21}) values based on the probability (P_{dis21}) values provided by the logistic regression:

$$F_{dis21} = \frac{P_{dis21}}{1 - P_{dis21}} / \left(\frac{n_1}{n_0} + \frac{P_{dis21}}{1 - P_{dis21}} \right)$$

where n_1 = number of presences, and n_0 = number of absences of yellow fever cases during the early 21st century.

F. Transmission risk models:

1. **20th-century transmission risk model:** Application of the fuzzy intersection (∩) between the 20th-century vector model (**D4.1**) and the 20th-century disease model (**E1**); i.e., in each hexagon, the minimum value shown by any of these models is selected.

SPSS syntax for fuzzy intersection between the vector and disease models, late 20th century
```
COMPUTE 20_century_transmission_model=MIN(20_century_vector_model,
20_century_disease_model).
EXECUTE.
```

2. **21st-century transmission risk model:** Application of the fuzzy intersection (∩) between the 21st-century vector model (**D4.2**) and the 21st -century disease model (**E2**); i.e., in each hexagon, the minimum value shown by any of these models is selected.

SPSS syntax for fuzzy intersection between the vector and disease models, late 21st century
```
COMPUTE 21_century_transmission_model=MIN(21_century_vector_model,
21_century_disease_model).
EXECUTE.
```

Appendix 21: Independent predictor variables considered for disease, vector, and transmission-risk modelling. Some variables were used only in specific models: *20th century models; ** enhanced 21st century models; ***enhanced 21st century vector models; ****disease models.

Factor	Code	Variable	Source
Climate	*Bio1*	Annual Mean Temperature	Chelsa (http://chelsa-climate.org)
	Bio5	Max Temperature of Warmest Month	
	Bio6	Min Temperature of Coldest Month	
	Bio7	Temperature Annual Range (Bio5-Bio6)	
	Bio12	Annual Precipitation	
	Bio15	Precipitation Seasonality (Coefficient of Variation)	
Human Concentration	*Pop_den*	Population density**	Administrative Centres & Populated Places shapefile at the Relational World Database II (RWDB2) updated in 2000 (http://www.fao.org/geonetwork)
	Dist_pop	Distance to populated places	
Infrastructures**	*Dist_road*	Distance to roads	Vector Map Level 0 at the Digital Chart of the World (DCW,http://worldmap.harvard.edu), updated in 2002
	Dist_rail	Distance to rail-roads	
Livestock***	*Buffaloes*	Density of buffaloes	FAO 2010(http://www.fao.org/livestock-systems/en/)
	Poultry	Density of poultry	
	Goats	Density of small ruminants (goats)	
	Pigs	Density of pigs	
	Sheep	Density of small ruminants (sheep)	
	Cattle	Density of cattle	
Topography	*Slope*	slope	From GTOPO30 (US Geological Survey 1996), using ArcGIS Desktop 10.3.
	Elev	Elevation	GTOPO30 (US Geological Survey 1996).
Hydrography	*Dist_riv*	Distance to rivers	Global Drainage Basin Database GDBD. Released Version 1.0: May 29, 2007 (http://www.cger.nies.go.jp/db/gdbd/gdbd_index_e.html).
Ecoregions*	*MedFWS*	Mediterranean Forest, Woodlands and Scrub	Terrestrial Ecoregions of the World: A New Map of Life on Earth: A new global map of terrestrial ecoregions provides an innovative tool for conserving biodiversity[1]
	TrosubDBF	Tropical and Subtropical Dry Broadleaf Forest	
	TempCF	Temperate Coniferous Forests	
	TempBMF	Temperate Broadleaf and Mixed Forests	
	TrosubCF	Tropical and Subtropical Coniferous Forests	
	DeXS	Deserts and Xeric Shrublands	
	Mangro	Mangroves	
	TrosubMBF	Tropical and Subtropical Moist Broadleaf Forest	
	BorFT	Boreal Forests/Taiga	
	TrosubGSS	Tropical and Subtropical Grasslands, Savannas and Shrublands	
	TempGSS	Temperate Grasslands, Savannas and Shrublands	
	FloGS	Flooded Grassland and Savannas	
	MonGS	Montane Grasslands and Shrublands	
	Tundra	Tundra	

Agriculture	*Class 11-14*	Croplands	GlobCover (GC) Land Cover version 2.3 database for 2009[2]
	Class 20	Mosaic Cropland (50-70%) / Vegetation (grassland, shrubland, forest) (20-50%)**	
	Class 30	Mosaic Vegetation (grassland, shrubland, forest) (50-70%) / Cropland (20-50%)**	
	Equi_irrig	Percentage of area equipped for irrigation***	Global Map of Irrigation Areas (version 4.0.1) around the year 2000 (http://www.fao.org/nr/water)
Ecosystem Types**	*Class 40*	Closed to open (>15%) broadleaved evergreen and/or semi-deciduous forest (>5m)	GlobCover (GC) Land Cover version 2.3 database for 2009[2]
	Class 50	Closed (>40%) broadleaved deciduous forest (>5m)	
	Class 60	Open (15-40%) broadleaved deciduous forest (>5m)	
	Class 70	Closed (>40%) needleleaved evergreen forest (>5m)	
	Class 90	Open (15-40%) needleleaved deciduous or evergreen forest (>5m)	
	Class 100	Closed to open (>15%) mixed broadleaved and needleleaved forest (>5m)	
	Class 110	Mosaic Forest/Shrubland (50-70%) / Grassland (20-50%)	
	Class 120	Mosaic Grassland (50-70%) / Forest/Shrubland (20-50%)	
	Class 130	Closed to open (>15%) shrubland (<5m)	
	Class 140	Closed to open (>15%) grassland	
	Class 150	Sparse (>15%) vegetation (woody vegetation, shrubs, grassland)	
	Class 160	Closed (>40%) broadleaved semi-deciduous and/or evergreen forest regularly flooded - Saline water	
	Class 170	Closed (>40%) broadleaved semi-deciduous and/or evergreen forest regularly flooded - Saline water	
	Class 180	Closed to open (>15%) vegetation (grassland, shrubland, woody vegetation) on regularly flooded or waterlogged soil - Fresh, brackish or saline water	
	Class 200	Bare areas	
	Class 220	Permanent snow and ice	
Forest loss**	*Forest loss*	Non intact forest	High-Resolution Global Maps of 21st-Century Forest Cover Change[3]
Logit equation	*Y-20th century*	20th-century-model logit equation	Linear combinations of predictor variables that form part of the logistic-regression equations
Spatial descriptors	*Fx*	Spatial trend, where "x" represents a continent	Linear combination of spatial variables derived from continental-scale trend surface analyses[4]
Primate chorotypes****	*SAx* and *AFy*	Chorotype species richness. *SAx*: South-American chorotype "x" and *AFy*: African chorotype "y"	Supplementary Figs. 5-7[5]

Supplementary References:

1. Olson DM, Dinerstein E, Wikramanayake E, Burgess ND, Powell G, Underwood E, et al. Terrestrial Ecoregions of the World: A New Map of Life on Earth: A new global map of terrestrial ecoregions provides an innovative tool for conserving biodiversity. Bioscience. 2001; 51: 933–938.
2. Bontemps S. GLOBCOVER 2009 Products Description and Validation Report. 2011.
3. Hansen MC. High-resolution global maps of 21st-century forest cover change. Science. 2013;342: 850–853
4. Legendre P. Spatial autocorrelation: Trouble or New Paradigm? Ecology. 1993;74: 1659–1673
5. Olivero J, Real R, Márquez AL. Fuzzy chorotypes as a conceptual tool to improve insight into biogeographic patterns. Syst Biol. 2011;60: 645–660. doi:10.1093/sysbio/syr026

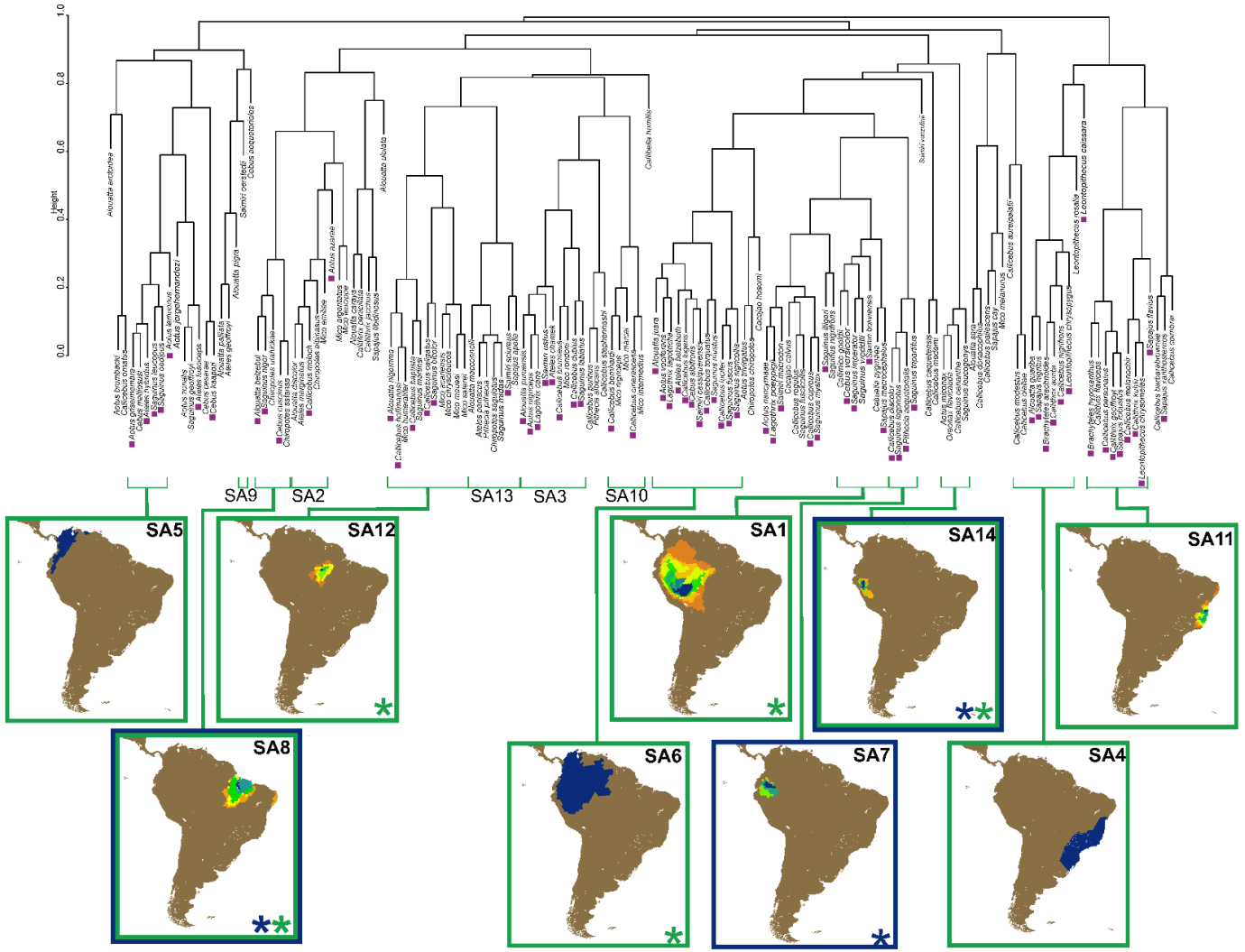

Appendix 22: Classification dendrograms of primate distributions in America. Blue rectangles: chorotypes significantly related to the distribution of the late 20th-century yellow fever cases according to a forward-stepwise logistic regression. Green rectangles: chorotypes significantly related only to the distribution of the 21st-century cases. Chorotypes that were finally included in disease models are highlighted with a blue asterisk for the late 20th century, and with a green asterisk for the 21st century. American chorotype names are coded as SA1 to SA14. Violet square: species belonging to chorotypes significantly related to the yellow fever distribution (degree of membership ≥ 0,5).

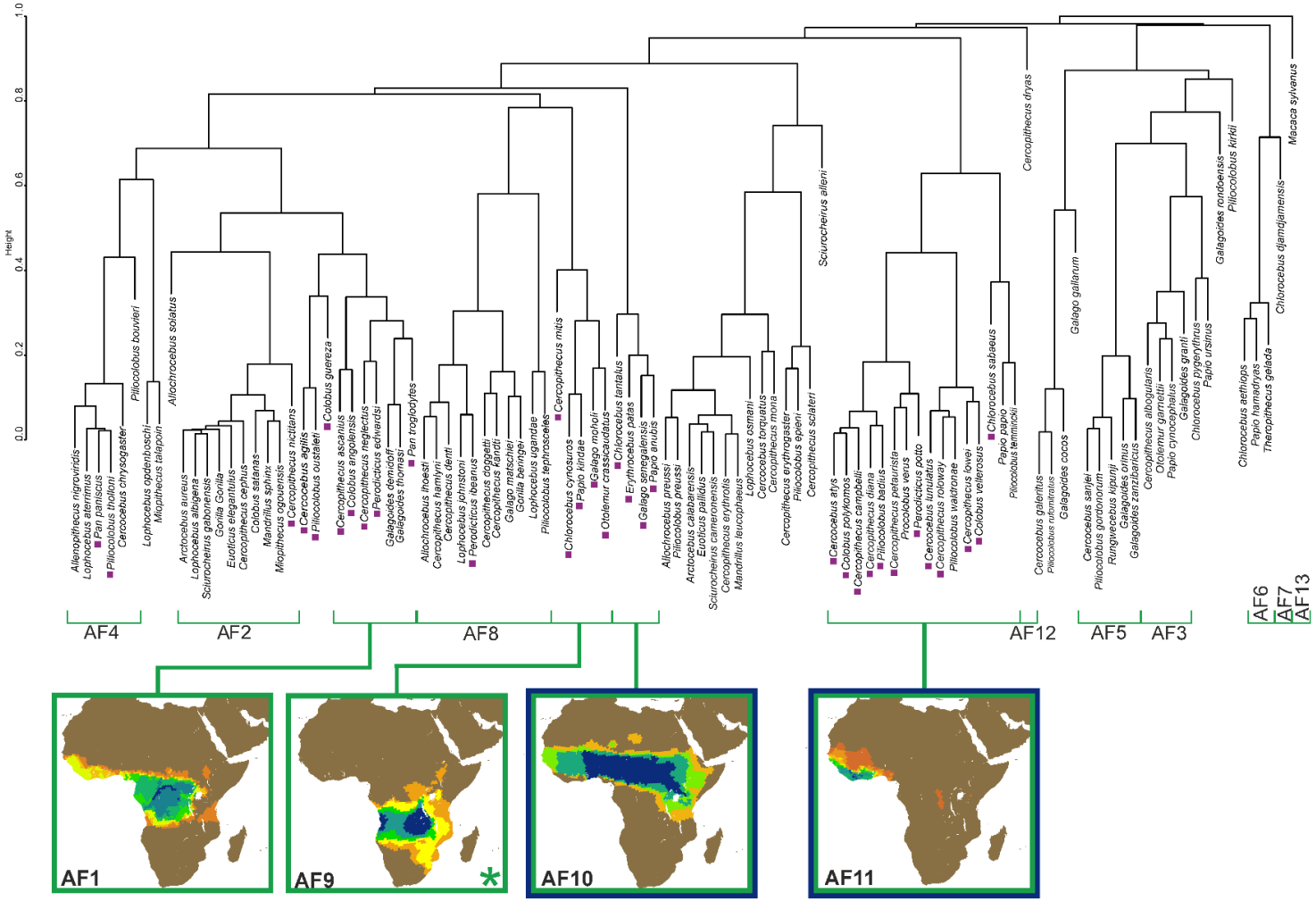

Appendix 23: Classification dendrograms of primate distributions in Africa. Blue rectangles: chorotypes significantly related to the distribution of the late 20th-century yellow fever cases according to a forward-stepwise logistic regression. Green rectangles: chorotypes significantly related only to the distribution of the 21st-century cases. Chorotypes that were finally included in disease models are highlighted with a blue asterisk for the late 20th century, and with a green asterisk for the 21st century. American chorotype names are coded as AF1 to AF13. Violet square: species belonging to chorotypes significantly related to the yellow fever distribution (degree of membership ≥ 0,5).

Appendix 24: Non-human primate genera included in the chorotypes that were significantly related to the distribution of yellow fever cases in the late 20th century and the early 21st century. SA: South-American chorotype; AF: African chorotype. See the classification dendrograms of primate distributions in South-America and Africa in Supplementary Fig. 1 and 2.

Model	Chorotype	Genera
20th century	SA7	*Callicebus*, *Pithecia*, *Saguinus*
	SA8	*Alouatta*, *Cebus*, *Chiropotes*
	SA14	*Saguinus*, *Brachyteles*, *Callithrix*, *Callicebus*, *Leontophitecus*
	AF10	*Chlorocebus*, *Erythrocebus*, *Galago*, *Papio*
	AF11	*Colobus*, *Cercopithecus*, *Piliocolobus*, *Cercocebus*, *Perodicticus*, *Procolobus*
21st century*	SA1	*Callimico*, *Cebus*, *Callithrix*, *Saguinus*, *Saimiri*, *Sapajus*
	SA4	*Alouatta*, *Sapajus*, *Brachyteles*, *Callithrix*, *Callicebus*, *Leontophitecus*
	SA5	*Aotus*, *Cebus*, *Ateles*, *Saguinus*
	SA6	*Alouatta*, *Aotus*, *Ateles*, *Callicebus*, *Saguinus*, *Saimiri*
	SA11	*Brachyteles*, *Callithrix*, *Callicebus*, *Sapajus*, *Leontopithecus*
	SA12	*Alouatta*, *Callicebus*, *Mico*, *Saguinus*
	AF1	*Cercopithecus*, *Colobus*, *Perodicticus*, *Galagoides, Pan*
	AF9	*Cercopithecus*, *Chlorocebus*, *Galago*, *Otolemur*, *Papio*

(*) All chorotypes in the 20th-century model are also included in the 21st-century model. Only additional chorotypes are shown here.

Appendix 25: Baseline disease model logit equations (i.e., linear combinations of predictor variables that form part of the logistic-regression equations). B: variable coefficient; SE: standard error; W: Wald parameter; DF: degrees of freedom; S: statistical significance. Variable codes as in Appendix 24.

20th-century model

Variable	B	SE	W	DF	S
Bio12	0.096×10^{-3}	0.104×10^{-3}	0.844	1	0.358
Dist_pop	-0.034×10^{-3}	0.005×10^{-3}	55.15	1	0.112×10^{-14}
Slope	0.121	0.048	6.492	1	0.011
DeXS	-2.784	0.947	8.636	1	0.003
Famerica	9.282	0.559	275.365	1	0.769×10^{-63}
Fafrica	6.805	0.422	260.479	1	0.135×10^{-59}
SA7	0.714	0.132	29.274	1	0.628×10^{-9}
SA8	0.334	0.084	16.01	1	0.063×10^{-3}
SA14	0.542	0.187	8.416	1	0.004
Constant	-6.959	0.388	321.032	1	0.863×10^{-73}
Goodness of fit		$\chi^2 = 4.214$; $n = 10$ bins; p=0.837			

21st-century model

Variable	B	SE	W	DF	S
Y-20th century	0.012	0.059	0.045	1	0.833
Bio12	0.161×10^{-3}	0.019×10^{-3}	2.165	1	0.141
Bio5	0.016	0.002	44.564	1	0.246×10^{-12}
Bio6	0.007	0.002	7.633	1	0.006
Dist_pop	-0.026×10^{-3}	0.003×10^{-3}	60.015	1	0.941×10^{-16}
Elev	0.001	0.219×10^{-3}	29.283	1	0.625×10^{-9}
DeXS	-2.759	0.688	16.068	1	0.061×10^{-3}
Famerica	7.983	0.605	174.096	1	0.943×10^{-42}
Fafrica	5.479	0.46	141.984	1	0.981×10^{-34}
SA1	0.26	0.047	31.12	1	0.243×10^{-9}
SA6	0.127	0.036	12.215	1	0.474×10^{-3}
SA8	0.625	0.084	55.567	1	0.903×10^{-15}
SA12	0.313	0.108	8.422	1	0.004
SA14	0.548	0.194	7.95	1	0.005
AF9	0.257	0.075	11.658	1	0.001
Constant	-12.354	1.349	83.913	1	0.517×10^{-21}
Goodness of fit		$\chi^2 = 6.499$; $n = 10$ bins; p=0.592			

21st-century enhanced model

Variable	B	SE	W	DF	S
Y-20th century	0.115	0.053	4.661	1	0.031
Bio12	0.202×10^{-3}	0.111×10^{-3}	3.303	1	0.069
Bio5	0.015	0.003	36.517	1	0.151×10^{-10}

Class 100	-752.147	831.976	0.817	1	0.366
Class 110	2.285	0.662	11.906	1	0.001
Class 130	-0.63	0.393	2.563	1	0.109
Class 200	-12.12	5.11	5.626	1	0.018
Dist_pop	-0.023×10^{-3}	0.003×10^{-3}	50.083	1	0.147×10^{-13}
Elev	0.001	0.176×10^{-3}	26.835	1	0.222×10^{-8}
Forest loss	3.967	0.903	19.287	1	0.011×10^{-3}
Famerica	6.845	0.583	137.899	1	0.766×10^{-33}
Fafrica	4.820	0.449	115.32	1	0.670×10^{-28}
SA1	0.265	0.048	30.900	1	0.272×10^{-9}
SA6	0.146	0.038	14.917	1	0.112×10^{-3}
SA8	0.508	0.085	35.764	1	0.223×10^{-10}
SA12	0.337	0.109	9.560	1	0.002
SA14	0.463	0.196	5.576	1	0.018
AF9	0.310	0.074	17.348	1	0.031×10^{-3}
Constant	-10.302	1.195	74.274	1	0.680×10^{-19}
Goodness of fit		$\chi^2 = 10.818$; *n* = 10 bins; p=0.212			

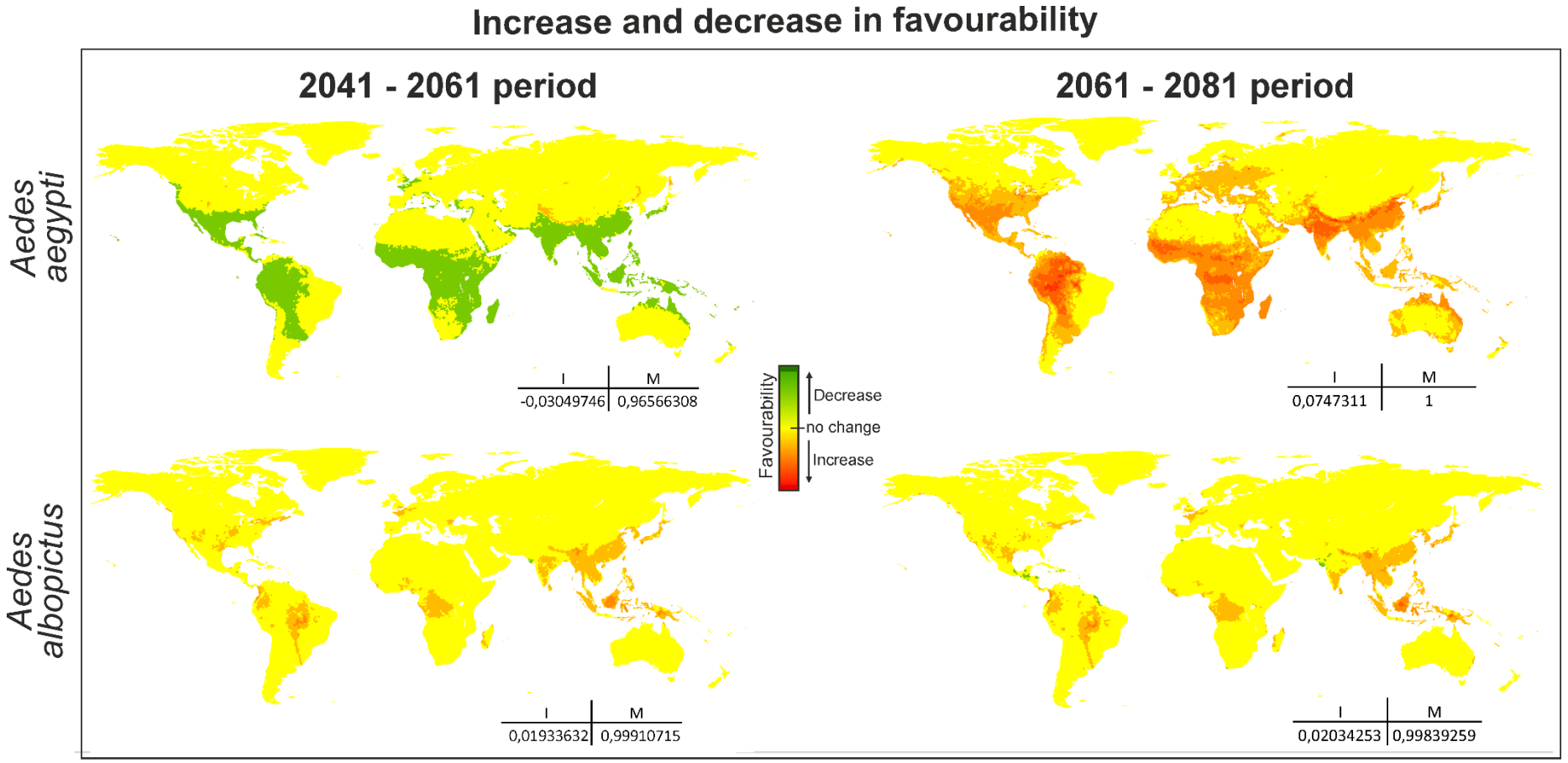

Appendix 26. Areas where favourability increases and decreases in the future relative to the present. Difference between the future projection and the current model. I: increment rate; B: maintenance rate (Romero et al. Journal of Biogeography 41.1 (2014): 111-121). Positive values of I indicate a net increase in favourability, that is, a gain in favourable areas, whereas negative values of I mean a net loss of favourable areas. M indicates the degree to which the favourable areas in the current model overlap with the favourable forecasted area.

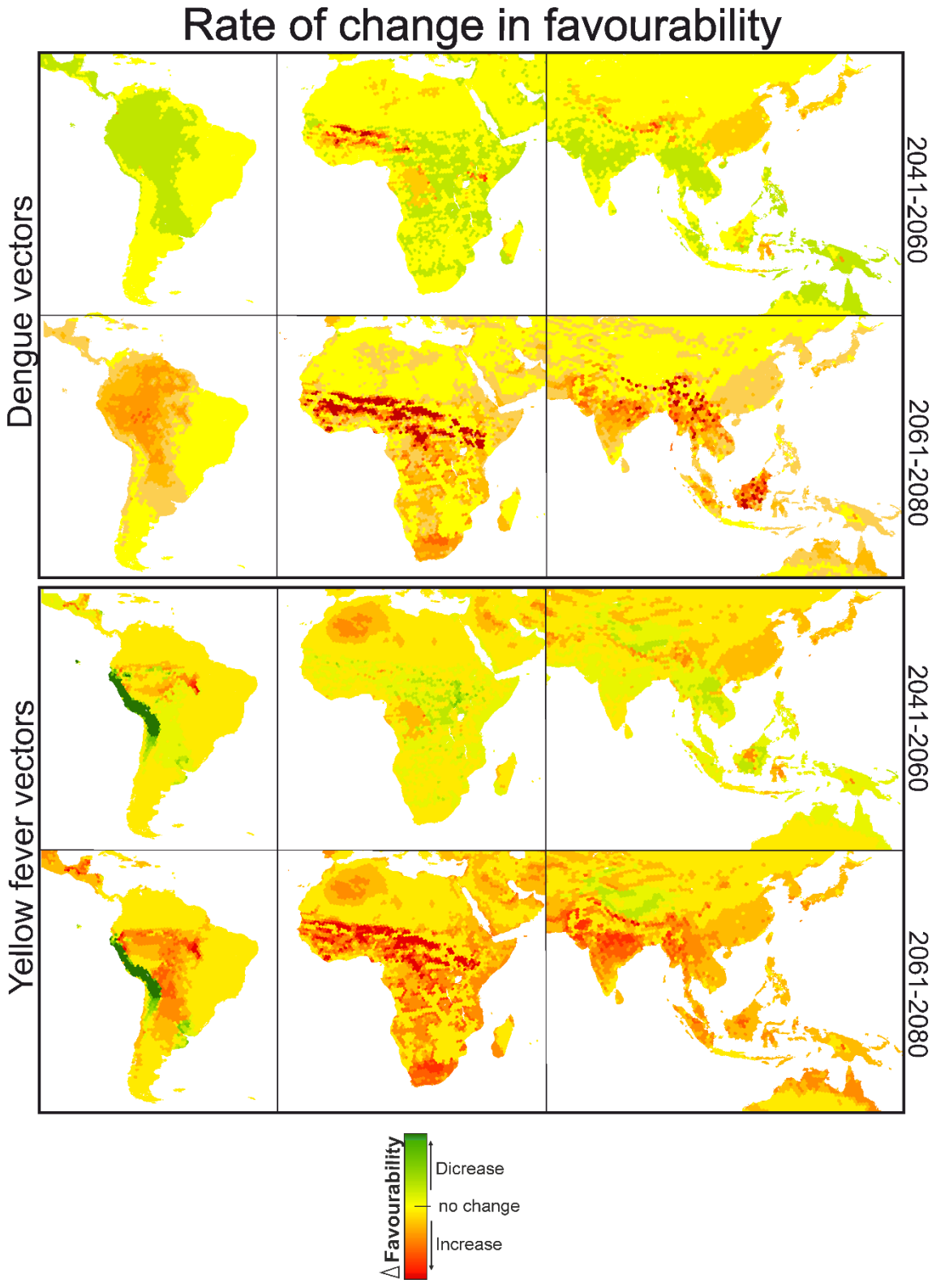

Appendix 27. Rate of change in favourability of dengue and yellow fever vectors models. Zoomed details of areas where favourability increases and decreases in the future relative (2041-2060 and 2061 – 2080) to the present.

13. Producción científica asociada a esta tesis doctoral / Scientific outputs of this PhD thesis

Artículos que avalan esta tesis doctoral / Articles from this PhD Thesis:

- **Aliaga-Samanez, A.**, Real, R., Vermeer, J., Olivero, J. (2020). Modelling species distributions limited by geographical barriers: A case study with African and American primates, *Global Ecology and Biogeography*, 29(3), 444-453, https://doi.org/10.1111/geb.13041 **(Q1)**
    - **Aliaga-Samanez, A**. et al. (2020), Data from: Modelling species distributions limited by geographic barriers: a case study with African and American primates, *Dryad*, *Dataset*, https://doi.org/10.5061/dryad.8pk0p2nj0
- Farfán, M., **Aliaga-Samanez, A.**, Olivero, J., Williams, D., Dupain, J., Guian, Z., Fa, J.E. et al. (2019). Spatial modelling for predicting potential wildlife distributions and human impacts in the Dja Forest Reserve, Cameroon, *Biological Conservation*, 230, 104-112, https://doi.org/10.1016/j.biocon.2018.12.015 **(Q1)**
- **Aliaga-Samanez, A.**, Cobos-Mayo, M., Real, R., Segura, M., Romero, D., Fa, J.E., Olivero, J. (2021) Worldwide dynamic biogeography of zoonotic and anthroponotic dengue, *PloS Neglected Tropical Dise*ases, 15(6), e0009496, https://doi.org/10.1371/journal.pntd.0009496 **(Q1)**
    - **Aliaga-Samanez, A.** et al. (2021), Compendium of dengue cases from 2013 to 2017, *Dryad*, *Dataset*, https://doi.org/10.5061/dryad.9w0vt4bfv

- **Aliaga-Samanez, A.**, Real, R., Segura, M., Marfil-Daza, C., Olivero, J. (2022) Yellow fever surveillance suggests zoonotic and anthroponotic emergent potential, *Communications Biology*, 5(1), 1-12, https://www.nature.com/articles/s42003-022-03492-9 (**Q1)**

- **Aliaga-Samanez, A.**, Romero, D., Murray, K., Cobos-Mayo, M., Segura, M., Real, R. & Olivero, J. (2023). Submitted. Climate change is aggravating dengue and yellow fever vectors spread.

Otras publicaciones surgidas durante el desarrollo de la presente tesis doctoral / Other publications that arose during the course of this doctoral thesis:

- Duque Sandoval, D.; **Aliaga-Samanez, A.**; Castellanos, A. H. G. (2019). El mono araña (*Ateles hybridus*) en la Reserva Forestal Caparo: Ecología y conservación. Urbani, B. & Ceballos-Mago. La primatología en Venezuela. pp. 57 - 79. Editorial Equinoccio (Colección Conjunta ACFIMAN/USB). https://equinoccio.com.ve/index.php/colecciones/acfiman-usb/la-primatologia-en-venezuela-detail.

- Martín Taboada, A., Romero, D., **Aliaga-Samanez A.**, Chamorro Sierra, D. (2020) Favorabilidad y lógica difusa como herramientas para el análisis biogeográfico de las interacciones competitivas entre especies. Carracedo, V.; García-Codron, J.C.; Garmendia, C.; Rivas, V. Conservación, Gestión y Restauración de la Biodiversidad. pp. 155 - 163.

- García Carrasco, J. M., **Aliaga-Samanez, A.**, Olivero, J.; Muñoz, A.; Santos, E.; Real, R. (2020) ¿Hay riesgo de establecimiento de encefalitis japonesa en Europa? Carracedo, V.; García-Codron, J.C.; Garmendia, C.; Rivas, V. Conservación, Gestión y Restauración de la Biodiversidad. pp. 73 - 82.

- **Aliaga-Samanez, A.**, Real, R., Segura, M., Marfil-Daza, C., Olivero, J. (2022). Emerging zoonotic and anthroponotic potential for yellow fever transmission. Nature Portfolio Health Community. https://healthcommunity.nature.com/posts/yellow-fever-surveillance-suggests-emergent-potential

Impacto en los medios de comunicación y en blogs de instituciones científicas surgidas durante el desarrollo de la presente tesis doctoral / Impact in the media and in blogs of scientific institutions that arose during the development of this doctoral thesis:

- Entrevista realizada por Global Infectious Disease Epidemiology Network (GIDEON): Tracking dengue: an interview with **Alisa Aliaga-Samanez**. (2021). https://www.gideononline.com/2021/07/07/tracking-dengue-an-interview-with-alisa-aliaga-samanez/

- Center for International Forestry Research (CIFOR): How deforestation poses dengue risk for Africa and Asia https://forestsnews.cifor.org/74205/how-deforestation-poses-dengue-pandemic-risk-for-africa-and-asia?fnl=enen

- GIDEON: New dengue study identifies new high-risk countries https://www.gideononline.com/2021/07/28/new-dengue-study-identifies-new-high-risk-countries/

- CIFOR: Deforestasi Picu Risiko Demam Berdarah di Afrika dan Asia https://forestsnews.cifor.org/74276/deforestasi-picu-risiko-demam-berdarah-di-afrika-dan-asia?fnl=en

- Investigadores de la UMA advierten del aumento del área de distribución de los mosquitos vectores del dengue. Sala de prensa de la *Universidad de Málaga*. https://www.uma.es/sala-de-prensa/noticias/investigadores-de-la-uma-advierten-del-aumento-del-area-de-distribucion-de-los-mosquitos-vectores-del-dengue/

- Investigadores de la UMA advierten del aumento de mosquitos vectores del dengue. *La opinión de Málaga*. https://www.laopiniondemalaga.es/malaga/2021/07/09/investigadores-uma-advierten-aumento-mosquitos-54849880.html

- Investigadores de la UMA advierten del aumento del área de distribución de mosquitos vectores del dengue. *Europapress*. https://www.europapress.es/andalucia/malaga-00356/noticia-investigadores-uma-advierten-aumento-area-distribucion-mosquitos-vectores-dengue-20210709123337.html

- Alerta por el aumento del área de distribución de mosquitos vectores del dengue. *Telecinco*. https://www.telecinco.es/informativos/salud/aumento-area-distribucion-mosquitos-vectores-dengue_18_3167598835.html

- Investigadores de la UMA advierten del aumento del área de distribución de mosquitos vectores del dengue. *20minutos*. https://www.20minutos.es/noticia/4759005/0/investigadores-de-la-uma-advierten-del-aumento-del-area-de-distribucion-de-mosquitos-vectores-del-dengue/

- Investigadores de la UMA advierten del aumento del área de distribución de mosquitos vectores del dengue. *Teleprensa*. https://www.teleprensa.com/articulo/malaga/investigadores-uma-advierten-aumento-area-distribucion-mosquitos-vectores-dengue/20210709104255978598.html

- Crece el área de distribución de los mosquitos que transmiten el dengue. *Novaciencia*. https://novaciencia.es/crece-el-area-de-distribucion-de-los-mosquitos-que-transmiten-el-dengue/

- Investigadores de la UMA advierten del aumento del área de distribución de mosquitos vectores del dengue. *Gente digital*. http://www.gentedigital.es/malaga/noticia/3176619/investigadores-de-la-uma-advierten-del-aumento-del-area-de-distribucion-de-mosquitos-vectores-del-dengue/

- How deforestation poses dengue pandemic risk. *Borneo bulletin*. https://borneobulletin.com.bn/how-deforestation-poses-dengue-pandemic-risk/

- Cómo la deforestación representa un riesgo de pandemia de dengue para África y Asia. *F1mundial*.

https://f1mundial.com/como-la-deforestacion-representa-un-riesgo-de-pandemia-de-dengue-para-africa-y-asia/

- El dengue ya no es una enfermedad tropical, está en el Mediterráneo y puede afectar al turismo. *Sport*. https://www.sport.es/es/noticias/dengue-enfermedad-tropical-mediterraneo-afectar-11906325

- El dengue ya no es una enfermedad tropical, está en el Mediterráneo y puede afectar al turismo. *Faro de Vigo*. https://www.farodevigo.es/medio-ambiente/2021/07/13/dengue-enfermedad-tropical-mediterraneo-afectar-54968682.html

- Científicos de la UMA profundizan en el crecimiento global de transimisión de la fiebre amarilla a humanos. *Europapress*. https://www.europapress.es/andalucia/malaga-00356/noticia-cientificos-uma-profundizan-crecimiento-global-transimision-fiebre-amarilla-humanos-20220620131459.html

- Científicos de la UMA profundizan en la biogeografía de la transmisión de la fiebre amarilla. Sala de prensa de la *Universidad de Málaga*. https://www.uma.es/sala-de-prensa/noticias/cientificos-de-la-uma-profundizan-en-la-biogeografia-de-la-transmision-de-la-fiebre-amarilla/

- La UMA indaga en el aumento de la transmisión de la fiebre amarilla a humanos. *La opinión de Malaga*. https://www.laopiniondemalaga.es/malaga/2022/06/21/uma-indaga-aumento-transmision-fiebre-67479586.html

- Cómo crece el riesgo global de transmisión de la fiebre amarilla a los humanos. *Fundación descubre*. https://idescubre.fundaciondescubre.es/noticias/profundizan-en-la-biogeografia-de-la-transmision-de-la-fiebre-amarilla/

- Científicos de la UMA indagan en la transimisión global de la fiebre amarilla a humanos. *Malaga Hoy*. https://www.malagahoy.es/malaga/Cientificos-UMA-fiebre-amarilla-humanos_0_1694531974.html

- Científicos de la UMA profundizan en la biogeografía de la transmisión de la fiebre amarilla. *Biotech-Spain*.

http://biotech-spain.com/en/articles/cient-ficos-de-la-uma-profundizan-en-la-biogeograf-a-de-la-transmisi-n-de-la-fiebre-amarilla/

- La UMA detecta nuevas zonas en las que se está extendiendo la fiebre amarilla. *Novaciencia*. https://novaciencia.es/la-uma-detecta-nuevas-zonas-en-las-que-se-esta-extendiendo-la-fiebre-amarilla/

14. Breve *curriculum vitae /* Brief cv

Alisa Aliaga Samanez es licenciada en Biología por la Universidad Nacional Federico Villarreal de Lima (Perú) con Máster en Diversidad Biológica y Medio Ambiente por la Universidad de Málaga (España). Actualmente está desarrollando su tesis doctoral en el Departamento de Biología Animal tras haber obtenido una beca predoctoral de la UMA y una beca predoctoral FPU del Ministerio de Universidades. Antes de empezar la etapa predoctoral participó en proyectos de investigación, en la Asociación Proyecto Mono Tocón en Perú, enfocado en el estudio la densidad y distribución del mono tócon en la Región de San Martín y en la Asociación Proyecto Mono Araña en Venezuela, enfocado en el estudio del comportamiento y la dieta de un grupo de monos araña en un fragmento de bosque en la Reserva Forestal Caparo, publicando 2 artículos científicos en revistas indexadas. Estos estudios fueron financiados por la IUCN-NL, Biocuencas Perú – Conservation International, Le conservatoire pour la protection des primates y por el Fondo de conservación de especies Mohamed Bin Zayed. Después de ello, realizó el máster en la Universidad de Málaga, obteniendo matrícula de honor en el Trabajo Fin de Máster. Luego participó en el Proyecto de Modelación de cybertracked y datos de amenazas para la planificación de la conservación de la Reserva Forestal de Dja (Camerún - África), financiado por African Wildlife Foundation. Durante su etapa predoctoral en la UMA ha publicado otros 4 artículos científicos de la tesis, todos en revistas indexadas en el JCR y en el 1º cuartil (Q1). Los dos últimos artículos científicos de la tesis publicados en PloS Neglected Tropical Diseases y en Communications Biology (Springer Nature) se han divulgado en medios de comunicación a nivel nacional y extranjero, en blogs de entidades científicas como CIFOR (Center for International Forestry Research) y GIDEON (Global Infectious Disease Epidemiology Network). Además, ha publicado 3 capítulos de libro y una publicación en el foro de Health Community de Nature Portfolio. Ha realizado

una estancia predoctoral de 3 meses en la London School of Hygiene and Tropical Medicines (MRC Unit The Gambia) tras obtener la Ayuda para Estancias Breves para beneficiarios del programa de FPU del Ministerio. También ha impartido horas de docencia en prácticas en el grado de Biología y Ciencias Ambientales. Ha presentado 25 contribuciones a congresos internacionales, obteniendo reconocimiento a mejor póster en el Congreso SINAPSIS 2022 celebrado en Londres. También ha complementado su formación con la asistencia a 41 conferencias, seminarios, talleres y cursos.